Aus dem Institut für Klinische Neuroimmunologie
der Ludwig-Maximilians-Universität München
Direktor: Prof. Dr. med. Reinhard Hohlfeld

Characterization of Disease-Related $CD8^+$ T Cells and their Antigens from Patients with Multiple Sclerosis

Dissertation

zum Erwerb des Doktorgrades der Naturwissenschaften
an der medizinischen Fakultät
der Ludwig-Maximilians-Universität München

vorgelegt von

Anna Gabriele Niedl
aus München

2013

Gedruckt mit der Genehmigung der medizinischen Fakultät
der Ludwig-Maximilians-Universität München

Betreuer:	PD Dr. rer. nat. Klaus Dornmair
Zweitgutachterin:	Prof. Dr. Elfriede Nößner
Dekan:	Prof. Dr. med. Dr. h. c. Maximilian Reiser, FACR, FRCR
Tag der mündlichen Prüfung:	22.08.2014

Danksagung

Ich möchte mich bei allen bedanken, die zum Gelingen dieser Arbeit beigetragen haben.

An erster Stelle möchte ich meinem Betreuer PD Dr. Klaus Dornmair für die Bereitstellung des interessanten und anspruchsvollen Themas, die intensive Betreuung, ständige Diskussionsbereitschaft und das begeisterte Interesse an meinem Projekt danken.

Ich danke Prof. Dr. Reinhard Hohlfeld für das ebenfalls sehr große Interesse an meiner Arbeit Sie haben so manchen Tag im abgeschotteten Sterilraum durch einen netten Plausch und auch mal einen Keks danach erheitert.

Besonders möchte ich mich bei den Kollaboratoren Prof. Dr. Lars Fugger, Dr. Kathrine Attfield, Dr. Wolfgang Klinkert, Dr. Stefan Pinkert und Dr. Peer-Hendrik Kuhn für die vielen, langen Gespräche und die fruchtbare Zusammenarbeit bedanken.

Ich danke allen Mitarbeitern für die angenehme Atmosphäre und die freundliche Aufnahme in beiden Abteilungen für Neuroimmunologie. Ein sehr großer Dank geht an Ingrid Eiglmeier, Joachim Malotka und Reinhard Mentele für die Einweisung in viele unterschiedliche Technologien und Geräte. Insbesondere bedanke ich mich auch bei Katherina und Jessica für das geduldige Erklären neuer Techniken und bei Simone für erfolgreiche Platz- und Geräteteilung. Außerdem bedanke ich mich bei Angelika, Kathrin, Judy, Latika, Makbule, Eduardo, Geraldine, Gintare, Birgit, Wakiro, Aline, Qingqing und Matea für die ständige Diskussionsbereitschaft und hilfreiche Kritik.

Abschließend möchte ich mich bei meiner Familie und meinen Freunden bedanken. Ohne euch wären gerade die letzten zwei Jahre nicht zu stemmen gewesen.

Zusammenfassung

Multiple Sklerose ist wahrscheinlich eine autoimmunvermittelte, entzündliche Erkrankung des zentralen Nervensystems. An verschiedenen Stellen im Gehirn und Rückenmark kommt es zu einer Zerstörung der Markscheiden und Axone. Diese Schädigung führt zu neurologischen Symptomen. Der Krankheits-verlauf ist nicht vorhersehbar und zugrundeliegende Mechanismen sind weitgehend unbekannt. Sowohl Umwelteinflüsse als auch genetische Prädisposition werden in diesem Zusammenhang diskutiert.

Vor kurzem wurde $CD8^+$ T Lymphozyten eine entscheidende Rolle bei der autoimmunvermittelten Pathogenese zugesprochen. Sie übertreffen deutlich die Anzahl an $CD4^+$ T Zellen in aktiven Läsionen aber Zielzellen oder erkannte Antigene sind bisher unbekannt. Schon sehr früh konnte eine genetische Verknüpfung zwischen der Wahrscheinlichkeit an Multipler Sklerose zu erkranken und dem humanen Leukozyten Antigen Genlocus festgestellt werden. Dabei wird das Risiko durch den Besitz des *HLA-A*0301* Allels erhöht und des *HLA-A*0201* Allels gesenkt. Demnach wurden in der vorliegenden Arbeit folgende zwei Fragestellungen bearbeitet:

1. Welche $CD8^+$ T Lymphozyten sind an dem Autoimmunangriff auf das zentrale Nervensystem beteiligt und welche Rezeptoren tragen sie zur Antigenerkennung?
2. Wie vermindert die Expression von HLA-A2 Molekülen das Erkrankungsrisiko?

Im ersten Teil wurden T Zell Rezeptoren von potentiell krankheitsrelevanten $CD8^+$ Einzelzellen aus gefrorenem Patientengewebe charakterisiert. Krankheitsrelevanz wurde durch Zugehörigkeit zu einer klonal expandierten Zellpopulation oder durch die Expression von Aktivierungsmarkern definiert. In einem klonspezifischen Ansatz wurden die T Zell Rezeptor beta Ketten von voruntersuchten, klonal expandierten T Zell Populationen analysiert. Zudem wurde eine neue, von Voruntersuchungen unabhängige Methode zur Charakterisierung von T Zell Rezeptor beta Ketten entwickelt.

Im zweiten Teil wurde die Antigenerkennung des möglicherweise krankheitsrelevanten T Zell Rezeptors 2D1 untersucht. Dieser Rezeptor wurde aus einem Multiple Sklerose Patienten isoliert. Der T Zell Rezeptor 2D1 erkennt ein Peptid, welches aus der Myelinscheide stammt und auf HLA-A3 Molekülen präsentiert wird. In einem Mausmodell entwickelten doppelt transgene Mäuse, die HLA-A3 und den T Zell Rezeptor 2D1 exprimierten, der Multiplen Sklerose ähnliche Symptome nach Immunisierung mit dem Myelinpeptid. Dreifach transgene Mäuse hingegen, die HLA-A3, den T Zell Rezeptor 2D1 und HLA-A2 exprimierten, blieben gesund. Die 2D1 T Zellen wurden in diesen Mäusen bereits im Thymus deletiert.

Um herauszufinden, welche HLA-A2 gebundenen Peptide diesen schützenden Effekt vermitteln, wurde eine neu entwickelte Methode angewandt, mit welcher Antigene von HLA Klasse I restringierten T Zellen identifiziert werden können. Dabei wurden 28 Peptide isoliert, welche von dem T Zell Rezeptor 2D1 auf HLA-A2 Molekülen erkannt werden. Diese Peptide wiesen hohe Sequenzähnlichkeiten auf. Acht Proteine aus der Maus – davon vier auch im Menschen vorhanden – kamen als Quellprotein in Frage. Schließlich wurden diese acht Proteine näher analysiert und Versuche zur Antigenprozessierung in unterschiedlichen antigenpräsentierenden Zellen durchgeführt.

Summary

Multiple Sclerosis is most probably an autoimmune inflammatory disease of the central nervous system. Demyelination of neurons and axonal loss occur in temporal and spatial resolution in multiple areas of the brain and spinal cord. This impairment manifests in neurological symptoms. The course of disease varies between individuals and the causing mechanisms still remain elusive. Environmental factors as well as genetic predispositions are widely discussed.

Recent studies stressed the prominent role of $CD8^+$ T lymphocytes in the autoimmune pathomechanism. They notably exceed the amount of $CD4^+$ T cells in acute lesions yet target cells and activating antigens remain elusive. A genetic linkage between the human leukocyte antigen gene locus and disease susceptibility was observed. Carrying the *HLA-A*0301* allele or the *HLA-A*0201* allele correlates with a risk factor or protective effect for Multiple Sclerosis susceptibility, respectively. Thus during this thesis two main questions were followed:

1. Which $CD8^+$ T lymphocytes participate in the autoimmune attack on central nervous system tissue and what are their receptors for antigen recognition?
2. How does the expression of HLA-A2 molecules lead to a decreased disease susceptibility?

In the first part, the T cell receptor molecules of potentially disease-related single $CD8^+$ T cells from frozen patient tissue samples were characterized. T lymphocytes were considered disease-related when they either belonged to a clonally expanded T cell population or expressed an activation marker on their cell surface. In a clone-specific approach, the T cell receptor beta chains of pre-analyzed, clonally expanded T cell populations were investigated. Further an unbiased approach independent of pre-analyses was established.

In the second part, antigen recognition of the probably disease-related T cell receptor 2D1 was investigated. This receptor was isolated from a Multiple Sclerosis patient and was known to be activated by a myelin-derived peptide presented on HLA-A3 molecules. In an animal model double-transgenic mice expressing HLA-A3 and the 2D1 T cell receptor developed a Multiple Sclerosis-like disease after immunization with the known peptide. Surprisingly not a single triple-transgenic mouse expressing HLA-A3, the T cell receptor 2D1 and HLA-A2 showed symptoms after immunization. In these mice 2D1 T lymphocytes were shown to be depleted in the thymus.

To characterize HLA-A2-bound peptides which mediate this protective effect a novel technology for unbiased identification of antigenic peptides recognized by human leukocyte antigen class I-restricted T lymphocytes was employed. 28 peptides presented on HLA-A2 molecules were found to be recognized by the T cell receptor 2D1. Those peptides displayed very closely related sequences. Eight possible parent proteins existing in mouse, therefrom even four equally expressed in humans were identified. Finally those putative parent proteins were further characterized and first investigations of antigen processing in different antigen presenting cell lines were performed.

Table of Contents

1 Introduction

1.1 Basics of the Mammalian Immune System

The mammalian immune system is responsible for the integrity of living organisms by protecting them from external pathogens like viruses, bacteria, fungi or multicellular parasites, as well as from harmful alterations of the body's own elements such as tumors (Chaplin 2010). Two main systems work together:

The innate immune defense consists of physical barriers, the complement system and immune cells such as granulocytes, monocytes and natural killer cells. These components recognize common features of many pathogens with genetically coded, invariant receptors. The main purpose is to keep reactions local and to mediate a fast response against common intruders.

The adaptive immune defense evolved in vertebrates and consists of the humoral and the cellular immunity. With highly variable receptors the cells of the adaptive immune system are able to specifically recognize distinct pathogenic structures, so called antigens. Further they provide enhanced protection against reinfection with the same pathogen by establishing immunological memory. B lymphocytes (B cells) express immunoglobulin molecules as antigen receptors on their surface. Following activation, they secrete these receptors as antibodies which neutralize toxins and viruses or mark extracellular pathogens for other immune cells. T lymphocytes (T cells) express immunoglobulin-like molecules as antigen receptors on their surface, the so called T cell receptor (TCR). They react against intracellular pathogens and altered-self structures or control a further immune response by secreting mediators.

1.2 T Lymphocytes

T cells originate from lymphatic precursor cells in the bone marrow and migrate into the thymus where they mature and rearrange their TCRs (Section 1.2.2., p. 3). The majority of T cells express a TCR consisting of an alpha and a beta chain. They are further subdivided according to their co-receptors into CD4 and CD8 expressing T lymphocytes.

$CD4^+$ T cells mainly coordinate the immune response by secreting mediators that attract other immune cells or influence their differentiation (Nakayamada et al., 2012). They recognize antigens in the context of human leukocyte antigen (HLA) class II molecules on specific antigen presenting cells (APC) such as dendritic cells, B lymphocytes or macrophages.

$CD8^+$ T cells mainly serve to eliminate infected or altered-self cells after direct cell contact and the release of granzyme B and perforin or signaling via the fas ligand CD95L (Harty et al., 2000). They recognize antigens in the context of HLA class I molecules that are expressed on all cells in the body containing a nucleus (Section 1.2.3, p. 4).

1.2.1 Structure of the Alpha Beta T Cell Receptor

As $CD8^+$ T lymphocytes are the main subject of this thesis, the structure of TCR molecules is explained regarding the alpha beta TCR complex and CD8 co-receptor (Figure 1, p. 2). The alpha and beta chains of the TCR molecule consist of an amino-terminal extracellular region, a hydrophobic transmembrane domain and a short intracellular carboxy-terminus (Kronenberg et al., 1986). The extracellular regions of both chains are composed of a variable and an immunoglobulin-like constant domain. Antigen recognition happens in the binding groove of both variable domains.

Due to the very short transmembrane region, the TCR dimer needs stabilization and cannot transduce signaling information on its own. These tasks are accomplished by the accessory CD3 complex (Clevers et al., 1988). It consists of epsilon-delta and epsilon-gamma heterodimers and a zeta-zeta homodimer. The first step in TCR signaling (Love and Hayes, 2010) is the phosphorylation of immunoreceptor tyrosine-based activation motifs that are located at the intracellular domains of the CD3 complex. After several steps the nuclear factor of activated T cells (NFAT) regulates the expression of activation-associated genes, such as the interleukin 2 (IL-2) locus.

The co-receptor CD8 may consist of an alpha-alpha homodimer or an alpha-beta heterodimer. CD8 reinforces and multiplies TCR signaling by laterally binding to HLA class I molecules and intracellular signal transduction (Gáspár et al., 2001). CD8 alpha-alpha homodimers are not only expressed on $CD8^+$ T lymphocytes but additionally on $CD4^+$ T lymphocytes, dendritic cells, macrophages and microglial cells of the central nervous system (CNS) (Gangadharan and Cheroutre, 2004).

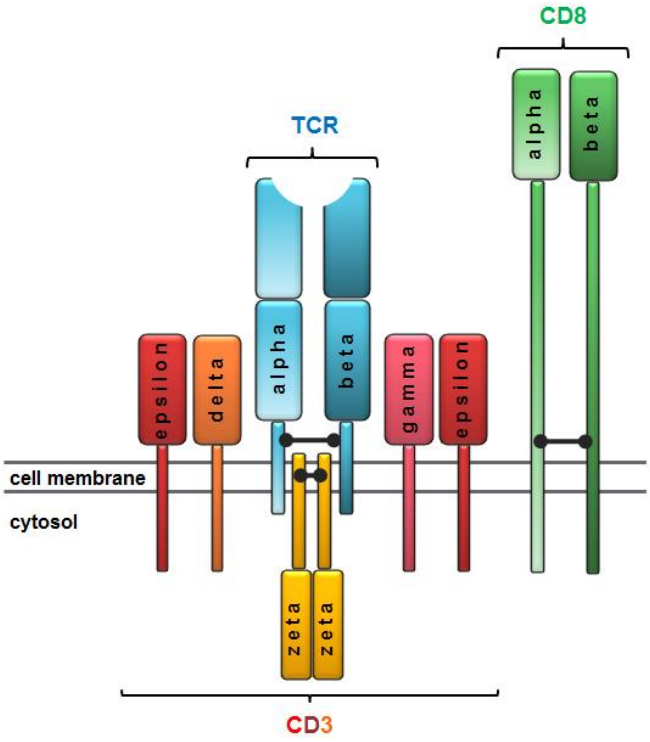

Figure 1: Alpha beta TCR complex.
The chains of the alpha beta TCR dimer (blue) consist of a variable amino-terminal and a constant carboxy-terminal region which ends in a short transmembrane domain. Antigen recognition takes place in the binding groove (white semicircle) at the variable region. The TCR is stabilized by the CD3 complex (red to yellow) which is responsible for signal transduction into the cell after antigen recognition. The co-receptor CD8 (green) may be composed of an alpha-alpha homodimer (not shown) or an alpha-beta heterodimer. Stabilizing disulphide bonds are depicted in black (modified from Backes, 2010).

1.2.2 Generation of the T Cell Receptor Diversity

T lymphocytes must recognize a broad spectrum of antigens. The variety of antigen recognition sites in the binding grooves of the variable domains is generated by somatic recombination of genetic segments. The rearrangements of TCR gene segments happen during T cell development in the thymus. TCR alpha chains consist of a variable (V), a joining (J) and a constant (C) gene segment whereas TCR beta chains contain additionally a diversity (D) segment.

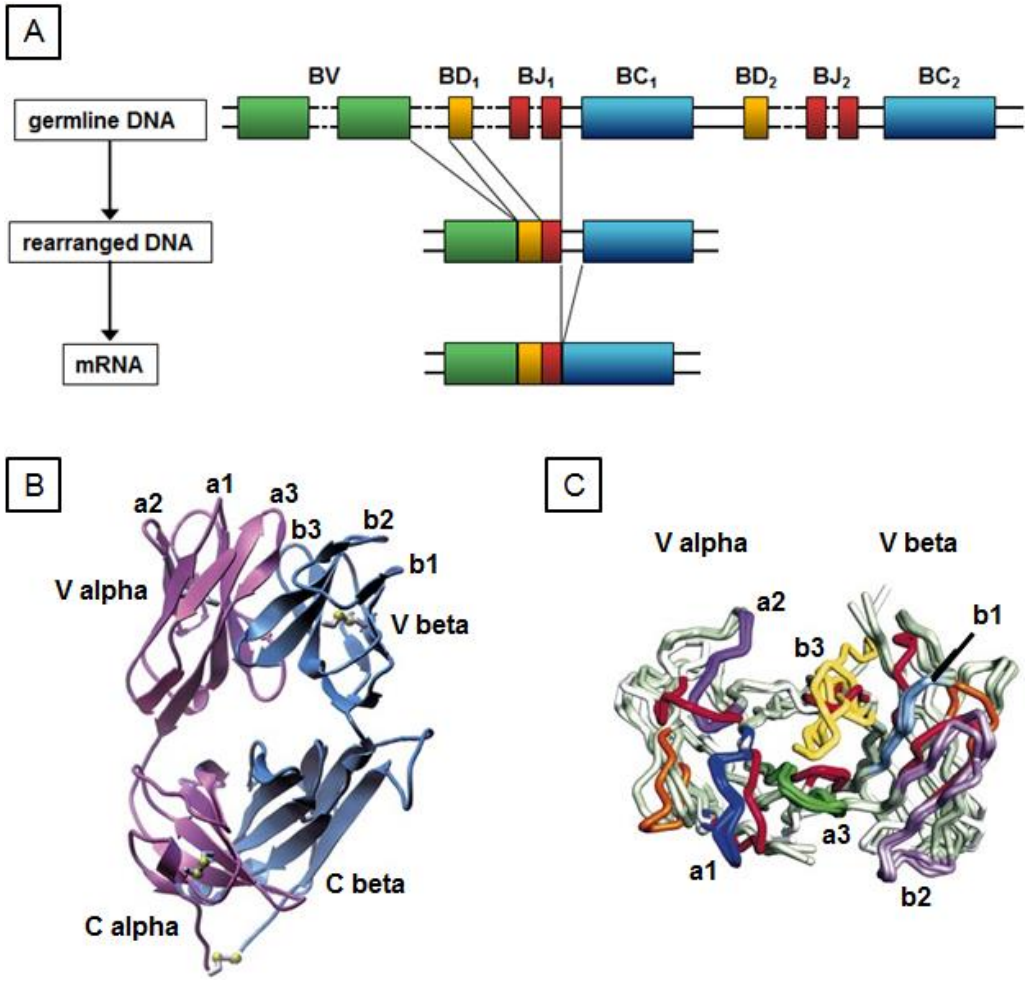

Figure 2: Generation of TCR diversity and crystal structure of an alpha beta TCR.
A: Rearrangement of the TCR beta gene locus. The human TCR beta gene locus consists of 52 V beta (BV, green), 2 D beta (BD, yellow), 13 J beta (BJ, red) and 2 C beta (BC, blue) gene segments. In a first step BV, BD and BJ segments are combined at the DNA level via somatic recombination, then the BC segment is added at the mRNA level via splicing. The TCR alpha gene locus is rearranged the same way but missing D gene segments. It consists of 70 to 80 V alpha (AV), 61 J alpha (AJ) and 1 C alpha (AC) gene segments (Arden et al., 1995; Rowen et al., 1996). **B:** Crystal structure of an alpha-beta TCR. The TCR alpha- (pink) and TCR beta chain (blue) consist each of a variable (V alpha and V beta) and constant (C alpha and C beta) domain. The chains are connected through disulphide bonds (yellow). CDR loops are numbered serially (modified from Murphy et al., 2008). **C:** Top view crystal structure of an alpha-beta TCR. CDR loops of the TCR alpha and beta chain are indicated (modified from Murphy et al., 2008).

First the TCR beta chain is generated by randomly joining a BD with a BV segment and then adding both to a BJ segment. Afterwards the TCR alpha chain is generated by joining an AV and AJ segment. These rearrangements occur on the DNA level. The rearrangements that produce a complete TCR beta chain are shown in Figure 2-A (p. 3) and further described in Krangel (2009). During this somatic

recombination random nucleotides are added or removed at the junctions between the V, D (only in TCR beta chains) and J gene segments. The resulting highly variable nucleotide sequence is called N(D)N. After transcription the V(D)J segments are combined with the C segment via splicing.
The antigen binding site of the variable domains consists at both TCR chains of three complementarity determining regions (CDR) (Figure 2-B and -C, p. 3). The CDR1 and CDR2 lie within the germline-coded V gene segments. However, the CDR3, which is mainly responsible for antigen recognition (Davis et al., 1998), is coded by the highly variable N(D)N sequence.

1.2.3 Antigen Recognition of $CD8^+$ T Lymphocytes

$CD8^+$ T cells with an alpha beta TCR do not recognize antigens in their native state like antibodies do, but recognize a composite ligand of an antigenic peptide bound to self-HLA class I molecules: the peptide:self-HLA complex.
HLA class I molecules consist of two distinct chains (Figure 3-A, p. 5). The alpha chain contains three extracellular domains and a fourth short transmembrane and intracellular domain. It is associated with a shorter non-polymorphic chain, the β_2-microglobulin. The alpha3 domain and the β_2-microglobulin are immunoglobulin-like domains. The alpha1 and alpha2 domains together form the peptide-binding groove. The HLA gene locus is polygenic and highly polymorphic. Each gene locus codes three HLA class I molecules called HLA-A, HLA-B and HLA-C which are co-dominantly expressed on the cell surface (Murphy et al., 2008). According to the IMGT (http://www.ebi.ac.uk/ipd/imgt/hla/stats.html) 1,695 HLA-A, 2,277 HLA-B and 1,321 HLA-C proteins are known to exist in the human population. The polymorphisms are mainly located in the peptide-binding groove which allows presentation of many different peptides (Falk et al., 1991).
HLA class I molecules usually present peptides of 8 to 10 amino acids (AA) in length (Madden et al., 1993) but in some cases bulging and consequently the presentation of peptides with up to 14 AAs in length is possible (Figure 3-D, p. 5; Speir et al., 2001). Peptides presented by one HLA variant usually consist of similar AAs at two or three positions, the anchor residues. The side chains of these AAs insert deep into pockets of the peptide-binding groove. The homepage http://www.syfpeithi.de/home.htm provides a huge database of HLA molecules, their anchor residues and confirmed binding peptides.
The peptides principally originate from intracellular proteins. These proteins are cleaved by the immunoproteasome and transported into the endoplasmatic reticulum where they are loaded onto the HLA class I molecule (Yewdell et al., 2003). $CD8^+$ T lymphocytes are provided degradation products of intracellular pathogens or aberrant self-peptides deriving from for example cancer cells amongst a huge pool of normal self-peptides. Thus, the pathogenic antigen recognition skills of T cells must be very sensitive. Few or even single contacts to pathogenic-peptide:self-HLA class I complexes suffice for T cell activation (Irvine et al., 2002).
Commonly the TCR lies slightly diagonal over the peptide:self-HLA class I complex and interacts with both the HLA molecule and the bound peptide (Figure 3-B and –C, p. 5) (Wang and Reinherz, 2012, Garcia and Adams, 2005). The CDR1 and CDR2 loops of the TCR alpha and beta chains

interact with AAs around the amino-terminus and the carboxy-terminus of the bound peptide respectively. The highly variable CDR3 loops of both TCR chains (Section 1.2.2, p. 3) meet over the central AAs of the bound peptide and mainly contribute to the antigen recognition (Davis et al., 1998). Different recognition patterns are possible when for example the TCR unconventionally interacts sideways with the peptide:HLA complex (Hahn et al., 2005; Sethi et al., 2011).

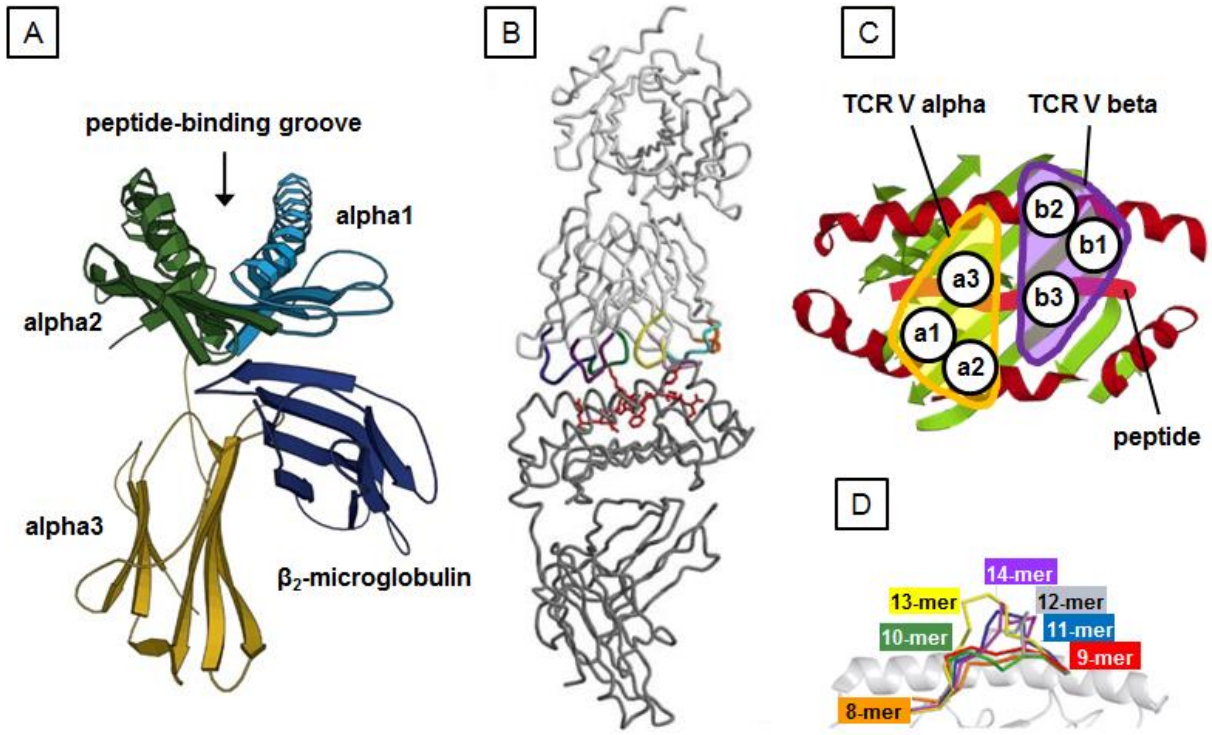

Figure 3: Peptide presentation on HLA class I molecules.
A: Crystal structure of extracellular domains of an HLA class I molecule. Light blue: alpha1 domain, green: alpha2 domain, yellow: alpha3 domain, dark blue: β_2-microglobulin (modified from Murphy et al., 2008). **B:** Crystal structure of a TCR:peptide:self-HLA class I complex. Light gray: TCR, dark gray: HLA class I molecule, red: peptide, dark blue: CDR1 alpha, purple: CDR2 alpha, green: CDR3 alpha, light blue: CDR1 beta, rose: CDR2 beta, yellow: CDR3 beta (modified from Rudolph et al., 2006) **C:** Scheme of interaction in the TCR:peptide:HLA class I complex. CDR loops of TCR alpha and beta chains and peptide are designated (modified from www.iayork.com). **D:** Binding mode of 8- to 14-mer peptides on HLA class I molecules (modified from Sewell, 2012).

1.2.4 T Cell Selection and Development

After successful rearrangement of TCR alpha- and beta-chains (Section 1.2.2, p. 3) T lymphocytes undergo further development in the thymus to ensure the recognition of self-HLA molecules loaded with peptides but to prevent autoreactivity (Griesemer et al., 2010). Thymic cortical epithelial cells can present nearly all possible self-peptides on both, HLA class I and HLA class II molecules (Anderson and Takahama, 2012).

In the first step, the positive selection, T cells only survive when their TCR can interact with self-peptide:self-HLA complexes (Nikolic-Zugic and Bevan, 1990). Here the decision between the $CD4^+$ and the $CD8^+$ T cell lineage happens according to the recognized HLA class. In the second step, the negative selection, T lymphocytes that react too strongly with self-peptide:self-HLA complexes are removed. With these two mechanisms over 95 % of precursor T cells are depleted and only those

which are both self-HLA restricted and self-tolerant enter into the blood and lymphoid system (Huesmann et al., 1991). These T lymphocytes interact at low affinity with self-peptide:self-HLA complexes but at high affinity with foreign antigens loaded onto self-HLA molecules (Morris and Allen, 2012).

Naïve T cells leave the thymus and circulate through the blood and lymphoid system until encountering a pathogenic antigen with their specific TCR. This encounter activates the naïve T cell (Smith-Garvin et al., 2009), which starts to divide and daughter cells maturate into effector cells fulfilling their role in the immune response. Other daughter cells maturate into memory cells that may be reactivated by the same pathogenic structure and then induce a fast, specific immune reaction even years after the first encounter with the antigen (Arens and Schoenberger, 2010).

1.2.5 T Cell Receptor Cross- and Alloreactivity

But one T cell may not only be activated by one specific peptide presented one specific HLA molecule. Crossreactivity describes the ability of T lymphocytes to recognize more than one distinct peptide:HLA ligand. To ensure sufficient efficiency of T cell mediated immunity in humans about 10^{15} distinct antigenic peptides need to be recognized (Davis and Bjorkman, 1988; Mason, 1998). 10^{15} single T lymphocytes would weigh more than 500 kg (Sewell, 2012). Studies have estimated that only about 10^{8} different TCRs exist in the human naïve T cell pool (Arstila et al., 1999). Consistently Wooldridge et al. (2012) demonstrated that one single $CD8^{+}$ T lymphocyte may be activated by more than 1.3 x 10^{6} different 10-mer peptides in the context of one distinct HLA molecule.

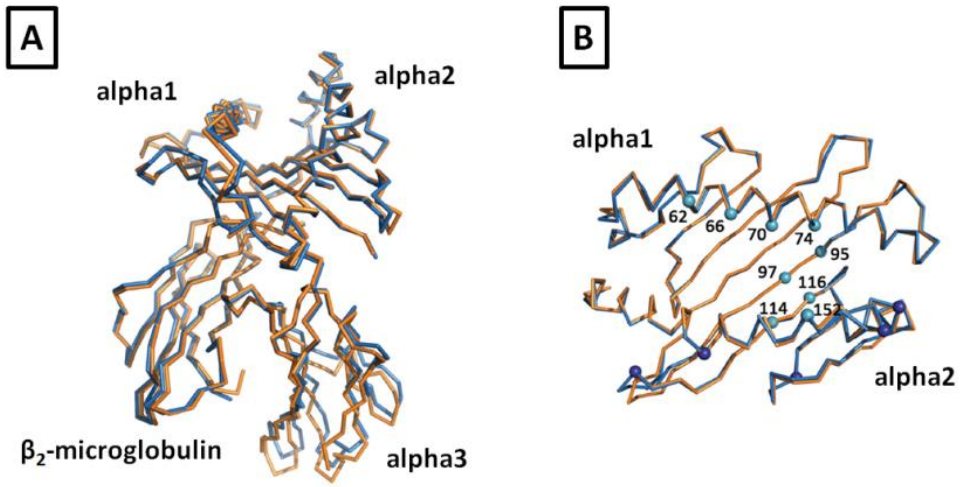

Figure 4: Structural comparison of HLA-A2 and HLA-A3 molecules.
Structures of HLA-A2 (orange) and HLA-A3 (blue) molecules are overlaid, alpha1, alpha2 and alpha3 domains as well as the β_2-microglobulin are denoted. HLA-A2 and HLA-A3 are over all structurally very equivalent (**A**), differing AAs in the peptide-binding groove are labeled as cyan or dark blue dots (**B**). (Modified from McMahon et al., 2011.)

Alloreactivity describes the ability of T lymphocytes to be activated by peptide:non-self-HLA complexes (Felix and Allen, 2007) which were not encountered during positive and negative selection in the thymus (Section 1.2.4, p. 5). This phenomenon occurs mainly in patients receiving a bone

marrow transplant that does not completely match the recipient's HLA repertoire. Donor T cells recognize peptides presented on recipient cells resulting in graft-versus-host disease (MacDonald et al, 2013). In solid organ transplantation recipient T cells recognize peptides presented on donor cells leading to graft rejection (Ibrahim et al., 1995).

The molecular mechanism of alloreactivity is widely discussed (D'Orsogna et al., 2013; Colf et al., 2007). One possible reason might be that most HLA alleles code for HLA molecules with only few different AAs. The resulting HLA molecules might for example differ in the peptide-binding groove but present very similar surfaces to the TCR like the HLA-A2 and HLA-A3 molecules (Figure 4, p. 6; McMahon et al., 2011). Thus the TCR that was selected in the thymus to interact with one specific type of HLA molecule can equally interact with the foreign HLA molecule but encounters a completely different set of bound peptides.

1.3 Autoimmunity

Unfortunately, during the generation of the adaptive receptor repertoire (Section 1.2.2, p. 3) reactivity against self-structures may arise. Despite many mechanisms eliminating or inactivating autoreactive immune cells like negative selection of T lymphocytes in the thymus (Section 1.2, p. 1), still some may escape and cause autoimmune diseases (Wekerle, 1992). Maybe selective pressure to establish an effective immune response against pathogenic structures causes self-tolerance inducing mechanisms to be limited and prone to failure.

Autoimmune diseases are generally characterized by the attack of adaptive immune cells against healthy structures of the body without previous demonstrable pathogenic infection. Autoimmune diseases may be classified into those that affect a single organ, such as type 1 diabetes or myositis, and those that affect tissues throughout the body such as systemic lupus erythematosus. In a third group of diseases such as multiple sclerosis (MS), it is still unknown whether autoimmunity or other pathological processes are the causation for illness.

The mechanisms causing autoimmune diseases are still largely unidentified. Environmental factors, molecular mimicry as well as genetic predisposition are discussed (Cusick et al., 2012; Rose and Bell, 2012).

1.4 Multiple Sclerosis

MS is most probably an autoimmune inflammatory disease of the CNS and one of the most common neurological diseases in young adults. Worldwide approximately 2.5 million people are affected. MS is more prevalent in females and gender likewise affects progression as well as treatment (Greer and McCombe, 2011). In the temperate zones of the northern and southern hemisphere MS prevalence exceeds that of equatorial regions. Environmental influences seem to play a crucial role as relocation to areas with less risk at young age reduces the risk of MS (Ebers, 2008) but also genetic predispositions may contribute to an elevated or reduced disease risk (Section 1.4.3, p. 8). The course of disease is not predictable for individuals and only symptomatic treatment is available. Recently

intense research rendered more specific treatment possible but still no cure is available (Ehling et al., 2010).

1.4.1 Pathomechanism of Multiple Sclerosis

During the course of disease, demyelination of neurons and axonal loss occur in temporal and spatial resolution in multiple areas of the brain and spinal cord (Brück and Stadelmann, 2003). This impairment manifests in neurological symptoms. The course of disease varies between individuals (Lucchinetti et al., 2000). Mostly patients first show relapse remitting MS with symptoms recovering after the relapse. Later the disease changes to secondary progressive MS leading to progressive accumulation of disability (Compston and Coles, 2008; Miller, 2012). Histologically four types of MS can be distinguished (Hu and Lucchinetti, 2009), yet the main characteristics are inflammatory plaques (lesions) and formation of scars in the CNS (Frohmann et al., 2006).

Previous findings indicate an autoimmune-mediated pathomechanism of MS. However, the inducing incident is not yet illuminated. MS is discussed as a latent or persistent viral infection, as a neurodegenerative and as an autoimmune disease (Owens et al., 2011; Trapp and Nave, 2008; Hohlfeld and Wekerle, 2001).

1.4.2 T Lymphocytes in Multiple Sclerosis

Despite varying inflammatory infiltrates, in almost all patients T lymphocytes, B cells and macrophages but also in lower amounts antibodies and complement deposits can be detected (Booss et al., 1983; Prineas and Wright, 1978; Lassmann et al., 2001). It was supposed that autoreactive $CD4^+$ T cells enter the CNS via the distorted blood brain barrier and provoke an inflammatory reaction (Noseworthy et al., 2000). The release of cytokines may harm the oligodendrocytes. Unfortunately patients who are treated with antibodies against CD4 did not show significant recovery even though depletion was successful (van Oosten et al., 1997).

Recent studies stressed the prominent role of $CD8^+$ T cells which probably harm the oligodendrocytes and neurons through direct cytotoxicity and release of cytokines (Mars et al., 2010; Friese and Fugger, 2009). In acute and chronic lesions the amount of $CD8^+$ T lymphocytes exceeds the number of $CD4^+$ T cells (Hauser et al., 1986; Babbe et al., 2000; Junker et al., 2007). Moreover mouse models studying the pathogenic role of $CD8^+$ T cells better reflect many aspects of MS than mouse models concentrating on $CD4^+$ T lymphocytes (Goverman et al., 2005; Mars et al., 2010).

1.4.3 HLA Class I-Related Genetic Predisposition for Multiple Sclerosis

Disease prevalence increases within family members of MS patients and the concordance rate in monozygotic twins is higher than in dizygotic twins (Baranzini et al., 2010; Dyment et al. 2004). According to the IMSGC and WTCCC2 genetic predisposition may play a key role in MS disease susceptibility. Many analyses have been performed and in 2011 the latest results of genome-wide association studies for MS were published. Besides many different gene loci, primarily different HLA

alleles are linked to disease susceptibility (http://www.well.ox.ac.uk/wtccc2/ms). Notably a risk factor is carrying the *HLA-A*0301* allele and a protective effect correlates with carrying the *HLA-A*0201* allele (Silva et al., 2009).

Honma et al. (1997) isolated an autoreactive $CD8^+$ T lymphocyte from an MS patient carrying both, the alleles *HLA-A*0201* and *HLA-A*0301*. This T cell clone was named 2D1 and proven to recognize the myelin sheath derived nine AA residues 45 to 53 of the proteolipid protein 1 (PLP) presented on HLA-A3. Friese et al. (2008) generated double-transgenic humanized mice expressing HLA-A3 and the TCR 2D1 as well as triple-transgenic humanized mice expressing HLA-A3, the TCR 2D1 and HLA-A2. 4 % of the double-transgenic mice showed mild spontaneous motor deficits and 25 % developed an MS-like disease after immunization with PLP_{45-53} peptide. Strikingly not a single triple-transgenic mouse showed symptoms even after immunization. Further investigations revealed negative selection of 2D1 T cells in the thymus which indicates cross-recognition of unknown peptide(s) presented on HLA-A2 molecules. As HLA-A2 and HLA-A3 molecules display a very similar surface to TCR molecules but present different peptides (Section 1.2.5, p. 6) this theory seems very likely. So far neither the cross-recognition of HLA-A2 molecules nor any other recognized peptide than PLP_{45-53} could be determined.

1.5 Current Knowledge Regarding the Characterization of Molecular Targets of Disease-Related T Lymphocytes

1.5.1 Identification of Disease-Related TCR Molecules

To better understand T cell mediated autoimmunity in MS the characterization of underlying pathogenic and possibly also protective mechanisms is crucial. In early studies the germline TCR beta chain repertoire was analyzed by restriction fragment length polymorphisms (Biddison et al., 1989) and reverse transcription of RNA from frozen MS brain tissue (Wucherpfennig et al., 1992). These methods were limited as they could not distinguish TCR sequences of disease-related T lymphocytes from the oligoclonal background.

Disease-related T cells should meet at least one of the following three criteria: First, the T lymphocyte carries a TCR belonging to a clonally expanded population, as T cells start to divide and proliferate upon activation. Second, the T lymphocyte expresses activation markers. Third, the T lymphocyte lies in direct contact with the target cell.

CDR3 spectratyping allows the identification of TCR beta chain sequences from clonally expanded T cell populations (Pannetier et al., 1995; Matsumoto et al., 2003). The development of monoclonal antibodies that recognize several TCR beta chains allows the staining of potentially disease-related T lymphocytes in tissue samples. Combining those two techniques, single expanded T cell clones around muscle fibers of patients with polymyositis were stained and isolated by laser microdissection. Subsequently clone-specific PCRs verified the sequences of TCR beta chains. Following multiplex PCRs revealed the sequences of corresponding TCR alpha chains (Seitz et al., 2006). This “clone-specific approach” is employed on MS brain tissue in this study.

As only a limited number of antibodies against TCR beta chains are available, the "clone-specific approach" is complemented by an "unbiased approach". Here brain tissue is double stained for the T cell co-receptor CD8 and the activation marker CD134 (formerly known as OX40). Activated T lymphocytes are isolated by laser microdissection. As the TCR beta chain is not known beforehand, an unbiased set of primers is used to identify its sequence (Kim et al., 2012). The corresponding TCR alpha chain is then determined as mentioned above.
Figure 5 (p. 10) summarizes the steps of the "clone-specific approach" and the "unbiased approach".

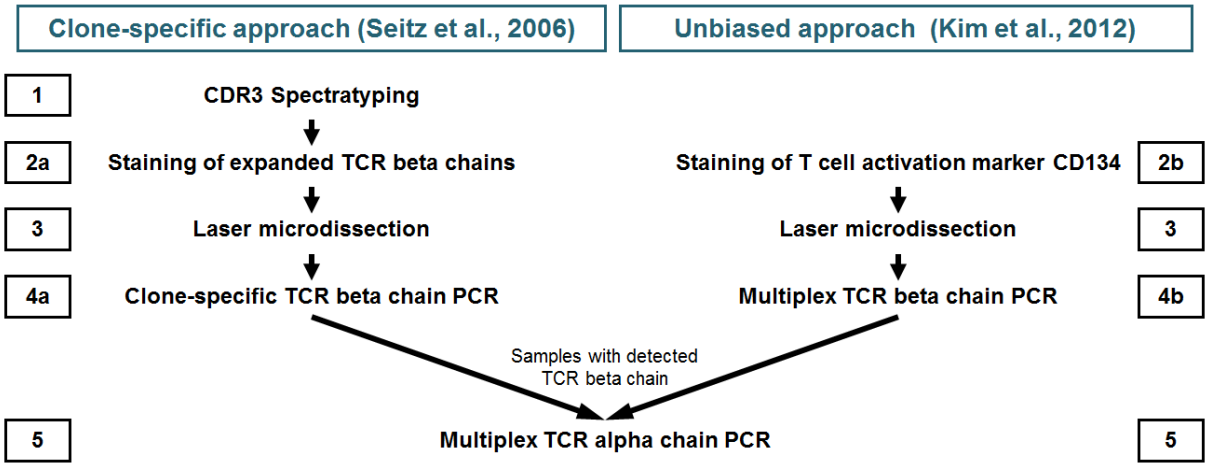

Figure 5: Workflow of the identification of paired TCR alpha- and beta-chains from disease-related T lymphocytes. Putatively autoaggressive T cells are either determined according to clonal expansion via CDR3 spectratyping (step 1) and staining of TCR beta chains (step 2a) or according to the expression of the activation marker CD134 (step 2b). Single cells are isolated by laser microdissection (step 3). In the "clone-specific approach" the TCR beta chain sequence is confirmed by a clone-specific PCR (step 4a), in the "unbiased approach" the TCR beta chain sequence is identified by multiplex PCR (step 4b). Multiplex alpha chain PCR (step 5) is performed on all samples that revealed a TCR beta chain (modified from Backes, 2010).

1.5.2 Antigen Identification of Putatively Disease-Related T Lymphocytes

In order to elucidate autoreactive mechanisms, antigen(-s) of putatively disease-related T cell receptors (Section 1.5.1, p. 9) need to be determined. Previous studies implicated candidate autoantigens like myelin basic protein (Lennon et al., 1970) or myelin oligodendrocyte protein (MOG) in animal models for MS (Schluesener et al., 1987). Additionally the Epstein-Barr virus was associated with MS (Sumaya et al., 1980; Serafini et al., 2010). After infection, immune cells that recognize the infectious agent might cross-react with epitopes in the healthy CNS (molecular mimicry) leading to an autoimmune reaction (Lucas et al., 2011).
Investigating the recognition of candidate antigenic proteins by certain disease-related TCRs is limited to rare cases where HLA-matched APCs are available. Only those cells can uptake and process the protein leading to proper antigen presentation. As an alternative van der Bruggen et al. (2007) transfected patient-derived full-length cDNA expression libraries into autologous APCs. Those APCs were scanned with patient-derived T lymphocytes. The major drawback of this method is the limited ability of APCs to correctly process antigens *in vitro*. Further peptide-based screening approaches were independent of antigen processing (Mohme et al., 2013; Nino-Vasquez et al., 2004; Sospedra et

al., 2003) but not all types of peptides may reach the HLA molecules on APC. For example hydrophobic candidates might accumulate and precipitate in aqueous cell culture media or disappear into cell membranes.

Siewert et al. (2012) solved these obstacles by stably transfecting COS-7 cells with plasmids encoding the patient's HLA class I alleles. Such COS-7 cells now can serve as APCs. In a next step those cells are transfected with plasmids coding for short peptides of random sequences but defined lengths, so called plasmid-encoded combinatorial peptide libraries (PECP libraries). In parallel T hybridoma cells are generated expressing the putatively disease-related TCR, human CD8 and sGFP under the control of the NFAT promoter. During co-culture T hybridoma cells that interact with an APC presenting an antigenic peptide are activated and fluoresce green. Now the underlying APC can be isolated under a fluorescence microscope. After several steps the antigen-coding plasmid can be determined. Figure 6 (p. 11) gives a schematic overview over this method, for detailed experimental procedures consult Section 2.8.4 (p. 60) and Figure 9 (p. 61).

With this novel technique one activating antigenic peptide out of a pool of millions can be detected *in vitro* circumventing the problems of defined antigen-processing in APCs. Consequentially for subsequent analysis of probable parent proteins no information regarding antigen-processing is available.

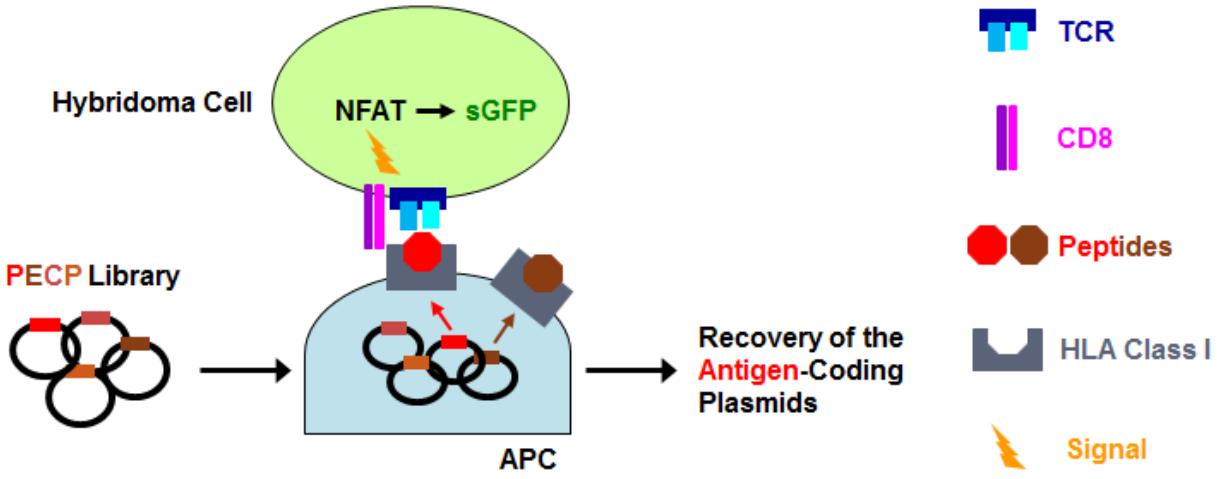

Figure 6: Identification of antigens from putatively disease-related TCR molecules.
As APC adherent COS-7 cells are stably transfected with plasmids coding for human HLA class I molecules and transiently transfected with PECP library-coding plasmids. As detector TCR-deficient mouse T hybridoma cells 58α^-/β^- are stably transfected with plasmids coding for a human putatively disease-related TCR and human CD8 as well as a plasmid coding for sGFP under the control of the NFAT promoter. When an APC presents a potentially autoantigen the T hybridoma cells above get activated and fluoresce green. All plasmids inside the APC are then purified and the potentially autoantigen can be identified by PCR and serial dilution experiments (modified from Backes, 2010).

1.6 Objective

Recent data have stressed the prominent role of $CD8^+$ T lymphocytes in the autoimmune pathomechanism of MS, yet the underlying mechanisms still remains elusive. Many of these results were based on immunohistochemistry and TCR repertoire studies. Moreover it is known for long that a genetic linkage between the HLA gene locus and disease susceptibility exists: Carrying the *HLA-A*0301* allele or the *HLA-A*0201* allele correlates with a risk factor or protective effect for disease susceptibility respectively. During this thesis therefore two main questions will be investigated:

1. Which $CD8^+$ T lymphocytes participate in the autoimmune attack on CNS tissue and what are their receptors for antigen recognition?
2. How does the expression of HLA-A2 lead to a decreased disease susceptibility?

To answer those questions first putatively disease-related single $CD8^+$ T cells will be isolated from frozen brain tissue of an MS patient by laser microdissection. Employing the clone-specific and the unbiased PCR techniques, their TCR molecules will be analyzed. In parallel, these PCR methods will be further optimized.
In the second part, antigen recognition of the probably disease-related TCR 2D1 will be investigated. It was shown to recognize the myelin-derived peptide PLP_{45-53} presented on HLA-A3 molecules. In a model system double-transgenic mice expressing HLA-A3 and the TCR 2D1 developed an MS-like disease after immunization with the PLP_{45-53} peptide. Surprisingly, when triple-transgenic mice expressing HLA-A3, the TCR 2D1 and HLA-A2 were created, not a single animal showed symptoms after immunization and 2D1 T lymphocytes were already depleted in the thymus of these mice.
An obvious question therefore is, which specific antigen(s) TCR 2Dq might recognize in the context of the protective HLA-A2 molecules. Therefore the antigen recognition properties of the TCR 2D1 will be characterized. To this end a novel technology for unbiased identification of antigenic peptides recognized by HLA class I-restricted T lymphocytes will be used. Then peptides presented on HLA-A2 molecules activating the TCR 2D1 will be investigated and probable parent proteins will be identified and further characterized.

2 Materials and Methods

2.1 Materials

2.1.1 Devices

Cell Disruptor	Sonifier 450	Branson (Danbury, USA)
Centrifuges	Avanti® J-26 XP	Beckman Coulter (Krefeld, D)
	Centrifuge 5417 R	Eppendorf (Hamburg, D)
	Heraeus® Megafuge 1.0 R	Thermo Fisher Scientific (Schwerte, D)
	OPTIMA XE90 Ultracentrifuge	Beckman Coulter
	Sprout Mini-centrifuge	Biozym (Hess, Oldendorf, D)
Cryotom	LEICA CM 3050	Leica Microsystems (Wetzlar, D)
Electroporator	Gene Pulser	Bio-Rad
Flow Cytometer	FACS Calibur	Becton Dickinson (Heidelberg, D)
	FACSVantage SE	Becton Dickinson
	FACSVerse	Becton Dickinson
Gel Electrophoresis	Power Supply LKB ECPS 3000/150	Pharmacia Biotech (Munich, D)
	Gel camera Universal Hood	Bio-Rad (Munich, D)
	Gel Doc XR	Bio-Rad
Microscopes and Accessories	Microscope Axioplan 2	Zeiss (Oberkochen, D)
	Microscope Axiovert 200M	Zeiss
	Robo-Mover	P.A.L.M. Microlaser Technologies (Bernried, D)
	Microinjector CellTram Vario	Eppendorf
	Micromanipulator LN25 Mini	Luigs und Neumann (Ratingen, D)
PCR Cyclers	GeneAmp PCR System 9600	Perkin Elmer
	T3 Thermocycler	Biometra (Göttingen, D)
	7900HT Fast Real-Time PCR System	Applied Biosystems (Foster City, USA)
Spectrophotometers	Nanodrop ND-1000	Thermo Fisher Scientific
	UV-VISIBLE Recording Spectrophotometer	Shimadzu (Duisburg, D)
	VICTOR² 1420 Multilabel Counter	Perkin Elmer (Wellesley, USA)
RNA Quality Analysis	2100 Bioanalyzer	Agilent (Santa Clara, USA)
Water Preparation	Milli Q Advantage	Millipore (Schwalbach, D)

2.1.2 Consumables and Chemicals

Consumables like pipet tips, reaction tubes, cell culture material and centrifugation tubes were purchased from Biozym, Eppendorf and Becton Dickinson. If necessary special sterile pipet tips and reaction tubes made of polypropylene from Biozym and Eppendorf were used to minimize adsorption of nucleic acids and proteins. Cell culture dishes were obtained from the companies BD Falcon (Heidelberg, D), Nunc (Langenselbold, D) and Corning (Wiesbaden, D). Chemicals were generally purchased from Merck (Darmstadt, D) or Sigma-Aldrich (St. Louis, USA).

2.1.3 Kits and Specific Reagents

Table 1: Kits and specific reagents.

Product	Company	Application
AatII Restriction Enzyme (20,000 U/mL)	New England Biolabs (Frankfurt a. M., D)	DNA digestion
AscI Restriction Enzyme (10,000 U/mL)	New England Biolabs	DNA digestion
BamHI-HF Restriction Enzyme (20,000 U/mL)	New England Biolabs	DNA digestion
BirA500 Biotin-Protein Ligase	Avidity (Aurora, USA)	protein biotinylation
Cut Smart™ Buffer (10x)	New England Biolabs	DNA digestion
Complete Protease Inhibitors	Roche (Mannheim, D)	protein experiments
dNTP (10 mM each)	Qiagen (Hilden, D)	PCR
Dynabeads® Protein G	Life Technologies (Oslo, N)	coupling of antibodies
Easy Pure® DNA-Purification Kit	Biozym	DNA purification from agarose gels
EB Buffer	Qiagen	DNA experiments
EcoRI-HF Restriction Enzyme (20.000 U/mL)	New England Biolabs	DNA digestion
FuGENE® HD Transfection Reagent	Promega (Madison, USA)	plasmid transfection in eukaryotic cells
Full Range Rainbow™ Recombinant Protein Molecular Weight Marker	Sigma-Aldrich	SDS-PAGE
Glycogen (20 mg/mL)	Roche	precipitation of nucleic acids
HiSpeed Plasmid Maxi Kit	Qiagen	library preparation
iProof™ High-Fidelity Master Mix (2x)	Bio-Rad	plasmid recovery PCR
MiniElute Gel Extraction Kit	Qiagen	DNA purification from agarose gels
NEB BSA (100x)	New England Biolabs	DNA digestion
NEB Buffer 4 (10x)	New England Biolabs	DNA digestion
NotI-HF Restriction Enzyme (20,000 U/mL)	New England Biolabs	DNA digestion
One-Step-RT-PCR-Kit	Qiagen	single cell PCR
pcDNA3.1™Directional TOPO® Expression Kit	Invitrogen (Karlsruhe, D)	cloning of PCR products
PCR Buffer (10x)	Roche	PCR
Pellet Paint® Coprecipitant	Novagen EMD Chemicals, San Diego (USA)	DNA precipitation
Pierce® BCA Protein Assay Kit	Thermo Scientific (Rockford, USA)	determination of protein concentration
Protector RNase Inhibitor	Roche	single cell isolation
QIAprep Spin Miniprep Kit	Qiagen	plasmid isolation
QIAquick® Gel Extraction Kit	Qiagen	DNA purification from agarose gels
QIAquick® PCR-Purification Kit	Qiagen	purification of PCR-products
Random Primers	Invitrogen	RT-PCR
Rapid DNA Dephos & Ligation Kit	Roche	DNA Dephosphorylation
RNA 6000 Pico Assay Reagent Kit	Agilent	quality analysis of RNA
RNase OUT™ Ribonuclease Inhibitor	Invitrogen	PCR
SalI-HF Restriction Enzyme (20,000 U/mL)	New England Biolabs	DNA digestion
See Blue® Plus 2 Prestained Standard	Life Technologies	SDS-PAGE
Sodium Acetate pH 5.2 (3 M)	Novagen	DNA precipitation
SuperScript® III Reverse Transcriptase Kit	Invitrogen	RT-PCR

Product	Company	Application
T4 Ligase (1 U/µL)	Invitrogen	DNA ligation
T4 Ligase Buffer (5x)	Invitrogen	DNA ligation
Taq-DNA-Polymerase (5 U/µL)	Roche	PCR
TaqMan® Gene Expression Master Mix	Applied Biosystems	qPCR
ToPro®-3 Iodide 642/661 (1 mM)	Invitrogen	FACS analysis
Wide Range Sigma Marker™	Sigma-Aldrich	SDS-PAGE

2.1.4 Buffers, Solutions and Media

Table 2: Buffers and solutions.

Name	Reagents	
3x reducing SDS loading buffer	0,15 M	Tris-HCl pH 6,8
	15 % (w/v)	Sodium dodecyl sulfate (SDS)
	45 % (v/v)	Glycerine
	6 % (v/v)	β mercaptoethanol
	0.01 % (w/v)	Bromphenol blue
		H_2O
5x SDS loading buffer	0.2 M	Tris-HCl pH 6.8
	7.5 % (w/v)	SDS
	20 % (v/v)	Glycerine
	0.02 % (w/v)	Bromphenol blue
		H_2O
6x DNA loading buffer	50 % (v/v)	Glycerine
	0.02 % (m/v)	Bromphenol blue
	0.02 % (m/v)	Xylenblue
	10 mM	Tris-HCl, pH 7.5
		H_2O
Anode buffer	50 mM	Boric acid
	20 % (v/v)	Methanol
		H_2O (pH 9.0)
Biotinylation buffer	100 mM	Tris-HCL, pH 7.5
	200 mM	NaCl
	5 mM	$MgCl_2$
	0.2 mM	Phenylmethanesulfonyl fluoride (PMSF) in 2-propanol
		H_2O
Cathode buffer	50 mM	Boric acid
	5 % (v/v)	Methanol
		H_2O (pH 9.0)
ConA 4B binding buffer	1 % (v/v)	IGEPAL
	20 mM	Tris-HCl, pH 7.4
	0.5 M	NaCl
	1 mM	$MnCl_2 \cdot 4\ H_2O$
	1 mM	$CaCl_2$
		H_2O
ConA 4B elution buffer	1 % (v/v)	IGEPAL
	20 mM	Tris-HCl, pH 7.4
	0.5 M	NaCl
	0.3 M	Methyl-α-D-mannopyranoside
		H_2O

Name	Reagents	
ConA 4B lysis buffer	1 % (v/v)	IGEPAL
	0.1 mM	PMSF in 2-propanol
		PBS
Coomassie® staining solution	0.1 % (w/v)	Coomassie® Brilliant-Blue R-250
	40 % (v/v)	Methanol
	10 % (v/v)	Acidic acid
		H_2O
DEPC treated water	Dissolve 0.1 % diethylpyrocarbonate (DEPC) in H_2O, incubate at room temperature over night, autoclave.	
Destaining solution	40 % (v/v)	Methanol
	10 % (v/v)	Acidic acid
		H_2O
Dynabead conjugation buffer	20 mM	NaH_2PO_4
	0.15 M	NaCl
		H_2O (pH 8.6)
ECL-A	0.25 % (w/v)	Luminol
	1 M	Tris-HCL, pH 8.6
		H_2O
ECL-B	0.11 % (w/v)	Para-hydroxycoumaric acid
		Dimethyl sulfoxide (DMSO)
Folding buffer	100 mM	Tris-HCl (pH 8.0)
	0.4 M	L-arginine
	2 mM	EDTA
		H_2O
IB detergent buffer	0.2 M	NaCl
	1 % (w/v)	Sodium deoxycholate
	1 %(v7v)	IGEPAL
	20 mM	Tris-HCl, pH 7.5
	2 mM	EDTA
		H_2O
IB lysis buffer	50 mM	Tris-HCl, pH 8.0
	25 % (w/v)	Sucrose
	1 mM	EDTA
		H_2O
IB wash buffer	0.5 % (v/v)	Triton X-100
	1 mM	EDTA
		H_2O
Injection buffer	3 mM	Guanidine HCl
	10 mM	Sodium acetate
	10 mM	EDTA
		H_2O (pH 4.2)
Lentil lectin elution buffer	2 mM	Dodecylmaltoside
	20 mM	Tris-HCl, pH 7.4
	0.5 M	NaCl
	0.3 M	Methyl-α-D-mannopyranisode
		H_2O
Lentil lectin equilibration buffer	20 mM	Tris-HCl, pH 7.4
	0.5 M	NaCl
	0.1 mM	PMSF in 2-propanol
	1 mM	$MnCl_2 \cdot 4\ H_2O$
	1 mM	$CaCl_2$
		H_2O

Name	Reagents	
Lentil lectin lysis buffer	20 mM	Tris-HCl, pH 7.4
	0.5 M	NaCl
	0.1 mM	PMSF in 2-propanol
	2 mM	Dodecylmaltoside
	1 mM	$MnCl_2 \cdot 4\ H_2O$
	1 mM	$CaCl_2$
		H_2O
Lentil lectin wash buffer	20 mM	Tris-HCl, pH 7.4
	0.5 M	NaCl
	2 mM	Dodecylmaltoside
	1 mM	$MnCl_2 \cdot 4\ H_2O$
	1 mM	$CaCl_2$
		H_2O
PBS	150 mM	NaCl
	8.4 mM	Na_2HPO_4
	2 mM	NaH_2PO_4
		H_2O
RIPA buffer	150 mM	NaCl
	1 % (v/v)	IGEPAL
	0.5 % (v/v)	Deoxycholic acid
	50 mM	Tris-HCl pH 8.0
	0.1 % (v/v)	SDS
		H_2O
SDS running buffer	0.1 % (w/v)	SDS
	24 mM	Tris
	192 mM	Glycine
		H_2O
TBE	90 mM	Tris-HCl pH 8.0
	90 mM	Boric acid
	2 mM	EDTA
		H_2O
Tryphanblue solution	0.1 % (w/v)	Tryphanblue
		PBS
Urea elution buffer	6 M	Urea
	50 mM	$NaH_2PO_4 \cdot H_2O$
	300 mM	NaCl
	250 mM	Imidazol
		H_2O (pH 8.0)
Urea lysis buffer	6 M	Urea
	50 mM	$NaH_2PO_4 \cdot H_2O$
	300 mM	NaCl
	10 mM	Imidazol
		H_2O (pH 8.0)
Urea solution	25 mM	MES
	8 M	Urea
	10 mM	EDTA
	0.1 mM	DTT
		H_2O
Urea wash buffer	6 M	Urea
	50 mM	$NaH_2PO_4 \cdot H_2O$
	300 mM	NaCl
	20 mM	Imidazol
		H_2O (pH 8.0)

Name	Reagents	
Western Blot blocking buffer	0.05 % (v/v) 5 % (w/v)	Tween-20 Blotting Grade Blocker Non-Fat Dry Milk (Bio-Rad) PBS

Table 3: Media for pro- and eukaryotic cell culture.

Name	Reagents		Company
FACS buffer	1 % (v/v)	Fetal calf serum (FCS) PBS	Invitrogen
Freezing medium	10 % (v/v)	DMSO FCS	 Invitrogen
Luria Bertani medium (with ampicillin: LB^{amp})	0.1 % (w/v) 0.05 % (w/v) 0.1 % (w/v) (100 µg/mL 	Bacto-Trypton Yeast extract NaCl Ampicillin) H_2O	Becton Dickinson Becton Dickinson
RPMI/complete	10 % (v/v) 100 U/mL 100 µg/mL 1x 1 mM	FCS Penicillin Streptomycin MEM non-essential amino acids MEM sodium pyruvate RPMI 1640 + L-Glutamine	Biochrom AG (Berlin, D) Invitrogen Invitrogen Invitrogen Invitrogen Invitrogen

2.1.5 Primers

All primers were purchased in a concentration of 100 pmol/µL and HPLC purified from Metabion (Martinsried, D). Primers designated with "for"(ward) elongate the coding strand and primers designated with "rev"(erse) elongate the non-coding strand of DNA. The appendages "out" or "in" refer to the position of primers in nested PCRs.

Table 4: Primers employed for RT-PCR of laser-captured single cells.

Name	Sequence
Cα-out	5′-GCA GAC AGA CTT GTC ACT GG-3′
Cα-RT-imp	5′-GCC ACA GCA CTG TTG C-3′
Cβ-out	5′-TGG TCG GGG WAG AAG CCT GTG-3′
Cβ-RT-2	5′-GWA GAA GCC TGT GGC C-3′

Table 5: Primers employed for clone specific amplification of $BV13S1^{+}BJ2.3^{+}$ and $BV22^{+}BJ2.1^{+}$ TCR sequences.

Name	Sequence
Cβ-mid1	5′-GTG GCC TTT TGG GTG TGG-3′
Cβ-mid2	5′-GGT GTG GGA GAT CTC TGC-3′
Cβ-in	5′-TCT GAT GGC TCA AAC ACA GC-3′
BV13S1-BJ2.3_for1	5′-AGG CTG ATT CAT TAC TCA GTT GG-3′
BV13S1-BJ2.3_rev1	5′-CGA GCA CTG TCA GCC GGG TGC-3′
BV13S1-BJ2.3_for2	5′-GTG CTG GTA TCA CTG ACC AAG G-3′
BV13S1-BJ2.3_rev2	5′-GTG CCT GGG CCA AAA TAC TGC-3′
BV13S1-BJ2.3_for3	5′-GTC TCC AGA TCA ACC ACA GAG G-3′
BV13S1-BJ2.3_rev3	5′-CCA AAA TAC TGC GTA TCT GCT CC-3′

Name	Sequence
BV13S1-BJ2.3_for1-new	5′-CTG ATT CAT TAC TCA GTT GG-3′
BV13S1-BJ2.3_rev1-new	5′-CAC TGT CAG CCG GGT GC-3′
BV13S1-BJ2.3_for2-new	5′-CTG GTA TCA CTG ACC AAG G-3′
BV13S1-BJ2.3_rev2-new	5′-CCT GGG CCA AAA TAC TGC-3′
BV13S1-BJ2.3_for3-new	5′-ATC AAC CAC AGA GGA TTT CC-3′
BV13S1-BJ2.3_rev3-new	5′-AAT ACT GCG TAT CTG CTC C-3′
BV13S1-for1	5′-TCC TGG TAT CGA CAA GAC C-3′
BV13S1-for2	5′-GAT TCA TTA CTC AGT TGG TGC-3′
BV13S1-for3	5′-ACT GAC CAA GGA GAA GTC C-3′
FE13S1-2.3-rev3	5′-AAA TAC TGC GTA TCT GCT CC-3′
BV22-BJ2.1_for1	5′-CTA TTG GTA CAG ACA AAT CTT GG-3′
BV22-BJ2.1_rev1	5′-CTA GCA CGG TGA GCC GTG TCC-3′
BV22-BJ2.1_for2	5′-AGA AGT CTG AAA TAT TCG ATG ATC-3′
BV22-BJ2.1_rev2	5′-AGC CGT GTC CCT GGC CCG AAG-3′
BV22-BJ2.1_for3	5′-GAT GAT CAA TTC TCA GTT GAA AGG-3′
BV22-BJ2.1_rev3	5′-AAG AAC TGC TCA TTG TGT TCT CC-3′
BV22-BJ2.1_for1-new	5′-TTG GTA CAG ACA AAT CTT GG-3′
BV22-BJ2.1_rev1-new	5′-CAC GGT GAG CCG TGT CC-3′
BV22-BJ2.1_for2-new	5′-CAG AGA AGT CTG AAA TAT TCG-3′
BV22-BJ2.1_rev2-new	5′-CTG GCC CGA AGA ACT GC-3′
BV22-BJ2.1_for3-new	5′-GAT CAA TTC TCA GTT GAA AGG-3′
BV22-BJ2.1_rev3-new	5′-ACT GCT CAT TGT GTT CTC C-3′

Table 6: Primers employed for unbiased amplification of TCR sequences.

Name	Sequence
Cβ-in	5′-TCT GAT GGC TCA AAC ACA GC-3′
UP	5′-ACA GCA CGA CTT CCA AGA CTC A-3′
UP-new	5′-AGC ACG ACT TCC AAG ACT CA-3′
VP1	5′-TSY TTT GTC TCC TGG GAG CA-3′
VP2	5′-CCT GAA GTC GCC CAG ACT CC-3′
VP3	5′-GTC ATS CAG AAC CCA AGA YAC C-3′
VP4	5′-GGW TAT CTG TMA GMG TGG AAC CTC-3′
VP5	5′-ATG TAC TGG TAT CGA CAA GAY C-3′
VP6	5′-CAC TGT GGA AGG AAC ATC AAA CC-3′
VP7	5′-TCT CCA CTC TSA AGA TCC AGC-3′
VP8	5′-CAG RAT GTA RAT YTC AGG TGT GAT CC-3′
VP9	5′-CCA GAC WCC AAR AYA CCT GGT CA-3′
VP1$^+$	5′-ACA GCA CGA CTT CCA AGA CTC ACY TTT GTC TCC TGG GAG CA-3′
VP2$^+$	5′-ACA GCA CGA CTT CCA AGA CTC ACC TGA TGT CGC CCA GAC TCC-3′
VP3$^+$	5′-ACA GCA CGA CTT CCA AGA CTC AGT CAT SCA GAA CCC AAG AYA CC-3′
VP4$^+$	5′-ACA GCA CGA CTT CCA AGA CTC AGG WTA TCT GTM AGM GTG GAA CCT C-3′
VP5$^+$	5′-ACA GCA CGA CTT CCA AGA CTC AAT GTA CTG GTA TCG ACA AGA YC-3′
VP6$^+$	5′-ACA GCA CGA CTT CCA AGA CTC ACA CTG TGG AAG GAA CAT CAA ACC-3′
VP7$^+$	5′-ACA GCA CGA CTT CCA AGA CTC ATC TCC ACT CTS AAG ATC CAG C-3′
VP8$^+$	5′-ACA GCA CGA CTT CCA AGA CTC ACA GRA TGT ARA TYT CAG GTG TGA TCC-3′
VP9$^+$	5′-ACA GCA CGA CTT CCA AGA CTC ATC AGA CWC CAA RAY ACC TGG TCA-3′

Table 7: Primers employed for first round amplification of TCR alpha chains.

Name	Sequence
Cα-out	5′-GAC GAC AGA CTT GTC ACT GG-‘3
Vα-1[14]-for-out	5′-AGS AGC CTC ACT GGA GTT G-3′
Vα-1[235]-for-out	5′-CTG AGG TGC AAC TAC TCA TC-3′
Vα-2-for-out	5′-CAR TGT TCC AGA GGG AGC C-3′
Vα-3,25-for-out	5′-GAA RAT GYC WCC ATG AAC TGC-3′
Vα-4,20-for-out	5′-WTG CTA AGA CCA CCC AGC C-3′
Vα-5-for-out	5′-AGA TAG AAC AGA ATT CCG AGG-3′
Vα-6,14-for-out	5′-RYT GCA CAT ATG ACA CCA GTG-3′
Vα-7-for-out	5′-CAC GTA CCA GAC ATC TGG G-3′
Vα-8,21-for-out	5′-CCT GAG YGT CCA GGA RGG-3′
Vα-9-for-out	5′-GTG CAA CTA TTC CTA TTC TGG-3′
Vα-10,24-for-out	5′-AST GGA GCA GAG YCC TCA G-3′
Vα-11-for-out	5′-TCT TCA GAG GGA GCT GTG G-3′
Vα-12-for-out	5′-GGT GGA GAA GGA GGA TGT G-3′
Vα-13,19,26-for-out	5′-SAA STG GAG CAG AGT CCT C-3′
Vα-15-for-out	5′-CCT GAG TGT CCG AGA GGG-3′
Vα-16-for-out	5′-ATG CAC CTA TTC AGT CTC TGG-3′
Vα-17-for-out	5′-TGA TAG TCC AGA AAG GAG GG-3′
Vα-18-for-out	5′-GTC ACT GCA TGT TCA GGA GG-3′
Vα-22,31-for-out	5′-CCC TWC CCT TTT CTG GTA TG-3′
Vα-23,30-for-out	5′-GGC ARG AYC CTG GGA AAG G-3′
Vα-27-for-out	5′-CTG TTC CTG AGC ATG CAG G-3′
Vα-28-for-out	5′-AGA CAA GGT GGT ACA AAG CC-3′
Vα-29-for-out	5′-CAA CCA GTG CAG AGT CCT C-3′
Vα-32-for-out	5′-GCA TGT ACA AGA AGG AGA GG-3′

Table 8: Primers employed for second round amplification of TCR alpha chains.

Set	Name	Sequence
#1	Vα-4/1-for-in	5′-ACA GAA GAC AGA AAG TCC AGC-3′
	Vα-4/2-for-in	5′-GTC CAG TAC CTT GAT CCT GC-3′
	Vα-6-for-in	5′-GCA AAA TGC AAC AGA AGG TCG-3′
	Vα-8/1-for-in	5′-CAG TGC CTC AAA CTA CTT CC-3′
	Vα-8/2-for-in	5′-GCC TCA GAC TAC TTC ATT TGG-3′
	Vα-14-for-in	5′-ACA GAA TGC AAC GGA GAA TCG-3′
	Vα-24-for-in	5′-CCT TCA GCA ACT TAA GGT GG-3′
	Vα-28-for-in	5′-TCT CTG GTT GTC CAC GAG G-3′
#2	Vα-2/1-for-in	5′-TGG AAG GTT TAC AGC ACA GC-3′
	Vα-2/2-for-in	5′-TGG AAG GTT TAC AGC ACA GG-3′
	Vα-5-for-in	5′-CAG CAT ACT TAC AGT GGT ACC-3′
	Vα-10-for-in	5′-TCA CTG TGT ACT GCA ACT CC-3′
	Vα-12-for-in	5′-TAC AAG CAA CCA CCA AGT GG-3′
	Vα-22-for-in	5′-AGG CTG ATG ACA AGG GAA GC-3′
	Vα-31-for-in	5′-GTG GAA TAC CCC AGC AAA CC-3′

Set	Name	Sequence
#3	Vα-7-for-in	5′-CTC CAG ATG AAA GAC TCT GC-3′
	Vα-13-for-in	5′-TTA AGC GCC ACG ACT GTC G-3′
	Vα-17-for-in	5′-CTG TGC TTA TGA GAA CAC TGC-3′
	Vα-18-for-in	5′-CC TTA CAC TGG TAC AGA TGG-3′
	Vα-21-for-in	5′-TGC TGA AGG TCC TAC ATT CC-3′
	Vα-23-for-in	5′-GTG GAA GAC TTA ATG CCT CG-3′
	Vα-32-for-in	5′-TCA CCA CGT ACT GCA ATT CC-3′
#4	Vα-3-for-in	5′-TTC AGG TAG AGG CCT TGT CC-3′
	Vα-11-for-in	5′-AGG GAC GAT ACA ACA TGA CC-3′
	Vα-15-for-in	5′-CCT CCA CCT ACT TAT ACT GG-3′
	Vα-19-for-in	5′-CCT GCA CAT CAC AGC CTC C-3′
	Vα-25-for-in	5′-AGA CTG ACT GCT CAG TTT GG-3′
	Vα-26-for-in	5′-CCT GCA TAT CAC AGC CTC C-3′
	Vα-29-for-in	5′-ACT GCA GTT CCT CCA AGG C-3′
#5	Vα-1^{235}-for-in	5′-AAG GCA TCA ACG GTT TTG AGG-3′
	Vα-1^{14}-for-in	5′-CTG AGG AAA CCC TCT GTG C-3′
	Vα-9-for-in	5′-ATC TTT CCA CCT GAA GAA ACC-3′
	Vα-16-for-in	5′-TCC TTC CAC CTG AAG AAA CC-3′
	Vα-20-for-in	5′-ACG TGG TAC CAA CAG TTT CC-3′
	Vα-27-for-in	5′-ACT TCA GAC AGA CTG TAT TGG-3′
	Vα-30-for-in	5′-CTC TTC ACC CTG TAT TCA GC-3′
	Cα-rev-in	5′-AGT CTC TCA GCT GGT ACA CG-3′

Table 9: Primers employed for the generation of plasmid-encoded combinatorial peptide libraries.

Name	Sequence
Lib-rev-new	5′-TAG TTT AGC GGC CGC TCA-3′
Lib-rev	5′-ATA GTT TAG CGG CCG CTC A-3′
N24-Lib-for	5‘-CAG GGA AGG CGC GCC ACC ATG NNK NNK NNK NNK NNK NNK NNK NNK TGA GCG GCC GCT AAA CTA T-3′
8L-Lib-for	5′-CAG GGA AGG CGC GCC ACC ATG NNK NNK NNK NNK NNK NNK NNK CTG TGA GCG GCC GCT AAA CTA T-3′
N30-Lib-for	5‘-CAG GGA AGG CGC GCC ACC ATG NNK NNK NNK NNK NNK NNK NNK NNK NNK NNK TGA GCG GCC GCT AAA CTA T-3′
10L-Lib-for	5′-CAG GGA AGG CGC GCC ACC ATG NNK NNK NNK NNK NNK NNK NNK NNK NNK CTN TGA GCG GCC GCT AAA CTA T-3′
N39-Lib-for	5‘-CAG GGA AGG CGC GCC ACC ATG NNK NNK NNK NNK NNK NNK NNK NNK NNK NNK NNK NNK TGA GCG GCC GCT AAA CTA T-3′

Table 10: Primers employed for the recovery of antigen-coding plasmids.

Name	Sequence
pcDNA-for-1	5′-CAC TGC TTA CTG GCT TAT CG-3′
pcDNA-2nd-for-TOPO	5′-CAC TCC GGC GCG CCA CCA TG-3′
pcDNA-rev-1	5′-ACT AGA AGG CAC AGT CGA GG-3′
pcDNA-rev-3	5′-TGG TGA TGG TGA TGATGA CC-3′

Table 11: Primers employed for the generation of truncated protein coding plasmids.

Name	Sequence
Prot-V5-rev	5′-ATC ATG TCG ACC TAC GTA GAA TCG AGA CCG A-3′
DMXL2-out-for	5′-TGG AGG AGT GTC AGA ATT GG-3′
DMXL2-out-rev	5′-CAG ACT GTC AGA TGA GAT GC-3′
exp-DMXL2-for	5′-GAG CAG AAT TCC ACC ATG AAC TCT TTA CAT ACC TCA GCC-3′
DMXL2-V5-rev	5′-TGA GCG GCC GCC TAC GTA GAA TCG AGA CCG AGG AGA GGG TTA GGG ATA GGC TTA CCT GCA GCT TTG GCT AAG CAC G-3′
Prot-Dmxl2-for	5′-CTA TTG GAT CCA ACT CTT TAC ATA CCT CAG CC-3′
EML5-out-for	5′-TGT GTG CAT CTG GAG AGA TG-3′
EML5-out-rev	5′-CTT TTT CAG TTT CCG GAC TGC-3′
exp-EML5-for	5′-GAG CAG AAT TCC ACC ATG AAA ACA GTT AAA GCC CAT GAT G-3′
EML5-V5-rev	5′-TGA GCG GCC GCC TAC GTA GAA TCG AGA CCG AGG AGA GGG TTA GGG ATA GGC TTA CCT TTC CGG ACT GCC AAC ATA C-3′
Prot-Eml5-for	5′-CTA TTG GAT CCA AAA CAG TTA AAG CCC ATG ATG-3′
GPCPD1-for	5′-CAG AAT GAC ACC TTC TCA GG-3′
GPCPD1-out-rev	5′-AGT GTT TCA ACA CCA TTG TGG-3′
exp-GPCPD1-for	5′-GAG CAG AAT TCC ACC ATG ACA CCT TCT CAG GTC AC-3′
GPCPD1-V5-rev	5′-TGA GCG GCC GCC TAC GTA GAA TCG AGA CCG AGG AGA GGG TTA GGG ATA GGC TTA CCA CCA TTG TGG ATG CCA AAC TG-3′
Prot-Gpcpd1-for	5′-CTA TTG GAT CCA TGA CAC CTT CTC AGG TCA C-3′
Prot-Ncan-for	5′-CTA TTG GAT CCG TGA CAG GCG TCG TGT TCC-3′

Table 12: Primers and probes employed for qPCR.
Primers were designed to span introns and mimotopes, probes were labeled with 5’ 6-FAM and 3’ Tamra.

Name	Sequence
ALOX12B-for	5′-CAA CAT GAT GCC CAT CGC C-3′
ALOX12B-rev	5′-GCA GGT TCC TCA GGA GGG-3′
ALOX12B-probe	5′-GAG TGG GAC TGG CTG TTG GCT AAA-3′
AP5S1-for	5′-TGC TGA CAC CAG TTT GTC C-3′
AP5S1-rev	5′-AGG CAG ATG CCA CAC TTC C-3′
AP5S1-probe	5′-CAG ACA AAG AGC GAG GGT AAA GGT T-3′
DMXL2-for	5′-ATT AGA TGA ACT GTC AGA CCC-3′
DMXL2-rev	5′-CAG TAG CTG TGT ATT TGA TCC-3′
DMXL2-probe	5′-AGA AGT GTT TAA CAT TGT GAG CCA ACA-3′
EML5-for	5′-AAT CAC TCT TCT GGT CCA GG-3‘
EML5-rev	5′-TGC CAA CAT ACA ATG ACT AGG-3‘
EML5-probe	5′-GTT TGG CCA CAC ATC CTT ACC TGC-3‘
EML6-for	5‘-TAA GAG TGG CCC GAT GAC C-3‘
EML6-rev	5‘-TAA GTT TCC GTA CAG CCA GC-3‘
EML6-probe	5‘-AGT GAT GAC AAA ACA CTT CGG ATC TG-3‘
GAPDH-for	5‘-TCA CCA CCA TGG AGA AGG C-3‘
GAPDH-rev	5‘-ATG CCC CCA TGT TTG TGA TGG GTG T-3‘
GAPDH-probe	5‘-GCT AAG CAG TTG GTG GTG CA-3‘
GPCPD1-for	5‘-CAG AAT GAC ACC TTC TCA GG-3‘
GPCPD1-rev	5‘-AGA GCC ACA GCA TTT TGA GG-3‘
GPCPD1-probe	5‘-CTT TGC AAT ATG TGG AAG CTG TGA TG-3‘

Name	Sequence
KLHL28-for	5‘-CTC TCG GAG TGG CAG TGC-3‘
KLHL28-rev	5‘-ACT CGG ATC GTA ACG CTC C-3‘
KLHL28-probe	5‘-GAA TGC TAT ACG CCA TTG GAG GCT A-3‘
MDH1b-for	5‘-ACC ATG AAA GAT CTC ATC AGC-3‘
MDH1b-rev	5‘-CTG ATC TCT GTG TGC ATC CC-3‘
MDH1b-probe	5‘-TAC TTA CGT GTG CTG CCA CTT AAT TC-3‘
NCAN-for	5‘-ACG ATG TCT ACT GCT TTG CC-3‘
NCAN-rev	5‘-ACC GAG GCC AGC GCT GC-3‘
NCAN-probe	5‘-AAG TCT TTT ACG TGG GCC CGG CC-3‘

2.1.6 Plasmids

Table 13: Plasmid constructs.

Plasmid	Size	Resistance Genes	Application	Reference
pcDNA6-NFAT-sGFP	7.4 kb	amp^R, bls^R	Stably transfected into B7 and 2D1 T hybridoma cells, activation marker for T hybridoma cells	D. Hackl, M. Ackmann, Katherina Siewert, Klaus Dornmair
pHSE3’-neo-B8	8.7 kb	amp^R, neo^R	Backbone plasmid for pHSE3’-HLA-A3	Klaus Dornmair, Katherina Siewert
pHSE3’-HLA-A2	9.2 kb	amp^R, neo^R	Expression of human HLA-A*0201 in COS-7 cells	Klaus Dornmair, Wakiro Sato
pHSE3’-HLA-A3‡	9.2 kb	amp^R, neo^R	Expression of human HLA-A*0301 in COS-7 cells	Section 2.5.7 (p. 41)
pRSVneo-HLA-A2	6.2 kb	amp^R, neo^R	Expression of human HLA-A*0201 in COS-7 cells	Katherina Siewert
pRSVneo-HLA-A3	6.2 kb	amp^R, neo^R	Expression of human HLA-A*0301 in COS-7 cells	Klaus Dornmair, Geraldine Rühl
pcDNA6/V5-HisA	5.1 kb	amp^R, bls^R	Backbone plasmid for truncated protein expression	Invitrogen, Supplements 5.7.1 (p. 120)
pcDNA6-DMXL2$_{748-926}$-V5‡	5.6 kb	amp^R, bls^R	Expression of mouse DMXL2$_{748-926}$ with V5 tag in COS-7 cells	Section 2.3.3 (p. 33), Supplements 5.7.1 (p. 120)
pcDNA6-EML5$_{897-1038}$-V5‡	5.5 kb	amp^R, bls^R	Expression of mouse EML5$_{897-1038}$ with V5 tag in COS-7 cells	Section 2.3.3 (p. 33), Supplements 5.7.1 (p. 120)
pcDNA6-GPCPD1$_{1-118}$-V5‡	5.2 kb	amp^R, bls^R	Expression of mouse GPCPD1$_{1-118}$ with V5 tag in COS-7 cells	Section 2.3.3 (p. 33), Supplements 5.7.1 (p. 120)
pcDNA6-NCAN$_{156-359}$-V5‡	5.7 kb	amp^R, bls^R	Expression of mouse NCAN$_{156-359}$ with V5 tag in COS-7 cells	Section 2.3.3 (p. 33), Supplements 5.7.1 (p. 120)
pQE-30	3.4 kb	amp^R	Backbone plasmid for truncated protein production	Jessica Bruder, Qiagen, Supplements 5.7.2 (p. 122)
pQE-30-His$_6$-DMXL2$_{748-926}$-V5‡	3.9 kb	amp^R	Production of mouse DMXL2$_{748-926}$ with His$_6$ and V5 tag in *E. coli*	Section 2.3.4 (p. 35), Supplements 5.7.2 (p. 122)
pQE-30-His$_6$-EML5$_{897-1038}$-V5‡	3.8 kb	amp^R	Production of mouse EML5$_{897-1038}$ with His$_6$ and V5 tag in *E. coli*	Section 2.3.4 (p. 35), Supplements 5.7.2 (p. 122)
pQE-30-His$_6$-GPCPD1$_{1-118}$-V5‡	3.5 kb	amp^R	Production of mouse GPCPD1$_{1-118}$ with His$_6$ and V5 tag in *E. coli*	Section 2.3.4 (p. 35), Supplements 5.7.2 (p. 122)

Plasmid	Size	Resistance Genes	Application	Reference
pQE-30-His_6-$NCAN_{156-359}$-V5‡	4.0 kb	amp^R	Production of mouse $NCAN_{156-359}$ with His_6 and V5 tag in *E. coli*	Section 2.3.4 (p. 35), Supplements 5.7.2 (p. 122)
pcDNArc-spacer	7.6 kb	amp^R, bls^R	Backbone plasmid for PECP libraries and peptide-coding plasmids	Katherina Siewert, Geraldine Rühl
N24‡	5.1 kb	amp^R, bls^R	PECP library, coding for random eightmer peptides	Section 2.3.1 (p. 30)
8L‡	5.1 kb	amp^R, bls^R	PECP library, coding for eightmer peptides with leucine at position 8	Section 2.3.1 (p. 30)
N27	5.1 kb	amp^R, bls^R	PECP library, coding for random nonamer peptides	Katherina Siewert
9L	5.1 kb	amp^R, bls^R	PECP library coding for nonamer peptides with leucine at position 9	Katherina Siewert
N30‡	5.1 kb	amp^R, bls^R	PECP library, coding for random decamer peptides	Section 2.3.1 (p. 30)
10L‡	5.1 kb	amp^R, bls^R	PECP library, coding for decamer peptides with leucine at position 10	Section 2.3.1 (p. 30)
N39‡	5.1 kb	amp^R, bls^R	PECP library, coding for random tridecamers peptides	Section 2.3.1 (p. 30)
$A2^{269}$	5.1 kb	amp^R, bls^R	PECP library, coding for nonamer peptides with I, V and L at the positions 2, 6 and 9, respectively	Katherina Siewert
pcDNA™3.1D/V5-His-TOPO®	5.5 kb	amp^R, neo^R	Recloning of peptides coded on PECP libraries for mimotope search	Invitrogen, Supplements 5.7.3 (p. 124)
13AAG64P_Ncan-V5_pMA-RQ	3.0 kb	amp^R	Cloning of $NCAN_{156-359}$-V5	Invitrogen, Supplements 5.7.4 (p. 125)

‡ The plasmid was constructed during this thesis.

2.1.7 Peptides

Peptides listed in Table 14 (p. 24) were synthesized by Thermo Fisher Scientific and purified by preparative HPLC to a final purity of >70% unless stated differently. Their sequences were verified by mass spectrometry. The peptides TAX_{11-19} and PLP_{45-53} were kindly provided by Prof. Dr. Lars Fugger, John Radcliffe Hospital (Oxford, GB). All peptides were delivered lyophilized and then dissolved in DMSO to a final concentration of 10 mg/mL.

Table 14: Peptides employed in TCR 2D1 and B7 antigen search experiments.

Name	Sequence	Parent Protein	Source Organism	Reference
PLP_{45-53}	KLIETYFSK	Proteolipid protein 1 (PLP)	*Homo sapiens*	CAM26805.1
-	YLIETYFRL	Hypothetical protein	*Haemophilus influenzae*	YP_005829445.1
-	KLIEKYFSK	Transcriptional regulator	*Bacillus cereus*	ZP_04220391.1
-	KLIEPYFSK	Protein MurG2	*Clostridium kluyveri*	YP_001397075.1
-	KLIGTYFSK	Oligoketide cyclase/lipid transport protein	*Rickettsia slovaca*	YP_005065446.1

Name	Sequence	Parent Protein	Source Organism	Reference
-	KLIDTYFTK	Oligoketide cyclase/lipid transport protein	*Rickettsia philipii*	YP_005300289.1
-	KLIDTYFSN	Borrelia ORF-A superfamily protein	*Borrelia burgdorferi*	YP_002455216.1
-	KLIQTYLSK	Cell wall surface anchor family protein	*Staphylococcus epidermidis*	AEU10801.1
-	KLIDTYFSG	Hypothetical protein LmonocyFSL_16611	*Listeria monocytogenes*	ZP_05296661.1
-	KLIETYFKK	Chain C, Crystal Structure Of A HLA Class I-Peptide Complex	*Homo sapiens*	2XPG_C
-	KMIETYFTT	GTP-binding protein YihA	*Bacillus thuringiensis*	ZP_04080665.1
-	KMLETYLSK	A/G-specific adenine glycosylase	*Streptococcus equi*	AEJ24562.1
-	KLIDTYFKK	Fe-S assembly protein, SufD	*Flavobacteria bacterium*	ZP_03702432.1
TAX_{11-19}	LLFGYPVYV	Tax	*Human T-lymphotropic virus 1*	BAB20130.1
-	PLFGYTVYG	Hypothetical protein	*Homo sapiens*	CAD28520.1
-	NLFGNPVYF	Solute carrier organic anion transporter family member 1C1 isoform 2	*Macaca mulatta*	AFE70069.1
-	IGFGYPAYI	Receptor accessory protein 5	*Mus musculus*	EDK97087.1
-	ALYGCPVYV	Diaminopimelate decarboxylase	*Capnocytophaga gingivalis*	ZP_04057540.1
-	IGFGYPAYI	Receptor accessory protein 5	*Mus musculus*	EDK97087.1
-	SEFSYPVYR	RCC1 and BTB domain-containing protein 2	*Macaca mulatta*	AFE71435.1
-	SLFAFPVYQ	Glucosidase	*Homo sapiens*	AAO14993.1
$ALOX12B_{404-411}$	LIGEAFCL	Arachidonate 12-lipoxygenase, 12R-type	*Mus musculus*	EDL10482.1
$AP5S1_{185-192}$	LLGEVWHL	AP-5 complex subunit sigma-1	*Mus musculus*	NP_081405.2
$DMXL2_{813-820}$	LIGEVFNI	Rabconnectin-3	*Homo sapiens / Mus musculus*	AAL93215.1 / CAQ12130.1
$EML5/6_{997-1004}$	MEGEVWGL	Echinoderm microtubule-associated protein-like 5 / -6	*Homo sapiens / Mus musculus*	AAQ62653.1, NP_001034842.2 / AAI58138.1, NP_666128.2
$GPCPD1_{15-22}$	LPGEVFAI	Glycerophosphocholine phosphodiesterase 1	*Homo sapiens / Mus musculus*	NP_062539.1 / NP_083078.3
$KLHL28_{384-391}$	LAGEVFAL	Kelch-like protein 28	*Mus musculus*	NP_079983.1
$MDH1B_{152-159}$	LSGEVFGM	Malate dehydrogenase 1B	*Mus musculus*	AAH50786.1
$NCAN_{257-264}$	LGGEVFYV	Neurocan	*Homo sapiens / Mus musculus*	AAC80576.1 / P55066.1

2.1.8 Antibodies

Table 15: Primary antibodies.
Apart from different notation all antibodies are directed against human antigens.

Specificity	Conjugate	Clone	Species/Isotype	Concentration	Company
CD8 alpha[†]	Cy3	LT8	Mouse / IgG1	-	AbD Serotec
CD8 beta	-	2ST8.5H7	Mouse / IgG2a	5.15 mg/mL	Beckman Coulter
CD8 beta[†‡]	Cy3	2ST8.5H7	Mouse / IgG2a	-	Beckman Coulter
CD134	FITC	ACT35	Mouse / IgG1	50 µg/mL	BD Pharmingen

Specificity	Conjugate	Clone	Species/Isotype	Concentration	Company
HLA-A2	-	BB7.2	Mouse / IgG2b	1 mg/mL	GeneTex (Irvine, USA)
HLA-A2	-	polyclonal	Rabbit / IgG	1 mg/mL	Abcam (Cambridge, UK)
HLA-A2	FITC	BB7.2	Mouse / IgG2b	0.1 mg/mL	ProImmune (Oxford, UK)
Mouse CD3e	-	145-2C11	Hamster / IgG	0.5 mg/mL	eBioscience (Frankfurt, D)
CD3	FITC	UCHT1	Mouse / IgG1	1.7 mg/mL	Dako (Glostrup, DK)
TCR BV13S1	FITC	IMMU222	Mouse / IgG2b	50 µg/mL	Beckman Coulter
TCR BV22	FITC	IMMU546	Mouse / IgG1	50 µg/mL	Beckman Coulter

† The antibody was labeled during Backes, 2010.
‡ The antibody was labeled during this thesis.

Table 16: Secondary antibodies.

Antibody	Conjugate	Concentration	Company	Abbreviation
Anti-V5	HRP	1.2 mg/mL	Life technologies	aV5-HRP
Goat anti FITC IgG	Alexa488	1 mg/mL	Invitrogen	aFITC-Alexa488
Goat anti Rabbit IgG (Fc)	HRP	1 mg/mL	AbD Serotec	-

Table 17: Isotype controls.

Antibody	Conjugate	Concentration	Company
Mouse IgG1	-	1 mg/mL	AbD Serotec
Mouse IgG2a	-	N/A	AbD Serotec
Mouse IgG2b	-	0.5 mg/mL	Abcam
Mouse IgG2b	FITC	N/A	BD Pharmingen

2.1.9 Eukaryotic Cell Lines and *Escherichia coli* Strains

Table 18: Eukaryotic cell lines.

Designation	Description	Source (reference)
2D1	Derivative cell line from 58$\alpha^-\beta^-$, expressing the TCR 2D1 and full length human CD8 alpha and beta	Lars Fugger, subclone from Harald von Boehmer
2D1-NFAT-sGFP‡	Derivative cell line from 2D1, additionally expressing sGFP under the control of the NFAT promoter	Section 2.5.6 (p. 40)
B7	Derivative cell line from 58$\alpha^-\beta^-$, expressing the TCR B7 and full length human CD8 alpha and beta	Lars Fugger, subclone from Harald von Boehmer
B7-NFAT-sGFP‡	Derivative cell line from B7, additionally expressing sGFP under the control of the NFAT promoter	Section 2.5.6 (p. 40)
COS-7	African green monkey kidney cell line, SV40 transformed, produces T antigen, adherent	ATCC (CRL-1651) (Gluzman, 1981)
COS-7-A2	COS-7 cells with stable expression of HLA-A*0201	Klaus Dornmair, Katherina Siewert
COS-7-A3‡	COS-7 cells with stable expression of HLA-A*0301	Section 2.5.7 (p. 41)
COS-7-Cw06	COS-7 cells with stable expression of HLA-Cw*0601	Klaus Dornmair, Geraldine Rühl
EBV-16488	EBV-transducted B cells, derived from polymyositis patient 16488, stable expression of HLA-A2, HLA-A26, HLA-B8, HLA-B38, HLA-Cw07, HLA-Cw12	Klaus Dornmair
EBV-17490	EBV-transducted B cells derived from polymyositis patient 17490, stable expression of HLA-A2, HLA-A3, HLA-B35, HLA-B40, HLA-Cw03, HLA-Cw04	Klaus Dornmair
EBV-FE	EBV-transducted B cells derived from MS patient FE, stable expression of HLA-A1, HLA-B8, HLA-Cw07	Klaus Dornmair

Designation	Description	Source (reference)
GP+E-A2	GP+E cells expressing HLA-A*0201	Klaus Dornmair, Katherina Siewert
GP+E-B38	GP+E cells expressing HLA-B*3801	Klaus Dornmair, Katherina Siewert
LTK-A1	LTK cells with stable expression of HLA-A*0101	Klaus Dornmair, Katherina Siewert
LTK-A2	LTK cells with stable expression of HLA-A*0201	Klaus Dornmair, Katherina Siewert
LTK-A3	LTK cells with stable expression of HLA-A*0301	Klaus Dornmair, Xiao Nong

‡ The cell line was generated during this thesis.

Table 19: Escherichia coli strains.
All *E. coli* strains were purchased from Invitrogen. Competence is given in colony forming units / µg pUC19 plasmid.

E. coli strain	Genotype	Competence
ElectroMAX™ DH10B™ T1 Phage Resistant Cells	F⁻ *mcr*A Δ(*mrr-hsd*RMS-*mcr*BC) Φ80*lacZ* ΔM15 Δ*lac*X74 *rec*A1 *end*A1 *ara*D139 Δ(*ara-leu*)7697 *gal*U *gal*K λ⁻ *rps*L *nup*G *ton*A	$1x10^{10}$
MAX Efficiency® DH5αF'IQ™ Competent Cells	F⁻Φ80*lac*ZΔM15 Δ(*lac*ZY A-*arg*F) U169 *rec*A1 *end*A1 *hsd*R17 (r_k-, m_k+) *pho*A *sup*E44 λ⁻ *thi*⁻1 *gyr*A96 *rel*A1 / F' *pro*AB+ *lac*IqZΔM15 zzf::Tn5 [KmR]	$3x10^{8}$
One Shot® BL21(DE3) Chemically Competent	F⁻ *ompT hsdS*$_B$ (r_B-m_B-) *gal dcm* (DE3)	$1x10^{8}$
One Shot® TOP10 Chemically Competent	F⁻ *mcr*A Δ(*mrr-hsd*RMS-*mcr*BC) Φ80*lacZ* ΔM15 Δ*lac*X74 *rec*A1 *ara*D139 Δ(*ara-leu*)7697 *gal*U *gal*K *rps*L (Str^R) *end*A1 *nup*G λ-	$1x10^{9}$

2.1.10 Human Tissue Samples and Blood Cells

Brain tissue from the male patient FE was used for analysis of TCR alpha and beta chains. This patient was diagnosed with a malignant glioma in the right temporooccipital lobe at the age of 49 in 1996. The affected brain area was surgically removed and stored frozen at -80°C. Presence of oligoclonal immunoglobulin bands in CSF and three relapses in the following five years led to the diagnosis of MS Type III (Hu and Lucchinetti, 2009). Patient FE is homozygous at the HLA class I gene locus (Skulina et al., 2004; recently confirmed by Geraldine Rühl). He possesses the alleles *HLA A*0101*, *HLA B*0801*, *HLA Cw*0701*, *HLA DRB1*0301*, *HLA DRB3*0101*, *HLA DQA1*05* and *HLA DQB1*0201*.

To establish fluorescent immunohistochemical staining, brain tissue from patient OIND-1 and tonsil tissue of two unknown patients was used. Patient OIND-1 suffered from a non-specified inflammatory brain disease. The tissue block was provided by Dr. Arzberger from the neuropathology of Klinikum Großhadern (Munich, D). The tonsils were provided by Dr. Markus Krumbholz from the otorhinolaryngology of Klinikum Großhadern.

$CD3^+$ blood lymphocytes from voluntary donors of the Max Planck Institute of Neurobiology were used as positive controls during the analysis of TCR alpha and beta chains.

All patients and voluntary donors allowed scientific examination of their biopsies or blood samples. These experiments were approved by the ethics committee of the Ludwig Maximilians University, Munich.

2.2 Analysis of Nucleic Acids

2.2.1 RNA isolation from Tissue Samples

Tissue samples were homogenized in TRIzol LS reagent by pipetting (10 µm tissue slides) or mechanical grinding (mouse thymus and brain). After adding 200 µL of chloroform per mL tissue suspension the samples were shaken for 15 seconds, incubated for 5 minutes at room temperature and centrifuged in the 5417 R Centrifuge (Eppendorf) at 4°C and 14,000 rpm (20,800 g). The upper, aqueous phase containing RNA was transferred into a new reaction tube. After adding 10 µL of glycogen (Novagen, final concentration of 200 µg) and 700 µL 70 % 2-propanol the samples were incubated for 20 minutes at -20°C and then centrifuged for 20 minutes at 4°C and 14,000 rpm (20,800 g). Subsequently the samples were washed with 1 mL 80 % ethanol via 5 minutes of centrifugation at 4°C and 14,000 rpm (20,800 g). The RNA pellet was air-dried, resuspended in 22 µL of DEPC-water (Invitrogen) and stored at -20°C. RNA concentration was determined as described in Section 2.2.2 (p. 28).

2.2.2 Determination of DNA and RNA Concentration

DNA and RNA concentration was measured at the spectrophotometer Nanodrop ND-1000 (Thermo Fisher Scientific) with the software "ND-1000 V3.2.1" according to the manufacturer's instructions at a wavelength of 260 nm.

2.2.3 Analysis of RNA Quality in Human Tissue Blocks

Human tissue blocks were stored at -80°C and warmed to -20°C for the generation of 10 µm thick cryostat tissue sections. Before usage, the cryotom was cleaned with RNase ZAP (Sigma-Aldrich), H_2O/DEPC and 80 % ethanol to provide an RNase-free working area. PET Membrane slides 1.0 (Zeiss) were baked 4 hours and 30 minutes at 180°C and coated 1 hour with 100 mL of a 2 µg/µL poly-L-lysine-hydrobromide solution inside a wet chamber. After rinsing with H_2O/DEPC the slides were dried and sterilized for 30 minutes through UV irradiation.

10 µm tissue sections were either collected directly after cutting in 1 mL TRIzol LS reagent or mounted on the prepared membrane slides and stored at -80°C. After different treatment of the stored slides (Section 3.2.1, p. 65), the tissue was collected by washing it with TRIzol LS reagent into 2 mL reaction tubes. TRIzol LS-tissue suspensions could be stored several days at -20°C. RNA isolation was performed as described in Section 2.2.1 (p. 28).

RNA quality analysis was performed in a chip at the 2100 Bioanalyzer (Agilent) using the "RNA 6000 Pico Assay" kit (Agilent). RNA samples were diluted 1:10 and 1:100 in DEPC-water (Invitrogen), denatured for 2 minutes at 70°C and then processed as described in the user manual. The data were obtained as gel-like images and electropherograms. For analyzing the data the software "Agilent Technologies 2100 Bioanalyzer 2100 Expert, VB.02.06.SI418" (Agilent) was employed. RNA quality was given as "RNA integrity number" (RIN). The RIN-value represented the ratio between 28S rRNA

and 18S rRNA offset against further factors. Values from 8 to 10 indicated good RNA quality, lower values meant less and higher values better quality, respectively.

2.2.4 Quantitative PCR

cDNA was transcribed from isolated RNA (Section 2.2.1, p. 28) using the SuperScript® III Reverse Transcriptase Kit (Invitrogen). First the reverse transcription PCR (RT-PCR) pre-mix was prepared according to the manufacturer's instructions:

Volume	Reagent	Final Concentration
10 µL	5x FS Buffer	1x
2.5 µL	dNTP-mix (10 mM each)	0.5 mM each
2.5 µL	DTT (0.1 M)	5 mM
2.5 µL	RNase OUT (40 U/µL)	100 U
2 µL	Random Primer	600 ng
2 µL	SuperScript III RT (200 U/µL)	500 U
1.5 µL	DMSO	3 %
x µL	total RNA	2.5 µg
50 µL		

The RT-PCR was performed in the T3 Thermocycler (Biometra) heating to 25°C for 5 minutes, to 50°C for 60 minutes and to 70°C for 15 minutes. cDNA samples were diluted to 50 ng/µL, aliquoted and stored at -20°C.

For quantitative PCR (qPCR) the primers were designed to span at least one intron and the region of interest in particular genes (Supplement 5.5, p. 113). Probes were labeled at 3' with 6-FAM and 5' with Tamra. Primers and probes for qPCR are listed in Table 12 (p. 22). Each qPCR was performed in 96-well optical reaction plates with 250 ng, 50 ng and 0 ng of template cDNA in triplets with the following mix:

Volume	Reagent	Final Concentration
10 µL	2x TaqMan gene expression master mix	1x
0.5 µL	x-for (10 µM)	0.25 µM
0.5 µL	x-rev (10 µM)	0.25 µM
0.5 µL	x-probe (5 µM)	0.125 µM
1 µL	cDNA	x ng
ad 20 µL	H_2O/DEPC	

qPCR was performed in the 7900HT Fast Real-Time PCR System (Applied Biosystems) under following conditions:

50°C	2 min		
95°C	10 min		
95°C	15 sec	denaturation	40 cycles
60°C	1 min	hybridization and elongation	

Data were acquired and analyzed with the software SDS Version 2.4.1 (Applied Biosystems). For calculation of ΔCt values Ct values of the house keeping gene *Gapdh* were subtracted from Ct values of genes of interest.

2.2.5 Agarose gel electrophoresis

According to the expected length of DNA 0.9 % to 2 % agarose gels were prepared in TBE buffer containing 0.5 µg/mL ethidium bromide. The samples were mixed with 6x DNA loading buffer to a final concentration of 1x. To determine the lengths of running DNA fragments 50 bp, 100 bp or 1 kb DNA markers (New England Biolabs) were used. The samples were run in TBE buffer at 180 V for 250 mL gels and 90 V for 35 mL gels. Ethidium bromide intercalates in DNA strands and absorbs UV light. Thus gels were documented at the Geldoc XR (Bio-Rad) device using the software "Quantity One V 4.6.5" (Bio-Rad). All buffers are given in Table 2 (p. 15).

2.2.6 Sequencing of DNA Samples

Sequencing analyses were performed at the sequencing service at the faculty of biology of the Ludwig Maximilians University, Munich employing the protocol "Cycle, Clean & Run BigDye v3.1". Resulting sequences were analyzed with the software "Chromas Lite V2.01" (Griffith University, AU) and "ApE - A plasmid Editor V2.0.44" (M. Wayne Davis).

2.3 Generation of diverse Plasmids

2.3.1 Plasmid-Encoded Combinatorial Peptide Libraries

First the primers N24-Lib-for, 8L-Lib-for, N30-Lib-for, 10L-Lib-for, N39-Lib-for and Lib-rev or Lib-rev-new (Table 9, p. 21) were denatured for 5 minutes at 99°C in the following setup in the T3 Thermocycler (Biometra):

Volume	Reagent	Final Concentration
5 µL	x-Lib-for (100 µM)	20 µM
5 µL	x-Lib-rev(-new) (100 µM)	20 µM
10 µL	10x PCR buffer	1x
ad 100 µL	H_2O/DEPC	

After cooling to room temperature the following PCR mix was added:

Volume	Reagent	Final Concentration
4 µL	dNTP-mix (10 mM each)	0.2 mM
10 µL	10x buffer	1x
2 µL	Taq-DNA-Polymerase (5 U/µL)	10 U
ad 100 µL	H_2O/DEPC	

Double strands were generated by gradual heating for 4 minutes at 60°C, 4 minutes at 63°C, 4 minutes at 65°C and finally 1 hour at 68°C in the T3 Thermocycler (Biometra).
For precipitation in 0.1 volumes of 3 M sodium acetate and 2.5 volumes of ethanol the samples were incubated for at least 30 minutes at -80°C and then centrifuged for 1 hour at 4°C and 14,000 rpm (20,800 g) in the 5417 R Centrifuge (Eppendorf). After discarding the supernatant the pellet was washed twice with 500 µL 70 % ethanol, air-dried and resuspended in 50 µL of EB buffer. DNA concentration was determined as described in Section 2.2.2 (p. 28).
To generate library inserts the double strands were first digested with the restriction enzyme AscI (New England Biolabs) over night at 37°C in the following setup:

Volume	Reagent	Final Concentration
x µL	DNA double strand	4 µg
10 µL	NEB buffer 4 (10x)	1x
7.2 µL	AscI (10,000 U/mL)	72 U
1 µL	NEB BSA (100x)	1x
ad 100 µL	H_2O/DEPC	

After heat-inactivation for 20 minutes at 65°C in the T3 Thermocycler (Biometra) 2 µL of the restriction enzyme NotI-HF (20,000 U/mL, New England Biolabs, final concentration of 40 U) were added and the samples were incubated for 4 hours at 37°C. Library inserts were purified with the QIAquick® PCR Purification Kit (Qiagen) and eluted in 50 µL EB buffer. DNA concentration was determined as described in Section 2.2.2 (p. 28).
The inserts were ligated into the previously AscI- and NotI-digested and dephosphorylated backbone plasmid pcDNArc-spacer (Table 13, p. 23) provided by Katherina Siewert or Geraldine Rühl.

Volume	Reagent	Final Concentration
x µL	Library insert	40 to 50 ng
x µL	backbone plasmid	1 µg
40 µL	5x T4 ligase buffer	1x
10 µL	T4 Ligase (1 U/µL)	10 U
ad 200 µL	H_2O/DEPC	

As negative control one sample in a final volume of 20 µL containing H_2O/DEPC instead of library insert was prepared. The samples were incubated at 16°C for 42 hours followed by precipitation of the DNA as described above but with addition of 20 µg Glycogen (Novagen) acting as a DNA carrier and 2 µL of Pellet Paint (Novagen). The pellet was resuspended in 20 µL of EB buffer.
The library plasmids were finally transformed into the *E. coli* strain ElectroMax DH10B™ (Invitrogen) as described in Section 2.4.4 (p. 37). To gain a very high yield of clones six times 50 µL of the bacteria were used. After growing each in 500 mL LB^{amp} medium (Section 2.4.1, p. 37) over night DNA purification was performed using the HiSpeed Plasmid Maxi Kit (Qiagen). After determination of the DNA concentration (Section 2.2.2, p. 28) samples of 10 to 15 µg DNA were stored at -20°C. Glycerol stocks were prepared from 500 mL of the bacteria (Section 2.4.3, p. 37).

2.3.2 Peptide-Coding Plasmids

The backbone plasmid pcDNArc-spacer (Table 13, p. 23) was digested with the restriction enzymes AscI and NotI (New England Biolabs) for at least 4 hours at 37°C in the following setup:

Volume	Reagent	Final Concentration
x µL	pcDNArc-spacer plasmid	40 µg
40 µL	NEB buffer 4 (10x)	1x
3 µL	NotI-HF (20,000 U/mL)	60 U
10 µL	AscI (10,000 U/mL)	100 U
4 µL	NEB BSA (100x)	1x
ad 400 µL	H_2O/DEPC	

The whole reaction volume was loaded on an agarose gel (Section 2.2.5, p. 30) and the digested plasmid backbone with the length of 5.1 kb was isolated using the QIAquick® Gel Extraction Kit (Qiagen) according to the manufacturer's description with elution in 200 µL of EB buffer. DNA concentration was determined as described in Section 2.2.2 (p. 28).

Primers listed in Supplements 5.5 (p. 113) were designed optimizing codons for expression in eukaryotic cells according to the webpage http://www.encorbio.com/protocols /Codon.htm (EnCor Biotechnology Inc., Florida, USA). To generate the inserts the corresponding forward and reverse primers were denatured in the T3 Thermocycler (Biometra) for 5 minutes at 95°C and annealed for 5 minutes at 75°C followed by cooling to room temperature in the following mix:

Volume	Reagent	Final Concentration
5 µL	x-for (100 µM)	20 µM
5 µL	x-rev (100 µM)	20 µM
ad 100 µL	EB buffer	

The backbone plasmid and the inserts were ligated for at least 30 minutes at room temperature according to the following setup:

Volume	Reagent	Final Concentration
1 µL	annealed insert	4 to 5 ng
1 µL	backbone plasmid	100 ng
4 µL	5x T4 Ligase Buffer	1x
1 µL	T4 Ligase (1 U/µL)	1 U
ad 20 µL	H_2O/DEPC	

As negative control one sample containing H_2O/DEPC instead of annealed insert was prepared. 2 µL of the ligation mix were transformed into the *E. coli* strain One Shot® TOP10 (Section 2.4.4, p. 37). The next day three clones were picked and grown in suspension. Plasmid purification was performed (Section 2.4.5, p. 38) and sequenced with the primer pcDNA-rev-3 (Table 10, p. 21). Glycerol stocks were prepared from 1 mL of the correct clones (Section 2.4.3, p. 37).

2.3.3 Truncated Proteins Coding Plasmid pcDNA6/V5-HisA

Domain-based truncation of the mouse proteins DMXL2, EML5, GPCPD1 and NCAN was conducted taking domain regions from http://www.uniprot.org/uniprot/Q8BPN8, http://www.uniprot.org/uniprot/Q8BQM8, http://www.uniprot.org/uniprot/Q8C0L9 and http://www.uniprot.org/uniprot/P55066 (Supplements 5.8, p. 126).

To generate adequate backbones, the plasmid pcDNA6/V5-HisA (Table 13, p. 23) was first digested with the restriction enzyme EcoRI-HF (New England Biolabs) for 2 hours at 37°C in the following setup:

Volume	Reagent	Final Concentration
x µL	pcDNA6/V5-HisA plasmid	4 µg
2 µL	NEB buffer 4 (10x)	1x
1 µL	EcoRI-HF (20,000 U/mL)	20 U
ad 20 µL	H_2O/DEPC	

After heat inactivation for 20 minutes at 65°C the following mix for the second digestion with the restriction enzyme NotI-HF was added:

Volume	Reagent	Final Concentration
1 µL	NEB buffer 4 (10x)	1x
1 µL	NotI-HF (20,000 U/mL)	20 U
0.3 µL	NEB BSA (100x)	1x
ad 10 µL	H_2O/DEPC	

The sample was incubated at 37°C for 2 hours. Subsequently the whole reaction volume was loaded on an agarose gel (Section 2.2.5, p. 30). The digested plasmid backbone with a length of 5.1 kb was isolated using the QIAquick® Gel Extraction Kit (Qiagen) according to the manufacturer's description with elution in 20 µL of EB buffer. DNA concentration was determined as described in Section 2.2.2 (p. 28). Afterwards 500 ng of digested plasmid were dephosphorylated using the Rapid DNA Dephos & Ligation Kit (Roche) according to the manufacturer's instructions.

To generate inserts coding for the truncated mouse proteins $DMXL2_{748\text{-}926}$, $EML5_{897\text{-}1038}$ and $GPCPD1_{1\text{-}118}$ cDNA from mouse thymus (Section 2.2.4, p. 29) was used as template for the following pre-amplification PCR with outer primers listed in Table 11 (p. 22):

Volume	Reagent	Final Concentration
2.0 µL	10x PCR buffer	1x
0.5 µL	dNTP-mix (10 mM each)	0.25 mM
0.5 µL	x-out-for (10 µM)	0.25 µM
0.5 µL	x-out-rev (10 µM)	0.25 µM
0.5 µL	Taq DNA Polymerase (5 U/µL)	2.5 U
1.0 µL	cDNA	50 ng
ad 20 µL	H_2O/DEPC	

The PCR was run in the T3 Thermocycler (Biometra) using the following conditions:

95°C	2 min		
95°C	30 sec	denaturation	
56°C	1 min	hybridization	40 cycles
72°C	1 min	elongation	
72°C	10 min		
4°C	∞		

The whole reaction volume was loaded on an agarose gel (Section 2.2.5, p. 30). The PCR products of expected lengths were isolated using the QIAquick® Gel Extraction Kit (Qiagen) according to the manufacturer's description with elution in 20 µL of EB buffer. DNA concentration was determined (Section 2.2.2, p. 28) and the products were sent for sequencing (Section 2.2.6, p. 30).
Next the actual gene region was amplified using the same protocol as mentioned above with 1 µL of the outer PCR product as template. The primers exp-x-for and x-V5-rev (Table 11, p. 22) were employed. They introduced 5' extensions with a restriction site for EcoRI, the Kozak sequence CCACC as well as the start codon ATG and 3' extensions with the V5 tag, the stop codon TAG and a restriction site for NotI. The products were sent for sequencing (Section 2.2.6, p. 30).
The required region of $NCAN_{156-359}$ was synthesized by GeneArt® Gene Synthesis (Invitrogen). The PCR products for $DMXL2_{748-926}$-V5, $EML5_{897-1038}$-V5 and $GPCPD1_{1-118}$-V5 and the plasmid 13AAG64P_Ncan-V5_pMA-RQ (Table 13, p. 23) containing $NCAN_{156-359}$-V5 were double digested for 2 hours at 37°C with the restriction enzymes EcoRI-HF and NotI-HF (New England Biolabs):

Volume	Reagent	Final Concentration
6 µL	PCR product / plasmid	
4 µL	NEB buffer 4 (10x)	1x
1 µL	NotI-HF (20,000 U/mL)	20 U
1 µL	EcoRI-HF (20,000 U/mL)	20 U
0.4 µL	NEB BSA (100x)	1x
ad 40 µL	H_2O/DEPC	

The whole reaction volume for $DMXL2_{748-926}$, $EML5_{897-1038}$ and $GPCPD1_{1-118}$ was purified using the QIAquick® Gel Extraction Kit (Qiagen) according to the manufacturer's description with elution in 20 µL of EB buffer. The whole reaction volume for $NCAN_{156-359}$-V5 was loaded on an agarose gel (Section 2.2.5, p. 30). The DNA fragment of the expected length was isolated using the QIAquick® Gel Extraction Kit (Qiagen) according to the manufacturer's description with elution in 20 µL of EB buffer. DNA concentration was determined (Section 2.2.2, p. 28).
The dephosphorylated backbone plasmid pcDNA6/V5-HisA and the inserts coding for the truncated mouse proteins $DMXL2_{748-926}$-V5, $EML5_{897-1038}$-V5, $GPCPD1_{1-118}$-V5 and $NCAN_{156-359}$-V5 were ligated for at least 30 minutes at room temperature according to the following setup:

Volume	Reagent	Final Concentration
x µL	insert	~18 ng
2 µL	dephosphorylated backbone plasmid	50 ng
4 µL	5x T4 Ligase Buffer	1x
1 µL	T4 Ligase (1 U/µL)	1 U
ad 20 µL	H_2O/DEPC	

As negative control one sample containing H_2O/DEPC instead of insert was prepared. 2 µL of the ligation mix were transformed into the *E. coli* strain One Shot® TOP10 (Section 2.4.4, p. 37). The next day three clones were picked and grown in suspension. Plasmid purification was performed (Section 2.4.5, p. 38) and sequenced with the primer pcDNA-for-1 and pcDNA-rev-1 (Table 10, p. 21). Sequences are given in Supplements 5.7.1 (p. 120).

2.3.4 Truncated Proteins Coding Plasmid pQE-30

For production and purification of the truncated proteins His_6-$DMXL2_{748-926}$-V5, His_6-$EML5_{897-1038}$-V5, His_6-$GPCPD1_{1-118}$-V5 and His_6-$NCAN_{156-359}$-V5 first the protein sequences of interest had to be cloned in the expression vector pQE-30 (Table 13, p. 23). This vector adds the sequence MRGS-His_6-GS at the amino-terminus of the truncated proteins.

$DMXL2_{748-926}$-V5-, $EML5_{897-1038}$-V5-, $GPCPD1_{1-118}$-V5- and $NCAN_{156-359}$-V5-coding inserts were amplified from corresponding pcDNA6/V5-HisA plasmids (Section 2.3.3, p. 33) using the primers given in Table 11 (p. 22) in the following setup:

Volume	Reagent	Final Concentration
10 µL	iProof™ High-Fidelity Master Mix (2x)	1x
1 µL	Prot-x-for (10 µM)	0.5 µM
1 µL	Prot-V5-rev (10 µM)	0.5 µM
0.5 µL	pcDNA6/V5-HisA-x	
ad 20 µL	H_2O/DEPC	

For amplification of the GC-rich sequence of $NCAN_{156-359}$-V5 3% DMSO was added. The PCR was run in the T3 Thermocycler (Biometra) using the following conditions:

98°C	1 min		
98°C	10 sec	denaturation	
56°C	30 sec	hybridization	35 cycles
72°C	30 sec	elongation	
72°C	10 min		
4°C	∞		

The whole reaction volume was loaded on an agarose gel (Section 2.2.5, p. 30). The PCR products of expected lengths were isolated using the QIAquick® Gel Extraction Kit (Qiagen) according to the manufacturer's description with elution in 12 µL of EB buffer. DNA concentration was determined (Section 2.2.2, p. 28) and the products were sequenced (Section 2.2.6, p. 30).

Correct PCR products were double digested for 3 hours at 37°C with the restriction enzymes BamHI-HF and SalI-HF (New England Biolabs):

Volume	Reagent	Final Concentration
6 µL	PCR product	300 ng
4 µL	Cut Smart™ buffer (10x)	1x
1 µL	BamHI-HF (20,000 U/mL)	20 U
1 µL	SalI-HF (20,000 U/mL)	20 U
ad 40 µL	H_2O/DEPC	

Digested PCR products were purified using the QIAquick® PCR-Purification Kit according to the manufacturer's instructions with elution in 12 µL of EB buffer. DNA concentration was determined (Section 2.2.2, p. 28).
The plasmid backbone pQE-30 was kindly provided by Jessica Bruder and digested for 3 hours at 37°C with the restriction enzymes BamHI-HF and SalI-HF (New England Biolabs):

Volume	Reagent	Final Concentration
7 µL	pQE-30 plasmid	4.9 µg
5 µL	Cut Smart™ buffer (10x)	1x
1.5 µL	BamHI-HF (20,000 U/mL)	30 U
1.5 µL	SalI-HF (20,000 U/mL)	30 U
ad 50 µL	H_2O/DEPC	

The whole reaction volume was loaded on an agarose gel (Section 2.2.5, p. 30). The digested plasmid backbone with length of 3.4 kb was isolated using the QIAquick® Gel Extraction Kit (Qiagen) according to the manufacturer's description with elution in 12 µL of EB buffer. DNA concentration was determined (Section 2.2.2, p. 28). 500 ng of digested plasmid were dephosphorylated using the Rapid DNA Dephos & Ligation Kit (Roche) according to the manufacturer's instructions.
The dephosphorylated backbone plasmid pQE-30 and the inserts coding for the truncated mouse proteins $DMXL2_{748-926}$-V5, $EML5_{897-1038}$-V5, $GPCPD1_{1-118}$-V5 and $NCAN_{156-359}$-V5 were ligated for 2 hours at room temperature according to the following setup:

Volume	Reagent	Final Concentration
x µL	insert	~90 ng
2 µL	dephosphorylated pQE-30 plasmid	50 ng
4 µL	5x T4 Ligase Buffer	1x
1 µL	T4 Ligase (1 U/µL)	1 U
ad 20 µL	H_2O/DEPC	

4 µL of the ligation mixes or non-digested pQE-30 plasmid were transformed into the *E. coli* strain MAX Efficiency® DH5αF'IQ (Section 2.4.4, p. 37). The next day five clones each were picked and grown in suspension. Plasmid purification was performed (Section 2.4.5, p. 38) and sequenced with

the primer pQE-for (5'-CCC GAA AAG TGC CAC CTG-3') and pQE-rev (5'-GTT CTG AGG TCA TTA CTG G-3'). Sequences are given in Supplements 5.7.2 (p. 122).

2.4 Handling of *E. coli* Cultures

2.4.1 Culture Conditions

As selection antibiotic ampicillin was used and added at a concentration of 0.1 mg/mL to either LB medium (Table 3, p. 18) or LB plates (LB medium supplemented with 0.15 % Bacto-Agar). *E. coli* bacteria were cultured in LB^{amp} medium or grown on LB^{amp} plates at 37°C. Suspension cultures shook at 225 rpm in receptacles containing 5x the culture volume of air to ensure sufficient aeration.

2.4.2 Determination of Cell Numbers

Cell numbers of *E. coli* bacteria were determined by measurement of the optical density (OD) at a wavelength of 600 nm. The OD was either measured in cuvettes with 1 cm of diameter at the UV-VISIBLE Recording spectrophotometer (Shimadzu) or at the spectrophotometer Nanodrop ND-1000 (Thermo Fisher Scientific) with the software "ND-1000 V3.2.1" (Thermo Fisher Scientific) in a 1 mm drop according to the user manual. At an OD of 1 or 0.1 respectively the culture was assumed to contain $1x10^9$ bacteria/mL.

Exact clone numbers were determined by spreading defined volumes of bacteria cultures on LB^{amp} plates (Section 2.4.1, p. 37), incubating them over night at 37°C and counting the clones at the next day.

2.4.3 Freezing and Thawing of *E. coli* Cultures

To store and preserve transformed *E. coli* cultures 50 % (v/v) of glycerol were added to LB^{amp} cultures and frozen at -80°C.

For thawing two times the volume of LB medium (Table 3, p. 18) was added. The bacteria were centrifuged for 15 minutes at 3000 g and 4°C and resuspended in at least five times the original volume of LB^{amp} medium (Section 2.4.1, p. 37). After shaking the cells for 1 hour at 225 rpm and 37°C they were diluted 1:8 and shook again for about 5 hours followed by plasmid isolation (Section 2.4.5, p. 38).

2.4.4 Plasmid Transformation in *E. coli* Cells

E. coli One Shot® TOP10 bacteria (Table 19, p. 27) were transformed by heat shock. The bacteria were thawn on ice. After adding 2 µL containing 10 pg to 100 ng of DNA sample the bacteria were incubated for 30 minutes on ice. As negative control samples containing pUC19 DNA were prepared which was provided by the manufacturer. The cells were heat-shocked for 30 seconds at 42°C in a water bath and cooled again for 2 minutes on ice. After adding 250 µL of pre-warmed S.O.C. medium (Invitrogen) the bacteria were shaken horizontally for 1 hour at 37°C and 225 rpm. Thereupon bacteria

were diluted to at least two different volumes and spread on LB^{amp} plates (Section 2.4.1, p. 37). At the next day single clones were resuspended in 3 mL of LB^{amp} medium and grown over night at 37°C (Section 2.4.1, p. 37).

E. coli MAX Efficiency® DH5αF'IQ bacteria (Table 19, p. 27) were transformed by heat shock as described above. Divergently 100 µL bacteria were thawed on ice in pre-cooled 10 mL round bottom tubes and 4 µL containing 10 ng DNA were added. Heat shock was performed for 45 seconds.

E. coli ElectroMAX DH10B™ bacteria (Table 19, p. 27) were transformed by electroporation. The bacteria were thawed on ice and 20 µL each were added to pre-cooled reaction tubes containing 2 µL DNA sample. As negative control samples containing pUC19 DNA which was provided by the manufacturer were prepared. The mixture was transferred into pre-cooled 0.1 cm electrode cuvettes (Bio-Rad) and shocked at 2.0 kV, 25 µF and 200 Ω using the Gene Pulser device (Bio-Rad). Immediately 1 mL of pre-warmed S.O.C. medium (Invitrogen) was added and after 1 hour of incubation at 37°C the bacteria were grown over night in 20 mL LB^{amp} medium (Section 2.4.1, p. 37) and in parallel diluted and spread on LB^{amp} plates to determine exact clone numbers (Section 2.4.2, p. 37).

2.4.5 Plasmid Isolation from *E. coli* Cells

Plasmids were isolated from 1 to 2 mL of *E. coli* cultures using the QIAprep Spin Miniprep Kit (Qiagen) according to the manufacturer's instructions. DNA was eluted in 35 µL EB buffer. For greater volumes of *E. coli* cultures, e.g. for the generation or PECP libraries (Section 2.3.1, p. 30), the HiSpeed Plasmid Maxi Kit (Qiagen) was employed according to the manufacturer's instructions.

2.5 Handling of Eukaryotic Cells

All centrifugation steps were performed for 6 minutes at 1,200 rpm (272 g) and 10°C in the centrifuge Heraeus® Megafuge 1.0 R.

2.5.1 Cultivation of Eukaryotic Cell Lines

Eukaryotic cells were cultured in tissue culture vessels of different sizes at 37°C and 5 % CO_2. Table 20 (p. 39) gives an overview over the used selection antibiotics for each eukaryotic cell line.

The cell line COS-7 and all its derivates, the cell lines LTK as well as the cell lines GP+E (Table 18, p. 26) grow adherent in the according media. When a cell density of 80 % was reached the cells had to be diluted. To singularize and detach them from the surface they were washed once in PBS (Table 2, p. 15) and incubated with Trypsin/EDTA (Invitrogen) for 15 minutes at 37°C and 5 % CO_2. After stopping the reaction with RPMI 1640 + L-Glutamine medium containing 5 % FCS the cells were centrifuged, counted (Section 2.4.2, p. 37) and cultivated again.

The cell lines 2D1 and B7 as well as their derivates grow in suspension in the according media. When a cell density of $1x10^6$/mL was reached the cells had to be diluted.

EBV-transduced B cells grow clotted in suspension in RPMI/complete medium (Table 3, p. 18) without antibiotic supplementation. Suspended single cells were removed and clots were downsized by soft shaking of the incubation bottle.

Table 20: Selection antibiotics for eukaryotic cell lines.
All cell lines (Table 18, p. 26) were cultivated in RPMI/complete medium (Table 3, p. 18) and the addition of according antibiotics. Concentrations of antibiotics for selection / normal cell culture are given in µg/mL.

Cell Line	Stable Transfection	Concentrations of Antibiotics	Antibiotics
2D1	TCR 2D1	- / 800	G418 (Invitrogen)
2D1-NFAT-sGFP‡	TCR 2D1, NFAT-sGFP	- / 800 2 to 6 / 3	G418 Blasticidin (Invitrogen)
B7	TCR B7	- / 800	G418
B7-NFAT-sGFP‡	TCR B7, NFAT-sGFP	- / 800 2 to 6 / 3	G418 Blasticidin
COS-7	-	-	
COS-7-A2	HLA-A*0201	- / 1500	G418
COS-7-A3‡	HLA-A*0301	3000 to 7000 / 1500	G418
COS-7-Cw06	HLA-Cw*0601	- / 1500	G418
GP+E-A2	HLA-A*0201	- / 500	G418
GP+E-B38	HLA-B*3801	- / 500	G418
LTK-A1	HLA-A*0101	- / 500	G418
LTK-A2	HLA-A*0201	- / 500	G418
LTK-A3	HLA-A*0301	- / 500	G418

‡ The cell line was generated during this thesis.

2.5.2 Counting of Eukaryotic Cells

Singularized adherent cells and cells growing in suspension were counted with an improved Neubauer counting chamber. Tryphanblue solution (Table 2, p. 15) was used as counter stain for dead cells as their perforated membranes allow transmigration of the colorant. Living cells in the four quadrants were counted under a light microscope, the average of this value was multiplied by the dilution factor of cell suspension with tryphanblue solution and the counting chamber constant of 10,000. The resulting value gave the number of cells per mL in the original suspension.

2.5.3 Freezing and Thawing of Eukaryotic Cells

For long term storage singularized adherent cells and cells growing in suspension were counted (Section 2.4.2, p. 37), centrifuged and resuspended in freezing medium (Table 3, p. 18) to a final concentration of $2x10^6$ cells/mL. 1.5 mL were filled in 1.8 mL cell freezing tubes and stored for 2 days at -80°C in freezing boxes (Thermo Scientific Nalgene, Langenselbold, D), allowing a temperature reduction of 1°C per hour. Then the tubes were transferred into liquid nitrogen tanks.

For thawing the cells were quickly warmed to 37°C, transferred in a 50 mL centrifugation tube filled with 40 mL RPMI 1640 + L-Glutamine medium and centrifuged. Freshly thawed cells were first

cultivated in RPMI/complete (Table 3, p. 18) medium for 2 days and then in medium containing the according antibiotics (Table 20, p. 39).

2.5.4 Fluorescence-Activated Cell Sorting of $CD3^+$ Blood Lymphocytes

Peripheral blood mononuclear cells (PBMC) were prepared from heparinized blood samples of voluntary donors by Ficoll density gradient centrifugation. 20 µL of a FITC-labeled antibody against CD3 (final concentration of 34 µg/mL, Table 15, p. 25) were added to 1 mL of PBMC, diluted to a final concentration of $1x10^6$ cells/mL in PBS (Table 2, p. 15) containing 1 % BSA. As isotype control FITC-labeled Mouse IgG1 was employed (Table 17, p. 26). After 30 minutes incubation on ice in the dark, the cells were washed with 1 mL PBS via centrifugation at 1,200 rpm (272 g) and 4°C for 6 minutes in the Megafuge 1.0 R (Heraeus). Samples of 1, 10 or 100 T cells were collected in 5.5 µL 5x buffer from the One Step RT-PCR Kit (Qiagen) via FACSorting at the FACSVantage SE (Becton Dickinson). FACSorting was performed by Wolfgang Klinkert.

2.5.5 FuGENE Transfection of Eukaryotic Cells

For the transfection of eukaryotic cells using the FuGENE® HD reagent the manufacturer's instructions were followed. Before transfection cells were cultivated in 3.5 cm dishes for at least 4 hours. Then 100 µL of RPMI 1640 + L-Glutamine medium containing 2 µg DNA were prepared and supplemented with 7 µL of pre-warmed FuGENE® HD transfection reagent. After an incubation of 10 minutes at room temperature the transfection mixture was dripped over the cells. Up and down scaling was performed according to these conditions. Empty-plasmid controls or samples containing no DNA served as negative controls.

2.5.6 Generation of the Stably Transfected Cell Lines 2D1-NFAT-sGFP and B7-NFAT-sGFP

The plasmid pcDNA6-NFAT-sGFP (Table 13, p. 23) was kindly provided by Katherina Siewert stored in samples of 30 µg at -20°C in precipitation mixture containing 0.1 volumes of 3 M sodium acetate and 2.5 volumes of ethanol. Two plasmid samples were centrifuged for 30 minutes at 4°C and 14,000 rpm (20,800 g) in the 5417 R Centrifuge (Eppendorf), washed twice in 500 µL ethanol, air dried and resuspended in 30 µL EB buffer (final concentration of 1 µg/µL).

2D1 and B7 T hybridoma cells (Table 18, p. 26) were washed twice in RPMI 1640 + L-Glutamine medium, counted (Section 2.5.2, p. 39) and resuspended in RPMI 1640 + L-Glutamine medium to a final concentration of $7x10^6$ cells per 800 µL.

First the plasmid suspensions were transferred in two 0.4 cm electrode cuvettes (Bio-Rad) on ice and then 800 µL of either B7 or 2D1 cells were added. Electroporation was performed at 280 V and 960 µF using the Gene Pulser device (Bio-Rad). After storing the cuvettes immediately on ice for 5 minutes the cells were transferred in 10 mL of pre-warmed RPMI/complete medium containing

0.8 mg/mL G418 (Table 20, p. 39). After leaving the cells at room temperature for 30 minutes they were incubated in total volumes of 30 mL in T75 cell culture flasks.
The next day the transfected cells were each separately cultivated in 48 wells of 24-well plates in RPMI/complete medium containing 0.8 mg/mL G418 and 2, 4 or 6 µg/mL blasticidin (Table 20, p. 39). To prevent evaporation of the medium the plates were stacked and wrapped in cling film. After 10 days grown single clones were isolated from wells containing 4 or 6 µg/mL blasticidin and further cultivated in 24-well plates in 1.5 mL RPMI/complete medium with 0.8 mg/mL G418 and 3 µg/mL blasticidin (Table 20, p. 39).
CD3 activation was performed from one tenth of each grown clone after 3 days (Section 2.5.8, p. 43). Clones that appeared green under the microscope (Section 2.5.9, p. 43) were analyzed by flow cytometry (Section 2.5.10, p. 43). The best clones were further cultivated in continuously greater volumes.

2.5.7 Generation of the Stably Transfected Cell Line COS-7-A3

The pRSV plasmid (Long et al., 1991) contains an SV40 origin of replication (ori) which allows replication in T antigen producing COS-7 cells. The plasmid pRSV-HLA-A3 (Table 13, p. 23) was kindly provided by Klaus Dornmair and purified by Geraldine Rühl. For stable transfection of COS-7 cells the HLA-A*0301 DNA fragment had to be inserted into the non-replicating plasmid backbone pHSE'-neo-B8 (Pircher et al., 1989, Table 13, p. 23). That would leave more replication capacity for later co-transfection with SV40 ori containing PECP library plasmids. Katherina Siewert kindly provided the backbone, which was digested with BamHI and SalI as well as dephosphorylated.
To obtain HLA-A*0301 DNA fragments pRSV-HLA-A3 plasmids were digested with the restriction enzymes BamHI and SalI (New England Biolabs) for 1 hour at 37°C:

Volume	Reagent	Final Concentration
2 µL	pRSV-HLA-A3 plasmid	5 µg
5 µL	NEB buffer 4 (10x)	1x
1 µL	BamHI-HF (20,000 U/mL)	20 U
1 µL	SalI-HF (20,000 U/mL)	20 U
ad 50 µL	H_2O/DEPC	

The whole reaction volume was loaded on an agarose gel (Section 2.2.5, p. 30) and the digested HLA-A*0301 DNA fragment with the length of 1.1 kb was isolated using the MinElute Gel Extraction Kit (Qiagen) according to the manufacturer's description with elution in 12 µL of EB buffer. DNA concentration was determined (Section 2.2.2, p. 28).
The backbone plasmid pHSE'-neo-B8 and the HLA-A*0301 DNA fragments were ligated for at least 30 minutes at room temperature according to the following setup:

Volume	Reagent	Final Concentration
x µL	HLA-A*0301 DNA fragments	25 ng
x µL	pHSE'-neo-B8 backbone plasmid	50 ng
4 µL	5x T4 ligase buffer	1x
1 µL	T4 Ligase (1 U/µL)	1 U
ad 20 µL	H_2O/DEPC	

As negative control one sample containing H_2O/DEPC instead of HLA-A*0301 DNA fragments was prepared. 2 µL of the ligation mix were transformed into the *E. coli* strain One Shot® TOP10 (Section 2.4.4, p. 37). The next day 5 clones were picked and grown in suspension. Plasmid purification was performed and sequenced with the primers pHSE3'-for (3'-CGC AGC CCG CAG AAC TCA GAA-5') and pHSE3'-rev (3'-AAA ACA TCA AGG GTC CCA TA-5'). DNA concentration was determined (Section 2.2.2, p. 28) and glycerol stocks were prepared from 1 mL of 2 colonies (Section 2.4.3, p. 37).

As transfection with linearized plasmids might render better stable transfectants pHSE3'-HLA-A3 plasmids were linearized from two colonies using the restriction enzyme AatII (New England Biolabs) according to the following setup:

Volume	Reagent	Final Concentration
x µL	pHSE3'-HLA-A3 plasmid	2 µg
2 µL	NEB buffer 4 (10x)	1x
1 µL	AatII (20,000 U/mL)	20 U
ad 20 µL	H_2O/DEPC	

Linearized as well as supercoiled plasmids of these two colonies were precipitated by adding 0.1 volumes of 3 M sodium acetate and 2.5 volumes of ethanol, incubation for at least 30 minutes at -80°C and centrifugation for 1 hour at 4°C and 14,000 rpm (20,800 g) in the 5417 R Centrifuge (Eppendorf). After discarding the supernatant the pellet was washed twice with 500 µL 70 % ethanol, air-dried and resuspended in 10 µL of EB buffer. DNA concentration was determined (Section 2.2.2, p. 28).

In 4 wells of a 24-well plate each 150,000 COS-7 cells were cultured (Section 2.5.1, p. 38) and transfected with either supercoiled or linearized pHSE3'-HLA-A3 plasmids using the FuGENE® transfection reagent (Section 2.5.5, p. 40). One additional well served as negative control.

After cultivation for 48 hours the transfected and non-transfected cells were singularized (Section 2.5.1, p. 38) and further cultivated in each 16 wells of 24-well plates containing 1.5 mL RPMI/complete medium with 3, 5 and 7 mg/mL G418 (Table 20, p. 39). To prevent evaporation of the medium the plates were stacked and wrapped in cling film. After 10 days, single clones were isolated and further cultivated in 1.5 mL RPMI/complete medium with 1.5 mg/mL G418 (Table 20, p. 39).

To verify the expression of HLA-A3 molecules one tenth of the best grown clones were resuspended in 100 µL of RPMI/complete medium (Table 3, p. 18), transferred in single wells of a 96-well plate and cultivated for 3 hours. Next 1 µL of PLP_{45-53} peptide (Table 14, p. 24) was loaded onto the cells, which is known to be presented on HLA-A3 and recognized by the TCR 2D1. After 3 hours to each

well 30,000 of 2D1-NFAT-sGFP T hybridoma cells (Table 18, p. 26) in 50 µL of RPMI/complete medium (Table 3, p. 18) were added. The next day expression of sGFP was analyzed under the fluorescence microscope Axiovert 200M (Section 2.5.9, p. 43). The best clones of the original 24-well plate were further cultivated in continuously greater volumes.

2.5.8 CD3 Activation of NFAT-sGFP T Hybridoma Cells

First the surface of different plates for cell cultures was coated with 1:500 in PBS diluted antibody against mouse CD3e (Table 15, p. 25) for 3 hours at 37°C. Then the supernatant was removed and NFAT-sGFP expressing T hybridoma cells were added (Section 2.5.6, p. 40). The next day sGFP expression in activated T hybridoma cells was analyzed at the fluorescence microscope (Section 2.5.9, p. 43) or by flow cytometry (Section 2.5.10, p. 43).

2.5.9 Fluorescence Microscopy for Detection of sGFP Expression in Eukaryotic Cells

Activated NFAT-sGFP expressing T hybridoma cells (Section 2.5.6, p. 40) were analyzed at the inverse fluorescence microscope AxioVert 200M (Zeiss). The expression of sGFP with an emission at 498/516 nm was detected with different Zeiss objectives (5x, NA 0.15; ∞/0, Epiplan-NEOFLUAR; 10x, NA 0.45 Plan Apochromat; 20x, NA 0.4; ∞/0-1.5 Achroplan, Korr Ph2), the CCD-camera CoolSNAP-HQ (Roper Scientific) and the fluorescence lamp HXP 120 (Visitron). To counter-check for autofluorescence a Cy3-filter (excitation/emission: 545(25)/605(70) nm, Zeiss) and to detect the sGFP expression a GFP-filter (excitation/emission at 472(30)/520(35) nm, BrightLine (Semrock, Rochester, USA)) were used. Light microscopy was performed with phase contrast illumination while the illumination times were 600 ms for the 5x and 20x objectives and 100 ms for the 10x objective. Pictures were taken in all three channels using the software "MetaMorph V6.3r6" from Visitron (Puchheim, D) and edited using the software "ImageJ 1.45s"(Wayne Rasband, National Institutes of Health, USA).

2.5.10 Flow Cytometry Analysis of sGFP Expression in Eukaryotic Cells

In single wells of a 96-well point button plate $1x10^5$ to $1x10^6$ cells were distributed (for cell counting Section 2.5.2, p. 39) and washed twice with 200 µL PBS (Table 2, p. 15). Next the cells were resuspended in 200 µL FACS buffer (Table 3, p. 18) containing 2 µg/mL of the dead cell stain ToPro-3 Iodide. 10,000 cells per sample were analyzed at the FACSCalibur device with excitation lasers for 488 nm and 633 nm. The data were analyzed using the software CellQuest V3.3 (Becton Dickinson) or FlowJo V7.6 (Tree Star, Ashland USA)

2.5.11 Flow Cytometry Analysis of HLA-A2 Expression

In single wells of a 96-well point button plate $1x10^5$ to $1x10^6$ cells (for cell counting Section 2.5.2, p. 39) were distributed and washed twice with 200 µL PBS (Table 2, p. 15). The cells were stained for

30 minutes on ice with either the FITC-conjugated antibody against HLA-A2 (Table 15, p. 25) or the FITC-conjugated isotype control (Table 17, p. 26) diluted 1:50 in FACS buffer (Table 3, p. 18). Next the cells were resuspended in 200 µL FACS buffer containing 0.17 µM of the dead cell stain ToPro-3 Iodide. 10,000 cells per sample were analyzed at the FACSVerse (BD Biosciences) with excitation lasers for 488 nm and 633 nm. The data were analyzed using the software FACSuite Version 1.0.4.2650 (BD Biosciences) and FlowJo V7.6 (Tree Star).

2.6 Analysis of Peptides and Proteins

2.6.1 Determination of Protein Concentration

Quick determination of protein concentration was performed at the spectrophotometer Nanodrop ND-1000 (Thermo Fisher Scientific) with the software "ND-1000 V3.2.1" according to the user manual at a wavelength of 280 nm. Final concentration was determined by multiplying the proteins molecular weight with the quotient of Nanodrop data and the extinction coefficient given by http://web.expasy.org/protparam/.

For determination of concrete protein concentration the Pierce® BCA Protein Assay Kit (Thermo Fisher Scientific) was employed according to the manufacturer's instructions. Right before use one tablet of Complete Protease Inhibitors (Roche) was added to 50 mL of RIPA buffer (Table 2, p. 15). Protein probes were measured in diluted series. Plates were analyzed at 540 nm wavelength with the VICTOR² 1420 Multilabel Counter (Perkin Elmer).

2.6.2 Peptide and Protein Lyophilization

For longtime storage peptides and proteins were lyophilized using the Scan Speed 40 centrifuge for speed vacuum concentration (Labogene, Lynge, DK). Lyophilization occurred after approximately 2 to 3 hours of centrifugation at 2,000 rpm and 37°C. In some cases centrifugation over night was necessary.

2.6.3 Mass Spectrometry of Peptides and Proteins

For rough sequence confirmation of proteins matrix-assisted laser desorption ionization - time of flight mass spectrometry (MALDI-TOF-MS) was performed. Probes were prepared from Coomassie-stained SDS polyacrylamide gels (Section 2.6.4, p. 44) and measured by Reinhard Mentele (Max Planck Institute of Biochemistry, Martinsried, D).

Peptide sequences were determined by electrospray ionization mass spectrometry (ESI-MS) by Peer-Hendrik Kuhn (German Center of Neurodegenerative Diseases, Munich, D).

2.6.4 SDS Polyacrylamide Gel Electrophoresis

For protein analysis SDS polyacrylamide gel electrophoresis (SDS-PAGE) was performed. Under reducing conditions samples were mixed with 3x reducing SDS loading buffer (Table 2, p. 15) and

incubated at 95°C for 5 minutes. Under non-reducing conditions, samples were mixed with 5x SDS loading buffer (Table 2, p. 15). After 3 minutes of centrifugation at 14,000 rpm (20,800 g) in the 5417 R Centrifuge (Eppendorf) up to 20 µL were loaded onto ready-to-use SDS gels.

For Novex® 4-20 % Tris-Glycine Mini Gels (Invitrogen) electrophoresis was performed in a "Mighty Small" device (Hoefer, San Francisco, USA) with SDS running buffer (Table 2, p. 15) for 90 minutes at 120 V. Either the molecular weight standard Wide Range Sigma Marker™ or the Sigma Full Range Rainbow™ Marker when subsequent Western Blot analysis should be performed (Section 2.6.5, p. 45) were used.

For Novex® NuPAGE 12 % Bis-Tris Gels (Life Technologies) electrophoresis was performed in a Mighty Small device with 1x NuPAGE® MOPS SDS running buffer (Life Technologies) for 60 minutes and 150 V. As molecular weight standard the See Blue® Plus 2 Prestained Standard (Life Technologies) was employed.

After running the gels they were either blotted (Section 2.6.5, p. 45) or directly swiveled in Coomassie staining solution for 30 minutes. Subsequently unspecific background staining was removed through washing in destaining solution for 1 hour (solutions see Table 2, p. 15). To gain even clearer stainings, the gels were swiveled over night at 4°C in 10 % acidic acid. SDS gels were shrink-wrapped and stored at 4°C.

For low amounts of protein silverstaining according to Shevchenko et al. (1996) was performed. Coomassie-stained SDS gels were shaken for 10 minutes each first in 50 % methanol supplemented with 5 % acidic acid, second in 50 % methanol and third in H_2O. After 1 minute of incubation in 0.02 % sodium thiosulfate the gel was washed three times for 1 minute in H_2O. Next the gel was shaken for 20 minutes in pre-cooled 0.1 % silver nitrate at 4°C. After washing twice for 1 minute in H_2O the staining was developed in freshly prepared 2 % sodium carbonate supplemented with 0.04 % formaldehyde. The staining reaction was stopped with 5 % acidic acid.

2.6.5 Western Blot

During Western Blot analysis proteins were transferred electrophoretically from SDS gels onto PVDF membranes for detection of specific proteins. Buffers are listed in Table 2 (p. 15).

An 8.5x8.5 cm square of PVDF membrane (Hybond™-P, GE Healthcare) was activated in methanol and rinsed in H_2O. In a semi-dry apparatus the following layers from bottom (anode) to top (cathode) were placed: two 9x9 cm squares of anode buffer-soaked Whatman paper (GE Healthcare), the activated 8.5x8.5 cm square of PVDF membrane, the SDS gel (Section 2.6.4, p. 44) and two 9x9 cm squares of cathode buffer-soaked Whatman paper. During 3 hours of electrophoresis at 35 mA per gel proteins, that are surrounded by negatively charged SDS, were transferred onto the positively charged PVDF membrane.

Subsequently the SDS gel was stained with Coomassie (Section 2.6.4, p. 44). The PVDF membrane was shaken for 1 hour at room temperature or over night at 4°C in Western Blot blocking buffer. After rinsing the blocking buffer, the membrane was stained for 1 hour with a protein-specific primary antibody diluted in Western Blot blocking buffer. After 3x washing for 5 minutes in 0.05 %

Tween-20/PBS the membrane was incubated for 1 hour with a secondary HRP-conjugated antibody diluted in Western Blot blocking buffer. Next the membrane was washed 3x for 5 minutes in 0.05 % Tween-20/PBS and placed on a piece of cling film. The membrane was covered with 10 mL enhanced chemiluminescence-A (ECL-A) solution complemented with 100 µL of ECL-B solution and 3.1 µL of H_2O_2. After rinsing the membrane was placed in a film cassette and developed on an Amersham HyperfilmTM ECL high performance chemiluminescence film at the x-ray developer machine OPTIMAX® (Protec, Oberstenfeld, D).

2.6.6 Coupling of IgG Antibodies to Protein G Dynabeads

For the purification of HLA-A2 molecules from cell lysates the anti-HLA-A2 antibody BB7.2 (Table 15, p. 25) was coupled to Protein G Dynabeads (Life Technologies).

After washing 3 mL (= 90 mg) of Protein G Dynabeads with 10 mL PBS (Table 2, p. 15) 720 µL (= 720 µg) anti-HLA-A2 antibody were added in a total amount of 10 mL PBS. The antibody was bound to Protein G during 1 hour of incubation at room temperature with shaking. Next the Dynabeads were washed once with 10 mL PBS and twice with Dynabead conjugation buffer (Table 2, p. 15) and coupled chemically to the antibody shaking for 30 minutes at room temperature in 12.6 mL Dynabead conjugation buffer containing 5 mM bis(sulfsuccinimidyl)suberate (BS^3). After washing the Dynabeads once in 10 mL of Dynabead conjugation buffer the coupling was repeated with fresh 12.6 mL of conjugation buffer containing 5 mM BS^3. The reaction was stopped by adding 600 µL 1 M Tris-HCl (pH 7.5). After washing the coupled Dynabeads three times with PBS they were stored at 4°C.

2.6.7 Preparation of Proteins from Eukaryotic Cell Lines

In each two wells of 6-well plates 500,000 COS-7-A2 cells were seeded (Table 18, p. 26) and transfected with pcDNA6-DMXL2$_{748-926}$-V5, pcDNA6-EML5$_{897-1038}$-V5, pcDNA6-GPCPD1$_{1-118}$-V5, pcDNA6-NCAN$_{156-359}$-V5 or empty pcDNA6/Vh-HisA plasmids (Section 2.3.3, p. 33) using the FuGENE® transfection reagent (Section 2.5.5, p. 40). After 24 and 48 hours one well each was singularized and centrifuged for 6 minutes at 1,200 rpm (272 g) and 10°C in the centrifuge Heraeus® Megafuge 1.0 R. The supernatants were removed and the cell pellets frozen at -20°C.

As lysis buffer one tablet Complete Protease Inhibitors (Roche) was solved in 50 mL PBS and stored in aliquots of 500 µL at -20°C. After thawing the cell pellets were resuspended in 500 µL of PBS/Complete, transferred in protein low-binding 1.5 mL reaction tubes (Eppendorf) and disrupted with 30 ultrasound pulses using the Sonifier 450 (Branson). Subsequently all samples were centrifuged for 30 minutes at 14,000 rpm (20,800 g) and 4°C in the 5417 R Centrifuge (Eppendorf). The supernatants were transferred in new protein low-binding 1.5 mL reaction tubes. Pellets and supernatants were stored at -20°C for further experiments.

2.6.8 Preparation of Peptides Presented on HLA-A2 by ConA 4B Chromatography

Peptides presented on HLA-A2 molecules were obtained from EBV-transducted B cells (Table 18, p. 26). EBV-16488 and EBV-17490 cells express human HLA-A2, EBV-FE cells served as negative control. All buffers are given in Table 2, p. 15.

1.5 x 10^9 of each EBV cell line were collected in PBS containing 0.05 % EDTA and stored at -20°C until further analysis. Cells were thawed on ice and washed twice with 20 mL PBS by centrifugation for 6 minutes and 1,200 rpm (272 g) at 4°C in the centrifuge Heraeus® Megafuge 1.0 R. After lysis in 100 mL of EBV lysis buffer freshly supplemented with two tablets of Complete protease inhibitors (Roche) for 30 minutes at 4°C the cells were centrifuged for 5 minutes at 4°C and 300 g in the Avanti® J-26 XP Centrifuge (Beckman Coulter) using the JA-10 rotor. The supernatants were transferred in 38.5 mL Ultra-Clear™ tubes (Beckman Coulter) and centrifuged for 30 minutes at 150,000 g and 4°C in the OPTIMA XE90 ultracentrifuge (Beckman Coulter).

After filtration of the supernatants through 45 µm filter units the contents of 1 mL HiTrapTM ConA 4B columns, 1 mM $MnCl_2$ and 1 mM $CaCl_2$ were added. To allow sufficient binding of glycosylated proteins in the batch procedure the suspensions of beads and samples were shaken on ice at 4°C for 1 hour. Following centrifugation for 5 minutes at 4°C and 1,200 rpm (272 g) in the centrifuge Heraeus® Megafuge 1.0 R the HiTrapTM ConA 4B column material was washed three times with 10 mL of EBV binding buffer freshly supplemented with Complete protease inhibitors (Roche). After centrifugation for 10 minutes at 1,200 rpm (272 g) and 4°C in the centrifuge Heraeus® Megafuge 1.0 R bound glycosylated proteins were eluted for 5 minutes in 2 mL EBV elution buffer freshly supplemented with Complete protease inhibitors (Roche). Centrifugation and elution were repeated, the total amount of 4 mL eluate was pooled and incubated with 1 mL (= 30 mg) anti-HLA-A2-coupled Protein G Dynabeads® (Section 2.6.6, p. 46) for 1 hour at room temperature.

The Dynabeads were washed 3x with 6 mL EBV elution buffer, twice with 6 mL PBS containing 2 mM dodecylmaltoside, twice with PBS and 11x with H_2O. The HLA-A2 alpha chain, the β_2-microglobulin and the bound peptides were denatured and eluted for 30 minutes in 2 mL of 0.2 % formic acid. The eluates were filtered for 90 minutes in 3 K Amicon® Ultra centrifugal filters (Millipore). The peptide-containing flow-through was additionally filtered through 0.22 µm filter units and 100 µL were cleaned using 0.5 mL Pierce® Detergent Removal spin columns according to the manufacturer's instructions with PBS as washing reagent.

All steps of the HLA-A2 purification were monitored by SDS-PAGE (Section 2.6.4, p. 44) and subsequent HLA-A2-specific western blot analysis (Section 2.6.5, p. 45). The peptides were analyzed by ESI mass spectrometry (Section 2.6.3, p. 44).

2.6.9 Preparation of Peptides Presented on HLA-A2 by Lentil-Lectin Chromatography

Peptides presented on HLA-A2 molecules were obtained from EBV-transducted B cells (Table 18, p. 26). EBV-16488 and EBV-17490 cells express human HLA-A2, EBV-FE cells served as negative control. All buffers are given in Table 2, p. 15.

1.5×10^9 of each EBV cell line were collected in PBS containing 0.05 % EDTA and stored at -20°C until further analysis. Cells were thawed on ice and washed twice with 20 mL PBS by centrifugation for 6 minutes and 1,200 rpm (272 g) at 4°C in the centrifuge Heraeus® Megafuge 1.0 R. After washing the pellets in 20 mL of lentil lectin equilibration buffer they were resuspended in 20 mL of lentil lectin lysis buffer freshly supplemented with Complete protease inhibitors (Roche) and disrupted for 15 minutes on ice with ultrasound pulses using the Sonifier 450 (Branson). The lysates were centrifuged for 5 minutes at 4°C and 300 g in the Avanti® J-26 XP Centrifuge (Beckman Coulter) using the JA-10 rotor. The supernatants were transferred in 38.5 mL Ultra-Clear™ tubes (Beckman Coulter) and centrifuged for 30 minutes at 150,000 g and 4°C in the OPTIMA XE90 ultracentrifuge (Beckman Coulter).

After filtration of the supernatants through 45 µm filter units they were loaded with a flow rate of 1 mL/min onto 1.5 x 10 cm Luer-Lock columns with flow adapters (Sigma-Aldrich) containing 1 mL lentil lectin agarose that were equilibrated with lentil lectin equilibration buffer and lentil lectin lysis buffer. The columns were washed with 15 mL of lentil lectin wash buffer freshly supplemented with Complete protease inhibitors (Roche). Glycosilated proteins were eluted in 4 mL of lentil lectin elution buffer and incubated with 1 mL (= 30 mg) anti-HLA-A2-coupled Protein G Dynabeads® (Section 2.6.6, p. 46) for 1 hour at room temperature.

Dynabeads were washed twice with 6 mL of lentil lectin elution buffer and 4x with H_2O. The HLA-A2 alpha chain, the β_2-microglobulin and the bound peptides were denatured and eluted for 30 minutes in 2 mL of 0.2 % formic acid. The eluates were filtered for 60 minutes in 3 K Amicon® Ultra centrifugal filters (Millipore). The peptide-containing flow-through was additionally filtered through 0.22 µm filter units and 100 µL were cleaned using 0.5 mL Pierce® Detergent Removal spin columns according to the manufacturer's instructions with PBS as washing reagent.

All steps of the HLA-A2 purification were monitored by SDS-PAGE (Section 2.6.4, p. 44) and subsequent HLA-A2-specific western blot analysis (Section 2.6.5, p. 45). The peptides were analyzed by ESI mass spectrometry (Section 2.6.3, p. 44).

2.6.10 Production and Purification of Soluble Proteins in *E. coli*

Truncated protein His_6-$DMXL2_{748-926}$-V5-, His_6-$EML5_{897-1038}$-V5-, His_6-$GPCPD1_{1-118}$-V5- and His_6-$NCAN_{156-359}$-V5-coding bacteria and bacteria carrying empty pQE-30 plasmids (Section 2.3.4, p. 35) were grown over night in 400 mL of LB^{amp} medium (Table 3, p. 18) containing 1 % glucose. Transport of glucose into the bacterial cell blocks activity of the *lac* operon.

To remove the glucose, bacteria were centrifuged for 10 minutes at 4,000 rpm (2,844 g) and 4°C in the Avanti® J-26 XP Centrifuge (Beckman Coulter) using the JA-10 rotor. The pellet was resuspended in 2 L LB medium and grown to an OD at 600 nm of 0.4 to 0.6. Protein production was induced by adding 1 mM isopropyl β-D-1-thiogalactopyranoside (IPTG). After 4 hours the 2 L of bacteria culture were centrifuged for 10 minutes at 4,000 rpm (2,844 g) and 4°C in the Avanti® J-26 XP Centrifuge (Beckman Coulter) using the JA-10 rotor. Bacterial pellets were transferred into 50 mL reaction tubes, weighed and stored at -20°C.

Soluble proteins containing a His_6 tag were purified by nickel chelate affinity chromatography according to the QIAexpressionist™ system of Qiagen. All steps in solutions containing 6 M urea were performed at room temperature. Buffers are given in Table 2 (p. 15).

About 3.3 g of bacterial pellet were thawed, resuspended in 100 mL of urea lysis buffer and disrupted for 15 minutes with ultrasound pulses using the Sonifier 450 (Branson). The lysate was centrifuged for 1 hour at 10,000 g and 20°C in the Avanti® J-26 XP Centrifuge (Beckman Coulter) using the JA-10 rotor. Pellets were stored at -20°C and the target protein-containing supernatant was loaded with a flow rate of 1 to 1.5 mL/min onto 5 mL Ni-NTA agarose in 1.5 x 10 cm Luer-Lock columns with flow adapters (Sigma-Aldrich). Imidazol in the urea lysis buffer should block unspecific binding of proteins to the Ni-NTA agarose. Columns were washed with 50 mL urea wash buffer.

The truncated proteins His_6-$DMXL2_{748-926}$-V5, His_6-$EML5_{897-1038}$-V5, His_6-$GPCPD1_{1-118}$-V5 and His_6-$NCAN_{156-359}$-V5 as well as the negative control from bacteria carrying the empty pQE-30 plasmid were eluted from the Ni-NTA columns at a fast protein liquid chromatography (FPLC) system. It contains a LCC-501 Plus controller that operates two pumps and an Uvicord SD UV-detector monitoring protein elution at 277 nm. Both pumps were first flushed with H_2O and then loaded with urea wash buffer and urea elution buffer. One Ni-NTA column was connected and washed with urea wash buffer until no more unspecific proteins were detected. Then the truncated protein His_6-$DMXL2_{748-926}$-V5, His_6-$EML5_{897-1038}$-V5, His_6-$GPCPD1_{1-118}$-V5 and His_6-$NCAN_{156-359}$-V5 or the negative control from bacteria carrying the empty pQE-30 plasmid were eluted with urea elution buffer.

The protein peaks were collected, concentrated in Ultracel® 10 K Amicon® Ultra Centrifugal Filters (Millipore) to an amount of 3 mL and dialyzed against H_2O over night in Novagen® D-Tube™ Dialyzer Maxi 3.5 kDa tubes (EMD Chemicals, San Diego, USA). Protein purity was analyzed by SDS-PAGE (Section 2.6.4, p. 44) and the dialyzed samples were lyophilized (Section 2.6.2, p. 44). Protein amount was determined using the Pierce® BCA Protein Assay Kit (Section 2.6.1, p. 44).

2.6.11 Production and Purification of the HLA-A2 alpha Chain in *E. coli*

Production and purification of the inclusion body (IB)-forming HLA-A2 alpha chain was performed according to the protocols in Altman and Davis (2003) and Nagai and Thøgersen (1987). All buffers are given in Table 2 (p. 15).

Geraldine Rühl kindly provided BL21(DE3) *E. coli* bacteria transformed with pET21c(+) plasmid coding for the avidin tagged HLA-A2 alpha chain. Bacteria were pre-cultured at 37°C over night in 100 mL LB^{amp} medium (Table 3, p. 18) containing 1% glucose. Transport of glucose into the bacterial cell blocks activity of the *lac* operon.

To remove the glucose 60 mL of the pre-culture were centrifuged for 5 minutes at 4,000 rpm (2,844 g) in the centrifuge Heraeus® Megafuge 1.0 R and resuspended in 3 L of LB^{amp} medium. After 3 to 4 hours the cells reached an OD of 0.6 to 1.0 at 600 nm and protein production was induced by adding 0.4 mM IPTG. After additional 4 hours of incubation the cells were centrifuged for 30 minutes at

4,000 rpm (2,844 g) and 4°C in the Avanti® J-26 XP Centrifuge (Beckman Coulter) using the JA-10 rotor. Bacterial pellets were transferred into 50 mL reaction tubes, weighed and stored at -80°C.

Cells (approximately 10 g) were thawed on ice and suspended in 12 mL of IB lysis buffer freshly supplemented with 20 mg of lysozyme. After incubation for 30 minutes on ice $MgCl_2$, $MnCl_2$ and DNase I were added to final concentrations of 10 mM, 1 mM and 10 µg/mL respectively. After incubation for 30 minutes on ice 20 mL of IB detergent buffer were added. The lysated cells were centrifuged twice for 10 minutes at 5,000 g in the Avanti® J-26 XP Centrifuge (Beckman Coulter) using the JA-10 rotor. The supernatant was removed and the pellet washed three times in 20 mL of IB wash buffer by centrifugation for 10 minutes at 5,000 g in the Avanti® J-26 XP Centrifuge (Beckman Coulter) using the JA-10 rotor.

Pellets were resuspended in 15 mL urea solution. After centrifugation of the solubilized IBs for 30 minutes at 150,000 g and 20°C in the OPTIMA XE90 ultracentrifuge (Beckman Coulter) and 38.5 mL Ultra-Clear™ tubes (Beckman Coulter) the supernatant was transferred into a 50 mL reaction tube. Protein concentration was measured using the Nanodrop ND-1000 (Section 2.6.1, p. 44) and aliquots of 1 mL were stored at -80°C.

2.6.12 Refolding of Peptide:HLA-A2 Complexes

Refolding of peptide:HLA-A2 complexes using the peptides $TAX_{11\text{-}19}$ (LLFGYPVYV), $DMXL2_{813\text{-}820}$ (LIGEVFNI), $EML5/6_{997\text{-}1004}$ (MEGEVWGL), $GPCPD1_{15\text{-}22}$ (LPGEVFAI) and $NCAN_{257\text{-}264}$ (LGGEVFYV) was performed as described in Altman and Davis (2003). All buffers are given in Table 2 (p. 15).

5 mM reduced glutathione, 0.5 mM oxidized glutathione and 0.2 mM PMSF in 2-propanol were added to folding buffer at 4°C. Vials of 620 ng HLA-A2 alpha chain (Section 2.6.11, p. 49) and 480 ng β_2-microglobulin (kindly provided by Geraldine Rühl) were thawn and filled up to 500 µL each by adding injection buffer. 20 mL of freshly supplemented folding buffer were stirred at high speed and 4°C. 200 ng of peptide dissolved in 40 µL DMSO were added drop wise. Next 500 µL β_2-microglobulin followed by 500 µL HLA-A2 alpha chain were injected forcefully close to the stirring rod. After 24 hours again 620 ng of HLA-A2 alpha chain were filled up to 500 µL with injection buffer and injected forcefully. The refolding reactions were stirred at 4°C for 16 hours.

Subsequently the refolding reactions were transferred in 38.5 mL Ultra-Clear™ tubes (Beckman Coulter) and centrifuged for 1 hour at 4°C and 200,000 g in the OPTIMA XE90 ultracentrifuge (Beckman Coulter). The supernatants were concentrated to a final volume of 1 mL in Ultracel® 10 K Amicon® Ultra Centrifugal Filters (Millipore).

The refolded peptide:HLA-A2 complexes were dialyzed for 60 hours against 1 L of biotinylation buffer using 4 Spectra/Por® Dialysis Membranes with a molecular weight cut-off of 12 to 14 kDa (Spectrum Laboratories, Rancho Dominguez, USA). The dialyzed samples were concentrated to a final volume of 150 µL using Ultracel® 10K Amicon® Centrifugal Filters (Millipore) at 4°C.

2.6.13 Enzymatic Biotinylation of Peptide:HLA-A2 Complexes

For enzymatic biotinylation of peptide:HLA-A2 complexes (Section 2.6.12, p. 50) the following setup was incubated over night at room temperature:

Volume	Reagent	Final Concentration
100 µL	1 M Tris-HCl (pH 7.5)	100 mM
40 µL	5 M NaCl	200 mM
5 µL	1 M $MgCl_2$	5 mM
4 µL	100 mM biotin in 200 mM Tris base	0.4 mM
50 µL	100 mM ATP	5 mM
2 µL	100 mM PMSF in 2-propanol	0.2 mM
100 µL	Peptide:HLA-A2 complex	
1.5 µL	BirA500 Biotin-Protein Ligase (1 mg/mL)	
ad 1 mL	H_2O	

Precipitated material was removed via 15 minutes of centrifugation at 14,000 rpm (20,800 g) and 4°C in the 5417 R Centrifuge (Eppendorf). The supernatants were concentrated to 100 µL in Ultracel® 10 K Amicon® Ultra Centrifugal Filters (Millipore). Finally the samples were washed six times in the centrifugal concentrator by adding 100 µL of 20 mM Tris-HCl (pH 8.0).

2.7 Characterization of Potentially Autoaggressive T Cells from Frozen Tissue Sections of MS Patient FE

TCR alpha- and beta-chains were generally designated according to IMGT nomenclature (Lefranc and Lefranc, 2001) but the V segments were named according to Arden et al., 1995.

2.7.1 Establishment of Immunofluorescent Staining

For the establishment of immunofluorescent staining 10 µm tissue sections of tonsil and an inflamed brain area of patient OIND-1 on glass slides (P.A.L.M. Microlaser Technologies) were employed. The customized bovine serum albumin (BSA)-free antibody anti-CD8 beta (Table 15, p. 25) (Beckman Coulter) was labeled with the Cy3™ mAb Labeling Kit (Amersham, Freiburg, D) according to the manufacturer's instructions. Final concentration of labeled antibody was not determined.

Prior to staining, the slides were thawed, fixed 5 minutes in pre-cooled 100 % acetone and blocked at room temperature for 5 minutes in PBS (Table 2, p. 15) containing 2 % BSA (Sigma-Aldrich) inside a wet chamber. Subsequently the sections were incubated in a dark, wet chamber for 5 minutes in 100 µL of primary antibody (Table 15, p. 25) diluted in PBS, then rinsed with 2 mL of PBS and incubated again in a dark, wet chamber for 5 minutes in 100 µL of secondary antibody (Table 16, p. 26) diluted in PBS. Negative controls were incubated in 100 µL of secondary antibody (Table 16, p. 26) diluted in PBS. After rinsing the slices again with 2 mL of PBS, one drop of "Fluorescent Mounting Medium" (Dako) and a cover glass were applied. The stainings were analyzed under an Axioplan 2 microscope (Zeiss).

2.7.2 Laser Microdissection of Single Cells from Tissue Sections of MS Patient FE

All steps needed strict RNase-free conditions. Therefore the laser microdissection was performed in a separate, UV-irradiated room, wearing protective clothing. The working surfaces and devices were cleaned with RNase ZAP (Sigma-Aldrich), H_2O/DEPC and 80 % ethanol before and after usage.

PET Membrane slides 1.0 (Zeiss) were prepared as described in Section 2.2.3 (p. 28) but were incubated for 1 min in RNase ZAP and washed twice with H_2O/DEPC between baking and coating. 10 µm thick cryostat sections from frozen tissue blocks of MS patient FE were mounted on the slides and stored them at -80°C.

For laser microdissection the slides were thawed, dried 1 minute in vacuum and dipped shortly in pre-cooled acetone. After rehydration with 100 µL PBS/DEPC (Table 2, p. 15) the slides were blocked 3 minutes in 100 µL PBS/DEPC containing 2 % BSA inside a wet chamber. Then the sections were co-incubated for 5 minutes in a wet, dark chamber with a 1:100 diluted, Cy3-labeled antibody against CD8 beta and either a 1:25 diluted, FITC-labeled antibody against TCR BV13S1, or a 1:25 diluted, FITC-labeled antibody against TCR BV22, or a 1:100, diluted FITC-labeled antibody against CD134 (Table 15, p. 25). After washing with 1 mL of PBS/DEPC the slides were incubated for 3 minutes inside a wet, dark chamber with the 1:100 diluted aFITC-Alexa488 antibody (Table 16, p. 26). Finally the slides were washed with 1 mL of PBS/DEPC, covered with 300 µL 1-propanol and analyzed immediately under the Axiovert 200M microscope (Zeiss).

Therefore the LD Plan-NEOFLUAR objective 40x/0.6 Korr, ∞/0-1.5 (Zeiss), the CCD-camera CoolSNAP-HQ (Roper Scientific, Martinsried, D), the fluorescence lamp HXP 120 (Visitron, Puchheim, D), the Robo Mover and the software "P.A.L.M. Robo Software V3.2.0.11" (P.A.L.M. Microlaser Technologies) were employed.

After evaporation of the 1-propanol, cells that were either double positive for CD8 beta and TCR BV13S1, TCR BV22 or CD134 or that were single positive for CD8 beta were marked and catapulted by laser pressure into mineral oil coated lids of single 200 µL reaction tubes. Single isolated cells were instantly stored on dry ice until reverse transcription PCR (RT-PCR) was performed (Section 2.7.3, p. 52).

2.7.3 RT-PCR of TCR Alpha- and Beta Chains

Two different approaches were employed for either unbiased (microdissected CD8 beta single positive or CD8 beta and CD134 double positive cells) or TCR-biased experiments (microdissected CD8 beta and TCR BV13S1 as well as CD8 beta and TCR BV22 double positive cells). The One Step RT-PCR kit (Qiagen) was used for both. Consecutively sets of six single isolated cells were transferred from dry-ice on ice before adding the RT-PCR mix and then directly put into the pre-cooled centrifuge.

For the "unbiased approach" 12.5 µL of RT-PCR reaction mix containing 0.625 µM of the Cα-out and Cβ-out primers (Table 4, p. 18) were added:

Volume	Reagent	Final Concentration
2.5 µL	5x buffer	1x
1 µL	dNTP-mix (10 mM each)	8 mM
0.078 µL	Cα-out (100 µM)	0.625 µM
0.078 µL	Cβ-out (100 µM)	0.625 µM
1 µL	enzyme mix	N/A
ad 12.5 µL	RNase-free H_2O	

For the TCR-biased "clone-specific approach" 20 µL of RT-PCR reaction mix containing 0.625 µM of the Cα-RT-imp and Cβ-RT-2 primers (Table 4, p. 18) were added:

Volume	Reagent	Final Concentration
4 µL	5x buffer	1x
0.8 µL	dNTP-mix (10 mM each)	4 mM
0.125 µL	Cα-RT-imp (100 µM)	0.625 µM
0.125 µL	Cβ-RT-2 (100 µM)	0.625 µM
0.8 µL	enzyme mix	N/A
ad 20 µL	RNase-free H_2O	

As microdissected cells stuck to the mineral oil coated lids of the reaction tubes (Section 2.7.2, p. 52), RT-PCR mixes had to be added into the lids and centrifuged down for 5 minutes at 4°C and 14,000 rpm (20,800 g) in the 5417 R Centrifuge (Eppendorf). RT-PCR was performed for 35 minutes at 50°C. Mineral oil-coated reaction tubes without microdissected cells served as negative control.
When RT-PCR was performed on FACS-sorted $CD3^+$ blood lymphocytes (Section 2.5.4, p. 40) or RNA samples, the volumes of the reaction mixes were adjusted to the mentioned final concentrations.
Later during the course of this thesis 0.2 U/µL of RNase OUT™ Ribonuclease Inhibitor (Invitrogen) were added into both RT-PCR reaction mixes for enhanced RNA preservation.

2.7.4 Basic Protocol of Clone Specific TCR Beta Chain PCR

Figure 7 (p. 54) gives an overview over all PCR steps of the TCR-biased "clone specific approach" to characterize TCR beta chains.

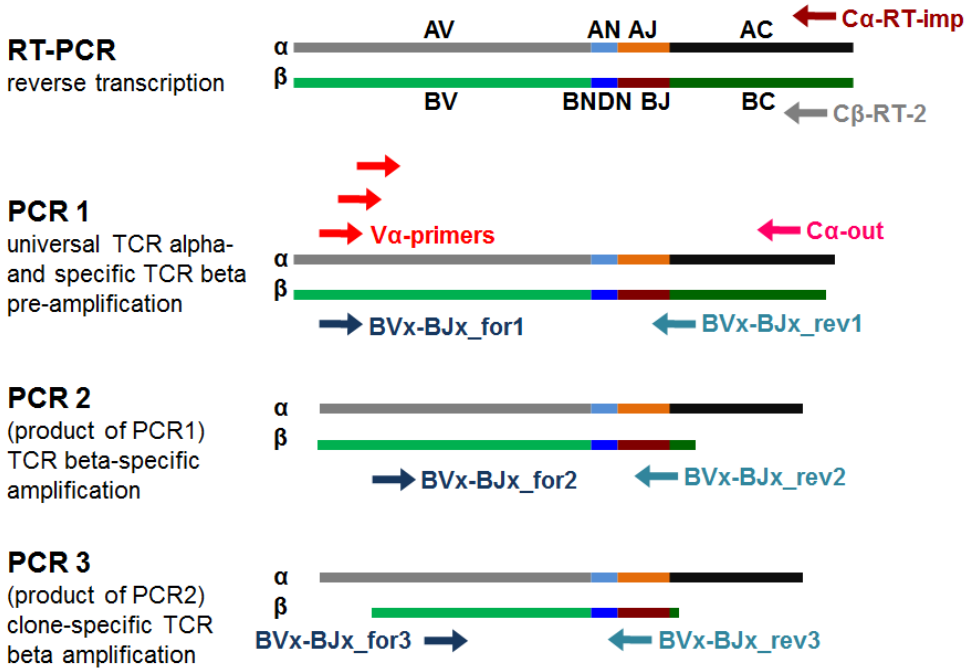

Figure 7: Relative positions of primers for the clone-specific amplification of TCR beta chains.
In the RT-PCR mRNA for TCR alpha- and beta-chains from single T cells was transcribed into cDNA via the primers Cα-RT-imp and Cβ-RT-2 which bind in the C-regions. In the PCR 1 the TCR alpha- and beta-chains were pre-amplified. For the TCR alpha chain a set of primers for all V alpha segments and the reverse primer Cα-out (closer to the J-segment) were used. For the TCR beta chain the first pair of V beta- and J beta-specific primers was used (BV13S1-BJ2.3_for1 and BV13S1-BJ2.3_rev1 or BV22-BJ2.1_for1 and BV22-BJ2.1_rev1).In the following nested PCRs (PCR 2 and PCR 3) we used the primers BV13S1-BJ2.3_for2 and BV13S1-BJ2.3_rev2 or BV22-BJ2.1_for2 and BV22-BJ2.1_rev2 and the primers BV13S1-BJ2.3_for3 and BV13S1-BJ2.3_rev3 or BV22-BJ2.1_for3 and BV22-BJ2.1_rev3 respectively. The third reverse primers reached into the clone-specific NDN-region. (gray: AV, light blue: AN, orange: AJ, black: AC, light green: BV, dark blue: BNDN, dark red: BJ, dark green: BC; figure modified from Backes, 2010)

A combined pre-amplification PCR (PCR 1 in Figure 7, p. 54) was performed for TCR alpha- and beta-chains on the product from the TCR-biased RT-PCR (Section 2.7.3, p. 52). 5 µL of PCR mix from the One Step RT-PCR kit (Qiagen) containing 0.6 µM Valpha primers (Vα-x-for-out in Table 7 (p. 20) and Seitz et al., 2006) and 0.6 µM of the primers Cα-rev-out, BV13S1-BJ2.3_for1 and BV13S1-BJ2.3_rev1 or BV22-BJ2.1_for1 and BV22-BJ2.1_rev1 (Table 5, p. 18 and Table 7, p. 20), respectively were added in the previous tubes to gain a final volume of 25 µL. A pre-mix of all the Valpha primers called "Vα-mix" was prepared.

Volume	Reagent	Final Concentration
1 µL	5x buffer	1x
0.2 µL	dNTP-mix (10 mM each)	4 mM
0.15 µL	Cα-rev-out (100 µM)	0.6 µM
0.45 µL	Vα-mix	0.062 µM each
0.15 µL	BVx-BJx_for1 (100 µM)	0.6 µM
0.15 µL	BVx-BJx_rev1 (100 µM)	0.6 µM
0.2 µL	enzyme mix	N/A
ad 5 µL	RNase-free H_2O	

Due to the huge amount of primers the pre-amplification PCR was performed as touch-down PCR in the GeneAmp PCR System 9600 (Perkin Elmer) with the following conditions:

95°C	15 min		
94°C	1 min	denaturation	
61°C	1 min	hybridization	4 cycles
72°C	1 min	elongation	
94°C	1 min	denaturation	
58°C	1 min	hybridization	4 cycles
72°C	1 min	elongation	
94°C	1 min	denaturation	
56°C	1 min	hybridization	4 cycles
72°C	1 min	elongation	
94°C	1 min	denaturation	
53°C	1 min	hybridization	30 cycles
72°C	1 min	elongation	
72°C	10 min		
4°C	∞		

Next followed two nested PCRs for the TCR beta chains (PCR 2 and PCR 3 in Figure 7, p. 54). For the primers consult Table 5 (p. 18). Samples containing 1 µL of H_2O/DEPC instead of previous PCR product served as negative controls.

Volume	Reagent	Final Concentration
2 µL	10x PCR buffer	1x
0.2 µL	dNTP-mix (10 mM each)	1 mM
0.1 µL	BVx-BJx_for2 or BVx-BJx_for3 (100 µM)	0.5 µM
0.1 µL	BVx-BJx_rev2 or BVx-BJx_rev3 (100 µM)	0.5 µM
0.3 µL	Taq-DNA-Polymerase (5 U/µL)	1.5 U
1 µL	product of previous PCR	
ad 20 µL	H_2O/DEPC	

The reactions were performed in the GeneAmp PCR System 9600 (Perkin Elmer) with the following conditions:

94°C	2 min		
94°C	1 min	denaturation	
53°C	1 min	hybridization	40 cycles
72°C	1 min	elongation	
72°C	10 min		
4°C	∞		

The PCR products of PCR 2 and PCR 3 were analyzed by agarose gel electrophoresis (Section 2.2.5, p. 30). Relevant bands were cut out, cleaned up with either the Easypure® DNA Purification kit

(Biozym, 10 µL elution volume) or the QIAquick Gel Extraction kit (Qiagen, 30 µL elution volume) and sent for sequencing (Section 2.2.6, p. 30) with a corresponding primer.

2.7.5 Basic Protocol of Unbiased TCR Beta Chain PCR

Figure 8 (p. 57) gives an overview over all PCR steps for the "unbiased approach" to characterize TCR beta chains.

The multiplex PCR to pre-amplificate TCR alpha- and beta-chains (PCR 1, Figure 8, p. 57) was performed directly after RT-PCR (Section 2.7.3, p. 52). 12.5 µL PCR mix from the OneStep RT-PCR kit (Qiagen) containing 3 µM Valpha- and Vbeta primers (Vα-x-for-out in Table 7 (p. 20) and Seitz et al., 2006, Vp-x in Table 6 (p. 19) and Kim et al., 2012) were added in the previous tubes to gain a final volume of 25 µL. A pre-mix of all the primers called "V primers" was prepared.

Volume	Reagent	Final Concentration
2.5 µL	5x buffer	1x
0.5 µL	dNTP-mix (10 mM each)	6 mM
0.6 µL	V primers	0.3 µM each
0.5 µL	enzyme mix	N/A
ad 12.5 µL	RNase-free H_2O	

The pre-amplification PCR was run as touch-down PCR in the PCR System 9600 (Perkin Elmer) due to the amount of primers using the following conditions:

95°C	15 min		
94°C	30 sec	denaturation	
60°C	1:30 min	hybridization	10 cycles
68°C	1 min	elongation	
94°C	30 sec	denaturation	
53°C	1:30 min	hybridization	30 cycles
68°C	1 min	elongation	
68°C	15 min		
4°C	∞		

The subsequent run-off PCR elongated the TCR beta chains for a 22 nucleotide "UP" segment (PCR 2, Figure 8, p. 57). A mix of all elongated primers Vp-x^+ (Table 6, p. 19) called "V^+-primers" was prepared. The PCR was run in the GeneAmp PCR System 9600 (Perkin Elmer) for 2 minutes at 94°C, 2:30 minutes at 53°C and 15 minutes at 68°C. Samples containing 1 µL of H_2O/DEPC instead of previous PCR product served as negative controls.

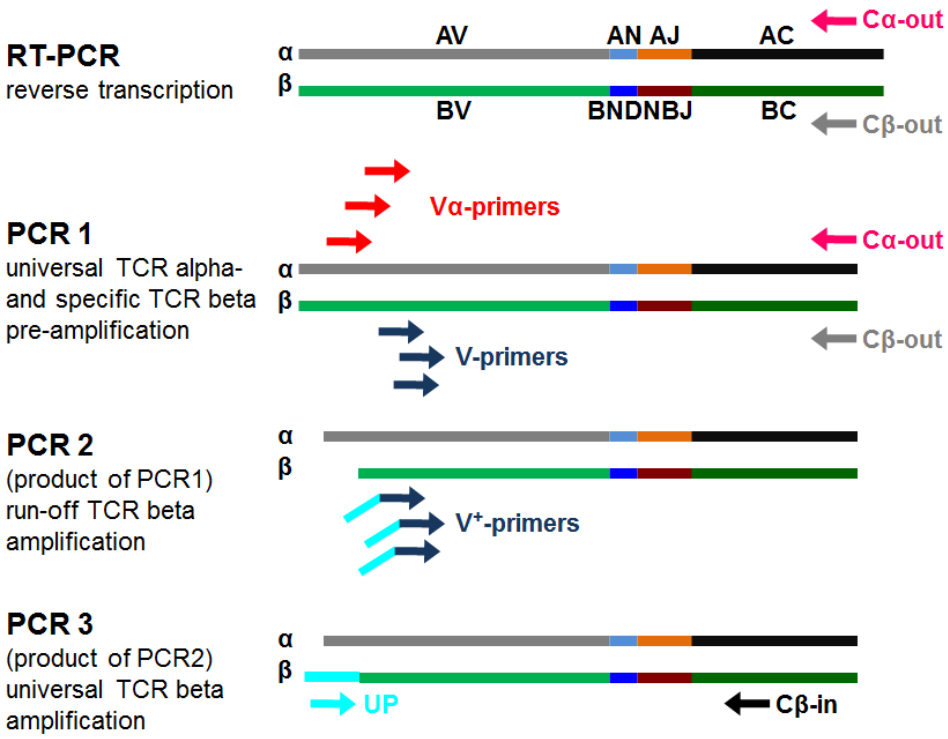

Figure 8: Relative positions of primers for the unbiased amplification of TCR beta chains.
In the RT-PCR mRNA for TCR alpha- and beta-chains from single T cells was transcribed into cDNA via the primers Cα-out and Cβ-out which bind in the C-regions. In the PCR 1 the TCR alpha- and beta-chains were pre-amplified. For the TCR alpha chain a set of primers for all AV segments and for the TCR beta chain a set of primers for all BV segments were used. No further reversed primers were added. The run-off PCR 2 elongates the TCR beta chain fragments for a 22 nucleotide "UP" sequence. In the PCR 3 TCR beta chains were amplified by the universal primer UP and the inner reverse primer Cβ-in. (gray: AV, light blue: AN, orange: AJ, black: AC, light green: BV, dark blue: BNDN, dark red: BJ, dark green: BC; figure modified from Backes, 2010)

Volume	Reagent	Final Concentration
2 µL	10x PCR buffer	1x
0.4 µL	dNTP-mix (10 mM each)	2 mM
0.2 µL	V^+-primers	0.062 µM each
0.1 µL	Taq-DNA-Polymerase (5 U/µL)	0.25 U
1 µL	product of PCR 1	
ad 20 µL	H_2O/DEPC	

Finally the products of the run-off PCR were amplified in the PCR 3 (Figure 8, p. 57) with universal primers. Samples containing 0.5 µL of H_2O/DEPC instead of previous PCR product served as negative controls.

Volume	Reagent	Final Concentration
2 µL	10x PCR buffer	1x
0.4 µL	dNTP-mix (10 mM each)	2 mM
2 µL	Cβ-in (10 µM)	1 µM
2 µL	UP (10 µM)	1 µM
0.2 µL	Taq-DNA-Polymerase (5 U/µL)	0.5 U
0.5 µL	product of PCR 2	
ad 20 µL	H_2O/DEPC	

The universal PCR 3 was run in the PCR System 9600 (Perkin Elmer) using the following conditions:

94°C	2 min		
94°C	30 sec	denaturation	
56°C	1 min	hybridization	35 cycles
68°C	1 min	elongation	
68°C	15 min		
4°C	∞		

The final PCR products were analyzed by agarose gel electrophoresis (Section 2.2.5, p. 30). Relevant bands were cut out, cleaned up with either the Easypure® DNA Purification kit (Biozym, 10 µL elution volume) or the QIAquick Gel Extraction kit (Qiagen, 30 µL elution volume) and sent for sequencing (Section 2.2.6, p. 30) with the primer Cβ-in.

2.7.6 TCR Alpha Chain PCR

PCR experiments to characterize TCR alpha chains were only performed on samples of PCR 1 which had yielded sequences of TCR beta chains in earlier experiments (Section 2.7.4, p. 53 and Section 2.7.5, p. 56). Mixes of the Vα-in primers listed in Table 8 (p. 20) called "Set 1" to "Set 5" were prepared. Samples containing 1 µL of H_2O/DEPC instead of the product of a PCR 1 served as negative controls.

Volume	Reagent	Final Concentration
2 µL	10x PCR buffer	1x
0.4 µL	dNTP-mix (10 mM each)	2 mM
2 µL	Vα-in Set-x	0.5 µM each
2 µL	Cα-rev-in (5 µM)	0.5 µM
0.2 µL	Taq-DNA-Polymerase (5 U/µL)	1 U
1 µL	product of PCR 1	
ad 20 µL	H_2O/DEPC	

Because of the huge amount of primers the TCR alpha chain PCR was performed as touch-down PCR in the GeneAmp PCR System 9600 (Perkin Elmer) with the following conditions:

94°C	2 min		
94°C	30 sec	denaturation	
61°C	1 min	hybridization	4 cycles
68°C	1 min	elongation	
94°C	30 sec	denaturation	
58°C	1 min	hybridization	4 cycles
68°C	1 min	elongation	
94°C	30 sec	denaturation	
56°C	1 min	hybridization	4 cycles
68°C	1 min	elongation	

94°C	30 sec	denaturation	
53°C	1 min	hybridization	40 cycles
68°C	1 min	elongation	
68°C	15 min		
4°C	∞		

The PCR products were analyzed by agarose gel electrophoresis (Section 2.2.5, p. 30). Relevant bands were cut out, cleaned up with either the Easypure® DNA Purification kit (Biozym, 10 µL elution volume) or the QIAquick Gel Extraction kit (Qiagen, 30 µL elution volume) and sent for sequencing (Section 2.2.6, p. 30) with the primer Cα-rev-in.

2.8 Characterization of Mimotopes Recognized by the TCRs 2D1 and B7

2.8.1 Peptide Assays with NFAT-sGFP-Expressing T Hybridoma Cells or IL-2 ELISA as Read-Out System

COS-7 cells were seeded in 96-well plates and transfected with pRSVneo-HLA-A2 or pRSVneo-HLA-A3 (Table 13, p. 23) using the FuGENE® HD transfection reagent (Section 2.5.5, p. 40). After 24 hours 10 µg of peptides (Table 14, p. 24) were loaded onto the cells. After incubation for 3 hours 2D1, B7, 2D1-NFAT-sGFP or B7-NFAT-sGFP T hybridoma cells (Section 2.5.6, p. 40 and Table 18, p. 26) were added. Later the stably transfected cell lines COS-7-A2 and COS-7-A3 (Section 2.5.7, p. 41) were employed. The next day the plates were either analyzed under the fluorescence microscope Axiovert 200M (Section 2.5.9, p. 43) or an IL-2 ELISA was performed.

Therefore the Mouse IL-2 ELISA Ready-SET-Go!® kit (eBioscience) and 96-well MaxiSorb® flat-bottom plates (Nunc) were employed according to the manufacturer's instructions. One well coated with 1:500 in PBS (Table 2, p. 15) diluted antibody against mouse CD3e (Table 15, p. 25) served as positive control. For the standard curves concentrations of IL-2 ranging from 5 to 500 pg/mL were used. The plates were analyzed at 450 nm wavelength with the VICTOR² 1420 Multilabel Counter (Perkin Elmer).

2.8.2 Assays with Peptide-Coding Plasmids

COS-7-A2 or COS-7-A3 cells (Table 18, p. 26) were seeded in 96-well or 24-well plates and transfected using the FuGENE® transfection reagent (Section 2.5.5, p. 40) with the peptide-coding plasmids listed in Table 13 (p. 23), which were prepared as described in Section 2.3.2 (p. 32). After 4 hours 2D1-NFAT-sGFP or B7-NFAT-sGFP T hybridoma cells were added (Section 2.5.6, p. 40 and Table 18, p. 26). The next day the plates were analyzed under the fluorescence microscope Axiovert 200M (Section 2.5.9, p. 43).

2.8.3 *In Vitro* Peptide:HLA-A2 Tetramer Recognition Assay

Pierce® High Sensitivity Streptavidin Coated Plates (Thermo Scientific) were washed tree times with wash buffer from the Mouse IL-2 ELISA Ready-SET-Go!® kit (eBioscience). After addition of 100 µL 1x PBS and 1 µL of biotinylated peptide:HLA-A2 complexes (Section 2.6.13, p. 51) the plates were incubated for 30 minutes at room temperature and then for 6 hours at 37°C. 2D1-NFAT-sGFP or B7-NFAT-sGFP T hybridoma cells were added (Section 2.5.6, p. 40 and Table 18, p. 26). The next day the plates were analyzed under the fluorescence microscope Axiovert 200M (Section 2.5.9, p. 43).

2.8.4 Assays with Plasmid-Encoded Combinatorial Peptide Libraries

The procedure was performed as described in Siewert et al., 2012. Figure 9 (p. 61) shows the workflow of the succeeding experiments.

2.8.4.1 Isolation of Positive APCs

COS-7-A2 (Table 18, p. 26) serving as APCs were seeded in 3.5 cm dishes in RPMI/complete medium (Table 3, p. 18) and transfected with PECP library plasmids (Table 13, p. 23) using the FuGENE® transfection reagent (Section 2.5.5, p. 40). After 48 hours of incubation 2D1-NFAT-sGFP T hybridoma cells (Section 2.5.6, p. 40 and Table 18, p. 26) were added in RPMI/complete medium (Table 3, p. 18). The next day the plates were analyzed under the fluorescence microscope Axiovert 200M (Section 2.5.9, p. 43).

When clusters of green fluorescing T hybridoma cells were observed, the underlying COS-7 cells were isolated using customized flexible capillaries with an inner diameter of 15 µm (custom-tips, Eppendorf) which were inserted into the LN25 Mini micromanipulator allowing movements in the range of micrometers. The latter device was connected to the CellTram Vario microinjector via an oil-filled tube that allowed applying very slight changes of pressure. The COS-7 cells were sucked into the capillary with some microliters of the surrounding medium and then expelled into pre-cooled 200 µL reaction tubes containing 7 µL H_2O/DEPC. The cells were shortly centrifuged in the Sprout Mini-centrifuge and stored on ice until the following plasmid recovery PCR could be performed. The capillaries were used for the consecutive isolation of COS-7 cells during one day's experiments.

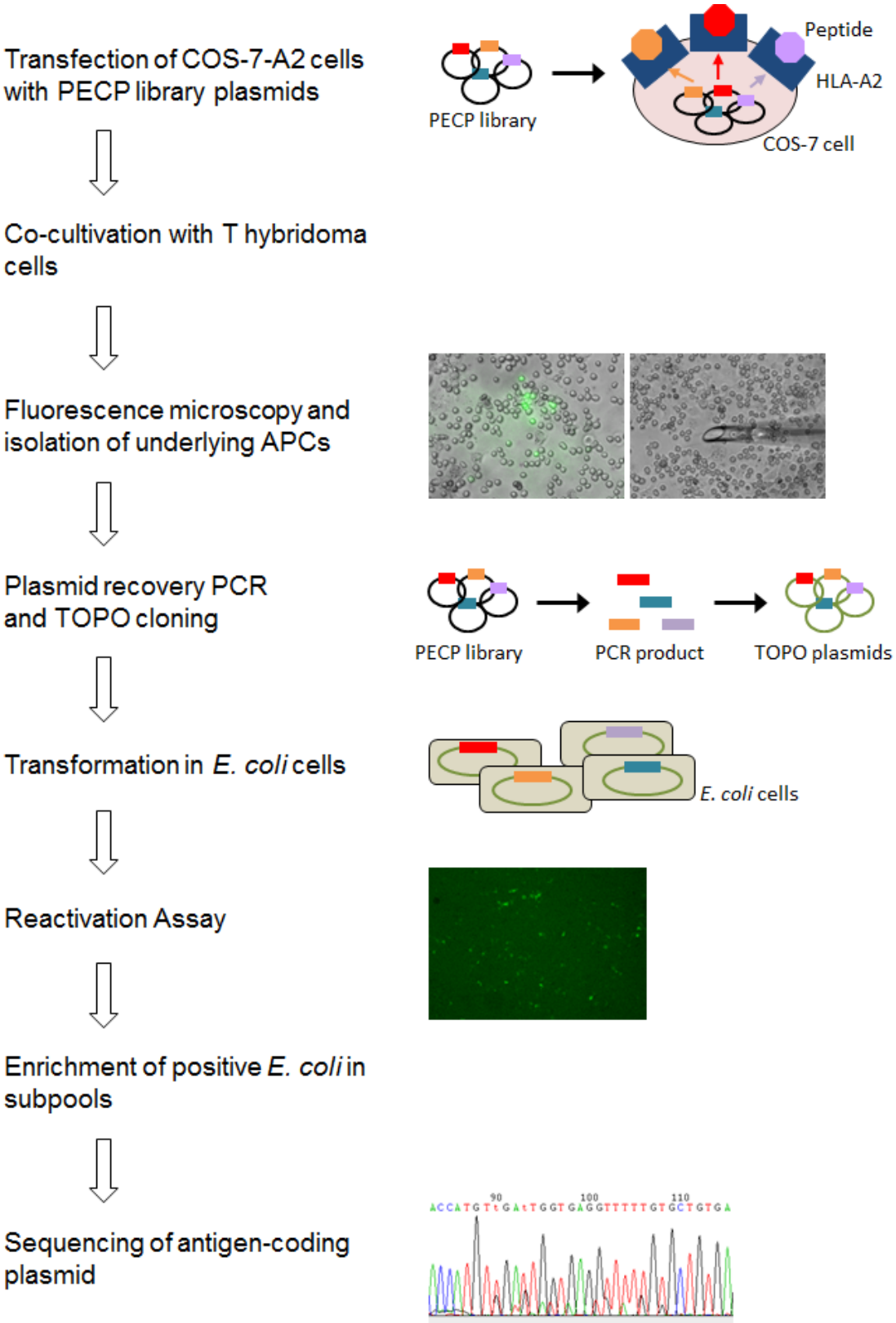

Figure 9: Workflow of mimotope search with PECP libraries.
The identification of antigen-coding plasmids using PECP libraries was performed as shown in this illustration. COS-7-A2 cells were transfected with PECP libraries (Section 2.5.5, p. 40 and Section 2.3.1, p. 30). After co-cultivation with 2D1-NFAT-sGFP T hybridoma cells underlying, activating COS-7-A2 cells were isolated (Section 2.8.4.1, p. 60). The peptide-coding region of the PECP library plasmids were amplified cloned and transformed in *E. coli* bacteria (Section 2.8.4.2, p. 62). After several rounds of reactivation and plasmid enrichment in subpools (Section 2.8.4.3, p. 63) the antigen-coding plasmid was sequenced (Section 2.8.4.4, p. 63).

2.8.4.2 Plasmid Recovery PCR and Recloning of PCR Products

The peptide-coding regions of intracellular plasmids from isolated COS-7 cells (Section 2.8.4.1, p. 60) were amplified using the following PCR setup with primers listed in Table 10 (p. 21):

Volume	Reagent	Final Concentration
50 µL	2x iProof™ High-Fidelity Master Mix	1x
0.5 µL	pcDNA-2nd-for-TOPO (100 µM)	0.5 µM
0.5 µL	pcDNA-rev-3 (100 µM)	0.5 µM
ad 100 µL	H_2O/DEPC	

The PCR was run in the T3 Thermocycler (Biometra) under the following conditions:

98°C	3 min		
98°C	20 sec	denaturation	
56°C	20 sec	hybridization	40 cycles
72°C	30 sec	elongation	
72°C	10 min		
4°C	∞		

Subsequently 10 µL of the PCR products were analyzed by agarose gel electrophoresis (Section 2.2.5, p. 30). Then 80 µL of the PCR products with visible bands were purified using the QIAquick® PCR-Purification kit (Qiagen) according to the manufacturer's instructions with elution in 30 µL EB buffer. DNA concentration was determined (Section 2.2.2, p. 28).
Next the samples were diluted to a final concentration of 1 ng/µL and ligated into the vector pcDNA3.1™D/V5-His-TOPO® using the pcDNA3.1™ Directional TOPO® Expression kit (Invitrogen):

Volume	Reagent	Final Concentration
1 µL	product of plasmid recovery PCR	1 ng
1 µL	salt solution (1.2 M NaCl, 0.06 M $MgCl_2$)	0.2 M NaCl, 0.01 M $MgCl_2$
0.5 µL	pcDNA3.1D/V5-His-TOPO® vector (15 to 20 ng/µL)	7.5 to 10 ng
ad 6 µL	H_2O/DEPC	

The ligation samples were incubated at room temperature for 30 minutes and then over night at 16°C. The next day the samples were precipitated in 0.1 volumes of 3 M sodium acetate and 2.5 volumes of ethanol with the addition of 20 µg Glycogen (Novagen) acting as a DNA carrier and 2 µL of Pellet Paint (Novagen) for at least 30 minutes at -80°C. After centrifugation for 1 hour at 4°C and 14,000 rpm (20,800 g) in the 5417 R Centrifuge (Eppendorf) the supernatant was discarded. The pellet was washed twice with 200 µL 70 % ethanol, air-dried and resuspended it in 2 µL of EB buffer.
Thereafter the probes were transformed into the *E. coli* strain ElectroMax DH10B™ (Invitrogen) (Section 2.4.4, p. 37). Plasmid purification was performed from 2 mL of the *E. coli* culture (Section 2.4.5, p. 38).

2.8.4.3 Reactivation Assay and Subpool Enrichment

COS-7-A2 cells (Table 18, p. 26) were seeded in 24-well plates in RPMI/complete medium (Table 3, p. 18) and transfected as duplicates with the previously purified plasmids (Section 2.8.4.2, p. 62) using the FuGENE® transfection reagent (Section 2.5.5, p. 40). After 24 or 48 hours of incubation 2D1-NFAT-sGFP T hybridoma cells (Section 2.5.6, p. 40 and Table 18, p. 26) were added in RPMI/complete medium (Table 3, p. 18). The next day the plates were analyzed under the fluorescence microscope Axiovert 200M (Section 2.5.9, p. 43). When reactivation was observed, the procedure to enrich the mimotope-coding plasmid was started.

Therefore the frequency of the mimotope-coding plasmid amongst bystander plasmids was estimated as 1 in the number of obtained clones after the transformation into the *E. coli* bacteria (Section 2.8.4.2, p. 62). 30 probes originating from the prior *E. coli* culture containing 1/10 of the previous clone number were cultivated in a volume of 1.25 mL in 96-well deep well plates and plasmid purification was performed from 1 mL of these *E. coli* cultures (Section 2.4.5, p. 38). Reactivation assays were performed as described above but in a single setup with incubation for 24 hours. This procedure was repeated until a dilution of the mimotope-coding plasmid of 1:300 or lower was obtained.

2.8.4.4 Final Enrichment and Sequencing of the Mimotope-Coding Plasmid

For the final dilutions *E. coli* bacteria of the last enriched culture were plated on agar plates (Section 2.4.1, p. 37). 30 streets of 30 colonies each were marked, picked individually with autoclaved toothpicks and cultivated over night in a volume of 20 mL LB^{amp} medium (Section 2.4.1, p. 37) in 50 mL reaction tubes. Reactivation assays were performed as described in Section 2.8.4.3 (p. 63) but in a single setup with incubation for 24 hours.

The colonies of positive streets were then analyzed individually and the final plasmid purification was sequenced (Section 2.2.6, p. 30) with the primer pcDNA-for-1or pcDNA-rev-3 (Table 10, p. 21).

2.8.5 Database Search for Parent Proteins

With all peptide sequences that were shown to activate T hybridoma cells protein BLAST search was performed using the webpage http://blast.ncbi.nlm.nih.gov/Blast.cgi and the database “non-redundant protein sequences” to identify possible parent proteins. Additionally a motif-based matrix search was accomplished in the case when more than one activating peptide was identified. In cooperation this search was performed by Stefan Pinkert, Max Planck Institute of Biochemistry (Martinsried, D).

3 Results

3.1 Characterization of Matching TCR Alpha and Beta Chains from Human Blood T Cells

Many autoimmune diseases such as MS or Psoriasis are characterized by tissue infiltrating $CD8^+$ T lymphocytes. These cells recognize so far unknown antigens with their TCR molecules and lead to destruction of target tissue structures.

A PCR method to identify TCR beta and matching alpha chains from putatively disease-related single cells was published (Seitz et al., 2006). This method allows cloning of TCR chains from cells belonging to expanded populations. T cell clones that contain a TCR V beta segment against which antibodies are available can be analyzed.

Based on this clone-specific approach a new PCR method to identify TCR beta chains in an unbiased manner was established. Song-Min Kim (Ludwig Maximilians University, Munich, department of dermatology) designed a set of primers that allows amplification of all possible human TCR beta chains originating from single T lymphocytes. The protocol and primers of Song-Min Kim were tested on human blood T cells.

Table 21: TCR beta (and matching alpha) chains from single sorted human blood T cells.
The unbiased method to identify human TCR beta- and subsequently alpha-chain sequences was tested on single human $CD3^+$ blood T lymphocytes. From 52 samples 2 TCR alpha- and beta-chain pairs as well as 5 single TCR beta chains were detected. Blue: amino acid sequence, green: V region, red: N(D)N, black: J region.

TCR chain	Sequence
BV8S1-BJ1.1	C A S T Q G W G D T E A F F G 5′-TGT GCC AGC ACC CAA GGG TGG GGA GAT ACT GAA GCT TTC TTT GGA-3′
AV20S1-AJ16.1	C V L L P R E V S D G Q K L L 5′-TGT GTA CTA CTG CCT CGT GAG GTC TCA GAT GGC CAG AAG CTG CTC-3′
BV12S3-BJ2.7	Y F C A S S T G T Y E Q Y F G 5′-TAT TTC TGC GCC AGT TCG ACA GGG ACC TAC GAG CAG TAC TTC GGG-3′
AV1S3-AJ56.1	Y F C A V S P G A N S K L T F 5′-TAC TTC TGT GCT GTG AGT CCC GGA GCC AAT AGT AAG CTG ACA TTT-3′
BV4S1-BJ2.3	Y L C S G S S F T S T D T Q Y 5′-TAT CTC TGC AGC GGT TCA TCG TTT ACT AGC ACA GAT ACG CAG TAT-3′
BV5S1-BJ1.1	L C A S S L V A D G E A F F G 5′-CTT TGC GCC AGC AGC TTG GTT GCG GAT GGC GAA GCT TTC TTT GGA-3′
BV12S1-BJ2.7	C A I S E S S L S Y E Q Y F G 5′-TGT GCC ATC AGT GAG TCA AGC CTT TCC TAC GAG CAG TAC TTC GGG-3′
BV13S2-BJ2.7	F C A S R P D R T L Y E Q Y F 5′-TTC TGT GCC AGC AGG CCG GAC AGG ACC CTC TAC GAG CAG TAC TTC-3′
BV22S1-BJ2.1	Y F C A S S L K A E Q F F G P 5′-TAC TTC TGT GCC AGC AGT TTG AAG GCT GAG CAG TTC TTC GGG CCA-3′

Human blood lymphocytes were isolated by gradient centrifugation and subsequent FACS-sorting into single reaction tubes using an anti-CD3 antibody. Samples were analyzed according to the protocol described in Section 2.7.5 (p. 56) and Section 2.7.6 (p. 58). From 52 sorted single $CD3^+$ blood lymphocytes 7 different TCR beta chains were identified (yield: 13.5 %). Of these seven samples two matching TCR alpha chains were detected (yield: 28.6 %) (Table 21, p. 64). All TCR alpha- and beta-

chains in this study are denoted according to Arden et al., 1995. The method including this experiment was published in Kim et al., 2012.

3.2 Optimization of the Methods to Identify Matching TCR Alpha and Beta Chains from Human Brain Tissue

The autoimmune mediated disease MS is characterized by demyelination, axonal loss, glial cell activation and the infiltration of immune cells into the CNS. Amongst all infiltrating cell populations $CD8^+$ T lymphocytes predominate and perform the direct autoimmune attack on CNS tissue structures (Friese and Fugger, 2009). Thus the identification of TCR molecules originating from disease-related T cells may provide further insights into the pathomechanisms of MS.

A clone-specific and an unbiased PCR method to characterize matching human TCR alpha- and beta-chains were established (Seitz et al., 2006; Kim et al., 2012). Here these methods were optimized for the use on human brain tissue samples. First the effects of different tissue treatment on the RNA quality were examined (Section 3.2.1, p. 65). Next liquid cover glass was tested for laser microdissection experiments (Section 3.2.2, p. 68). Finally the clone-specific PCR protocol was adapted to the use on human brain tissue samples (Section 3.2.3, p. 69).

3.2.1 Effects of Different Tissue Treatment on RNA Quality

During my Diploma thesis all available brain tissue blocks from MS patient FE were investigated according to MS lesions and T lymphocyte infiltrates. The blocks 9a, 10a and 11b appeared most promising for T cell analyses. Now the initial state of RNA quality in these brain tissue blocks was determined.

RNA was isolated from fresh cryosections and analyzed (Section 2.2.3, p. 28). Signals of 18S and 28S rRNA from all blocks were visible in the densitometry plot (Figure 10-A, p. 66) and electropherograms (Figure 10-B, p. 66). Despite detection of degradation products the RNA quality was considered well enough for single cell PCR experiments.

In the second experiment the loss of RNA quality in the brain tissue 9a and 11b was monitored from cutting cryosections until the end of the staining procedure for laser microdissection. To this end RNA was isolated from fresh cryosections, from each two sections stored on PET Membrane slides at -80°C and from each two sections on PET Membrane slides after storage at -80°C and the staining procedure for laser microdissection (Section 2.7.2, p. 52). Resulting RNA quality was analyzed (Section 2.2.3, p. 28).

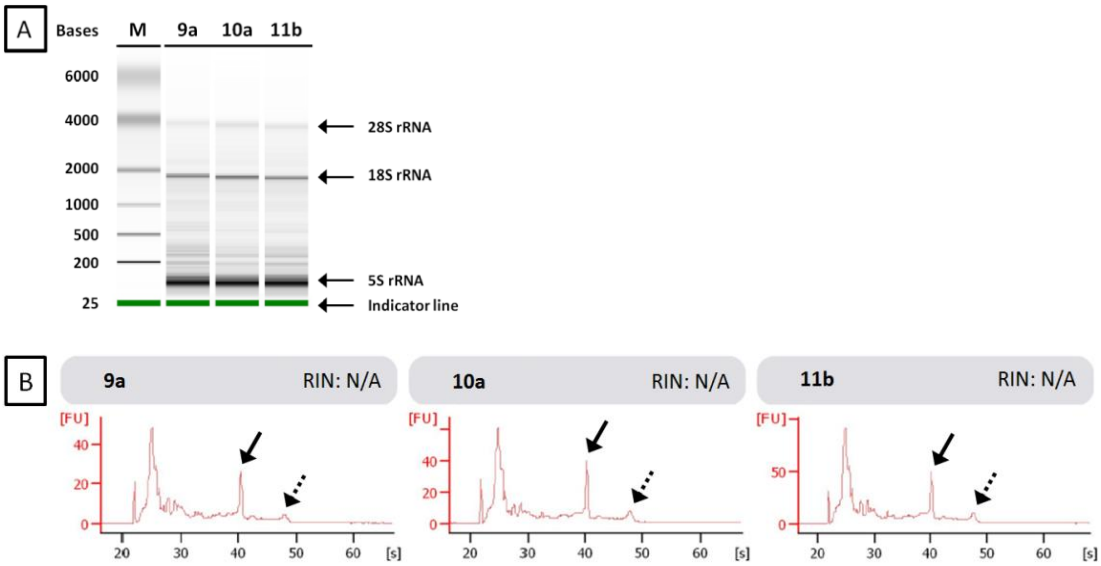

Figure 10: RNA quality of different tissue blocks from MS patient FE.
The initial RNA quality in tissue blocks 9a, 10a and 11b of the brain biopsy from MS patient FE was determined. **A:** Densitometry plot. **B:** Single electropherograms show RNA signals as a function of runtime in seconds against fluorescence intensity in relative fluorescence units (FU). RIN values were not available. Solid arrow: 18S rRNA, dashed arrow: 28S rRNA.

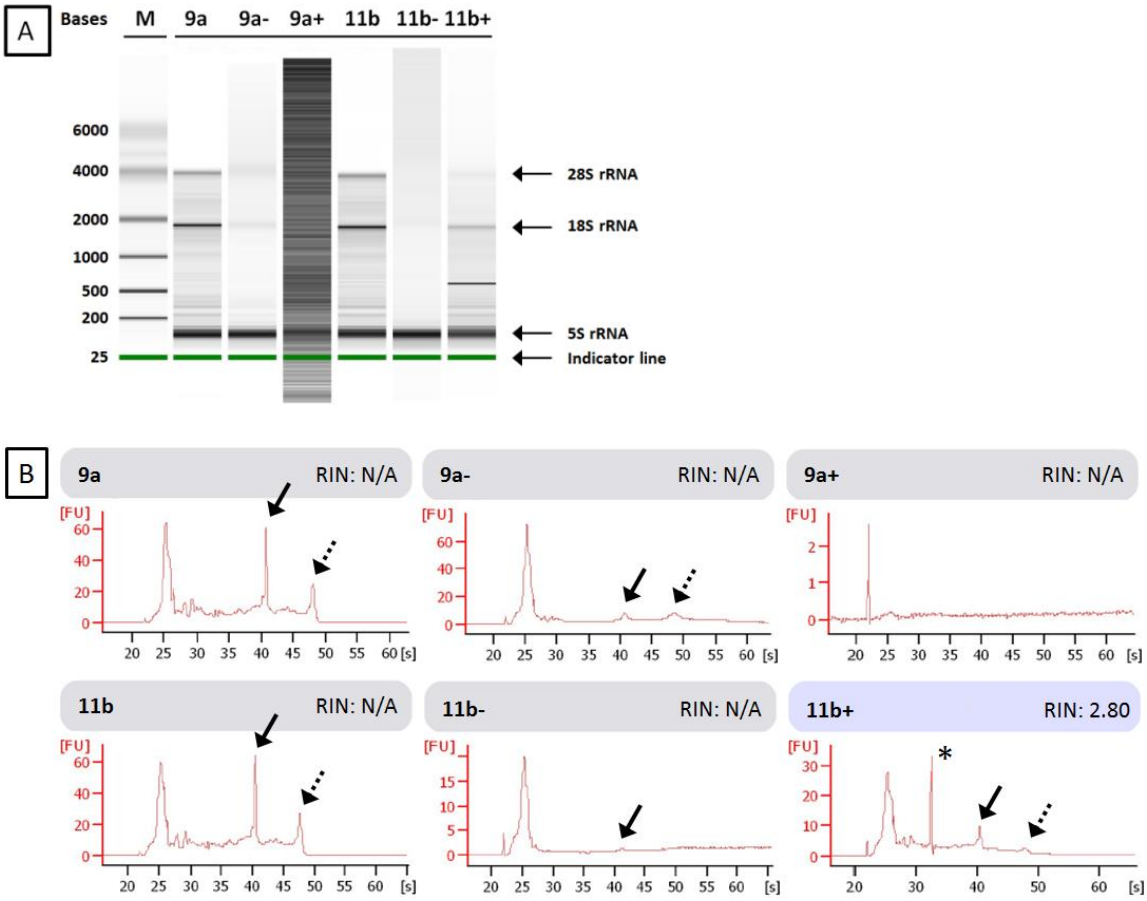

Figure 11: Loss of RNA quality in brain tissue during the laser microdissection protocol.
Slices of human brain blocks 9a and 11b were collected after cutting at the cryotom, after storage at -80°C on PET Membrane slides 1.0 (Zeiss) (samples 9a- and 11b-) and after the staining procedure for laser microdissection (samples 9a+ and 11b+). **A:** Densitometry plot. **B:** Single electropherograms show RNA signals as a function of runtime in seconds against fluorescence intensity in relative FU. Solid arrow: 18S rRNA, dashed arrow: 28S rRNA, asterisk: measurement artifact.

Fresh cryosections from block 9a and 11b yielded both comparable initial RNA quality as seen in the first experiment above. Signals of 18S and 28S rRNA were visible in the densitometry plot (Figure 11-A, p. 66). Storage at -80°C led to RNA degradation, but faint signals of 18S and 28S rRNA were detectable. After subsequent staining RNA was completely lost in the sections from block 9a. RNA quality in the stained sections of block 11b was better as in the sections stored at -80°C. This result might be due to the fact that different sections were used and that those for analysis after staining might have already had better initial RNA quality (Figure 11-B, p. 66).

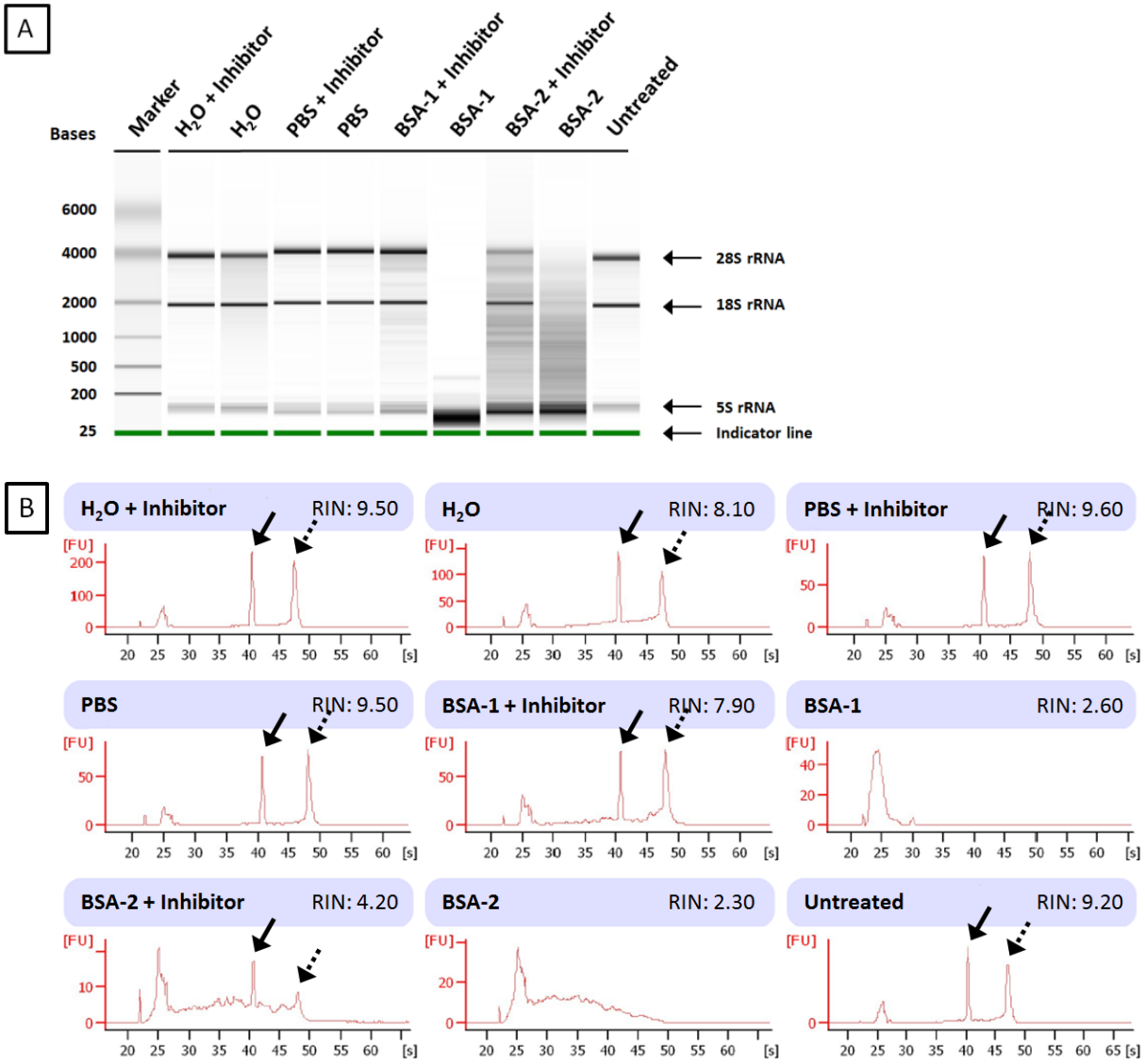

Figure 12: RNA quality after incubation in different solutions.
Each 500 ng RNA were left at room temperature for 2 hours in water, 2 % BSA/PBS of different batches or PBS, each with and without RNase inhibitor. Untreated RNA stored on dry ice served as positive control. **A:** Densitometry plot. **B:** Single electropherograms show RNA signals as a function of runtime in seconds against fluorescence intensity in FU. Solid arrow: 18S rRNA, dashed arrow: 28S rRNA, BSA-1: SIGMA Albumin from Bovine Serum (Sigma-Aldrich), BSA-2: Protease/DNase free Powder BSA (Equitech-Bio, Inc.).

As complete RNA degradation was observed in the stained sections of block 9a, the influence of different reagents on RNA quality which were used in the staining procedure was examined. It was

hypothesized that BSA samples might contain RNases. Therefore 500 ng of RNA that was isolated from T hybridoma cells, were left at room temperature for 2 hours in 10 µL H_2O/DEPC, PBS/DEPC or 2 % BSA/PBS/DEPC of two different batches. BSA-1 was SIGMA Albumin from Bovine Serum (Sigma-Aldrich), BSA-2 was Protease/DNase free Powder BSA (Equitech-Bio, Inc.; Kerreville, USA). Each approach was performed with and without the addition of 1 U/µL Protector RNase Inhibitor (Roche). An untreated RNA sample which was stored on dry-ice served as positive control. The resulting RNA quality was analyzed (Figure 12, p. 67; Section 2.2.3, p. 28).

As expected, the untreated RNA yielded very good quality with an RIN value of 9.20 and strong signals of 18S as well as 28S rRNA. Even the RNA incubated with H_2O/DEPC or PBS/DEPC in absence of RNase inhibitor yielded good qualities with RIN values of 8.10 and 9.50 and still strong signals of 18S and 28S rRNA. The addition of RNase inhibitor ameliorated these RNA qualities to RIN values of even 9.50 and 9.60 respectively.

Incubation with 2 % BSA/PBS/DEPC led to massive RNA degradation. Treatment with BSA batch 1 degraded RNA completely. The densitometry plot (Figure 12-A, p. 67) shows many unspecific signals of fractionized RNA in the sample of BSA batch 2. In both samples no signals of 18S and 28S rRNA could be detected. The addition of RNase inhibitor improved or completely restored RNA quality in the samples incubated with BSA batch 2 and BSA batch 1 respectively. The sample treated with BSA batch 2 and RNase inhibitor yielded an RIN value of 4.20 and detectable signals of 18S and 28S rRNA. The sample treated with BSA batch 1 and RNase inhibitor yielded a good RIN value of 7.90 and strong signals of 18S as well as 28S rRNA.

For later laser microdissection experiments the addition of Protector RNase Inhibitor (Roche) to each staining and washing solution was essential. SIGMA Albumin from Bovine Serum (Sigma-Aldrich) was used for blocking and staining solutions. In the timeframe of 2 hours RNA quality could be preserved well enough for subsequent PCR experiments.

3.2.2 Liquid Cover Glass

Image quality at conditions of laser microdissection is very poor (Section 2.7.2, p. 52; Figure 14-A to -D, p. 69). For microscopy usually tissue is covered with a glass cover slip. This allows light to pass straightly through the two layers of glass with tissue and aqueous solution in between (Figure 13-left, p. 69). Covering the tissue is not possible during microdissection experiments, catapulting tissue fragments into a reaction tube using a laser beam. In order to sustain RNA quality, so far the stained tissue was covered with a drop of fast evaporating 1-propanol. The alcohol covers the tissue but adapts to its surface formations. Thus light rays get refracted in various directions, rendering the image blurred (Figure 13-middle, p. 69).

To solve this problem Liquid Cover Glass introduced by the company Zeiss was tested. The reagent is claimed to embed the tissue and to smoothen rough surface structures. This should result in high resolution of even minute details such as nuclei and cell boundaries comparable to coverslipped specimens (Figure 13-right, p. 69). The reagent is dissolved in 1-propanol so RNA quality should not be affected. According to the manufacturer detection of fluorescence staining should be enhanced.

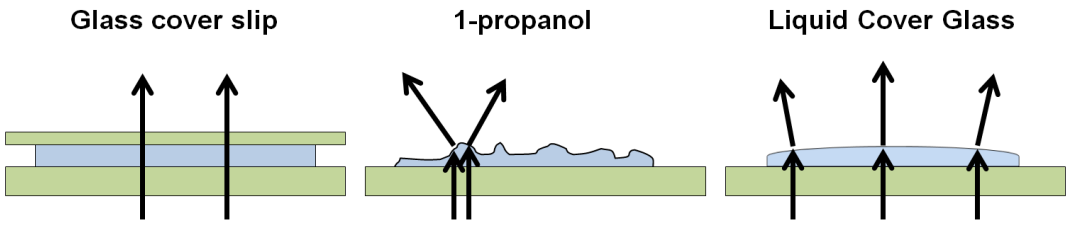

Figure 13: Refraction of light in different media.
Light rays (arrows) pass almost straightly through tissue specimens in aqueous solution covered with a glass cover slip (left) but are refracted at the rough surface of tissue covered with 1-propanol (middle). Liquid Cover Glass (Carl Zeiss MicroImaging) should embed tissue and smooth the surface to reduce refraction (right). Illustration modified from Backes (2010).

Hence brain tissue slides of MS patient FE were stained with the primary antibodies anti-CD8b-Cy3 and BV13S1-FITC and the secondary antibody aFITC-Alexa488 under the conditions of laser microdissection (Section 2.7.2, p. 52). One slide was covered with 1-propanol, the other with Liquid Cover Glass as recommended by the manufacturer. Unfortunately the Liquid Cover Glass emitted intense autofluorescence. Thus no fluorescence staining could be detected. Even the tissue structure and single cells were better detectable in the slide covered with 1-propanol (Figure 14, p. 69). In conclusion, Liquid Cover Glass was no option for our stainings under laser microdissection conditions.

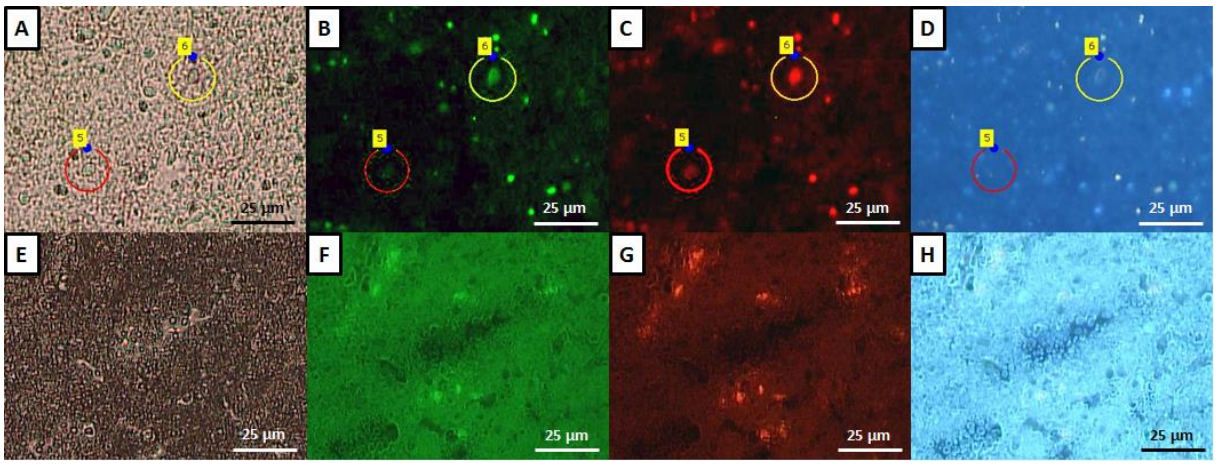

Figure 14: Test staining for Liquid Cover Glass.
Brain tissue slides were stained with the primary antibodies anti-TCR BV13S1-FITC (1:25) and anti-CD8b-Cy3 (1:100) as well as the secondary antibody aFITC-Alexa488 (1:100). **A-D:** coverage with 1-propanol, red circle: CD8 beta$^+$ cell, yellow circle: CD8 beta$^+$/BV13S1$^+$ cell; **E-H:** coverage with Liquid Cover Glass.

3.2.3 Optimization of the Clone-Specific TCR Beta Chain PCR Protocol

In MS patient FE the TCR beta chains BV13S1-BJ2.3 and BV22-BJ2.1 belong to clonally expanded T lymphocyte populations (Skulina et al., 2004, Backes, 2010). The sequences of the TCR beta chains were therefore known, but the corresponding TCR alpha chains still needed to be identified. Thus single CD8$^+$BV13S1$^+$ and CD8$^+$BV22$^+$ T cells were isolated by laser microdissection from brain tissue. Then the already known sequences of the TCR beta chains had to be confirmed before the PCR for identification of the TCR alpha chain could be performed. The protocol for clone-specific

amplification of TCR beta chains was published in Seitz et al., 2006. Here this protocol was optimized for the TCR beta chains BV13S1-BJ2.3 and BV22-BJ2.1.

Therefore two different primer sets were evaluated, which selectively amplify the published BV13S1-BJ2.3 and BV22-BJ2.1 sequences. The basic protocol for clone-specific amplification of the TCR beta chains BV13S1-BJ2.3 and BV22-BJ2.1 was performed (Section 2.7.4, p. 53) until PCR2 employing either the primer sets BV13S1-BJ2.3 (#13) and BV22-BJ2.1 (#22) or BV13S1-BJ2.3-new (#13-new) and BV22-BJ2.1-new (#22-new) (Table 5, p. 18). Precise positions of these primers on the TCR beta chain sequences are displayed in Supplement 5.1 (p. 109). As templates either samples of 100 pooled, FACS-sorted blood T lymphocytes from a healthy donor (Section 2.5.4, p. 40) or 1 µL of total RNA isolated from the tissue blocks 2a, 6, 9a, 10a, 11a and 12a of MS patient FE were used. Negative controls without template were included. The numbers of obtained sequences are summarized in Table 22 (p. 70); detailed sequences are given in Table 23 (p. 70).

Table 22: Number of sequences obtained in test PCR for TCR BV13S1-BJ2.3 and BV22-BJ2.1 specific primers.
The primer sets BV13S1-BJ2.3 (#13), BV13S1-BJ2.3-new (#13-new), BV22-BJ2.1 (#22) and BV22-BJ2.1-new (#22-new) were tested six times on 100 pooled blood $CD3^+$ T-lymphocytes of a healthy donor and twice on total RNA prepared from the tissue blocks 2, 6, 9a, 10a, 11a and 12a from MS patient FE. The left number gives the amount of samples, the right number gives the amount of obtained sequences.

	Blood	FE-2a	FE-6	FE-9a	FE-10a	FE-11a	FE-12a
#13	6 – 1	2 – 0	2 – 1	2 – 1	2 – 2	2 – 0	2 – 0
#13-new	6 – 0	2 – 0	2 – 2	2 – 0	2 – 1	2 – 0	2 – 0
#22	6 – 0	2 – 0	2 – 0	2 – 0	2 – 1	2 – 1	2 – 0
#22-new	6 – 0	2 – 1	2 – 0	2 – 0	2 – 1	2 – 0	2 – 0

Table 23: Sequences obtained from test PCR for TCR BV13S1-BJ2.3 and BV22-BJ2.1 specific primers.
The primer sets BV13S1-BJ2.3 (#13), BV13S1-BJ2.3-new (#13-new), BV22-BJ2.1 (#22) and BV22-BJ2.1-new (#22-new) were tested on samples of 100 blood $CD3^+$ T-lymphocytes of a healthy donor and samples of RNA prepared from the tissue blocks 2, 6, 9a, 10a, 11a and 12a from MS patient FE. Blue: amino acid sequence, green: V region, red: N(D)N, black: J region.

Primer set	Template	Sequence
#13	Blood	F C A S S Y G T S S T D T Q 5′-TTC TGT GCC AGC AGT TAC GGG ACT AGC AGC ACA GAT ACG CAG-3′
#13	FE-6	Y F C A S C E G G S T D T Q 5′-TAC TTC TGT GCC AGC TGC GAG GGC GGC AGC ACA GAT ACG CAG-3′
#13	FE-9a	Y F C A S S L G A D T Q Y F 5′-TAC TTC TGT GCC AGC AGC CTG GGA GCA GAT ACG CAG TAT TTT-3′
#13	FE-10a	Y F C A S S L G A D T Q Y F 5′-TAC TTC TGT GCC AGC AGC CTG GGA GCA GAT ACG CAG TAT TTT-3′
#13	FE-10a	Y F C A S S L G A D T Q Y F 5′-TAC TTC TGT GCC AGC AGC CTG GGA GCA GAT ACG CAG TAT TTT-3′
#13-new	FE-6	Y F C A S S L G A D T Q Y F 5′-TAC TTC TGT GCC AGC AGC CTG GGA GCA GAT ACG CAG TAT TTT-3′
#13-new	FE-6	Y F C A S S L G A D T Q Y F 5′-TAC TTC TGT GCC AGC AGC CTG GGA GCA GAT ACG CAG TAT TTT-3′
#13-new	FE-10a	Y F C A S S L G A D T Q Y F 5′-TAC TTC TGT GCC AGC AGC CTG GGA GCA GAT ACG CAG TAT TTT-3′
#22	FE-10a	C A S S E G A G E H N E Q F 5′-TGT GCC AGC AGT GAA GGG GCG GGA GAA CAC AAT GAG CAG TTC-3′
#22	FE-11a	C A S S E G A G E H N E Q F 5′-TGT GCC AGC AGT GAA GGG GCG GGA GAA CAC AAT GAG CAG TTC-3′
#22-new	FE-2a	C A S S E G A G E H N E Q F 5′-TGT GCC AGC AGT GAA GGG GCG GGA GAA CAC AAT GAG CAG TTC-3′
#22-new	FE-10a	F C A S S P L A N S Y N E Q 5′-TTC TGT GCC AGC AGT CCG CTA GCG AAC TCC TAC AAT GAG CAG-3′

Using the primer set #13 a TCR beta chain was obtained from one out of six blood cell samples. The primer sets #13-new, #22 and #22-new did not yield any sequence from blood cell samples. Employing the primer set #13 on RNA samples from MS patient FE further four sequences were detected. The primer set #13-new yielded three TCR beta chains. Of these in total seven sequences six were identical, originating from the clonal expanded T cell population which was described in Skulina et al. (2004) and Backes (2010). Using the primer set #22 on RNA samples from MS patient FE two sequences were detected. The primer set #22-new yielded further two TCR beta chains. Of these in total four sequences three were identical, originating from the clonal expanded T cell population which was described in Skulina et al. (2004) and Backes (2010).
In summary, for both TCR beta chains both primer pairs rendered comparable results. For later experiments the primer sets #13-new and #22-new were employed since their T_m was better suited to the applied PCR conditions (Supplement 5.1, p. 109).

3.3 Establishment of a Semi-Biased TCR Beta Chain PCR Protocol

So far tissue specimens from MS patient FE were stained with antibodies against CD8 beta and TCR BV13S1 or TCR BV22. Double positive cells were isolated via laser microdissection and analyzed using the clone-specific PCR protocol for the TCR beta chains BV13S1-BJ2.3 and BV22-BJ2.1. It was presumed that all TCR BV13S1 and TCR BV22 positive cells possess the already described TCR beta chains containing the BJ segment 2.3 and 2.1 respectively (Skulina et al., 2004). Through this assumption all TCR beta chain sequences which contain any of the other possible twelve BJ segments were neglected.

Table 24: Primer combinations for establishment of the semi-biased TCR beta chain PCR.

Setup	Pre-Amplification PCR	1st Nested PCR	2nd Nested PCR
#1	BV13S1-BJ2.3_for1 BV13S1-BJ2.3_rev1	BV13S1-BJ2.3_for2 BV13S1-BJ2.3_rev2	BV13S1-BJ2.3_for3 BV13S1-BJ2.3_rev3
#2	BV13S1-for1 BV13S1-BJ2.3_rev1-new	BV13S1-for2 BV13S1-BJ2.3_rev2-new	BV13S1-for3 FE13S1-2.3-rev3
#3	BV13S1-for1 Cβ-mid1	BV13S1-for2 Cβ-in	- -
#4	BV13S1-for1 Cβ-mid2	BV13S1-for2 Cβ-in	- -
#5	BV13S1-for1 Cβ-mid1	BV13S1-for3 Cβ-in	- -
#6	BV13S1-for1 Cβ-mid2	BV13S1-for3 Cβ-in	- -

Thus a semi-biased TCR beta chain PCR was designed using forward primers annealing in the specific BV regions and reverse primers annealing in the constant BC region. The reverse primers and their positions are given in Supplement 5.2 (p. 110). The PCR protocol was basically performed as described in Section 2.7.4 (p. 53). For the pre-amplification PCR the reverse primers Cβ-mid1 or Cβ-mid2 were designed. Afterwards only one further nested PCR was performed using the reverse primer

Cβ-in from the unbiased TCR beta chain PCR protocol. All primer sequences are listed in Table 5 (p. 18).

The feasibility of this new protocol was investigated using RNA isolated from tonsil tissue as template. For each setup displayed in Table 24 (p. 71) eight independent reactions on 4.63 ng RNA were performed. Negative controls without template were included. From the primer setups #1 and #2 both, the 1st and 2nd nested PCR were analyzed by agarose gel electrophoresis. The obtained sequences are listed in Table 25 (p. 72).

The primer setup #1 did not yield any TCR beta chain sequence containing the BV13S1 gene segment, the primer setups #2, #3, #5 and #6 yielded one sequence each and the primer setup #4 yielded two sequences. Surprisingly one more sequence containing the BV3S1 gene segment was contained after the 2nd nested PCR using the primer setup #2. The underlined part of the primer BV13S1-for1 (5'-TCCTGGTATCGACAAGACC-3') perfectly anneals in the BV3S1 gene segment. Obviously this primer was carried through all three subsequently performed reactions leading to the received PCR product.

In conclusion both reverse primers Cβ-mid1 and Cβ-mid2 performed equally well and were suited for semi-biased amplification of TCR beta chain sequences. The forward primer BV13S1-for1 can be used on single isolated cells already stained for TCR BV13S1 but may also amplify TCR beta chains containing the BV3S1 gene segment. The primer setup #1 should not be used in further experiments possibly due to the high T_m (Supplement 5.1, p. 109).

Table 25: Sequences obtained from the test PCR for semi-biased TCR beta chain amplification.
The protocol for semi-biased amplification of TCR beta chains with the known BV13S1 gene segment was tested with six different primer setups (Table 24, p. 71) on each eight samples of RNA isolated from tonsil tissue. #2-1: primer setup #2, 1st nested PCR; #2-2: primer setup #2, 2nd nested PCR; blue: amino acid sequence, green: V region, red: N(D)N, black: J region.

Setup	TCR beta chain	Sequence
#2-1	BV13S1-BJ2.3	F C A S S S G T A S T D T Q 5′-TTC TGT GCC AGC AGT TCC GGG ACG GCT AGC ACA GAT ACG CAG-3′
#2-2	BV3S1-BJ2.3	Y L C A S S P Q G A D T Q Y 5′-TAC CTC TGT GCC AGC AGT CCC CAG GGA GCA GAT ACG CAG TAT-3′
#3	BV13S1-BJ1.5	C A S S S S N S N Q P Q H F 5′-TGT GCC AGC AGT TCC TCG AAT AGC AAT CAG CCC CAG CAT TTT-3′
#4	BV13S1-BJ1.4	C A S S Y G S A G G E K L F 5′-TGT GCC AGC AGT TAT GGG TCG GCA GGG GGG GAA AAA CTG TTT-3′
#4	BV13S1-BJ2.7	C A S S Y G G V G T Y E Q Y 5′-TGT GCC AGC AGT TAC GGA GGG GTT GGC ACC TAC GAG CAG TAC-3′
#5	BV13S1-BJ1.5	C A S S S S N S N Q P Q H F 5′-TGT GCC AGC AGT TCC TCG AAT AGC AAT CAG CCC CAG CAT TTT-3′
#6	BV13S1-BJ2.1	A S S Y S S R A F N N E Q G 5′-GCC AGC AGT TAC TCG AGT CGA GCC TTC AAC AAT GAG CAG TTC-3′

3.4 Characterization of TCR Beta Chains from Brain Tissue of MS Patient FE

The aim of this thesis' first main project was to characterize the TCR molecules of putatively disease-related T lymphocytes from the MS patient FE. After several optimization steps the protocol was applicable to human frozen brain tissue samples. In line with the lesion mapping performed during

Backes (2010) the search for matching TCR alpha- and TCR beta-chains was continued using the tissue blocks 9a and 11b.

Potentially autoaggressive T cells had to be distinguished from bystander cells. Hence certain criteria were followed. First, the cell's morphology had to display T lymphocyte appearance (relatively round, 8 to 20 µm in diameter), second the T cell had to be activated carrying the surface marker CD134 (OX-40) or third, the T cell had to belong to a clonally expanded cell population. CDR3 spectratyping from earlier analyses revealed several TCR beta chains of clonally expanded T cell populations in the MS patient FE (Babbe et al., 2000; Skulina et al., 2004). Of these we focused on cells carrying the TCR beta chains BV13S1-BJ2.3 and BV22-BJ2.1 as monoclonal antibodies against TCR BV13S1 and TCR BV22 were commercially available. The DNA sequence of these two TCR beta chains is given in Supplement 5.1 (p. 109).

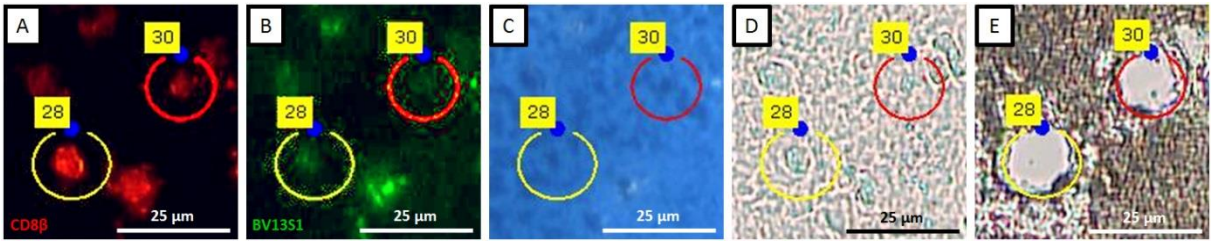

Figure 15: Staining and laser microdissection of CD8$^+$ T lymphocytes from human MS brain tissue.
A 10 µm brain tissue section from MS patient FE was double stained for CD8 beta (**A**, red) and BV13S1 (**B**, green). CD8 beta$^+$ (element 30) and CD8 beta$^+$/BV13S1$^+$ (element 28) cells without autofluorescent background (**C**, blue) were marked with red and yellow circles respectively. Marked elements were individually isolated by laser microdissection. **D:** Bright-light image of the tissue before and **E:** after laser microdissection.

For the clone-specific approach 10 µm frozen brain tissue section from MS patient FE were stained with antibodies against CD8 beta and TCR BV13S1 or TCR BV22. For the unbiased approach antibodies against CD8 beta and CD134 were employed. Double positive or single CD8 beta$^+$ T lymphocytes were isolated via laser microdissection and further analyzed using the adequate TCR beta chain PCR protocol. An exemplary staining and cell isolation is depicted in Figure 15 (p. 73). Cells that are single positive for CD8 beta do not immediately qualify as potentially disease-related T lymphocytes. But if the TCR beta chain sequence obtained from such cells additionally shows up in the CDR3 spectratyping analysis, the criterion of clonal expansion would be met.

Table 26: TCR beta chain sequences obtained from isolated single cells from MS patient FE brain tissue.
Single T lymphocytes were isolated by laser microdissection from 10 µm brain tissue sections of MS patient FE. CD8 beta$^+$/BV13S1$^+$ T cells were analyzed using the clone-specific TCR beta chain PCR protocol; the CD8 beta$^+$/CD134$^+$ T cells was analyzed using the unbiased TCR beta chain PCR protocol. Blue: amino acid sequence, green: V region, red: N(D)N, black: J region.

Phenotype	TCR beta chain	Sequence
CD8 beta$^+$/CD134$^+$	BV6S2-BJ2.2	C A S S L A P N G E L F F 5′-TGT GCC AGC AGC TTA GCC CCT AAC GGG GAG CTG TTT TTT-3′
CD8 beta$^+$/BV13S1$^+$	BV13S1-BJ2.3	C A S S Y G T S S T D T Q 5′-TGT GCC AGC AGT TAC GGG ACT AGC AGC ACA GAT ACG CAG-3′
CD8 beta$^+$/BV13S1$^+$	BV13S1-BJ2.3	S V P A A R A A G A D T Q 5′-TCT GTG CCA GCT GCG AGG GCG GCA GGA GCA GAT ACG CAG-3′

From 42 CD8 beta$^+$/TCR BV13S1$^+$ cells isolated from 69 tissue slides 2 TCR beta chain sequences were recovered. Both were composed of the BV13S1 and BJ2.3 gene segments but differed from the earlier detected clonally expanded T cell population. From 23 CD8 beta$^+$/TCR BV22$^+$ cells isolated from 15 tissue slides no TCR beta chain sequence was identified. 474 CD8 beta$^+$/CD134$^+$ cells isolated from 26 tissue slides and 578 CD8beta$^+$ cells isolated from 84 tissue slides were analyzed using the unbiased PCR protocol. One new TCR beta chain sequence of a CD8 beta$^+$/CD134$^+$ T lymphocyte was identified. Unfortunately no corresponding TCR alpha chains could be recovered. The detected TCR beta chain sequences are presented in Table 26 (p. 73). The low yield compared to single blood T lymphocytes (Section 3.1, p. 64) is mainly due to moderate RNA quality in the frozen tissue sections.

3.5 Preliminaries to Mimotope Searches of the TCR 2D1 on HLA-A2 Molecules

For better understanding of T cell-mediated processes in MS two major questions need to be answered. First the TCRs of disease-related effector cells and second the recognized autoantigenic peptides have to be characterized. To answer the second question Siewert et al. (2012) established a technology for identification of antigenic peptides recognized by HLA class I-restricted T lymphocytes. The method of mimotope search employs plasmid-encoded combinatorial peptide libraries (PECP libraries) which are transfected in antigen presenting cells (APC) stably expressing patient relevant HLA class I molecules. Reporter cells expressing the TCR of interest, human CD8 and sGFP under control of the NFAT promoter fluoresce green upon TCR activation and allow subsequent antigen identification (Section 2.8.4, p. 60).

This technique was now employed to better understand the molecular basis of the genetic linkage to HLA class I molecules in MS. Carrying the *HLA-A*0301* allele correlates with a risk factor, whereas carrying the *HLA-A*0201* allele correlates with a protective effect for MS susceptibility (IMSGC and WTCCC2, 2011). The TCR 2D1 was isolated from an MS patient and shown to recognize the PLP_{45-53} peptide (KLIETYFSK) on HLA-A3 molecules (Honma et al, 1997). Friese et al. (2008) discovered that double-transgenic mice expressing HLA-A3 and the 2D1 TCR develop an MS-like disease after immunization with PLP_{45-53} peptide. Surprisingly, not a single triple-transgenic mouse expressing HLA-A3, the TCR 2D1 and HLA-A2 showed symptoms after immunization as 2D1 T lymphocytes were depleted in the thymus. The underlying molecular mechanism still remained elusive. Therefore we focused on characterizing mimotope peptides presented on HLA-A2 molecules that result in TCR 2D1 activation. The control TCR B7 was employed as it recognizes the known peptide TAX_{11-19} (LLFGYPVYV) on HLA-A2 molecules (Ding et al., 1998).

Before the mimotope search experiments could be started some preliminaries were necessary. First the COS-7 lines stably expressing HLA-A3 and reporter cell lines stably expressing the TCR 2D1 or TCR B7 and sGFP under control of the NFAT promoter as well as five new PECP libraries were generated. Then the question whether the TCR 2D1 can be activated through any endogenous peptides presented by different cell lines was followed. Next the peptide positions important for recognition by the TCR 2D1 based on the PLP_{45-53} peptide presented on HLA-A3 were investigated. Finally the question arose

whether derivatives of the PLP_{45-53} and TAX_{11-19} peptide presented on either HLA-A2 or HLA-A3 molecules resulted in TCR 2D1 or TCR B7 activation.

3.5.1 Cell Lines 2D1-NFAT-sGFP and B7-NFAT-sGFP

To generate the reporter cell lines 2D1-NFAT-sGFP and B7-NFAT-sGFP intrinsic TCR-deficient T hybridoma cell lines expressing the human TCR 2D1 or B7 were stably transfected with pcDNA6-NFAT-sGFP containing blasticidin resistance (Section 2.5.6, p. 40). This plasmid codes for sGFP under control of the NFAT promoter, causing the cells to fluoresce green upon TCR activation. 57 and 89 blasticidin resistant clones of 2D1-NFAT-sGFP and B7-NFAT-sGFP cells respectively were isolated. Of these all 57 clones of 2D1-NFAT-sGFP cells and 38 clones of B7-NFAT-sGFP cells were activated with an antibody against CD3 (Section 2.5.8, p. 43). sGFP expression was detected by fluorescence microscopy and flow cytometry (data not shown). Of each cell line the two strongest fluorescing clones were cultivated and used as reporter cells for further experiments.

3.5.2 Cell Lines COS-7-A2 and COS-7-A3

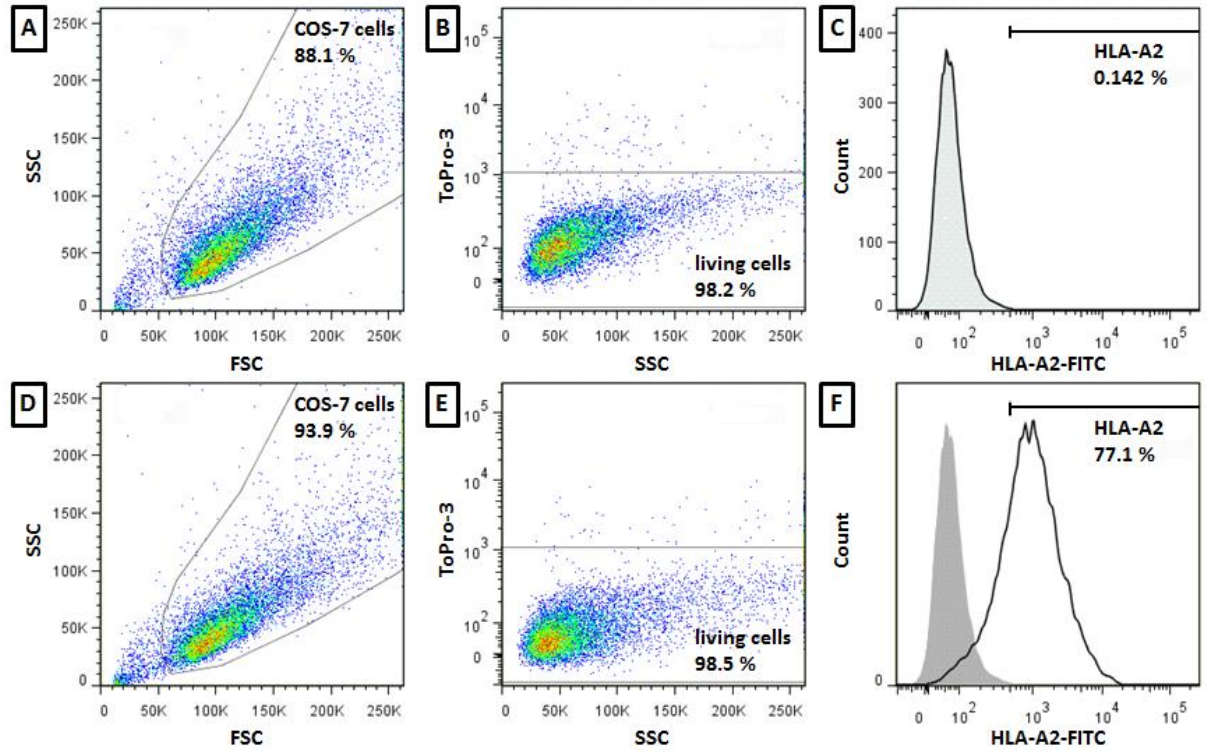

Figure 16: HLA-A2 expression of COS-7-A2 cells.
COS-7-A2 cells were stained with the antibody anti-HLA-A2-FITC (**D-F**) or the isotype control IgG2b-FITC (**A-C**) and the dead cell stain ToPro-3. **A and D:** Gate for COS-7 cells. **B and E:** Subsequent gate for living cells. **C and F:** Subsequent gate for HLA-A2 expression. **F:** Overlay of unstained (gray) and stained (white) COS-7-A2 cells. SSC: side scatter, FSC: forward scatter.

The cell line COS-7-A3 was generated as described in Section 2.5.7 (p. 41). There was no antibody against HLA-A3 commercially available. Thus the expression of HLA-A3 was verified by incubating the cells with PLP_{45-53} peptide, which was known to be presented on HLA-A3 and recognized by the TCR 2D1 (Honma et al, 1997). After co-cultivation the sGFP-expression of the reporter cell line 2D1-NFAT-sGFP was detected by fluorescence microscopy (data not shown). The COS-7-A3 clones that activated the most 2D1-NFAT-sGFP cells were further cultivated and used as APCs for later experiments.
The cell line COS-7-A2 was kindly provided by Katherina Siewert. HLA-A2 expression was verified by flow cytometry (Figure 16, p. 75).

3.5.3 Generation of Plasmid-Encoded Combinatorial Peptide Libraries

A technology to identify antigenic peptides recognized by HLA class I-restricted T lymphocytes was established by Siewert et al. (2012). This method employs PECP libraries coding for potentially antigenic peptides. A library for random nonamer peptides (N27), a library with eight random AAs and leucine at position 9 (9L) and several HLA-specific PECP libraries, for example the nonamer HLA-A2-specific $A2^{269}$ library with I, V and L at the positions 2, 6 and 9 were already generated.
For the mimotope search with TCR 2D1 on HLA-A2 five new libraries were designed (Section 2.3.2, p. 32). The TCR 2D1 recognizes the nonamer peptide PLP_{45-53} (KLIETYFSK) presented on HLA-A3 molecules (Honma et al., 1997), but the lengths of peptides which would be recognized on HLA-A2 molecules was not known. Therefore PECP libraries for random eight-, ten- and tridecamers (N24, N30 and N39) were generated. According to the database for HLA-binding motifs www.syfpeithi.com, peptides that bind to HLA-A2 molecules display often a leucine at the last position. Correspondingly two more PECP libraries with seven or nine random AAs and leucine at position 8 or 10 respectively (8L and 10L) were produced.
The main goal was to obtain a high number of clones to cover a broad spectrum of all statistically possible AA combinations (Table 27, p. 76). To verify the libraries' quality and to survey the amount of stop codons at the random positions 30 single bacteria clones for each library (data not shown) and the libraries in total were sequenced (Supplements 5.3, p. 111).

Table 27: Features of the 8L, N24, 10L, N30 and N39 PECP libraries.

PECP library	AA sequence	Statistically possible AA combinations		Gained clone numbers
8L	X X X X X X X L	20^7 =	1,280,000,000	394,327,500
N24	X X X X X X X X	20^8 =	25,600,000,000	2,520,000
10L	X X X X X X X X X L	20^9 =	512,000,000,000	406,455,000
N30	X X X X X X X X X X	20^{10} =	10,240,000,000,000	11,529,000
N39	X X X X X X X X X X X X X	20^{13} =	81,920,000,000,000,000	277,830,000

The gained clones of the 8L library covered 30.8 % of all possible AA combinations. The clone numbers of the 10L and N39 libraries were still sufficient for following experiments. In contrast, the N24 and N30 libraries contained comparably low numbers of individual clones. Later these two

libraries were again generated by Geraldine Rühl with yields of 229.25x10^6 and 27.65x10^6 clones for the N24 and N30 PECP library respectively.

3.5.4 Investigation of Endogenous Antigens on Different Cell Lines

After generation of all required cell lines (Section 3.5.1, p. 75) first the question whether the TCR 2D1 or the control TCR B7 are intrinsically activated by different cell lines was followed. Such cell lines would be excluded as APC in later experiments.

According to former knowledge, activation of the TCR 2D1 or B7 was restricted to antigen presentation on HLA-A3 or HLA-A2 molecules respectively. 2D1-NFAT-sGFP and B7-NFAT-sGFP cells were co-cultured with COS-7-A2, COS-7-A3, COS-7-Cw06, LTK-A2, LTK-A3, LTK-A1, GP+E-A2, GP+E-B38, EBV-16488 and EBV-FE cells (Table 18, p. 26). All cell lines were either untreated, loaded with 10 µg of PLP$_{45-53}$ peptide (KLIETYFSK) for TCR 2D1 and TAX$_{11-19}$ peptide (LLFGYPVYV) for TCR B7 in 1 µL DMSO or treated with 1 µL of pure DMSO as control. Cell activation was monitored by IL-2 ELISA (Figure 17, p. 77). All obtained results were confirmed by fluorescence microscopy (data not shown).

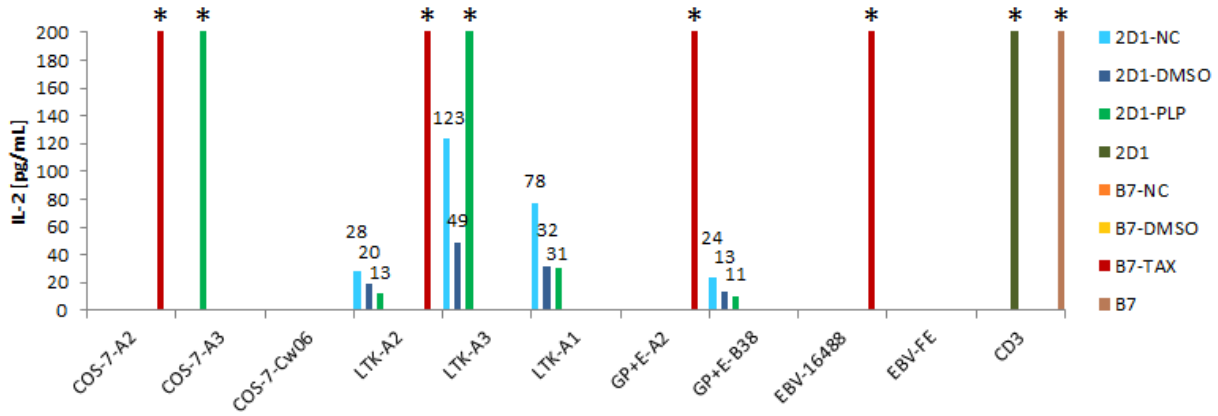

Figure 17: IL-2 ELISA for endogenous antigen recognition of TCR 2D1 and TCR B7 on different cell lines.
The cell lines COS-7-A2, COS-7-A3, COS-7-Cw06, LTK-A2, LTK-A3, LTK-A1, GP+E-A2, GP+E-B38, EBV-16488 and EBV-FE were untreated (NC), treated with 1 µL pure DMSO (DMSO) or loaded with 10 µg of PLP$_{45-53}$ peptide (KLIETYFSK) or and TAX$_{11-19}$ peptide (LLFGYPVYV) in 1 µL DMSO (PLP or TAX) and incubated with either 2D1-NFAT-sGFP or B7-NFAT-sGFP cells. Anti-CD3 activation served as positive control. Cell activation was measured by IL-2 ELISA with detection minimum at 5 pg/mL. Data represent two independent experiments. Asterisks: IL-2 concentration > 200 pg/mL - saturation effect in optical density occurred (OD > 1).

The control cell line B7-NFAT-sGFP was activated by cell lines expressing HLA-A2 molecules when those were loaded with the TAX$_{11-19}$ peptide. No further combination resulted in cell activation.

In contrast 2D1-NFAT-sGFP cells were activated by cell lines expressing HLA-A3 molecules loaded with the PLP$_{45-53}$ peptide but also recognized endogenous antigens on all different LTK and the GP+E-B38 cells. Endogenous activation was reduced through addition of pure DMSO or PLP$_{45-53}$ peptide in DMSO. This effect might be due to cytotoxicity of DMSO.

In the context of GP+E cells expression of HLA-B38 seemed accountable for antigen recognition as GP+E-A2 cells did not activate 2D1-NFAT-sGFP cells. This is a first indication that the TCR 2D1

might be activated by other HLA molecules than HLA-A3. In the context of LTK cells activation of 2D1-NFAT-sGFP cells was HLA-independent. Here xenorecognition of mouse antigen presentation molecules by the human TCR 2D1 might be the underlying mechanism which was not further investigated.

EBV-transducted cells could be used as APC. They did not result in endogenous activation of 2D1-NFAT-sGFP or B7-NFAT-sGFP cells. Major drawbacks were their expression of three to six different HLA molecules and the clotty growing which prevented proper contact to the reporter cells. COS-7 cells were suited as APC for later experiments because no endogenous antigens of this cell line activated 2D1-NFAT-sGFP or B7-NFAT-sGFP cells and they grow in an adherent cell layer.

3.5.5 Position Screening for Contacts of TCR 2D1 and PLP_{45-53}:HLA-A3 Complex

Next the interaction motif of the TCR 2D1 with peptide:HLA-A3 complexes was investigated. All HLA binding motifs were taken from the database www.syfpeithi.com.

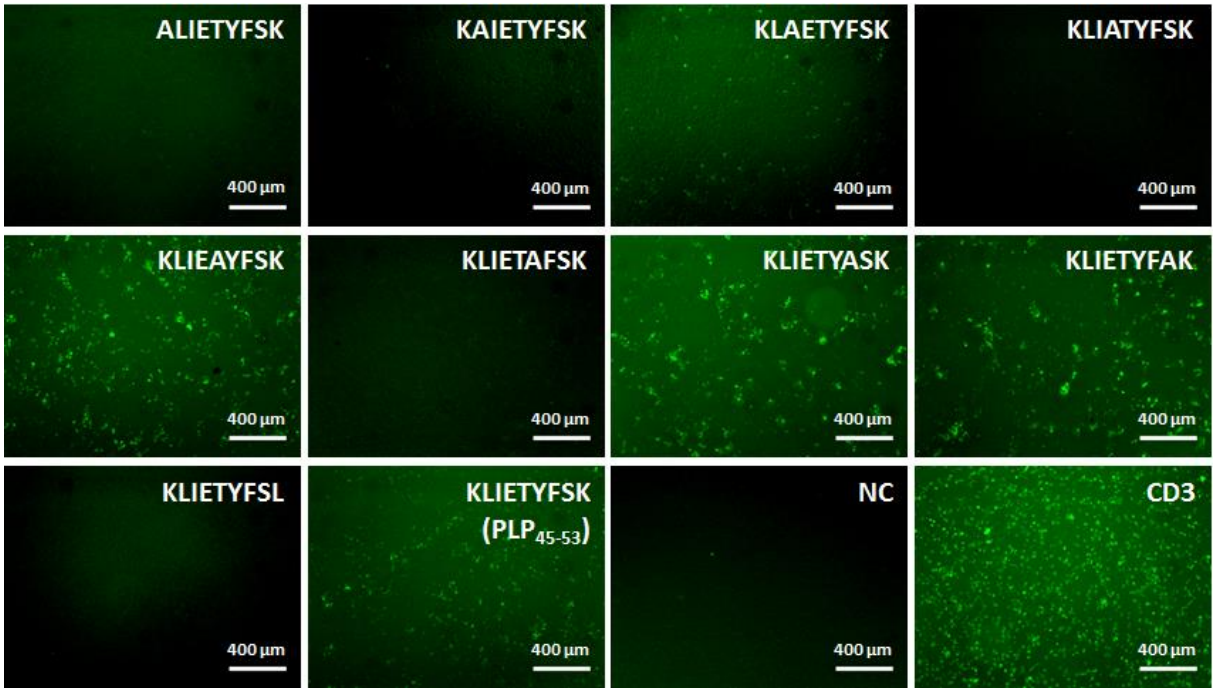

Figure 18: PLP_{45-53}-dependent position screening for contacts of TCR 2D1 and peptide:HLA-A3 complexes.
COS-7-A3 cells were transfected with PECP library-like plasmids coding for the peptide KLIETYFSK (PLP_{45-53}), eight derivatives with alanine substituting the positions 1 to 8 and the peptide KLIETYFSL and co-cultured with 2D1-NFAT-sGFP cells. Empty plasmid served as negative (NC) and CD3 activation as positive control for activation capability of 2D1-NFAT-sGFP cells.

The TCR 2D1 recognizes the peptide PLP_{45-53} (KLIETYFSK) presented on HLA-A3 molecules (Honma et al., 1997). Thus PECP library-like plasmids coding for the peptide KLIETYFSK as positive control and eight derivatives with alanine separately substituting the positions 1 to 8 were generated (Section 2.3.2, p. 32). Additionally plasmids coding for the peptide KLIETYFSL with leucine at the ninth position being a known binding anchor for HLA-A2 molecules were prepared.

After transfection of COS-7-A2 and COS-7-A3 cells with the ten plasmids separately and co-cultivation with 2D1-NFAT-sGFP cells in two independent experiments, TCR activation was monitored by fluorescence microscopy (Figure 18, p. 78).

No cell activation was observed in any approach using COS-7-A2 as APC (data not shown). Hence not even substitution of lysine at position 9 by leucine did result in either peptide presentation on HLA-A2 molecules or the recognition of KLIETYFSL:HLA-A2 complexes by the TCR 2D1.

Using COS-7-A3 cells as APC the positive control KLIETYFSK (PLP_{45-53}) as well as the derivatives KLIEAYFSK, KLIETYASK and KLIETYFAK resulted in activation of 2D1-NFAT-sGFP cells. Furthermore the peptide KLAETYFSK activated few 2D1-NFAT-sGFP cells. The peptides ALIETYFSK, KAIETYFSK, KLIATYFSK, KLIETAFSK and KLIETYFSL did not result in TCR 2D1 activation.

The peptides with substitutions at position 2 and 9 were probably not presented on HLA-A3 molecules as these are the two known major anchor positions for peptide:HLA-A3 interaction and should contain the AAs L/V/M or K/Y/F, respectively. Low TCR activation after alanine substitution of position 3 may also be due to peptide:HLA-A3 interaction. Position 3 is an auxiliary anchor position of HLA-A3 that should contain the AAs F/Y. The positions 1, 4 and 6 seemed to be important for peptide-TCR 2D1 interaction, whereas the positions 5, 7 and 8 may be variable.

3.5.6 Peptide recognition of TCR 2D1 and TCR B7 on HLA-A2 and HLA-A3 Molecules

Some TCRs may recognize over a million different peptides presented on one HLA molecule (Wooldridge et al., 2012) others have a much narrower recognition spectrum. Hence next the spectrum of peptides that can be recognized by the TCR 2D1 in comparison to the better characterized TCR B7 was analyzed.

To this end the known peptides PLP_{45-53} (KLIETYFSK) and TAX_{11-19} (LLFGYPVYV) were entered in the BLAST protein search matrix (http://blast.ncbi.nlm.nih.gov). Employing the "non-redundant protein sequences" database and "blastp" algorithm twelve derivatives of the PLP_{45-53} peptide and seven derivatives of the TAX_{11-19} peptide were chosen by "best-guess". All 19 "best-guess" candidates and the two original PLP_{45-53} and TAX_{11-19} peptides were loaded onto COS-7-A2 and COS-7-A3 cells. After co-cultivation with either 2D1-NFAT-sGFP or B7-NFAT-sGFP cells, activation was monitored by IL-2 ELISA (Figure 19, p. 80). All obtained results were confirmed by fluorescence microscopy (data not shown).

In line with Hausmann et al. (1999) the TCR B7 was capable of recognizing a broad antigenic spectrum presented on HLA-A2 molecules. Besides the TAX_{11-19} peptide (LLFGYPVYV) it was activated by four of its derivatives (PLFGYTVYG, IGFGYPAYI, SEFSYPVYR and SLFAFPVYQ) and further seven derivatives of PLP_{45-53} (KLIEKYFSK, KLIEPYFSK, KLIGTYFSK, KLIDTYFTK, KLIDTYFSN, KLIETYFKK and KMLETYLSK) presented on HLA-A2 molecules. No peptide was recognized in the context of HLA-A3 molecules.

On the contrary the TCR 2D1 displayed a very narrow recognition pattern of peptides presented on HLA-A3 molecules. It was activated by the known PLP_{45-53} peptide (KLIETYFSK) and one of its derivatives (KLIETYFKK) with a single AA exchange at position 7. This position was already shown to not be important for peptide-TCR interactions by alanine substitution (Section 3.5.3, p. 76). Strikingly one nonamer peptide (NLFGNPVYF) that mediated TCR activation in the context of HLA-A2 molecules was detected. Thus, for the first time cross-recognition of a peptide presented on HLA-A2 instead of HLA-A3 molecules by the TCR 2D1 was identified.

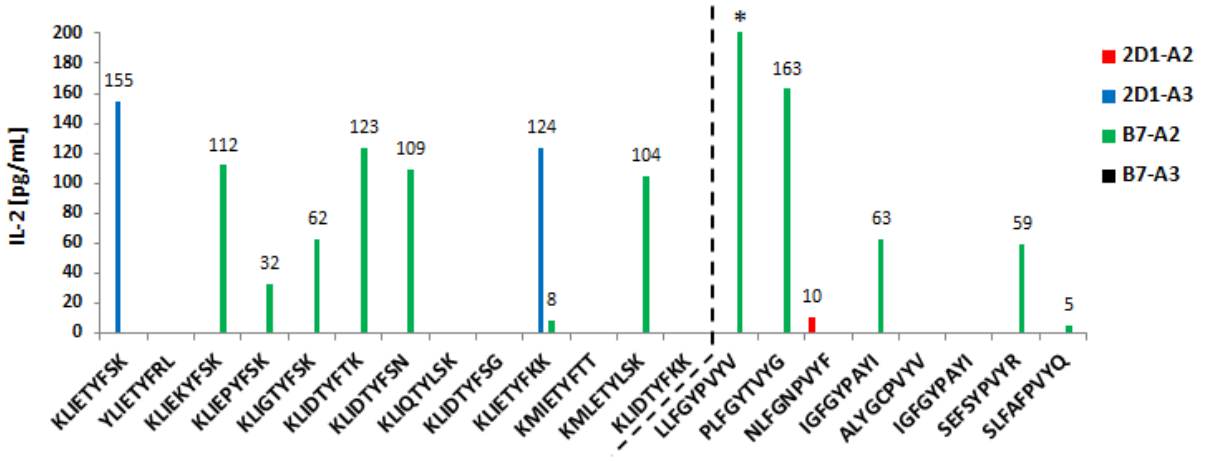

Figure 19: IL-2 ELISA for peptide recognition of TCR 2D1 and TCR B7 on HLA-A2 and HLA-A3 molecules.
COS-7-A2 and COS-7-A3 cells were loaded with 21 different synthetic peptides and incubated with either 2D1-NFAT-sGFP or B7-NFAT-sGFP cells. Cell activation was measured by IL-2 ELISA with detection minimum at 5 pg/mL. Data represent two independent experiments. Dashed line: division between PLP_{45-53} (KLIETYFSK) with derivatives and TAX_{11-19} (LLFGYPVYV) with derivatives; asterisk: IL-2 concentration > 200 pg/mL - saturation effect in optical density occurred (OD > 1).

3.6 Mimotope Search with TCR 2D1 on HLA-A2 Molecules

In a first step all necessary tools for mimotope search of TCR 2D1 on HLA-A2 molecules were prepared - the cell lines COS-7-A2 and 2D1-NFAT-sGFP as well as several PECP libraries. Second the interaction motif of the TCR 2D1 with peptide:HLA-A3 complexes was investigated revealing the importance of the peptide positions 1, 4 and 6 for nonamer peptide-TCR 2D1 contacts. Third the TCR 2D1 was characterized as quite specific for few peptides presented on HLA-A3 molecules and capable of cross-recognizing one nonamer peptide presented on HLA-A2 molecules.

In the previous experiments the investigated peptides were all derivatives of the PLP_{45-53} (KLIETYFSK) and TAX_{11-19} peptide (LLFGYPVYV). In a current step unbiased identification of further peptides that are cross-recognized by the TCR 2D1 on HLA-A2 molecules was examined. To this end mimotopes were investigated employing the technology described in Siewert et al. (2012). This method yields mimotopes which are non-natural peptides. From these a shared motif was determined. Based on this, motif database search for related existing peptides was performed and those were tested using peptide-coding plasmids. Finally it was investigated whether or not the identified

mimotope sequences from human existed in the endogenous pool of peptides presented on HLA-A2 molecules in EBV-transducted B cell lines.

3.6.1 Mimotope Search with Plasmid-Encoded Combinatorial Peptide Libraries

For unbiased detection of mimotopes of the TCR 2D1 on HLA-A2 molecules COS-7-A2 cells were transfected with different PECP libraries (Section 3.5.3, p. 76) and co-cultivated with 2D1-NFAT-sGFP reporter cells. Latter cells expressed sGFP under control of the NFAT promoter. These cells fluoresce green upon activation through the TCR 2D1 recognizing a peptide:HLA complex (Figure 20, p. 81). Underlying APCs were isolated and the mimotope-coding plasmid was then recovered according to the protocol given in Section 2.8.4 (p. 60).

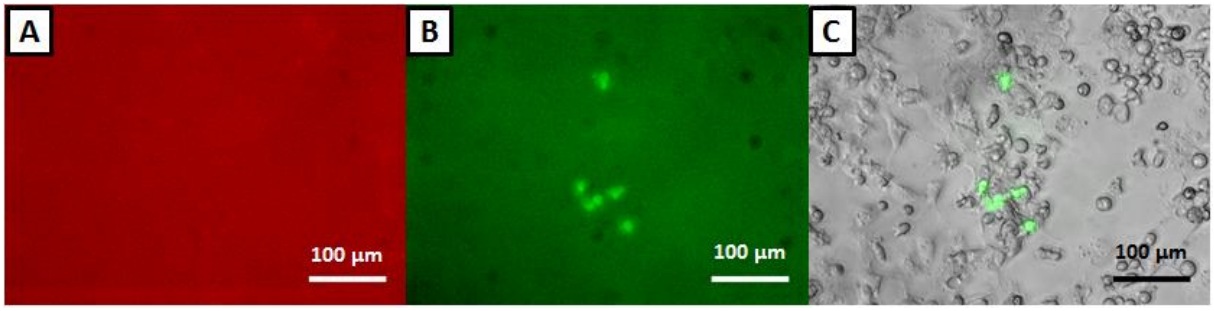

Figure 20: Cluster of activated reporter 2D1-NFAT-sGFP over mimotope-presenting COS-7-A2 cells.
COS-7-A2 cells were transfected with the 8L PECP library and co-cultivated with 2D1-NFAT-sGFP cells. Accumulation of activated, green fluorescing reporter cells indicates presence of an antigen-coding plasmid in the underlying COS-7-A2 cells. **A:** red fluorescence channel, **B:** green fluorescence channel, **C:** overlay of green fluorescence and transmitted light.

Table 28: Summary of mimotope search for TCR 2D1 with PECP libraries on HLA-A2 molecules.
For details related to PECP libraries consult Table 27 (p. 76).

PECP library	Investigated APCs [x10^6]	Isolated clusters	Mimotopes
$A2^{269}$	7.7	4	-
N24	27.0	9	-
8L	25.5	27	LIGEVFVL LVGEVWGL LLGEVFEL
N27	27.7	19	-
9L	8.0	-	-
N30	6.5	14	-
10L	5.5	-	-
N39	2.0	-	-

Table 28 (p. 81) summarizes the number of investigated APCs, isolated cell clusters and recovered mimotope sequences according to the employed PECP libraries. Transfection of COS-7-A2 cells with the 9L, 10L and N39 libraries did not yield activated 2D1-NFAT-sGPF reporter cells. Employing the $A2^{269}$, N24, N27 and N30 PECP libraries in total 46 clusters with 2 to 4 green fluorescing reporter cells above were isolated. No mimotopes were identified. Strikingly transfection of COS-7-A2 cells

with the 8L PECP library yielded accumulations of at least six activated 2D1-NFAT-sGFP cells. Here 27 clusters of underlying COS-7-A2 cells were isolated and 3 mimotopes were recovered. The eightmer peptide sequences LIGEVFVL, LVGEVWGL and LLGEVFEL were the first unbiasedly identified mimotopes presented on HLA-A2 molecules that are recognized by the TCR 2D1.

3.6.2 Database Searches and Identification of Mimotope Peptides with Peptide-Coding Plasmids

As shown in Section 3.5.6 (p. 79) the TCR 2D1 displays a very strict peptide recognition pattern compared to the TCR B7. In line with this result the three unbiasedly identified eightmer mimotopes presented on HLA-A2 molecules (LIGEVFVL, LVGEVWGL and LLGEVFEL) shared identical AAs at the positions 1, 3, 4, 5 and 8. AAs at position 2 were aliphatic and AAs at position 6 were aromatic. Position 7 seemed variable.

The computational biologist Stefan Pinkert (Max Planck Institute of Biochemistry, Martinsried, D) developed a motif-based matrix search for peptides resembling given sequences. A search matrix based on the three eightmer mimotopes was designed where probabilities for certain AAs at each position were assigned (Table 29, p. 82). Using this matrix Stefan Pinkert searched protein databases for the taxa 10090 (mouse), 9606 (human), 408170 (human gut metagenome), 2 (bacteria) and 10239 (viruses).

From this first motif-based database search 69 peptides from mouse, 64 peptides from human, 19 peptides from human gut metagenome, 269 peptides from bacteria and 22 peptides from viruses were obtained. In these peptide lists peptides existing in both mouse and human were accented and for example peptides from lethal bacteria as *Bacillus anthracis* or endemic bacteria of the deep sea were given less importance. Further less importance was given to peptides that did not contain AAs in line with at least two HLA-A2 anchor and/or TCR 2D1 contact positions.

Table 29: Initial matrix for database search based on three 2D1 - HLA-A2 mimotopes.
According to the three mimotopes each AA was given a probability in percent at each peptide position. Yellow: anchor position of HLA-A2, orange: presumed TCR 2D1 - peptide contact position, AAP: amino acid position.

AAP	Mimotopes			A	C	D	E	F	G	H	I	K	L	M	N	P	Q	R	S	T	V	W	Y	Sum
1	L	L	L	0	0	0	0	0	0	0	0	0	**80**	**20**	0	0	0	0	0	0	0	0	0	100 %
2	I	V	L	**5**	0	0	0	0	**5**	0	**30**	0	**30**	0	0	0	0	0	0	0	**30**	0	0	100 %
3	G	G	G	0	0	0	0	0	**100**	0	0	0	0	0	0	0	0	0	0	0	0	0	0	100 %
4	E	E	E	0	0	**10**	**80**	0	0	0	0	0	0	0	0	0	**10**	0	0	0	0	0	0	100 %
5	V	V	V	0	0	0	0	0	0	0	0	0	0	0	0	0	0	0	0	0	**100**	0	0	100 %
6	F	W	F	0	0	0	0	**40**	0	**5**	0	0	0	0	0	0	0	0	0	0	0	**40**	**15**	100 %
7	V	G	E	**5**	**5**	**5**	**5**	**5**	**5**	**5**	**5**	**5**	**5**	**5**	**5**	**5**	**5**	**5**	**5**	**5**	**5**	**5**	**5**	100 %
8	L	L	L	0	0	0	0	0	0	0	**10**	0	**70**	**10**	0	0	0	0	0	0	**10**	0	0	100 %

According to these criteria the lists were reduced to 37 candidates, therefrom 6 peptides shared in mouse and human, 3 peptides from mouse, 3 peptides from human, 3 peptides from human gut metagenome, 20 peptides from bacteria and 2 peptides from viruses. For these candidates peptide-

coding plasmids were produced (Section 2.3.2, p. 32) and TCR 2D1 activation was tested applying the protocol given in Section 2.8.2 (p. 59). From the 37 examined peptide sequences 16 induced TCR 2D1 activation when presented on HLA-A2 molecules.

Based on the information of the now 19 recognized mimotopes and 21 not-recognized peptide sequences a second motif-based matrix search was performed (Supplements 5.4, p. 112). A list of related peptides with descending matching scores was obtained. The list was cut at a score of 76 % conformity. Now 199 peptides from mouse, 194 peptides from human and 102 peptides from human gut metagenome were obtained. The same reduction rules as mentioned above were applied and further 19 candidates were studied, therefrom 8 peptides shared in mouse and human, 5 peptides from mouse, 5 peptides from human and 1 peptide from human gut metagenome.

Table 30: Mimotopes presented on HLA-A2 molecules, recognized by the TCR 2D1.
AAP: amino acid position, M&H: mouse and human, HGM: human gut metagenome.

AAP	Mouse					M&H				Human			HGM			Bacteria									
1	L	L	L	L	L	L	L	L	M	L	L	L	L	L	L	L	L	L	L	L	I	M	L	L
2	A	L	I	S	P	I	P	G	E	G	L	Q	I	P	I	I	I	I	I	I	L	I	V	G	A
3	G	G	G	G	G	G	G	G	G	G	G	G	G	G	G	G	G	G	G	G	G	G	G	G	G
4	E	E	E	E	E	E	E	E	E	E	E	E	E	E	E	E	E	E	E	E	E	E	E	E	E
5	V	V	A	V	V	V	V	V	V	V	V	V	V	V	V	V	V	V	V	A	V	V	V	V	V
6	F	W	F	F	W	F	F	F	W	Y	W	F	W	W	W	F	Y	F	F	F	F	W	W	W	F
7	A	H	C	G	M	N	A	Y	G	R	N	G	V	E	L	I	V	V	A	I	I	G	S	L	N
8	L	L	L	M	V	I	I	V	L	L	A	A	L	L	A	L	L	I	L	L	L	L	L	L	L

In summary, from 56 candidates 25 mimotopes presented on HLA-A2 molecules were detected that activated the TCR 2D1 (Table 30, p. 83). The other peptide sequences were either not presented on HLA-A2 molecules or did not result in activation of the TCR 2D1 (Table 31, p. 83).

Table 31: Sequences of peptides not recognized by the TCR 2D1 on HLA-A2 molecules.
AAP: amino acid position, HGM: human gut metagenome.

AAP	Mouse			Mouse and Human									Human					HGM	Bacteria									Virus	
1	L	L	L	L	L	L	L	L	L	L	L	L	L	L	L	L	L	L	L	L	L	L	L	L	L	L	L	L	I
2	I	L	E	I	T	V	V	T	L	L	E	R	R	L	V	L	S	E	V	V	I	I	V	P	T	Y	V	L	G	H	V
3	G	G	G	G	G	G	G	G	G	G	G	G	G	G	G	G	G	G	G	G	G	G	G	G	G	G	G	G	G	G	G
4	E	E	E	E	E	E	E	E	E	E	E	E	E	N	D	A	E	E	E	E	E	D	D	E	E	E	Q	Q	D	E	E
5	M	V	A	I	V	V	V	V	L	V	G	V	V	V	L	V	V	V	V	I	G	L	V	V	V	V	V	V	V	V	V
6	F	V	F	F	A	G	D	V	W	Q	F	W	W	F	W	W	H	F	F	F	F	W	H	F	F	F	F	F	Y	Y
7	E	A	P	E	K	E	F	A	C	A	I	Q	A	V	N	L	L	I	G	V	V	V	G	V	P	P	A	E	V	N	V
8	L	L	L	L	L	L	L	L	L	L	L	L	L	L	L	L	L	V	T	L	L	L	V	L	L	L	L	L	L	L	L

3.6.3 Search for Human Candidate Peptides in the Endogenous Repertoire of HLA-A2$^+$ EBV-Transducted B Cells

In the mimotope search three peptides from human (SPDL1$_{473-480}$ (LGGEVYRL), TAP1$_{260-267}$ (LQGEVFGA) and WDR25$_{14-21}$ (LLGEVWNA)) and interestingly four peptides present in mouse and human (DMXL2$_{813-820}$ (LIGEVFNI), EML5$_{997-1004}$ / EML6$_{997-1004}$ (MEGEVWGL), GPCPD1$_{15-22}$ (LPGEVFAI) and NCAN$_{257-264}$ (LGGEVFYV)) were identified to activate the TCR 2D1 in the context of HLA-A2 (Section 3.6.2, p. 82).

Earlier experiments showed that the TCR 2D1 was not intrinsically activated by the HLA-A2$^+$ EBV-transduced cell line EBV-16488 (Section 3.5.4, p. 77). This could have been due to either very low amounts of presented peptides or the clumpy growth of EBV-transduced B cells. Thus the interaction between the underlying EBV-transduced B cells and the 2D1-NFAT-sGFP reporter cells could have been impeded. Thus the question arouse whether or not the activating peptides occurred in the endogenous antigen repertoire of HLA-A2$^+$ EBV-transduced cell lines EBV-16488 or EBV-17490. The HLA-A2$^-$ cell line EBV-FE served as negative control.

HLA-A2 expression on the cell surface was verified by flow cytometry (Figure 21, p. 85). Peptide:HLA-A2 complexes were isolated from 1.5 x 10^9 cells of each type using two different purification methods (Section 2.6.8, p. 47 and Section 2.6.9, p. 47). After denaturation the endogenously presented peptides were collected and in collaboration with Peer-Hendrik Kuhn (German Center of Neurodegenerative Diseases, Munich, D) analyzed by ESI-TOF.

In line with the earlier endogenous activation experiment (Section 3.5.4, p. 77), none of the seven mimotopes could be found in the peptide pool deriving from the HLA-A2$^+$ cell lines EBV-16488 or EBV-17490.

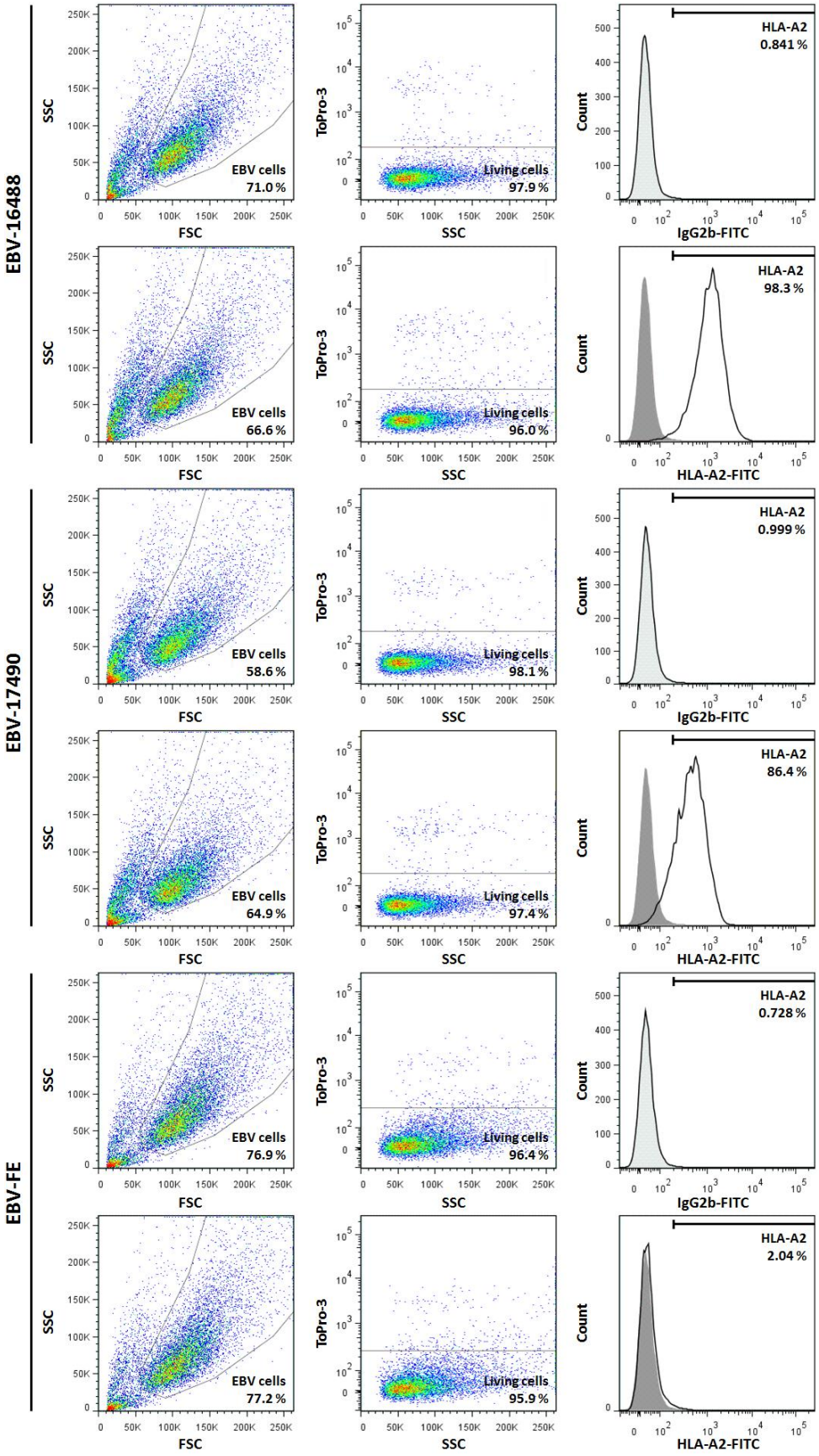

Figure 21: HLA-A2 expression of EBV-transducted B cell lines.
EBV-16488, EBV-17490 and EBV-FE cells were stained with the isotype control IgG2b-FITC (upper row) or the antibody anti-HLA-A2-FITC (lower row) and the dead cell stain ToPro-3. Gates from left to right were subsequently set for EBV cells, living cells and HLA-A2 expression. The lower right panel of each cell line presents overlay of isotype control (gray) and stained cells (white). SSC: side scatter, FSC: forward scatter.

3.7 Characterization of Mouse Peptides recognized by TCR 2D1 on HLA-A2 Molecules

In an unbiased experiment three mimotopes were detected that were presented on HLA-A2 molecules and activated the TCR 2D1 (Section 3.6.1, p. 81). Based on those mimotopes further 4 peptide sequences shared in mouse and human, 5 from mouse, 3 from human, 3 from human gut metagenome and 10 from bacteria were identified (Section 3.6.2, p. 82 and Table 30, p. 83).

Recognition of peptides presented on HLA-A2 molecules by the TCR 2D1 might cause thymic depletion of TCR $2D1^+$ T cells and prevent MS-like disease in HLA-A2, HLA-A3 and TCR 2D1 triple-transgenic mice (Friese et al., 2008). Thus in these mice thymic cells might present endogenous peptides that induce depletion of 2D1 T lymphocytes.

Here we aimed at identifying parent proteins from mouse that might be cleaved resulting in presentation of mimotope peptides. Thus the focus was put on mimotopes existing in mice ($ALOX12B_{404\text{-}411}$ (LIGEAFCL), $AP5S1_{185\text{-}192}$ (LLGEVWHL), $KLHL28_{384\text{-}391}$ (LAGEVFAL) and $MDH1B_{152\text{-}159}$ (LSGEVFGM)) and those also present in humans were emphasized ($DMXL2_{813\text{-}820}$ (LIGEVFNI), $EML5_{997\text{-}1004}$ / $EML6_{997\text{-}1004}$ (MEGEVWGL), $GPCPD1_{15\text{-}22}$ (LPGEVFAI) and $NCAN_{257\text{-}264}$ (LGGEVFYV)). Hereby the mimotope LPGEVWMV from mouse was excluded as its existence was stated by the protein database UniProt but not could not be verified by protein BLAST.

First the expression of potential parent proteins for the eight detected mimotopes in mouse tissue was verified. Concentrating on mimotopes present in mouse and human next the recognition of synthetic peptides loaded on HLA-A2 molecules by the TCR 2D1 was studied. Finally it was examined whether or not different APCs could cleave potential parent proteins existing in mouse and human resulting in mimotope presentation on HLA-A2 molecules and recognition by the TCR 2D1

3.7.1 Expression of Potential Parent Proteins in Mouse Tissue

In Section 3.6.2 (p. 82) it was shown that the mouse peptides $ALOX12B_{404\text{-}411}$, $AP5S1_{185\text{-}192}$, $DMXL2_{813\text{-}820}$, $EML5_{997\text{-}1004}$ / $EML6_{997\text{-}1004}$, $GPCPD1_{15\text{-}22}$, $KLHL28_{384\text{-}391}$, $MDH1B_{152\text{-}159}$ and $NCAN_{257\text{-}264}$ were recognized by the TCR 2D1 on HLA-A2 molecules when they were transfected as peptide-coding plasmids. Now the expression of genes coding for the parent proteins in mouse tissue was studied. Brain and thymus tissue was examined as HLA-A3 and TCR 2D1 double-transgenic mice developed MS-like neurological symptoms and 2D1 TCR^+ T lymphocytes were depleted in the thymus of HLA-A2, HLA-A3 and TCR 2D1 triple-transgenic mice (Friese et al., 2008).

qPCR was performed (Section 2.2.4, p. 29) using primers that span at least one intron and amplify gene regions coding for the mimotope peptide sequences (Supplements 5.5, p. 113). Thymus and brain tissue as template derived from a 10 week old female C57BL/6 wild type mouse and a 9 week old male SJL/J wild type mouse respectively (Kerstin Berer, Max Planck Institute of Neurobiology, Martinsried, D).

All parent genes were expressed in mouse thymus as well as mouse brain tissue (Figure 22, p. 87). The *Ncan* gene is specifically transcribed in the nervous system. Thus low expression level of *Ncan* in thymus (ΔCt value of 22.5) might be due to exclusive gene expression in the very few medullary

thymic epithelial cells. In these cells expression of the *Aire* gene drives transcription of organ-specific genes allowing maturing T cells to be exposed to a huge set of self-antigens during negative selection (Derbinski et al, 2001).

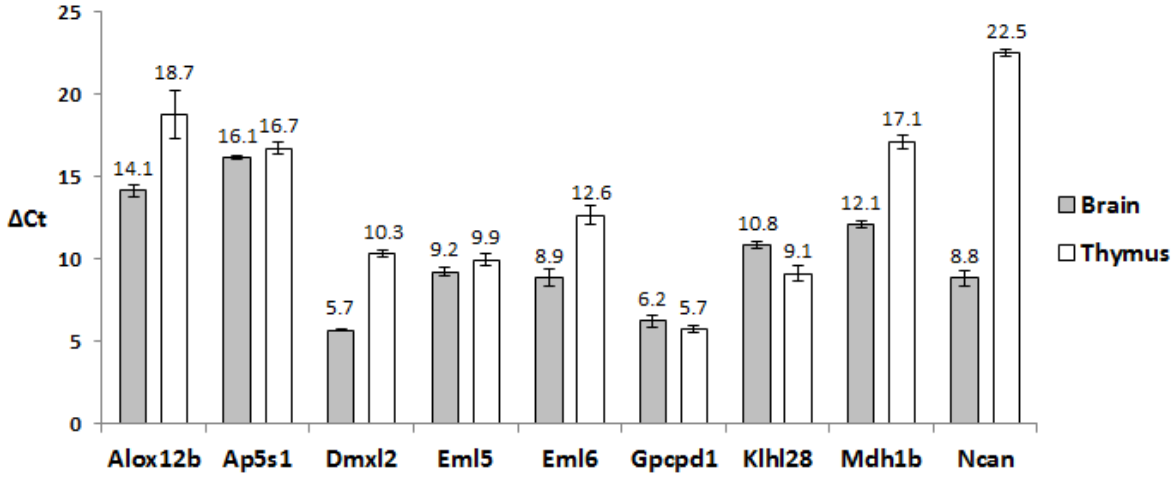

Figure 22: Gene expression of parent proteins for mimotopes in mouse tissue.
Expression of parent proteins for mimotopes in mouse brain and thymus tissue was examined by qPCR. Data represent triplicates from two independent experiments. ΔCt values were calculated using Ct values of the house keeping gene *Gapdh*. Error bars indicate standard deviation.

3.7.2 Recognition of Mouse and Human Mimotopes on HLA-A2 Tetrameres by the TCR 2D1

The TCR 2D1 was able to recognize the plasmid-coded peptides $DMXL2_{813-820}$ (LIGEVFNI), $EML5_{997-1004}$ / $EML6_{997-1004}$ (MEGEVWGL), $GPCPD1_{15-22}$ (LPGEVFAI) and $NCAN_{257-264}$ (LGGEVFYV) presented on HLA-A2 molecules (Section 3.6.2, p. 82). Those peptides were of special interest as they are present in mouse and human. Due to the very high hydrophobicity of those peptides COS-7-A2 cells could not be loaded with synthetic peptides (data not shown). It is assumed that the extremely hydrophobic peptides get dissolved in lipid membranes before they may interact with the HLA bincing groove. Hence HLA-A2 molecules were refolded *in vitro* in complex with the mentioned peptides (Section 2.6.12, p. 50). As the control TCR B7 but not the TCR 2D1 can be activated with the TAX_{11-19} peptide (LLFGYPVYV) presented on HLA-A2 molecules (Ding et al., 1998), this complex was additionally generated.

After biotinylation (Section 2.6.13, p. 51) the peptide:HLA-A2 tetramers were adsorbed at streptavidin-coated plates and incubated with 2D1-NFAT-sGFP and B7-NFAT-sGFP cells in two independent experiments. Empty wells served as negative and anti-CD3 activation as positive control. TCR activation was monitored by fluorescence microscopy (Figure 23, p. 88).

As expected the cell line 2D1-NFAT-sGFP was activated by the peptides $DMXL2_{813-820}$, $EML5_{997-1004}$ / $EML6_{997-1004}$, $GPCPD1_{15-22}$, and $NCAN_{257-264}$ presented on HLA-A2 molecules but not by the TAX_{11-19}:HLA-A2 complex. On the contrary, the cell line B7-NFAT-sGFP was exclusively activated by the TAX_{11-19} peptide presented on HLA-A2 molecules.

Thus the candidate sequences DMXL2$_{813-820}$, EML5$_{997-1004}$ / EML6$_{997-1004}$, GPCPD1$_{15-22}$, and NCAN$_{257-264}$ were not only recognized by the TCR 2D1 in form of plasmid-coded peptides presented on COS-7-A2 cells but also as synthesized peptides in complex with HLA-A2 molecules.

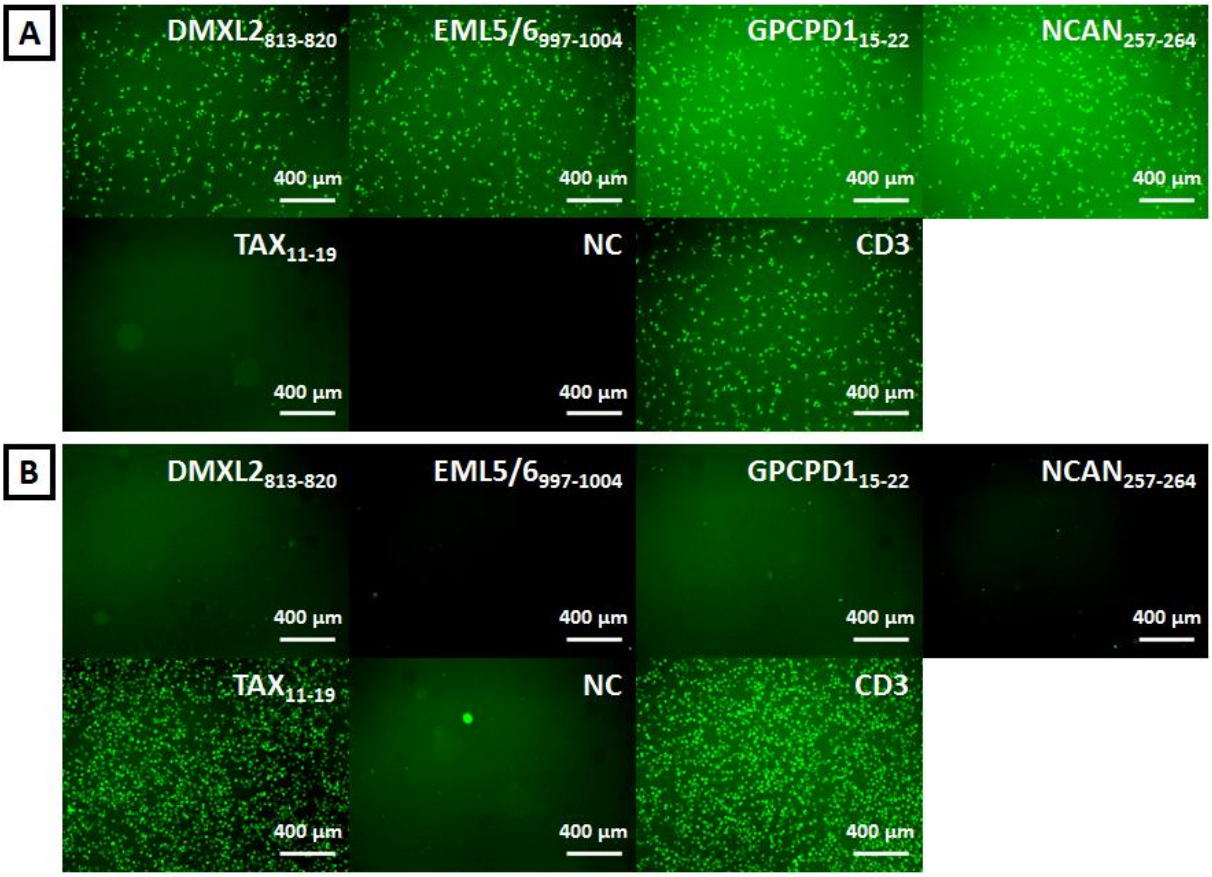

Figure 23: Recognition of peptides presented on HLA-A2 tetramers by TCR 2D1 and TCR B7.
Biotinylated HLA-A2 tetrameres loaded with the peptides DMXL2$_{813-820}$ (LIGEVFNI), EML5$_{997-1004}$ / EML6$_{997-1004}$ (MEGEVWGL), GPCPD1$_{15-22}$ (LPGEVFAI), NCAN$_{257-264}$ (LGGEVFYV) and TAX$_{11-19}$ (LLFGYPVYV) were adsorbed at streptavidin-coated plates. Empty wells served as negative (NC) and CD3-coated wells as positive control. Plates were incubated with 2D1-NFAT-sGFP **(A)** or B7-NFAT-sGFP **(B)** reporter cells.

3.7.3 Investigation of Protein Processing in COS-7-A2 Cells

The mimotopes DMXL2$_{813-820}$ (LIGEVFNI), EML5$_{997-1004}$ / EML6$_{997-1004}$ (MEGEVWGL), GPCPD1$_{15-22}$ (LPGEVFAI) and NCAN$_{257-264}$ (LGGEVFYV) present in mouse and human were recognized by the TCR 2D1 either coded on plasmids and presented by COS-7-A2 cells or as synthetic peptides on HLA-A2 tetramers. Now the question was asked whether or not COS-7-A2 cells are able to process the potential parent proteins leading to presentation of the mimotope peptides on the cell surface.

pcDNA plasmids coding for the truncated mouse proteins DMXL2$_{748-926}$, EML5$_{897-1038}$, GPCPD1$_{1-118}$ and NCAN$_{156-359}$ with a V5 tag at the carboxy-terminus were generated (Section 2.3.3, p. 33, Supplements 5.7.1, p. 120). The proteins were truncated according to their domain structure (Supplements 5.8, p. 126). Empty plasmid served as negative control. COS-7-A2 cells were transiently

transfected with these plasmids (Section 2.5.5, p. 40). Protein expression was monitored independently by SDS-PAGE (Section 2.6.4, p. 44) and western blot analysis (Section 2.6.5, p. 45) using the aV5-HRP antibody (Table 16, p. 26). Therefore supernatant and pellets of cell lysis were loaded (Section 2.6.7, p. 46).

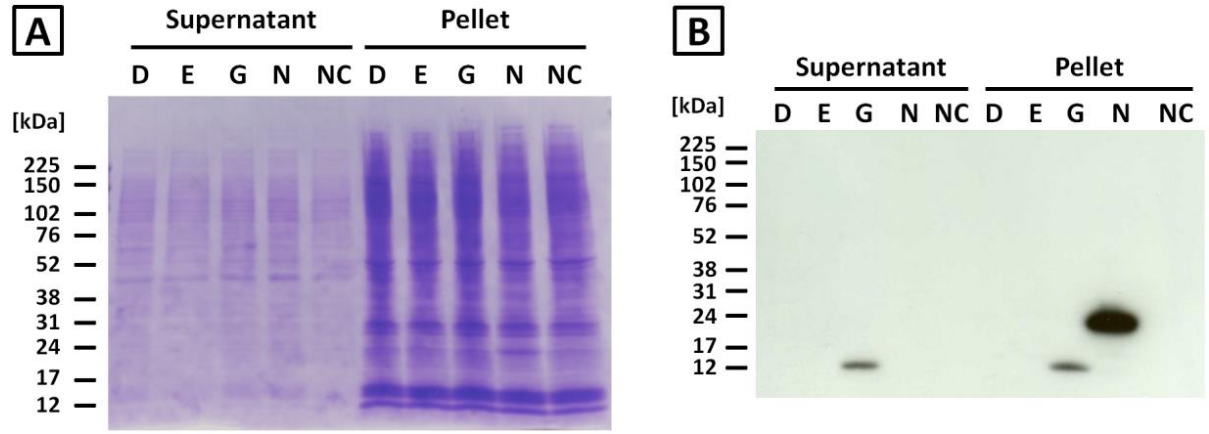

Figure 24: Truncated protein expression in COS-7-A2 cells.
COS-7-A2 cells were transiently transfected with pcDNA6/V5-HisA plasmids coding for the truncated mouse proteins $DMXL2_{748-926}$ (D), $EML5_{897-1038}$ (E), $GPCPD1_{1-118}$ (G) and $NCAN_{156-359}$ (N) with V5 tag at the carboxy-terminus. Empty plasmid served as negative control (NC). Supernatants and pellets of cell lysis were analyzed by SDS-PAGE (**A**) and western blot (**B**) employing 0.12 µg/mL of the aV5-HRP antibody and 20 seconds exposure time. Expected molecular weights: D 21.5 kDa, E 16.9 kDa, G 14.4 kDa, N 24.1 kDa.

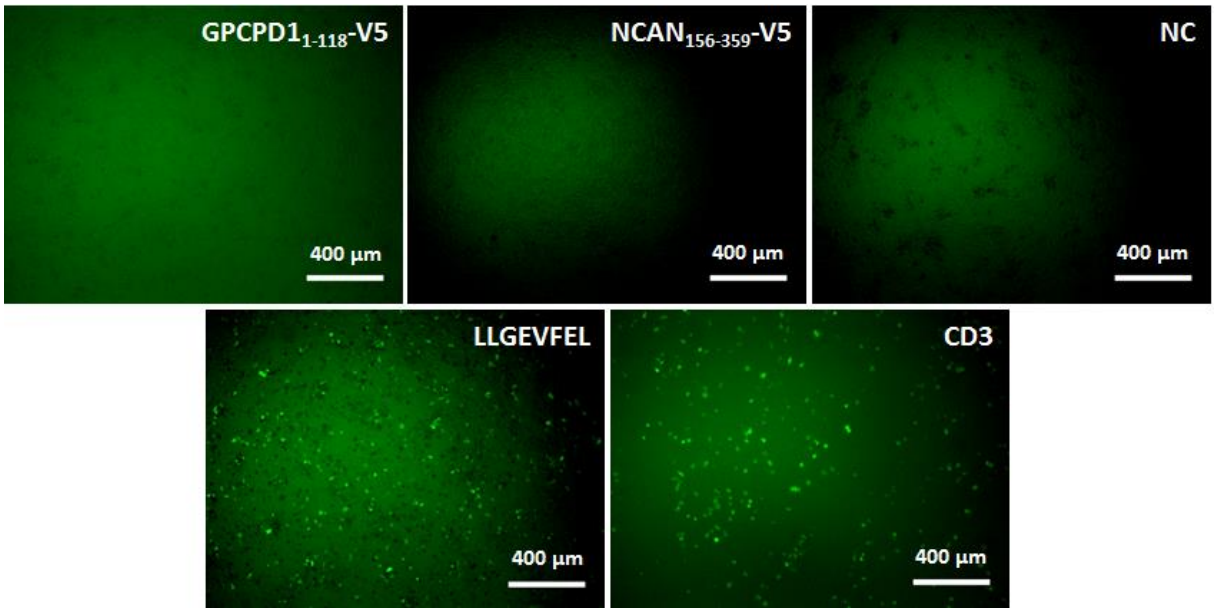

Figure 25: Protein processing in COS-7-A2 cells.
COS-7-A2 cells were transfected with pcDNA plasmids coding for the truncated mouse proteins $GPCPD1_{1-118}$ and $NCAN_{156-359}$ with a V5 tag at the carboxy-terminus and co-cultured with 2D1-NFAT-sGFP cells. Empty plasmid served as negative control (NC) and pcDNA plasmid coding for the mimotope LLGEVFEL as positive control. CD3 activation served as control for activation capability of 2D1-NFAT-sGFP cells.

COS-7-A2 cells expressed GPCPD1$_{1\text{-}118}$-V5 (14.4 kDa) in low amounts. NCAN$_{156\text{-}359}$-V5 (24.1 kDa) was expressed stronger but sticking to membranes due to intense hydrophobicity. Surprisingly, DMXL2$_{748\text{-}926}$-V5 and EML5$_{897\text{-}1038}$-V5 were not expressed in COS-7-A2 cells (Figure 24, p. 89). GPCPD1$_{1\text{-}118}$-V5- or NCAN$_{156\text{-}359}$-V5-expressing COS-7-A2 cells did not activate co-cultured 2D1-NFAT-sGFP cells (Figure 25, p. 89). Thus COS-7-A2 cells could not process the truncated potential parent proteins leading to mimotope presentation on HLA-A2 molecules.

3.7.4 Investigation of Protein Cross-Presentation in EBV-Transducted B Cells

As the cell line COS-7 was not able to process potential parent proteins leading to mimotope presentation on HLA-A2 molecules, better suited cell lines were investigated. B cells serve besides dendritic cells or macrophages as APC in the immune system. The capability of dendritic cells to cross-present antigens that were taken up from the milieu surrounding the cell on HLA class I molecules is well known (Ackerman and Cresswell, 2004). Additionally it was shown that also B cells and other non-professional APCs are capable of cross-presentation (Bennett et al., 1998; Gnjatic et al., 2003). As no adequate dendritic cells were available, the HLA-A2^{+} EBV-transducted B cell lines EBV-16488 and EBV-17490 (Section 3.6.3, p. 84) were employed to investigate whether or not the potential parent proteins DMXL2, EML5, GPCPD1, and NCAN could be processed correctly leading to presentation of the mimotopes DMXL2$_{813\text{-}820}$, EML5$_{997\text{-}1004}$ / EML6$_{997\text{-}1004}$, GPCPD1$_{15\text{-}22}$, and NCAN$_{257\text{-}264}$.

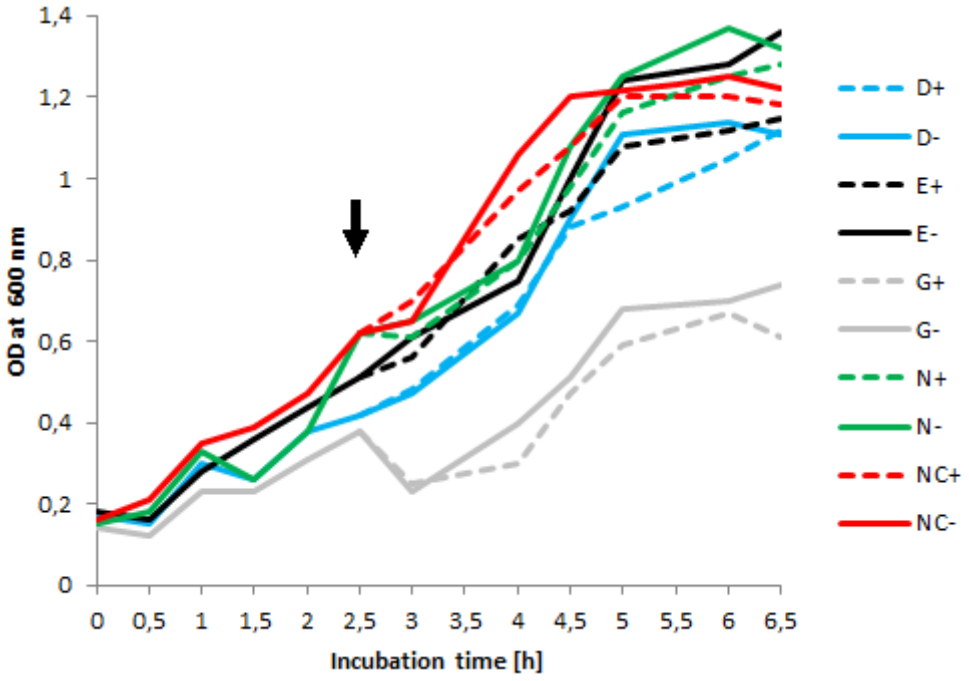

Figure 26: Growing curve of *E. coli* bacteria with and without induction of protein production.
MAX Efficiency® DH5αF'IQ bacteria transformed with pQE-30 plasmids coding for His$_6$-DMXL2$_{748\text{-}926}$-V5 (D), His$_6$-EML5$_{897\text{-}1038}$-V5 (E), His$_6$-GPCPD1$_{1\text{-}118}$-V5 (G) and His$_6$-NCAN$_{156\text{-}359}$-V5 (N) or the empty plasmid control (NC) were shaken at 37°C for 6.5 hours with (+) or without (-) induction of protein production after 2.5 hours through addition of 1 mM IPTG (arrow). OD was measured at 600 nm.

The truncated potential parent proteins $DMXL2_{748-926}$, $EML5_{897-1038}$, $GPCPD1_{1-118}$ and $NCAN_{156-359}$ with a V5 tag at the carboxy-terminus for detection in western blot analysis and a His_6-tag at the amino-terminus for protein purification were produced (Section 2.6.10, p. 48). To this end the sequences of $DMXL2_{748-926}$-V5, $EML5_{897-1038}$-V5, $GPCPD1_{1-118}$-V5 and $NCAN_{156-359}$-V5 were cloned into the pQE-30 vector which added the sequence MRGS-His_6-GS at the amino-terminus of the truncated proteins (Section 2.3.4, p. 35).

Before large scale protein production first the growth curve and behavior of the MAX Efficiency® DH5αF'IQ bacteria transformed with pQE-30 plasmids coding for His_6-$DMXL2_{748-926}$-V5, His_6-$EML5_{897-1038}$-V5, His_6-$GPCPD1_{1-118}$-V5 and His_6-$NCAN_{156-359}$-V5 with and without induction through IPTG was determined. Empty plasmid transformed bacteria served as negative control (Figure 26, p. 90).

The growth of all bacterial strains was slightly retarded through addition of IPTG after 2.5 hours. Non-induced bacteria grew to an in total higher cell density. The lac promoter appeared leaky so even non-induced bacteria produced protein albeit in lower amounts (data not shown). The growth peak was reached after 5.5 hours of incubation. The maximum of cell density reversely correlated with the amount of produced protein (Figure 26, p. 90 and Figure 27-B, p. 91).

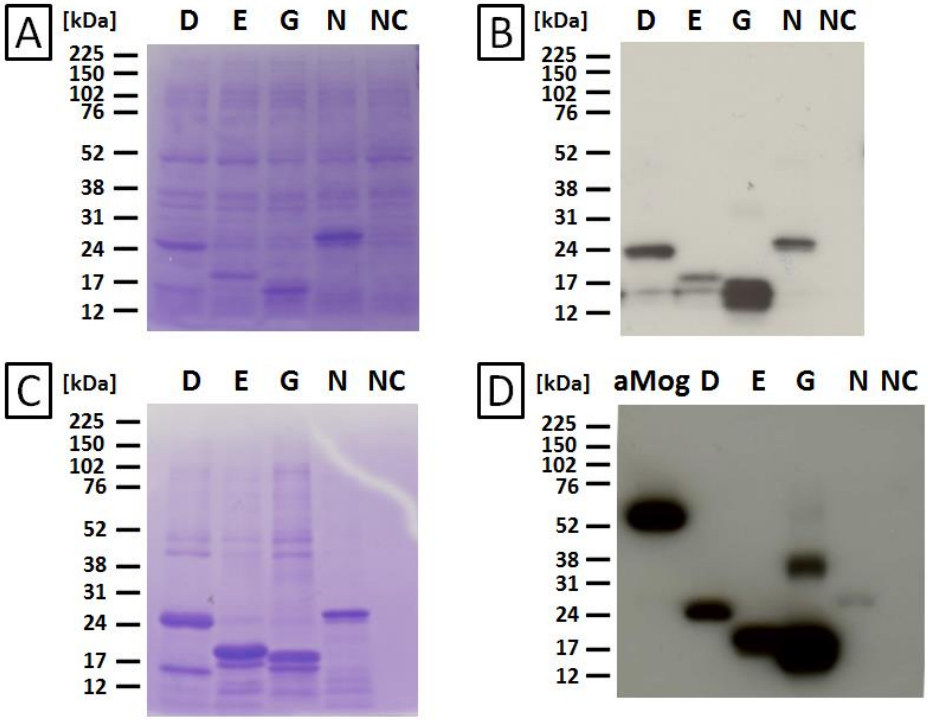

Figure 27: Production of truncated parent proteins in *E. coli* bacteria and their purification.
MAX Efficiency® DH5αF'IQ bacteria were transformed with pQE-30 plasmids coding for His_6-$DMXL2_{748-926}$-V5 (D), His_6-$EML5_{897-1038}$-V5 (E), His_6-$GPCPD1_{1-118}$-V5 (G) and His_6-$NCAN_{156-359}$-V5 (N) or the empty plasmid control (NC). Protein production was monitored by SDS-PAGE (**A**) and western blot (**B**) employing 0.12 µg/mL of the aV5-HRP antibody and 2 seconds exposure time. Protein purity after nickel chelate affinity chromatography was monitored by SDS-PAGE (**C**) and western blot (**D**) employing 0.12 µg/mL of the aV5-HRP antibody and 10 seconds exposure time. V5-tagged heavy chain of anti-MOG antibody served as positive control. Expected molecular weights: D 22.8 kDa, E 18.2 kDa, G 15.8 kDa, N 25.4 kDa.

The protocol for large scale protein production was adapted to the observed bacterial behavior. Protein amounts and purity were monitored by SDS-PAGE (Figure 27-A and -C, p. 91) and western blot (Figure 27-B and -D, p. 91) before and after nickel chelate affinity chromatography (Section 2.6.10, p. 48). Protein sequences were verified by MALDI-TOF-MS (Supplements 5.9, p. 140).

As expected from the slow growth rate, His_6-$GPCPD1_{1-118}$-V5 protein was produced and purified in very high amounts even leading to dimerization in SDS-PAGE with subsequent western blot analysis (Figure 27-B and -D, p. 91). Compared to His_6-$DMXL2_{748-926}$-V5 and His_6-$EML5_{897-1038}$-V5 proteins His_6-$NCAN_{156-359}$-V5 protein was purified in low but sufficient amounts (Figure 27-D, p. 91).

The HLA-$A2^+$ cell lines EBV-16488 and EBV-17490 were incubated with purified proteins or the purification eluate of empty plasmid control bacteria. Equally treated EBV-FE cells served as negative control. In none of the experiments co-cultured 2D1-NFAT-sGFP cells were activated (data not shown). Thus EBV-transducted B cells were not able to process and cross-present the truncated potential parent proteins leading to mimotope presentation on HLA-A2 molecules.

4 Discussion

MS is most probably an autoimmune inflammatory disease of the CNS. Demyelination of neurons and axonal loss occur in temporal and spatial resolution in multiple areas of the brain and spinal cord (Brück and Stadelmann, 2003). This impairment manifests in neurological symptoms. In acute and chronic brain lesions the amount of $CD8^+$ T lymphocytes exceeds the number of $CD4^+$ T cells (Babbe et al., 2000; Junker et al., 2007). Recent studies further stressed the prominent role of $CD8^+$ T cells which probably harm the oligodendrocytes and neurons through direct cytotoxicity and release of cytokines (Mars et al., 2010; Friese and Fugger, 2009).

The course of disease varies between individuals (Lucchinetti et al., 2000) and the causing mechanisms still remain elusive. Environmental factors as well as genetic predispositions are widely discussed. Very early a genetic linkage between the HLA gene locus and disease susceptibility was observed (Jersild et al., 1972; Naito et al., 1972). In 2011 the IMSGC and WTCCC2 published the latest results of genome-wide association studies for MS, stating that carrying the *HLA-A*0201* allele correlates with a protective effect (Silva et al., 2009). Therefore during this thesis two main questions were followed:

3. Which $CD8^+$ T lymphocytes participate in the autoimmune attack on CNS tissue and what are their receptors for antigen recognition?
4. How does the expression of HLA-A2 molecules lead to a decreased disease susceptibility?

To address the first questions potentially disease-related single $CD8^+$ T cells were isolated from brain tissue of MS patient FE via laser microdissection. Employing two different PCR techniques, their TCR molecules were analyzed (Seitz et al., 2006; Kim et al., 2012). In the second part antigen recognition of the disease-related TCR 2D1 in context of HLA-A2 molecules was investigated using a novel technique developed by Siewert et al. (2012). This led to the identification of several peptide antigens that might eventually induce depletion of specific T cell clones and thereby mediate protection. Finally potential parent proteins of the detected antigens were further characterized.

4.1 Identification of Disease-Related Alpha-Beta TCRs from $CD8^+$ T Cells in MS Patient FE

Patient FE was initially diagnosed with a malignant glioma in 1996, the affected brain area was surgically removed and stored frozen. Presence of oligoclonal immunoglobulin bands in CSF and three relapses in the following five years finally led to the diagnosis of MS. In contrast to already rarely available autopsy tissue, the stored brain biopsy from 1996 provided the unique opportunity to investigate very early immunological processes in MS brain tissue. In the course of my diploma thesis (Backes, 2010) all tissue blocks of MS patient FE were mapped according to accumulated immune

cells, actively inflamed areas and scar formation. Based on these results, the blocks 9a and 11b were used for the characterization of potentially disease-related $CD8^+$ T lymphocytes.

Therefore the potentially disease-related $CD8^+$ T cells had to be distinguished from non-involved bystander cells. In an earlier study, Seitz et al. (2006) analyzed disease-related T lymphocytes in polymyositis patients. During this disease muscle fibers are attacked by the immune system. In muscle biopsies muscle fibers and immune cells intruding into them were obvious. In the frozen tissue specimens from MS patient FE borders between brain cells were not distinguishable. Direct cell contact between autoreactive $CD8^+$ T lymphocytes and target cells could not be observed. Hence two other criteria were applied: Disease-related T cells had either to belong to a clonally expanded cell population or had to be activated.

The clone-specific approach for TCR characterization was based on earlier results from single cell analysis and CDR3 spectratyping that revealed several TCR beta chains of clonally expanded and persistent T cell populations in brain and blood samples of the MS patient FE (Babbe et al., 2000; Skulina et al., 2004). To analyze $CD8^+$ T lymphocytes carrying already known TCR beta chains, brain tissue was stained for CD8 and the specific TCR beta chains. As monoclonal antibodies against TCR BV13S1 and TCR BV22 were commercially available, persisting T cells carrying the TCR beta chains BV13S1-BJ2.3 and BV22-BJ2.1 were further investigated.

In the unbiased approach for TCR characterization brain tissue was stained for CD8 and the activation marker CD134 (formerly known as OX40). CD134 is expressed on activated T cells (Paterson et al., 1987) and was found on activated T lymphocytes involved in autoimmune encephalomyelitis (Weinberg et al., 1996).

Despite several technical obstacles the clone-specific PCR protocol for TCR identification could be optimized, the functionality of the unbiased PCR protocol was verified and disease-related TCR molecules from $CD8^+$ T cells in brain tissue of MS patient FE were characterized.

4.1.1 Technical Obstacles

During the identification of disease-related alpha beta TCRs from $CD8^+$ T cells in MS patient FE three major technical obstacles were met. First, T lymphocytes were cut in varying thicknesses in brain tissue sections and RNA might have been lost. Second, the image quality had to suffice for fluorescence microscopy and isolation of single cells by laser microdissection (Section 2.7.2, p. 52). Third, the RNA quality in the isolated single cells had to be adequate for subsequent PCR analyses (Section 2.7.3, p. 52).

4.1.1.1 Positioning of Cells in Tissue Sections

When preparing tissue sections, potentially disease-related $CD8^+$ T lymphocytes were cut open and RNA might have been swiped out. For single cell isolation the slides were stained according to the criteria mentioned above (Section 4.1, p. 93). During the washing and incubation steps again RNA might have been lost. Attempts to cross-link mRNA molecules to cell skeleton particles did not improve the yield of subsequent PCR analyses (Kathrin Held, data not published).

Stained T cells appear as rounded dots under the microscope. This appearance does not correlate with the amount of cell contained in the tissue section. The 10 µm tissue section might bear the main part containing a lot of mRNA molecules but also just a marginal part of the T lymphocyte (Figure 28-A, p. 95). The latter would not bear enough mRNA for later PCR analyses. In thicker tissue sections the probability of cutting bigger cell parts is higher, but two overlaying cells might appear as one (Figure 28-B, p. 95) and would potentially reveal two sequences for TCR molecules. It would not be possible to tell whether or not obtained TCR alpha- and beta-chain sequences are matching and truly deriving from one single disease-related T cell.

Taking those two points together, only approximately 50% of isolated single cells from 10 µm tissue sections contained enough RNA for subsequent PCR analyses.

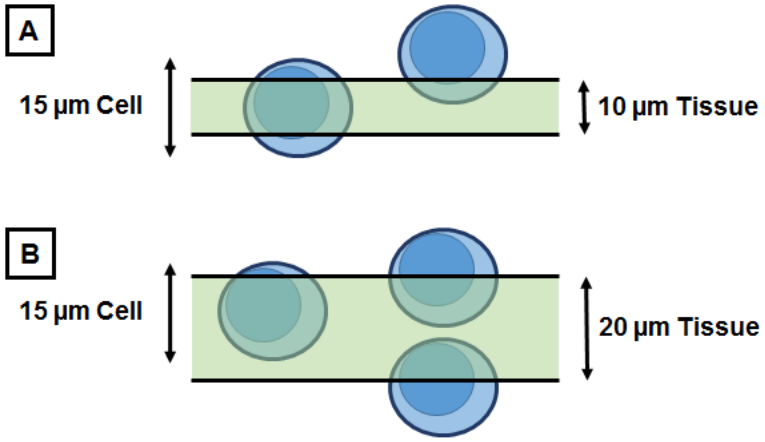

Figure 28: Position of cells and their nuclei in tissue sections.
A: In 10 µm tissue sections cells with a diameter of 15 µm may appear the same when stained for microscopy, but may be cut in different layers. The tissue section only contains the nucleus of the left cell. **B:** In thicker tissue sections the probability of cutting bigger cell parts is higher, but two overlaying cells might appear as one. (Modified from Backes, 2010.)

4.1.1.2 Image Quality

For conventional fluorescence staining, tissue slides are incubated as long as possible with blocking solution, primary and secondary antibodies. Due to the inevitable need of RNA preservation for subsequent PCR analyses, the staining protocol for laser microdissection was shortened to minimal incubation times (Section 2.7.2, p. 52). Despite further loss of image quality, the washing steps were reduced (Section 4.1.1.1, p. 94).

Usually tissue is covered with fluorescence mounting medium and a glass cover slip. This allows light to pass straightly resulting in sharp images with stark contrast. Covering the tissue is not possible during microdissection where tissue fragments are catapulted into a reaction tube using a laser beam. The application of Liquid Cover Glass impeded detection of stained cells due to strong auto-fluorescence (Section 3.2.2, p. 68). Thus stained tissue was covered with a drop of fast evaporating 1-propanol. The alcohol covers the tissue but adapts to its surface formations. Hence light rays get refracted in various directions (Figure 13, p. 69).

Those drawbacks resulted in blurred images (coverage with 1-propanol) with intense background staining (short incubation with blocking solution and minimal washing steps) (Figure 15, p. 73) but maintained RNA quality.

4.1.1.3 RNA Quality

To characterize the TCR molecules of potentially disease-related $CD8^+$ T lymphocytes, single cells were isolated by laser microdissection from frozen brain tissue sections. Thereupon mRNA coding for the TCR alpha- and beta-chains was transcribed into cDNA in a first RT-PCR (Section 2.7.3, p. 52). In earlier studies TCR molecules were analyzed employing more stable genomic DNA from single cells as PCR template (Roers et al., 1998; Babbe et al., 2000). This approach is applicable on TCR beta chains as in the gene locus only 13 BJ segments exist (Arden et al., 1995; Rowen et al., 1996). Thus for unbiased characterization of TCR beta chains a forward primer set annealing to all possible BV segments could be paired in 13 separate reactions with reverse primers annealing to each BJ segment. However, in this study additionally matching TCR alpha chains should be analyzed. In the TCR alpha chain gene locus 70 to 80 AV and 61 AJ gene segments are known (Arden et al., 1995; Rowen et al., 1996). Based on one single cell not enough separate PCR reactions are performable to cover all possible combinations. Thus genomic DNA was not suited as template in this approach.

Despite lower molecular stability of RNA compared to DNA a huge amount of mRNA molecules exists in one single cell. Additionally, on mRNA molecules the exon between the rearranged V(D)J segment and the C segment is removed (Section 1.2.2, p. 3). Forward primers annealing to all known BV or BA gene segments could be paired with reverse primers annealing to the BC or AC gene segment. Hence good initial RNA quality in the investigated patient tissue and RNA preservation throughout the cell isolation was crucial.

The biopsy of MS patient FE employed for the characterization of potentially disease-related $CD8^+$ T cells was taken in 1996. Right after surgery the biopsy was divided into several blocks and frozen at -80°C. Later the blocks were moved numerous times on dry ice between different laboratories and freezers. For preparation of tissue slices, the blocks were warmed to -20°C. All these cycles of warming and cooling during the last 16 years influenced the tissue and notably RNA quality.

Compared to RNA from fresh T hybridoma cells incubated with H_2O (Figure 12, p. 67) the RNA quality in the frozen biopsy parts 9a and 11b was expectedly worse (Figure 10, p. 66). However, despite many degradation products still intact 18S and 28S rRNA was detectable, rendering the initial RNA quality not very good but sufficient for subsequent single cell PCR experiments. It was considered highly probable for at least some TCR alpha- and beta-chain-coding mRNA molecules to be still intact and serve as RT-PCR template. Notably the RNA quality decreased after tissue slices were cut, mounted on PET slides and stored at -80°C (Figure 11, p. 66). Moreover after the staining procedure for single cell isolation (Section 2.7.2, p. 52) almost all RNA was degraded. Thus tissue slides were stored at -80°C for two weeks at most and RNase inhibitors were added into each staining solution. These changes of protocol and the employment of SIGMA Albumin from Bovine Serum as blocking solution improved the RNA preservation during single cell isolation experiments (Figure 12, p. 67).

4.1.2 The Clone-Specific PCR Method for TCR Identification

In the clone-specific approach for identification of alpha beta TCR molecules from potentially disease-related $CD8^+$ T lymphocytes, cells with an already known TCR beta chain were investigated. Spectratyping analyses revealed that in MS patient FE the TCR beta chains BV13S1-BJ2.3 and BV22-BJ2.1 belong to clonally expanded T lymphocyte populations with the N(D)N sequences SLGA and GAGEH, respectively (Skulina et al., 2004, Backes, 2010). The protocol for clone-specific amplification of TCR beta chains was published (Seitz et al., 2006). In Backes (2010) the protocol was applied on brain tissue sections from MS patient FE, but the TCR beta chains BV13S1-BJ2.3 and BV22-BJ2.1 were not recovered from isolated single cells.

Here new primer combinations for amplification of the two TCR beta chains were designed and evaluated (Section 3.2.3, p. 69). Employing them on RNA prepared from brain tissue slices of MS patient FE, the BV13S1-BJ2.3 and BV22-BJ2.1 sequences were found six and four times respectively. These results proofed the existence of the clonally expanded T cells in the investigated brain tissue of MS patient FE. Further, this experiment indicated that the tissue block 10a might be best suited for clone specific single cell isolation. From the RNA of this block three times the clonal expanded TCR beta chain sequence BV13S1-BJ2.3 and once the clonal expanded TCR beta chain sequence BV22-BJ2.1 was detected. But in line with mapping highly active lesion in the block 10a (Backes 2010), this tissue block was considered too precious for isolation of potentially disease-related $CD8^+$ T lymphocytes.

Positive staining for CD8 and the TCR beta chains BV13S1 or BV22 in brain tissue slides from the blocks 9a and 11b was a rare event. In these brain blocks mainly old lesions were present, indicating that the BV13S1-BJ2.3 and BV22-BJ2.1 T cell populations were participating in the pathomechanism of active lesions. Only 42 CD8 $beta^+$/TCR $BV13S1^+$ and 23 CD8 $beta^+$/TCR $BV22^+$ single cells were isolated from 69 and 15 slides, respectively (Section 3.4, p. 72). Employing the strictly clone-specific primers annealing to the BV and BJ segments only 1 of 13 possible TCR beta chains would have been detectable. Because TCR beta chains of T lymphocytes that consist of the BV13S1 or BV22 gene segments combined with one of the other 12 possible BJ gene segments would have been lost (Rowen et al., 1996), a semi-biased TCR beta chain PCR protocol was established (Section 3.3, p. 71).

Instead of employing reverse primers annealing to the BJ segment, primers annealing to the BC region were designed. Combining those with the BV13S1- or BV22-specific forward primers, all 13 possible TCR beta chain arrangements could be amplified. The new primer combination employing the BV13S1-specific forward primers was evaluated using RNA isolated from inflamed tonsil tissue. Six different $BV13S1^+$ TCR beta chain sequences were determined (Table 25, p. 72). With this semi-specific TCR beta chain PCR protocol now the probability for obtaining a sequence from isolated single cells stained for a specific TCR V beta segment was raised significantly.

Unfortunately, from the 42 CD8 $beta^+$/TCR $BV13S1^+$ and 23 CD8 $beta^+$/TCR $BV22^+$ isolated single cells the clonally expanded TCR beta chains BV13S1-BJ2.3 and BV22-BJ2.1 could not be amplified (Section 3.4, p. 72). Instead two different TCR beta chains BV13S1-BJ2.3 with the N(D)N sequences GTS and ARAAGA were detected (Table 26, p. 73). Those did not belong to clonally expanded T cell populations and no correlating TCR alpha chains could be identified. The latter might be due to

statistical reasons resulting from the huge amount of applied primers. Even from freshly isolated human blood lymphocytes only in 28.6 % the TCR alpha chain could be amplified (Section 3.1, p. 64). Taken together, these results strongly indicate an important role in active lesions of the T lymphocyte populations carrying the TCR beta chains BV13S1-BJ2.3 and BV22-BJ2.1 with the N(D)N sequences SLGA and GAGEH, respectively. For future experiments single cell isolation from tissue block 10a should be considered to finally reveal the matching TCR alpha chain.

4.1.3 The Unbiased PCR Method for TCR Identification

In the unbiased approach for identification of alpha beta TCR molecules from potentially disease-related $CD8^+$ T lymphocytes, mainly cells expressing the activation marker CD134 were investigated. Here the sequence of the TCR beta chains was not known beforehand. Thus a new set of primers amplifying TCR beta chains irrespectively of the rearranged BV and BJ segments was needed.

Song-Min Kim designed a set of nine forward primers (Table 6, p. 19) annealing to all known human BV gene segments. Those were combined with reverse primers annealing to the BC region, allowing the amplification of all possible human TCR beta chain sequences. During this thesis and as part of the publication Kim et al., 2012 the PCR protocol was tested on single human $CD3^+$ blood T lymphocytes (Section 3.1, p. 64). From 52 blood T cells 7 different TCR beta chains were identified (13.5 %). For these seven TCR beta chains two matching TCR alpha chains were detected yielding matching TCR alpha- and beta-chain sequences in 3.8 % of all analyzed single cells (Table 21, p. 64).

The yield of paired TCR alpha- and beta-chain sequences was relatively low compared to experiments performed on viable T cells from explant cell cultures from lesional biopsies of patients with chronic plaque psoriasis (Kim et al., 2012). There in 78 % of all analyzed single cells matching TCR beta- and alpha-chain sequences were obtained. This difference might be due to the following two reasons: First, the sorting of single $CD3^+$ blood T lymphocytes was performed by Wolfgang Klinkert employing the FACSVantage SE machine. He claimed that due to technical problems only in every third tube actually a sorted single cell could be expected. Second, the sorted single cells were frozen at –80°C before PCR analysis was performed. Thus strand breakage of mRNA molecules during freezing and thawing could have occurred and decreased the PCR efficiency.

As the functionality of the newly developed unspecific PCR protocol was proven and published, analysis of alpha beta TCR molecules from potentially disease-related $CD8^+$ T lymphocytes in brain tissue of MS patient FE was performed. Mainly T cells expressing the activation marker CD134 were investigated. As mentioned above, positive staining of CD8 and the TCR beta chains BV13S1 or BV22 for the clone-specific approach in brain tissue slides of the MS patient FE was a rare event (Section 4.1.2, p. 97). Thus also CD8 single positive cells were isolated from these slides and analyzed employing the unbiased TCR beta chain PCR protocol.

From 578 $CD8beta^+$ cells isolated from 84 tissue slides none and from 474 CD8 $beta^+/CD134^+$ cells isolated from 26 tissue slides one TCR beta chain sequence and no corresponding TCR alpha chain sequence was obtained (Section 3.4, p. 72). The TCR beta chain originated from an activated T lymphocyte which did not belong to a clonally expanded population in MS patient FE (Backes,

2010). However, a low yield of matching TCR alpha and beta chains obtained from single cells in frozen brain biopsies was already observed during the establishment of the unbiased PCR protocol (Kim et al., 2012). In these earlier experiments from 643 isolated single cells 68 TCR beta chains (10,6 %) and 13 TCR alpha chains were identified yielding 2 % paired TCR alpha and beta chains.
The very low output might be due to the initial RNA quality in the frozen tissue blocks of MS patient FE and loss of RNA quality during the staining protocol for single cell isolation (Section 4.1.1.3, p. 96). A lot of tissue fractions appearing like a CD8 single positively stained T lymphocyte could have been isolated because of the low image quality (Section 4.1.1.1, p. 94). To maintain RNA quality in future experiments isolated single cells should be processed faster. The recent acquisition of a pipetting robot might improve the technical basis for these requirements.

4.2 Future Prospects (I)

After pre-investigation by spectratyping, TCR beta chains of clonally expanded T cell populations can be detected and their matching TCR alpha chains may be identified employing the clone-specific PCR protocol (Seitz et al., 2006). Based on this method, here a semi-biased PCR protocol was established, allowing the amplification of all possible TCR beta chains that were arranged employing one specified BV gene segment independent of the BJ gene segment. In future experiments the characterization of TCR beta chains will not be restricted to pre-detected clones but also TCR beta chains containing different BJ segments may be identified. Despite differences in the BJ gene segments, those TCR beta chains might reveal closely related CDR3 sequences and antigen specificities. Further, spectratyping can be replaced by commercially available pyrosequencing analysis. This approach would save time and a lot of precious biopsy material.
Clinically it would be very interesting to finally identify the matching TCR alpha chains of the clonally expanded T cell populations carrying the BV13S1-BJ2.3 and BV22-BJ2.1 TCR beta chain in MS patient FE. As these T cell clones persisted for at least five years, they probably play a crucial role in the disease mechanism. In further experiments the complete TCR alpha- and beta-chain sequences could be reconstructed and employed for antigen search experiments.
Development of the PCR protocol for unbiased identification of TCR beta chains provides an even more powerful tool for characterization of disease-related alpha beta TCR molecules (Kim et al., 2012). Employing a universal primer set for all known BV gene segments no pre-investigation of the T cell repertoire is needed. The TCR beta chains of all T cells considered disease-related due to their activation status or morphology is now possible.
Further, Sun et al. (2012) designed an alternative pool of primers for unbiased amplification of TCR beta chains from single T lymphocytes. Their experiments were performed on viable sorted single T cells originating from human blood leading to high yields of TCR beta chain sequences. This unbiased pool of primers for the TCR beta chain could be applied using the PCR protocol for identification of TCR alpha chains (Section 2.7.6, p. 58) combined with reverse primers annealing to the BC region.

Taken together, the described methods for identification of matching TCR alpha and beta chains might be extended on further T cell subsets. Instead of staining for CD8 or CD134, staining for CD4 and markers of e.g. regulatory T cells, NK T cells or MAIT cells might be performed. For instance this would provide more profound insights into the molecular mechanisms underlying different kinds of autoimmune-mediated diseases, immune attacks on tumor cells or complications after organ transplantation.

4.3 Mimotope Identification of the MS-Related TCR 2D1 on HLA-A2 Molecules

Parallel to the characterization of disease-related $CD8^+$ T lymphocytes from brain tissue sections of MS patient FE, the linkage of moderate disease susceptibility to the expression of HLA-A2 molecules was investigated. In 2011 the IMSGC and WTCCC2 published the latest results of genome-wide association studies for MS. Primarily different HLA alleles are linked to disease susceptibility. Notably a risk factor is carrying the *HLA-A*0301* allele and a protective effect correlates with carrying the *HLA-A*0201* allele (Brynedal et al., 2007; Burfoot et al., 2008).

In 1997, Honma et al. isolated the $CD8^+$ T cell clone 2D1 from an MS patient. Further, they determined activation of the T cell clone 2D1 by the PLP_{45-53} peptide (KLIETYFSK) presented on HLA-A3 molecules. In 2008, Friese et al. used humanized mouse models to define the contributions of both HLA alleles to MS susceptibility. They generated double-transgenic mice expressing HLA-A3 and the TCR 2D1 as well as triple-transgenic mice expressing HLA-A3, the TCR 2D1 and HLA-A2. 4 % of the double-transgenic mice showed mild spontaneous motor deficits and 25 % developed an MS-like disease after immunization with PLP_{45-53} peptide. Strikingly even after immunization not a single triple-transgenic mouse showed symptoms. Further investigation revealed depletion of 2D1 T cells in the thymus of triple-transgenic mice. This observation indicated recognition of unknown peptide(s) in the context of HLA-A2 molecules leading to negative selection. The hypothesis was affirmed by the molecular similarity of HLA-A2 and HLA-A3 molecules (Figure 4, p. 6; McMahon et al., 2011).

The T cell clone 2D1 was isolated from an MS patient carrying both, the *HLA-A*0201* and *HLA-A*0301* alleles. The events during positive and negative selection of the clone 2D1 in the patient's thymus cannot be reconstructed. Thus it cannot be known whether the TCR 2D1 was initially selected due to interaction with HLA-A2 or HLA-A3 molecules. However, the TCR 2D1 appeared double-restricted by HLA-A3 as well as HLA-A2 molecules.

In a first round of experiments the capability of TCR 2D1 to allorecognize peptides bound to HLA-B38 molecules and to even xenorecognize murine antigen presenting molecules was observed. Additionally the TCR 2D1 was proven to crossrecognize one closely related nonamer derivative of the PLP_{45-53} peptide presented on HLA-A3 molecules. Then the first nonamer peptide presented on HLA-A2 molecules activating the TCR 2D1 was identified. Finally mimotopes presented on HLA-A2 molecules were identified. Based on the 3 structurally closely related mimotopes a motif-based

database search was performed revealing further 25 mimotopes presented on HLA-A2 molecules and recognized by the TCR 2D1.

4.3.1 First Evidence for Allo- and Crossreactivity of the TCR 2D1

The properties of TCR 2D1 were compared to the well-characterized TCR B7. This TCR was initially shown to recognize the TAX_{11-19} peptide (LLFGYPVYV) on HLA-A2 molecules (Ding et al., 1998). Crossrecognition of the peptides LGYGFVNYI, LGYGFVNYV, MLWGYLQYV and ILYGFIHIV presented on HLA-A2 molecules was later detected by Hausmann et al. (1999).

Unlike TCR B7, the TCR 2D1 showed signs of allo- and even xenorecognition in the very first experiment examining different cell lines as APC (Section 3.5.4, p. 77). 2D1-NFAT-sGFP reporter cells were activated by murine GP+E cells stably expressing HLA-B38 molecules. Allorecognition of endogenous peptides presented on HLA-B38 molecules might have been the underlying mechanism as GP+E cells stably expressing HLA-A2 molecules failed to activate the 2D1-NFAT-sGFP reporter cells. Further, murine LTK cells stably expressing human HLA-A1, HLA-A2 or HLA-A3 molecules activated 2D1-NFAT-sGFP reporter cells in an HLA- and PLP_{45-53} peptide-independent manner. Thus xenorecognition of murine antigen-presenting molecules on the surface of all different LTK cell lines might have occurred. These characteristics strongly indicated a high probability for the TCR 2D1 to additionally recognize peptides presented on HLA-A2 molecules.

In further experiments crossrecognition of nonamer peptides similar to the known peptides PLP_{45-53} (KLIETYFSK) and TAX_{11-19} (LLFGYPVYV) on the HLA-A3 and HLA-A2 molecules by the TCRs 2D1 and B7 was investigated (Section 3.5.6, p. 79). Therefore the two known peptides were entered into the protein search matrix of BLAST. As “best-guess” candidates twelve and seven derivatives of the PLP_{45-53} and TAX_{11-19} peptide respectively were chosen according to their source organisms or source proteins (Table 14, p. 24). Hereby neither HLA anchor positions nor potential TCR interaction residues were taken into account. This experiment aimed at categorizing the capability of crossrecognition of the TCR 2D1 compared to the TCR B7.

In line with Hausmann et al. (1999) a broad spectrum of crossrecognized peptides presented on HLA-A2 molecules was detected for the TCR B7. Besides four derivatives of the TAX_{11-19} peptide even seven derivatives of the structurally non-related PLP_{45-53} peptide resulted in activation of the B7-NFAT-sGFP reporter cell line. Recognition of the PLP_{45-53} derived peptide candidates presented on HLA-A2 molecules was surprising, as they did not display sequences in line with typical HLA-A2 anchor residues and thus should not be presented on those molecules. Although the TCR 2D1 showed some crossrecognition, this appeared in a very strict manner. Only one derivative of the PLP_{45-53} (KLIETYFSK) peptide with only one exchanged AA at position 8 (KLIETYF<u>K</u>K) activated the reporter cell line 2D1-NFAT-sGFP in the context of HLA-A3.

Strikingly, during this experiment the first recognition of a peptide presented on HLA-A2 molecules by the TCR 2D1 was verified. Whereas the reporter cell line B7-NFAT-sGFP was not activated by any peptide presented on HLA-A3 molecules, the cell line 2D1-NFAT-sGFP was capable of recognizing the TAX_{11-19} peptide derivative NLFGNPVYF in the context of HLA-A2 molecules. This peptide

showed a similar sequence to the later detected eightmer mimotopes (Section 4.3.2.2, p. 103). The mode of activation was not as strong as activation through the PLP_{45-53} peptide and its derivative (KLIETYFSK and KLIETYFKK) but still detectable in two independent experiments (Figure 19, p. 80). For the first time the TCR 2D1, which originated from an MS patient carrying both, the *HLA-A*0201* and *HLA-A*0301* alleles, was shown to be double-restricted.

4.3.2 Identification of Mimotopes Recognized by the TCR 2D1 on HLA-A2 Molecules

After the capability of the TCR 2D1 to recognize peptides presented on HLA-A2 molecules was verified, experiments for unbiased identification of mimotopes were performed. Therefore a new technique for the identification of antigenic peptides recognized by HLA class I-restricted T lymphocytes was employed (Siewert et al., 2012). Based on the three thereby identified mimotopes a shared motif was determined and database search for related existing peptides was conducted. In total 28 new peptide sequences were described to activate the TCR 2D1 in the context of HLA-A2 molecules.

4.3.2.1 Unbiased Identification of Antigenic Peptides

The technique developed by Siewert et al. (2012) was the first method for unbiased *in vitro* antigen search applicable for all HLA class I restricted TCRs (Section 2.8.4, p. 60). In an earlier approach van der Bruggen et al. (2007) transfected patient-derived full-length cDNA expression libraries into autologous APCs. Those APCs were scanned with patient-derived T cells. Only in very rare cases autologous APCs of a patient are available and the ability of APCs to correctly process antigens *in vitro* is very limited. Further, peptide-based screening approaches were independent of antigen processing (Mohme et al., 2013; Nino-Vasquez et al., 2004; Sospedra et al., 2003) but not all types of peptides may reach the HLA molecules on APCs if applied from the outside. For example hydrophobic candidates might accumulate and precipitate in aqueous cell culture media or disappear into cell membranes.

For the unbiased identification of mimotopes presented on HLA-A2 molecules and recognized by the TCR 2D1, COS-7 cells stably expressing HLA-A2 molecules served as APC (Section 3.5.2, p. 75). COS-7 cells derive from kidney tissue of the African green monkey. These cells are closer related to human than any rodent-derived cell lines, such as LTK or GP+E cells. Hence mechanisms associated with intracellular signaling or protein turnover might be better comparable to human cells. In 2007 Godelaine et al. successfully employed COS-7 cells as APCs for antigen search of $CD8^+$ T cells.

The COS-7-A2 cells were transfected with PECP libraries, coding for millions of different peptides of defined lengths with or without fixed AAs at certain positions. Co-cultured 2D1-NFAT-sGFP reporter cells stably expressed the TCR 2D1 as well as sGFP under the control of the NFAT promoter, leading to green fluorescence upon TCR activation (Section 3.5.1, p. 75).

As in earlier experiments recognition of the nonamer peptide NLFGNPVYF presented on HLA-A2 molecules was observed, first the N27 library from Katherina Siewert coding for random nonamer peptides was applied. Screening 27.7 $x10^6$ transfected APCs, no mimotope sequences were obtained.

According to Siewert, 2011 the employed N27 library coded for approximately 4×10^6 of all statistically possible 512×10^9 different nonamer peptides. The N27 library was one of the first libraries produced in our laboratory. The low clone number was obtained due to lacking experience. Thus no peptide sequence activating the TCR 2D1 in the context of HLA-A2 molecules might have been coded as the stated clone number was screened in almost 7-fold excess. As in recent attempts of library generation clone numbers of up to 4×10^8 were obtained (Section 3.5.3, p. 76), for future experiments a new N27 library should be generated.

Next the PECP libraries $A2^{269}$ and 9L kindly provided by Katherina Siewert were applied. In line with the HLA-A2 anchor motif stated at http://www.syfpeithi.de/home.htm, those libraries coded for nonamer peptides with I, V and L at the positions 2, 6 and 9 respectively or merely L at the position 9. Again no mimotope sequence was obtained. These results were not too surprising as in the analysis of "best-guess" candidates the antigenic peptide NLFGNPVYF did fit into the fixed AA scheme. Additionally presentation on HLA-A2 molecules and recognition by the TCR B7 of peptides could be demonstrated which did not match the stated anchor residues (Section 3.5.6, p. 79).

Five new PECP libraries of different lengths were designed. The PECP libraries N24, N30 and N39 coded for random eight-, ten- and tridecamers, whereas the PECP libraries 8L and 24L coded for peptides with seven or nine random AAs and L at position 8 or 10 respectively (Section 3.5.3, p. 76). Here except for the N30 library very high clone numbers were obtained. However, screening APCs transfected with the N24, N30, N39 and 10L libraries no mimotope sequences were obtained.

In contrast, screening of APCs transfected with the 8L library resulted in 27 clusters of at least six activated 2D1-NFAT-sGFP reporter cells and finally the three mimotope sequences LIGEVFVL, LVGEVWGL and LLGEVFEL were identified. For the first time the TCR 2D1 was shown to recognize three structurally closely related eightmer peptides presented on HLA-A2 molecules (Section 3.6.1, p. 81).

In antigen search experiments employing other TCRs, mimotopes were obtained from clusters containing only two to four activated reporter cells (Siewert, 2011). In these studies the TCR molecules of interest were cloned into different subtypes of $58\alpha^-\beta^-$ reporter cells. The T hybridoma cells employed during this thesis revealed "true" antigenic activation only then, when clusters of at least six activated cells were observed. Employing such cells in further experiments will save a lot of time and money. Microscopic screening can be performed very fast, because huge clusters of activated cells are very obvious compared to small accumulations. Those clusters might even facilitate future automation of cell search experiments.

4.3.2.2 Motif-Based Database Search

The TCR 2D1 displayed very strict recognition patterns for peptides presented on both, the HLA-A3 and HLA-A2 molecules. Presented on HLA-A3 besides the already known PLP_{45-53} peptide (KLIETYFSK) only nonamer derivatives with one AA exchange at the positions 3, 5, 7 or 8 (KLAETYFSK, KLIEAYFSK, KLIETYASK, KLIETYFAK and KLIETYFKK) activated the TCR 2D1 (Section 3.5.5, p. 78 and Section 3.5.6, p. 79). The unbiasedly detected eightmer mimotopes LIGEVFVL, LVGEVWGL and LLGEVFEL recognized on HLA-A2 molecules again presented a

very strict shared AA motif. AAs at the positions 1, 3, 4, 5 and 8 were identical, AAs at position 2 were aliphatic and AAs at position 6 were aromatic. Only position 7 seemed variable.

Falk et al. discovered in 1991 that nonamer peptides bound to HLA-A2 molecules should present L or M at position 2, V or L at position 9 and V at the auxiliary anchor position 6. Adapted to eightmer peptides all tree mimotopes were consistent with this claim. As HLA-A2 interaction motif they displayed L at position 1 and 9 and V at the auxiliary anchor position 5. Hence the positions 2 (aliphatic AAs I, L or V), 3 (G), 4 (E) and 6 (aromatic AAs F or W) seemed to interact with the TCR 2D1.

Based on the very strict motif a matrix for the search of related peptides was designed, which assigned probabilities to certain AAs at each position of eightmer peptides (Table 29, p. 82). With this matrix our collaborator Stefan Pinkert searched for matching peptides in protein databases for the taxa 9606 (human), 10090 (mouse), 408170 (human gut metagenome), 2 (bacteria) and 10239 (viruses). The taxa were chosen according to the following criteria:

First, the TCR 2D1 was isolated from a human MS patient carrying both the *HLA-A*0201* and *HLA-A*0301* alleles (Honma et al., 1997). Second, in a triple-transgenic mouse model the expression of HLA-A2 besides the TCR 2D1 and HLA-A3 prevented spontaneous and provoked MS-like symptoms (Friese et al., 2008). Peptides occurring in mouse and human were of special interest. Such candidates might allow to transfer the molecular basis of the protective effect in the mouse model to actual mechanisms in human MS. Third, recent evidence stretched the role of bacteria and especially those of the human gut microbiota in MS susceptibility and course of disease (Berer et al., 2011; Collins et al., 2012; Fung et al., 2012). Forth, several viruses were associated with MS (Virtanen and Jacobson, 2012; Rainey-Barger et al., 2013; Sundqvist et al., 2013). Candidate peptides deriving from pathogenic or commensal bacteria and viruses might activate immune cells. Due to a mechanism called “molecular mimicry”, such activated immune cells might then recognize endogenous peptides as well and perform tasks related to disease (Lucas et al., 2011).

The resulting list of hundreds of peptides was reduced excluding both, peptides that did not contain AAs with at least two HLA-A2 anchor and/or TCR 2D1 contact positions and peptides deriving from lethal or endemic bacteria from for example the deep sea. The now 37 candidate peptides were cloned into peptide-coding plasmids, transfected into COS-7-A2 cells and screened for the activation of 2D1-NFAT-sGFP cells (Section 3.6.2, p. 82). Subsequently a second matrix was designed according to all activating and non-activating peptide sequences (Supplements 5.4, p. 112). The resulting list of even more peptides was reduced according to the same criteria. Finally from 56 investigated candidates 25 mimotopes presented on HLA-A2 molecules activated the TCR 2D1 (Table 30, p. 83). The other peptide sequences were either not presented on HLA-A2 molecules or did not result in activation of the TCR 2D1 (Table 31, p. 83). Amongst the recognized eightmer peptides four derived from human and mouse, five from mouse, three from human, three from human gut metagenome, ten from bacteria and none from viruses.

4.3.3 Viral Association with Pathogenesis of Multiple Sclerosis

Surprisingly the motif-based database search did not reveal any antigenic candidate peptide deriving from viruses. Since the discovery of intrathecal antibodies against measles virus in MS patients (Adams and Imagawa, 1962) viruses were discussed as cause of MS pathogenesis. Varying viruses such as JC virus, HTLV-1, chlamydia or viruses of the herpes family were associated (Agostini et al., 2000; Poser et al., 1990; Rostasy et al., 2003; Olival et al., 2013). Especially the role of EBV was highlighted, as almost all MS patients are seropositive for EBV and infected B cells were detected in the meninges of MS patients (Serafini et al., 2007; Owens and Bennett, 2012; Pakpoor et al., 2013).
In follow-up experiments here the profile of peptides presented on HLA-A2 molecules from EBV-transduced B cells was investigated (Section 3.6.3, p. 84). None of the detected mimotopes was present on EBV-transducted HLA-A2 positive B cells. Hence here the hypothesized association of EBV infection with MS could not be affirmed. Investigation of other disease-related TCRs might shed some more light on the association between viruses and the pathogenesis of MS.

4.3.4 Application of Mimotopes as Synthetic Peptides

Recognition of peptides presented on HLA-A2 molecules might cause thymic depletion of TCR 2D1$^+$ T cells and prevent MS-like disease in HLA-A2, HLA-A3 and TCR 2D1 triple-transgenic mice (Friese et al., 2008). Thus the focus of further experiments was put on mimotopes existing in mice with emphasis on those also present in humans (Table 32, p. 105). Hereby the mimotope LPGEVWMV from mouse was excluded as its existence was stated by the protein database UniProt but not verified by NCBI protein BLAST. The expression of the resulting eight potential parent proteins in mouse brain and thymus tissue was verified by qPCR (Section 3.7.1, p. 86).

Table 32: Mimotopes presented on HLA-A2 molecules activating the TCR 2D1 originating from mouse or human and mouse.

Mimotope	Parent protein	Source Organism
LIGEVFNI	DMXL2	human, mouse
MEGEVWGL	EML5	human, mouse
	EML6	human, mouse
LPGEVFAI	GPCPD1	human, mouse
LGGEVFYV	NCAN	human, mouse
LIGEAFCL	ALOX12B	mouse
LLGEVWHL	AP5S1	mouse
LAGEVFAL	KLHL28	mouse
LSGEVFGM	MDH1B	mouse

Up to this stage, COS-7-A2 cells transfected with peptide-coding plasmids served as APCs. To confirm recognition of the mimotopes by the TCR 2D1 they were synthesized as peptides. Unlike in earlier experiments with synthetic peptides (Section 3.5.6, p. 79), the eight mimotope peptides originating from mouse could not be loaded onto COS-7-A2 cells. The peptides were too hydrophobic leading to aggregation and precipitation in the aqueous cell culture medium.

To circumvent this problem, HLA-A2 molecules were refolded *in vitro* (Section 3.7.2, p. 87). As this is a very costly and complex procedure, only the four mimotopes present in mouse and human were investigated. The candidate peptides $DMXL2_{813-820}$, $EML5_{997-1004}$ / $EML6_{997-1004}$, $GPCPD1_{15-22}$, and $NCAN_{257-264}$ in complex with HLA-A2 molecules resulted in activation of 2D1-NFAT-sGFP reporter cells. Employing this method, peptides of any characteristics may be loaded onto HLA class I molecules. Activation capacity of those complexes can then easily be investigated in an *in vitro* system.

4.4 *In Vitro* Processing of Potential Parent Proteins

The eight detected mimotopes originating from mouse cannot intrinsically be linked to processes preventing MS-like symptoms in triple-transgenic mice expressing the TCR 2D1, HLA-A2 and HLA-A3 (Friese et al., 2008). Expression of all potential parent proteins in brain and thymus was verified (Section 3.7.1, p. 86), but antigen processing resulting in presentation of antigenic peptides still remained unproven.

Ideally, professional APCs originating from triple-transgenic mice might be cultured *in vitro* and fed with purified potential parent proteins. As read-out system they would be co-cultured with 2D1-NFAT-sGFP reporter cells. In general, autologous APCs present the best option for the analysis of antigen processing. However, for most immune-mediated diseases the question of which cell type actually is the APC in the pathogenic mechanism remains unsolved. Should the correct cell type be identified, cells still might not be available in sufficient numbers or be generally suited for *in vitro* experiments. Thus here the antigen processing capability of first COS-7-A2 and second HLA-A2 positive EBV-transduced B cells was investigated. These cells were available in our laboratories and could be cultured with minor efforts.

For antigen presentation in the context of HLA class I molecules, proteins are degraded in the cytosol by the immunoproteasome (Rock et al., 2002). Peptides are then transported into the endoplasmatic reticulum and loaded onto HLA class I molecules (Yewdell et al., 2003). Those complexes finally reach the cell surface. This process can be performed by almost all nucleated cells in the body. In expectation of correct antigen processing, COS-7-A2 cells were transfected with plasmids coding for truncated versions of the potential parent proteins that contained the antigenic mimotope sequences (Section 3.7.3, p. 88).

The proteins were truncated according to their domain structure (Supplements 5.8, p. 126). The database “UniProt” provided known and predicted domains according to the AA sequence of the proteins of interest. The candidate peptides $DMXL2_{813-820}$, $EML5_{997-1004}$ / $EML6_{997-1004}$, and $NCAN_{257-264}$ were positioned between two of such domains. Thus the parent proteins were truncated before the first and after the second domain. The mimotope $GPCPD1_{15-22}$ was positioned closely to the amino terminus of the parent protein in a carbohydrate-binding module. In this case the truncation was performed after this module, leading to expression of only one domain.

The single-domain truncated protein $GPCPD1_{1-118}$-V5 was expressed in low amounts. $NCAN_{156-359}$-V5 was expressed stronger but sticking to membranes due to strong hydrophobicity. For unknown reasons $DMXL2_{748-926}$-V5 and $EML5_{897-1038}$-V5 were not expressed in COS-7-A2 cells (Figure 24, p. 89). The

plasmid constructs were based on those coding for mimotope peptide sequences and contained all the same regulatory sequences. Nonetheless COS-7-A2 cells expressing the truncated proteins $GPCPD1_{1\text{-}118}$-V5 and $NCAN_{156\text{-}359}$-V5 were co-cultivated with 2D1-NFAT-sGFP reporter cells but failed to activate them (Figure 25, p. 89). In line with earlier experiments, COS-7-A2 cells were not capable of correct antigen processing (Siewert, 2011; Bhonsle 2011).

In a second approach, HLA-A2 positive EBV-transducted B cell lines were employed as APCs (Section 3.7.4, p. 90). Those cells did not express the truncated proteins but might be capable of cross-presentation (Groothuis and Neefjes, 2005). B cells serve besides dendritic cells or macrophages as APC in the immune system. Cross-presentation of antigens that were taken up from the surrounding milieu on HLA class I molecules by dendritic cells is well known (Ackerman and Cresswell, 2004). Additionally it was shown that also B cells and other non-professional APCs are capable of cross-presentation (Bennett et al., 1998; Gnjatic et al., 2003).

Thus the truncated potential parent proteins His_6-$DMXL2_{748\text{-}926}$-V5, His_6-$EML5_{897\text{-}1038}$-V5, His_6-$GPCPD1_{1\text{-}118}$-V5 and His_6-$NCAN_{156\text{-}359}$-V5 were purified and fed to HLA-A2 positive EBV-transducted B cells. They were co-cultivated with 2D1-NFAT-sGFP reporter cells but failed to activate them. First of all the EBV-transduced B cells might not be able to uptake proteins from the cell culture medium and process them leading to mimotope presentation in this artificial setup. Second their clumpy growing might have impeded antigen presentation to 2D1-NFAT-sGFP reporter cells.

4.5 Future Prospects (II)

Here for the first time one nonamer and 28 eightmer peptides presented on HLA-A2 molecules were verified to activate the 2D1 TCR. Thus the TCR 2D1 was demonstrated to be crossreactive and double-restricted. The structural similarity of the eightmer mimotopes allowed fast identification of eight potential parent proteins originating from mouse, therefrom four additionally existing in human.

In future experiments the role of those proteins in the immunological processes of the investigated mice should be studied. First professional APCs originating from triple-transgenic mice should be cultured *in vitro* and fed with purified potential parent proteins. As read-out system they could be co-cultured with 2D1-NFAT-sGFP reporter cells generated during this thesis. When these APCs succeed in correct antigen processing and presentation of the mimotope peptides, the gene(-s) coding for the parent protein(-s) could be knocked out or knocked down in the triple-transgenic mice. Despite probable polygenetic influences now these mice might develop MS-like symptoms again.

Interestingly, the T cell clone 2D1 was isolated from an MS patient carrying both, the *HLA-A*0201* and *HLA-A*0301* alleles. In contrast to the effects observed in the triple-transgenic mouse model, expression of HLA-A2 molecules did not protect the patient from MS. Even though critical disparities between animal models and human are observed for various diseases, such models contribute to the understanding of health and disease and the development of new treatments.

Taken together, the methods for the characterization of disease-related alpha beta TCRs from $CD8^+$ T cells and for the identification of antigenic peptides recognized by HLA class I-restricted T lymphocytes provide powerful tools to better understand underlying mechanisms in T cell-mediated

diseases. Large patient cohorts might be studied and perhaps some common patterns could be detected. The obtained knowledge would allow development of new therapeutic approaches, diagnostic or prognostic biomarkers or even T cell based vaccinations. In terms of personalized medicine in the far future one might even think of developing a peptide vaccine against MS applicable for individuals carrying the *HLA-A*0201* allele based on the mimotopes identified in this thesis.

5 Supplements

5.1 Position of Primers for Clone-Specific TCR Beta Chain PCR

Blue: protein sequence, green: V region, red: N(D)N, black: J region.

BV13S1 - BJ2.3

```
    P  G  M  G  L  R  L  I  H  Y  S  V  G  A  G  I  T  D  Q  G  E  V  P  N
5′-CCAGGCATGGGGCTGAGGCTGATTCATTACTCAGTTGGTGCTGGTATCACTGACCAAGGAGAAGTCCCCAAT
 G  Y  N  V  S  R  S  T  T  E  D  F  P  L  R  L  L  S  A  A  P  S  Q  T  S
GGCTACAATGTCTCCAGATCAACCACAGAGGATTTCCCGCTCAGGCTGCTGTCGGCTGCTCCCTCCCAGACATCT
 V  Y  F  C  A  S  S  L  G  A  D  T  Q  Y  F  G  P  G  T  R  L  T  V  L
GTGTACTTCTGTGCCAGCAGCCTGGGAGCAGATACGCAGTATTTTGGCCCAGGCACCCGGCTGACAGTGCTCG-3′
```

Primer	Sequence	T_m [°C]
BV13S1-BJ2.3_for1	5’-AGG CTG ATT CAT TAC TCA GTT GG-3’	66
BV13S1-BJ2.3_rev1	5’-CGA GCA CTG TCA GCC GGG TGC-3’	72
BV13S1-BJ2.3_for2	5’-GTG CTG GTA TCA CTG ACC AAG G-3’	68
BV13S1-BJ2.3_rev2	5’-GTG CCT GGG CCA AAA TAC TGC-3’	66
BV13S1-BJ2.3_for3	5’-GTC TCC AGA TCA ACC ACA GAG G-3’	68
BV13S1-BJ2.3_rev3	5’-CCA AAA TAC TGC GTA TCT GCT CC-3’	68

BV13S1 - BJ2.3

```
    D  P  G  M  G  L  R  L  I  H  Y  S  V  G  A  G  I  T  D  Q  G  E  V  P
5′-GACCCAGGCATGGGGCTGAGGCTGATTCATTACTCAGTTGGTGCTGGTATCACTGACCAAGGAGAAGTCCCC
 N  G  Y  N  V  S  R  S  T  T  E  D  F  P  L  R  L  L  S  A  A  P  S  Q  T
AATGGCTACAATGTCTCCAGATCAACCACAGAGGATTTCCCGCTCAGGCTGCTGTCGGCTGCTCCCTCCCAGACA
 S  V  Y  F  C  A  S  S  L  G  A  D  T  Q  Y  F  G  P  G  T  R  L  T  V
TCTGTGTACTTCTGTGCCAGCAGCCTGGGAGCAGATACGCAGTATTTTGGCCCAGGCACCCGGCTGACAGTG-3′
```

Primer	Sequence	T_m [°C]
BV13S1-BJ2.3_for1-new	5’-CTG ATT CAT TAC TCA GTT GG-3’	56
BV13S1-BJ2.3_rev1-new	5’-CAC TGT CAG CCG GGT GC-3’	58
BV13S1-BJ2.3_for2-new	5’-CTG GTA TCA CTG ACC AAG G-3’	58
BV13S1-BJ2.3_rev2-new	5’-CCT GGG CCA AAA TAC TGC-3’	56
BV13S1-BJ2.3_for3-new	5’-ATC AAC CAC AGA GGA TTT CC-3’	58
BV13S1-BJ2.3_rev3-new	5’-AAT ACT GCG TAT CTG CTC C-3’	56

BV22 - BJ2.1

```
    I  S  N  H  L  Y  F  Y  W  Y  R  Q  I  L  G  Q  K  V  E  F  L  V  S  F
5′-ATCTCTAATCACTTATACTTCTATTGGTACAGACAAATCTTGGGGCAGAAAGTCGAGTTTCTGGTTTCCTTT
 Y  N  N  E  I  S  E  K  S  E  I  F  D  D  Q  F  S  V  E  R  P  D  G  S  N
TATAATAATGAAATCTCAGAGAAGTCTGAAATATTCGATGATCAATTCTCAGTTGAAAGGCCTGATGGATCAAAT
 F  T  L  K  I  R  S  T  K  L  E  D  S  A  M  Y  F  C  A  S  S  E  G  A  G
TTCACTCTGAAGATCCGGTCCACAAAGCTGGAGGACTCAGCCATGTACTTCTGTGCCAGCAGTGAAGGGCGGGA
 E  H  N  E  Q  F  F  G  P  G  T  R  L  T  V  L
GAACACAATGAGCAGTTCTTCGGGCCAGGGACACGGCTCACCGTGCTAG-3′
```

Primer	Sequence	T_m [°C]
BV22-BJ2.1_for1	5'-CTA TTG GTA CAG ACA AAT CTT GG-3'	64
BV22-BJ2.1_rev1	5'-CTA GCA CGG TGA GCC GTG TCC-3'	70
BV22-BJ2.1_for2	5'-AGA AGT CTG AAA TAT TCG ATG ATC-3'	64
BV22-BJ2.1_rev2	5'-AGC CGT GTC CCT GGC CCG AAG-3'	72
BV22-BJ2.1_for3	5'-GAT GAT CAA TTC TCA GTT GAA AGG-3'	66
BV22-BJ2.1_rev3	5'-AAG AAC TGC TCA TTG TGT TCT CC-3'	66

BV22 - BJ2.1

```
    I  S  N  H  L  Y  F  Y  W  Y  R  Q  I  L  G  Q  K  V  E  F  L  V  S  F
5'-ATCTCTAATCACTTATACTTCTATTGGTACAGACAAATCTTGGGGCAGAAAGTCGAGTTTCTGGTTTCCTTT
 Y  N  N  E  I  S  E  K  S  E  I  F  D  D  Q  F  S  V  E  R  P  D  G  S  N
TATAATAATGAAATCTCAGAGAAGTCTGAAATATTCGATGATCAATTCTCAGTTGAAAGGCCTGATGGATCAAAT
 F  T  L  K  I  R  S  T  K  L  E  D  S  A  M  Y  F  C  A  S  S  E  G  A  G
TTCACTCTGAAGATCCGGTCCACAAAGCTGGAGGACTCAGCCATGTACTTCTGTGCCAGCAGTGAAGGGGCGGGA
 E  H  N  E  Q  F  F  G  P  G  T  R  L  T  V
GAACACAATGAGCAGTTCTTCGGGCCAGGGACACGGCTCACCGTG-3'
```

Primer	Sequence	T_m [°C]
BV22-BJ2.1_for1-new	5'-TTG GTA CAG ACA AAT CTT GG-3'	56
BV22-BJ2.1_rev1-new	5'-CAC GGT GAG CCG TGT CC-3'	58
BV22-BJ2.1_for2-new	5'-CAG AGA AGT CTG AAA TAT TCG-3'	58
BV22-BJ2.1_rev2-new	5'-CTG GCC CGA AGA ACT GC-3'	56
BV22-BJ2.1_for3-new	5'-GAT CAA TTC TCA GTT GAA AGG-3'	58
BV22-BJ2.1_rev3-new	5'-ACT GCT CAT TGT GTT CTC C-3'	56

5.2 Position of Primers in the TCR Beta Chain Constant Gene Segment

Red: single nucleotide polymorphism between allele 1 and allele 2.

Human TCR beta chain C segment allele 1

```
5'-GAGGACCTGAACAAGGTGTTCCCACCCGAGGTCGCTGTGTTTGAGCCATCAGAAGCAGAGATCTCCCACACC
CAAAAGGCCACACTGGTGTGCCTGGCCACAGGCTTCTTCCCCGACCACGTGGAGCTGAGCTGGTGGGTGAATGGG
AAGGAGGTGCACAGTGGGGTCAGCACGGACCCGCAGCCCCTCAAGGAGCAGCCCGCCCTCAATGACTCCAGATAC
TGC-3'
```

Human TCR beta chain C segment allele 2

```
5'-GAGGACCTGAAAAACGTGTTCCCACCCGAGGTCGCTGTGTTTGAGCCATCAGAAGCAGAGATCTCCCACACC
CAAAAGGCCACACTGGTGTGCCTGGCCACAGGCTTCTACCCCGACCACGTGGAGCTGAGCTGGTGGGTGAATGGG
AAGGAGGTGCACAGTGGGGTCAGCACAGACCCGCAGCCCCTCAAGGAGCAGCCCGCCCTCAATGACTCCAGATAC
TGC-3'
```

Primer	Sequence	T_m [°C]
Cβ out	5'-TGG TCG GGG WAG AAG CCT GTG-3'	68°C
Cβ-RT-2	5'-GWA GAA GCC TGT GGC C-3'	52°C
Cβ-mid1	5'-GTG GCC TTT TGG GTG TGG-3'	58°C
Cβ-mid2	5'-GGT GTG GGA GAT CTC TGC-3'	58°C
Cβ-in	5'-TCT GAT GGC TCA AAC ACA GC-3'	60°C

5.3 Library Sequencing

Samples of the PECP libraries 8L, N24, 10L, N30 and N39 were sequenced after plasmid isolation (Section 2.3.1, p. 30 and Section 3.5.3, p. 76).

NNK: all amino acids, 1x stop; CTG: leucine.

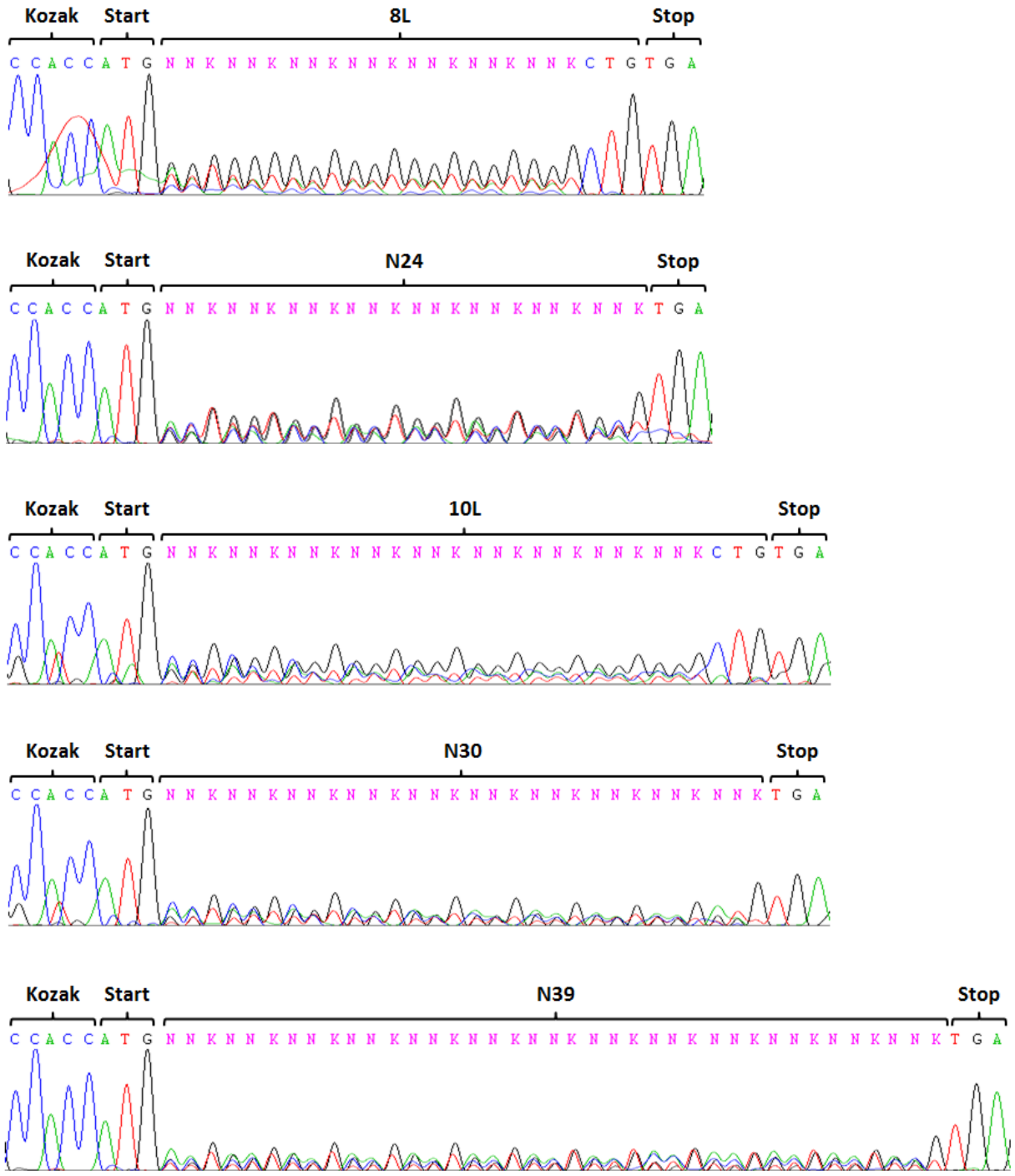

5.4 Second Matrix for Database Search Based on TCR 2D1-HLA-A2 Mimotopes and Candidates

According to the 3 mimotopes and 16 recognized candidates as well as the 21 not recognized candidates each AA is given a probability in percent at each peptide position.

Yellow: anchor position of HLA-A2, orange: presumed TCR 2D1 - peptide contact position, AAP: amino acid position.

AAP	Recognized mimotopes and candidates																		
1	L	L	L	L	L	L	L	L	L	L	I	M	L	L	L	L	L	L	
2	I	V	L	I	I	I	A	I	I	I	L	I	V	L	I	G	P	G	A
3	G	G	G	G	G	G	G	G	G	G	G	G	G	G	G	G	G	G	G
4	E	E	E	E	E	E	E	E	E	E	E	E	E	E	E	E	E	E	E
5	V	V	V	V	V	V	V	V	V	A	V	V	V	V	V	V	V	V	V
6	F	W	F	F	Y	F	F	W	F	F	F	W	W	W	F	Y	W	W	F
7	V	G	E	I	V	V	A	V	A	I	I	G	S	H	N	R	E	L	N
8	L	L	L	L	L	I	L	L	L	L	L	L	L	L	I	L	L	L	L

AAP	Not recognized candidates																		
1	L	L	I	L	L	L	L	L	L	L	L	L	L	L	L	L	L	L	L
2	I	I	V	L	V	V	I	I	V	V	P	T	V	V	T	T	Y	V	L	G	H
3	G	G	G	G	G	G	G	G	G	G	G	G	G	G	G	G	G	G	G	G	G
4	E	E	E	N	D	E	E	D	D	E	E	E	E	E	E	E	Q	Q	D	E
5	I	M	V	V	L	I	G	L	V	V	V	V	V	V	V	V	V	V	V	V
6	F	F	Y	F	W	F	F	F	W	F	H	A	G	D	V	F	F	F	F	F	Y
7	E	E	V	V	N	V	V	V	G	G	V	K	E	F	A	P	P	A	E	V	N
8	L	L	L	L	L	L	L	L	V	T	L	L	L	L	L	L	L	L	L	L	L

Second matrix for database search:

AAP	A	C	D	E	F	G	H	I	K	L	M	N	P	Q	R	S	T	V	W	Y	Sum
1	0	0	0	0	0	0	0	**20**	0	**50**	**30**	0	0	0	0	0	0	0	0	0	100%
2	**10**	0	0	0	0	**10**	0	**20**	0	**20**	0	0	**20**	0	0	0	0	**20**	0	0	100%
3	**20**	0	0	0	0	**80**	0	0	0	0	0	0	0	0	0	0	0	0	0	0	100%
4	0	0	0	**100**	0	0	0	0	0	0	0	0	0	0	0	0	0	0	0	0	100%
5	**30**	0	0	0	0	0	0	0	0	0	0	0	0	0	0	0	0	**70**	0	0	100%
6	0	0	0	0	**30**	0	**20**	0	0	0	0	0	0	0	0	0	0	0	**30**	**20**	100%
7	**5**	**5**	**5**	**5**	**5**	**5**	**5**	**5**	**5**	**5**	**5**	**5**	**5**	**5**	**5**	**5**	**5**	**5**	**5**	**5**	100%
8	0	0	0	0	0	0	0	**40**	0	**60**	0	0	0	0	0	0	0	0	0	0	100%

5.5 Primers and Plasmids for Peptide-Coding Plasmids

All primers were purchased in a concentration of 100 pmol/µL and HPLC purified from Metabion. Primers designated with "for"(ward) elongate the coding stand and primers designated with "rev"(erse) elongate the non-coding strand of DNA. Primers were optimized for expression in mammalian cells with the tool provided on the webpage http://www.encorbio.com/protocols/Codon.htm.

Name	Sequence
PLP_{45-53}-for	5′-CGC GCC ACC ATG AAA CTG ATT GAA ACC TAT TTT AGC AAA TGA GC-3′
PLP_{45-53}-rev	5′-GGC CGC TCA TTT GCT AAA ATA GGT TTC AAT CAG TTT CAT GGT GG-3′
TAX_{11-19}-for	5′-CGC GCC ACC ATG CTG CTG TTT GGC TAT CCG GTG TAT GTG TGA GC-3′
TAX_{11-19}-rev	5′-GGC CGC TCA CAC ATA CAC CGG ATA GCC AAA CAG CAG CAT GGT GG-3′
KLIETYFSL-for	5′-CGC GCC ACC ATG AAA CTG ATT GAA ACC TAT TTT AGC CTG TGA GC-3′
KLIETYFSL-rev	5′-GGC CGC TCA CAG GCT AAA ATA GGT TTC AAT CAG TTT CAT GGT GG-3′
ALIETYFSK-for	5′-CGC GCC ACC ATG GCG CTG ATT GAA ACC TAT TTT AGC AAA TGA GC-3′
ALIETYFSK-rev	5′-GGC CGC TCA TTT GCT AAA ATA GGT TTC AAT CAG CGC CAT GGT GG-3′
KAIETYFSK-for	5′-CGC GCC ACC ATG AAA GCG ATT GAA ACC TAT TTT AGC AAA TGA GC-3′
KAIETYFSK-rev	5′-GGC CGC TCA TTT GCT AAA ATA GGT TTC AAT CGC TTT CAT GGT GG-3′
KLAETYFSK-for	5′-CGC GCC ACC ATG AAA CTG GCG GAA ACC TAT TTT AGC AAA TGA GC-3′
KLAETYFSK-rev	5′-GGC CGC TCA TTT GCT AAA ATA GGT TTC CGC CAG TTT CAT GGT GG-3′
KLIATYFSK-for	5′-CGC GCC ACC ATG AAA CTG ATT GCG ACC TAT TTT AGC AAA TGA GC-3′
KLIATYFSK-rev	5′-GGC CGC TCA TTT GCT AAA ATA GGT CGC AAT CAG TTT CAT GGT GG-3′
KLIEAYFSK-for	5′-CGC GCC ACC ATG AAA CTG ATT GAA GCG TAT TTT AGC AAA TGA GC-3′
KLIEAYFSK-rev	5′-GGC CGC TCA TTT GCT AAA ATA CGC TTC AAT CAG TTT CAT GGT GG-3′
KLIETAFSK-for	5′-CGC GCC ACC ATG AAA CTG ATT GAA ACC GCG TTT AGC AAA TGA GC-3′
KLIETAFSK-rev	5′-GGC CGC TCA TTT GCT AAA CGC GGT TTC AAT CAG TTT CAT GGT GG-3′
KLIETYASK-for	5′-CGC GCC ACC ATG AAA CTG ATT GAA ACC TAT GCG AGC AAA TGA GC-3′
KLIETYASK-rev	5′-GGC CGC TCA TTT GCT CGC ATA GGT TTC AAT CAG TTT CAT GGT GG-3′
KLIETYFAK-for	5′-CGC GCC ACC ATG AAA CTG ATT GAA ACC TAT TTT GCG AAA TGA GC-3′
KLIETYFAK-rev	5′-GGC CGC TCA TTT CGC AAA ATA GGT TTC AAT CAG TTT CAT GGT GG-3′
LIGEVFIL-for	5′-CGC GCC ACC ATG CTG ATC GGC GAG GTG TTC ATC CTG TGA GC-3′
LIGEVFIL-rev	5′-GGC CGC TCA CAG GAT GAA CAC CTC GCC GAT CAG CAT GGT GG-3′
LIGEVYVL-for	5′-CGC GCC ACC ATG CTG ATC GGC GAG GTG TAC GTG CTG TGA GC-3′
LIGEVYVL-rev	5′-GGC CGC TCA CAG CAC GTA CAC CTC GCC GAT CAG CAT GGT GG-3′
LIGEVFVI-for	5′-CGC GCC ACC ATG CTG ATC GGC GAG GTG TTC GTG ATC TGA GC-3′
LIGEVFVI-rev	5′-GGC CGC TCA GAT CAC GAA CAC CTC GCC GAT CAG CAT GGT GG-3′
LIGEIFEL-for	5′-CGC GCC ACC ATG CTG ATC GGC GAG ATC TTC GAG CTG TGA GC-3′
LIGEIFEL-rev	5′-GGC CGC TCA CAG CTC GAA GAT CTC GCC GAT CAG CAT GGT GG-3′
LIGEMFEL-for	5′-CGC GCC ACC ATG CTG ATC GGC GAG ATG TTC GAG CTG TGA GC-3′
LIGEMFEL-rev	5′-GGC CGC TCA CAG CTC GAA CAT CTC GCC GAT CAG CAT GGT GG-3′
LAGEVFAL-for	5′-CGC GCC ACC ATG CTG GCC GGC GAG GTG TTC GCC CTG TGA GC-3′
LAGEVFAL-rev	5′-GGC CGC TCA CAG GGC GAA CAC CTC GCC GGC CAG CAT GGT GG-3′
IVGEVYVL-for	5′-CGC GCC ACC ATG ATC GTG GGC GAG GTG TAC GTG CTG TGA GC-3′
IVGEVYVL-rev	5′-GGC CGC TCA CAG CAC GTA CAC CTC GCC CAC GAT CAT GGT GG-3′
LIGEVWVL-for	5′-CGC GCC ACC ATG CTG ATC GGC GAG GTG TGG GTG CTG TGA GC-3′
LIGEVWVL-rev	5′-GGC CGC TCA CAG CAC CCA CAC CTC GCC GAT CAG CAT GGT GG-3′
LLGNVFVL-for	5′-CGC GCC ACC ATG CTG CTG GGC AAC GTG TTC GTG CTG TGA GC-3′

Name	Sequence
LLGNVFVL-rev	5′-GGC CGC TCA CAG CAC GAA CAC GTT GCC CAG CAG CAT GGT GG-3′
LVGDLWNL-for	5′-CGC GCC ACC ATG CTG GTG GGC GAC CTG TGG AAC CTG TGA GC-3′
LVGDLWNL-rev	5′-GGC CGC TCA CAG GTT CCA CAG GTC GCC CAC CAG CAT GGT GG-3′
LIGEVFAL-for	5′-CGC GCC ACC ATG CTG ATC GGC GAG GTG TTC GCC CTG TGA GC-3′
LIGEVFAL-rev	5′-GGC CGC TCA CAG GGC GAA CAC CTC GCC GAT CAG CAT GGT GG-3′
LVGEIFVL-for	5′-CGC GCC ACC ATG CTG GTG GGC GAG ATC TTC GTG CTG TGA GC-3′
LVGEIFVL-rev	5′-GGC CGC TCA CAG CAC GAA GAT CTC GCC CAC CAG CAT GGT GG-3′
LIGEGFVL-for	5′-CGC GCC ACC ATG CTG ATC GGC GAG GGC TTC GTG CTG TGA GC-3′
LIGEGFVL-rev	5′-GGC CGC TCA CAG CAC GAA GCC CTC GCC GAT CAG CAT GGT GG-3′
LIGEAFIL-for	5′-CGC GCC ACC ATG CTG ATC GGC GAG GCC TTC ATC CTG TGA GC-3′
LIGEAFIL-rev	5′-GGC CGC TCA CAG GAT GAA GGC CTC GCC GAT CAG CAT GGT GG-3′
LLGEVFIL-for	5′-CGC GCC ACC ATG CTG CTG GGC GAG GTG TTC ATC CTG TGA GC-3′
LLGEVFIL-rev	5′-GGC CGC TCA CAG GAT GAA CAC CTC GCC CAG CAG CAT GGT GG-3′
LIGDLFVL-for	5′-CGC GCC ACC ATG CTG ATC GGC GAC CTG TTC GTG CTG TGA GC-3′
LIGDLFVL-rev	5′-GGC CGC TCA CAG CAC GAA CAG GTC GCC GAT CAG CAT GGT GG-3′
IIGEVWGL-for	5′-CGC GCC ACC ATG ATC ATC GGC GAG GTG TGG GGC CTG TGA GC-3′
IIGEVWGL-rev	5′-GGC CGC TCA CAG GCC CCA CAC CTC GCC GAT GAT CAT GGT GG-3′
LVGDVWGV-for	5′-CGC GCC ACC ATG CTG GTG GGC GAC GTG TGG GGC GTG TGA GC-3′
LVGDVWGV-rev	5′-GGC CGC TCA CAC GCC CCA CAC GTC GCC CAC CAG CAT GGT GG-3′
MVGEVWSL-for	5′-CGC GCC ACC ATG ATG GTG GGC GAG GTG TGG AGC CTG TGA GC-3′
MVGEVWSL-rev	5′-GGC CGC TCA CAG GCT CCA CAC CTC GCC CAC CAT CAT GGT GG-3′
LLGEVWHL-for	5′-CGC GCC ACC ATG CTG CTG GGC GAG GTG TGG CAC CTG TGA GC-3′
LLGEVWHL-rev	5′-GGC CGC TCA CAG GTG CCA CAC CTC GCC CAG CAG CAT GGT GG-3′
LIGEVFNI-for	5′-CGC GCC ACC ATG CTG ATC GGC GAG GTG TTC AAC ATC TGA GC-3′
LIGEVFNI-rev	5′-GGC CGC TCA GAT GTT GAA CAC CTC GCC GAT CAG CAT GGT GG-3′
LGGEVYRL-for	5′-CGC GCC ACC ATG CTG GGC GGC GAG GTG TAC AGA CTG TGA GC-3′
LGGEVYRL-rev	5′-GGC CGC TCA CAG TCT GTA CAC CTC GCC GCC CAG CAT GGT GG-3′
LPGEVWEL-for	5′-CGC GCC ACC ATG CTG CCC GGC GAG GTG TGG GAG CTG TGA GC-3′
LPGEVWEL-rev	5′-GGC CGC TCA CAG CTC CCA CAC CTC GCC GGG CAG CAT GGT GG-3′
LVGEVFGT-for	5′-CGC GCC ACC ATG CTG GTG GGC GAG GTG TTC GGC ACC TGA GC-3′
LVGEVFGT-rev	5′-GGC CGC TCA GGT GCC GAA CAC CTC GCC CAC CAG CAT GGT GG-3′
LGGEVWLL-for	5′-CGC GCC ACC ATG CTG GGC GGC GAG GTG TGG CTG CTG TGA GC-3′
LGGEVWLL-rev	5′-GGC CGC TCA CAG CAG CCA CAC CTC GCC GCC CAG CAT GGT GG-3′
LAGEVFNL-for	5′-CGC GCC ACC ATG CTG GCC GGC GAG GTG TTC AAC CTG TGA GC-3′
LAGEVFNL-rev	5′-GGC CGC TCA CAG GTT GAA CAC CTC GCC GGC CAG CAT GGT GG-3′
LPGEVHVL-for	5′-CGC GCC ACC ATG CTG CCC GGC GAG GTG CAC GTG CTG TGA GC-3′
LPGEVHVL-rev	5′-GGC CGC TCA CAG CAC GTG CAC CTC GCC GGG CAG CAT GGT GG-3′
LTGEVAKL-for	5′-CGC GCC ACC ATG CTG ACC GGC GAG GTG GCC AAG CTG TGA GC-3′
LTGEVAKL-rev	5′-GGC CGC TCA CAG CTT GGC CAC CTC GCC GGT CAG CAT GGT GG-3′
LVGEVGEL-for	5′-CGC GCC ACC ATG CTG GTG GGC GAG GTG GGC GAG CTG TGA GC-3′
LVGEVGEL-rev	5′-GGC CGC TCA CAG CTC GCC CAC CTC GCC CAC CAG CAT GGT GG-3′
LVGEVDFL-for	5′-CGC GCC ACC ATG CTG GTG GGC GAG GTG GAC TTC CTG TGA GC-3′
LVGEVDFL-rev	5′-GGC CGC TCA CAG GAA GTC CAC CTC GCC CAC CAG CAT GGT GG-3′
LTGEVVAL-for	5′-CGC GCC ACC ATG CTG ACC GGC GAG GTG GTG GCC CTG TGA GC-3′
LTGEVVAL-rev	5′-GGC CGC TCA CAG GGC CAC CAC CTC GCC GGT CAG CAT GGT GG-3′
LTGEVFPL-for	5′-CGC GCC ACC ATG CTG ACC GGC GAG GTG TTC CCC CTG TGA GC-3′
LTGEVFPL-rev	5′-GGC CGC TCA CAG GGG GAA CAC CTC GCC GGT CAG CAT GGT GG-3′
LYGEVFPL-for	5′-CGC GCC ACC ATG CTG TAC GGC GAG GTG TTC CCC CTG TGA GC-3′

Name	Sequence
LYGEVFPL-rev	5′-GGC CGC TCA CAG GGG GAA CAC CTC GCC GTA CAG CAT GGT GG-3′
LVGQVFAL-for	5′-CGC GCC ACC ATG CTG GTG GGC CAG GTG TTC GCC CTG TGA GC-3′
LVGQVFAL-rev	5′-GGC CGC TCA CAG GGC GAA CAC CTG GCC CAC CAG CAT GGT GG-3′
LLGQVFEL-for	5′-CGC GCC ACC ATG CTG CTG GGC CAG GTG TTC GAG CTG TGA GC-3′
LLGQVFEL-rev	5′-GGC CGC TCA CAG CTC GAA CAC CTG GCC CAG CAG CAT GGT GG-3′
LGGDVFVL-for	5′-CGC GCC ACC ATG CTG GGC GGC GAC GTG TTC GTG CTG TGA GC-3′
LGGDVFVL-rev	5′-GGC CGC TCA CAG CAC GAA CAC GTC GCC GCC CAG CAT GGT GG-3′
LHGEVYNL-for	5′-CGC GCC ACC ATG CTG CAC GGC GAG GTG TAC AAC CTG TGA GC-3′
LHGEVYNL-rev	5′-GGC CGC TCA CAG GTT GTA CAC CTC GCC GTG CAG CAT GGT GG-3′
LPGEVFAI-for	5′-CGC GCC ACC ATG CTG CCC GGC GAG GTG TTC GCC ATC TGA GC-3′
LPGEVFAI-rev	5′-GGC CGC TCA GAT GGC GAA CAC CTC GCC GGG CAG CAT GGT GG-3′
LLGELWCL-for	5′-CGC GCC ACC ATG CTG CTG GGC GAG CTG TGG TGC CTG TGA GC-3′
LLGELWCL-rev	5′-GGC CGC TCA CAG GCA CCA CAG CTC GCC CAG CAG CAT GGT GG-3′
LGGEVFYV-for	5′-CGC GCC ACC ATG CTG GGC GGC GAG GTG TTC TAC GTG TGA GC-3′
LGGEVFYV-rev	5′-GGC CGC TCA CAC GTA GAA CAC CTC GCC GCC CAG CAT GGT GG-3′
LLGEVQAL-for	5′-CGC GCC ACC ATG CTG CTG GGC GAG GTG CAG GCC CTG TGA GC-3′
LLGEVQAL-rev	5′-GGC CGC TCA CAG GGC CTG CAC CTC GCC CAG CAG CAT GGT GG-3′
LEGEGFIL-for	5′-CGC GCC ACC ATG CTG GAG GGC GAG GGC TTC ATC CTG TGA GC-3′
LEGEGFIL-rev	5′-GGC CGC TCA CAG GAT GAA GCC CTC GCC CTC CAG CAT GGT GG-3′
MEGEVWGL-for	5′-CGC GCC ACC ATG ATG GAG GGC GAG GTG TGG GGC CTG TGA GC-3′
MEGEVWGL-rev	5′-GGC CGC TCA CAG GCC CCA CAC CTC GCC CTC CAT CAT GGT GG-3′
LRGEVWQL-for	5′-CGC GCC ACC ATG CTG AGA GGC GAG GTG TGG CAG CTG TGA GC-3′
LRGEVWQL-rev	5′-GGC CGC TCA CAG CTG CCA CAC CTC GCC TCT CAG CAT GGT GG-3′
LRGEVWAL-for	5′-CGC GCC ACC ATG CTG AGA GGC GAG GTG TGG GCC CTG TGA GC-3′
LRGEVWAL-rev	5′-GGC CGC TCA CAG GGC CCA CAC CTC GCC TCT CAG CAT GGT GG-3′
LIGEVWLA-for	5′-CGC GCC ACC ATG CTG ATC GGC GAG GTG TGG CTG GCC TGA GC-3′
LIGEVWLA-rev	5′-GGC CGC TCA GGC CAG CCA CAC CTC GCC GAT CAG CAT GGT GG-3′
LLGEVVAL-for	5′-CGC GCC ACC ATG CTG CTG GGC GAG GTG GTG GCC CTG TGA GC-3′
LLGEVVAL-rev	5′-GGC CGC TCA CAG GGC CAC CAC CTC GCC CAG CAG CAT GGT GG-3′
LIGEAFCL-for	5′-CGC GCC ACC ATG CTG ATC GGC GAG GCC TTC TGC CTG TGA GC-3′
LIGEAFCL-rev	5′-GGC CGC TCA CAG GCA GAA GGC CTC GCC GAT CAG CAT GGT GG-3′
LLGEVWNA-for	5′-CGC GCC ACC ATG CTG CTG GGC GAG GTG TGG AAC GCC TGA GC-3′
LLGEVWNA-rev	5′-GGC CGC TCA GGC GTT CCA CAC CTC GCC CAG CAG CAT GGT GG-3′
LLGAVWLL-for	5′-CGC GCC ACC ATG CTG CTG GGC GCC GTG TGG CTG CTG TGA GC-3′
LLGAVWLL-rev	5′-GGC CGC TCA CAG CAG CCA CAC GGC GCC CAG CAG CAT GGT GG-3′
LEGEAFPL-for	5′-CGC GCC ACC ATG CTG GAG GGC GAG GCC TTC CCC CTG TGA GC-3′
LEGEAFPL-rev	5′-GGC CGC TCA CAG GGG GAA GGC CTC GCC CTC CAG CAT GGT GG-3′
LSGEVFGM-for	5′-CGC GCC ACC ATG CTG AGC GGC GAG GTG TTC GGC ATG TGA GC-3′
LSGEVFGM-rev	5′-GGC CGC TCA CAT GCC GAA CAC CTC GCC GCT CAG CAT GGT GG-3′
LPGEVWMV-for	5′-CGC GCC ACC ATG CTG CCC GGC GAG GTG TGG ATG GTG TGA GC-3′
LPGEVWMV-rev	5′-GGC CGC TCA CAC CAT CCA CAC CTC GCC GGG CAG CAT GGT GG-3′
LSGEVHLL-for	5′-CGC GCC ACC ATG CTG AGC GGC GAG GTG CAC CTG CTG TGA GC-3′
LSGEVHLL-rev	5′-GGC CGC TCA CAG CAG GTG CAC CTC GCC GCT CAG CAT GGT GG-3′
LEGEVFIV-for	5′-CGC GCC ACC ATG CTG GAG GGC GAG GTG TTC ATC GTG TGA GC-3′
LEGEVFIV-rev	5′-GGC CGC TCA CAC GAT GAA CAC CTC GCC CTC CAG CAT GGT GG-3′
LQGEVFGA-for	5′-CGC GCC ACC ATG CTG CAG GGC GAG GTG TTC GGC GCC TGA GC-3′
LQGEVFGA-rev	5′-GGC CGC TCA GGC GCC GAA CAC CTC GCC CTG CAG CAT GGT GG-3′

All following plasmids were constructed during this thesis employing the primers above (Section 2.3.2, p. 32).

Plasmid	Size	Resistance Genes	Application
pcDNArc-PLP_{45-53}	5.1 kb	amp^R, bls^R	Expression of PLP_{45-53} peptide in COS-7 cells
pcDNArc-TAX_{11-19}	5.1 kb	amp^R, bls^R	Expression of TAX_{11-19} peptide in COS-7 cells
pcDNArc-KLIETYFSL	5.1 kb	amp^R, bls^R	Expression of KLIETYFSL peptide in COS-7 cells
pcDNArc-ALIETYFSK	5.1 kb	amp^R, bls^R	Expression of ALIETYFSK peptide in COS-7 cells
pcDNArc-KAIETYFSK	5.1 kb	amp^R, bls^R	Expression of KAIETYFSK peptide in COS-7 cells
pcDNArc-KLAETYFSK	5.1 kb	amp^R, bls^R	Expression of KLAETYFSK peptide in COS-7 cells
pcDNArc-KLIATYFSK	5.1 kb	amp^R, bls^R	Expression of KLIATYFSK peptide in COS-7 cells
pcDNArc-KLIEAYFSK	5.1 kb	amp^R, bls^R	Expression of KLIEAYFSK peptide in COS-7 cells
pcDNArc-KLIETAFSK	5.1 kb	amp^R, bls^R	Expression of KLIETAFSK peptide in COS-7 cells
pcDNArc-KLIETYASK	5.1 kb	amp^R, bls^R	Expression of KLIETYASK peptide in COS-7 cells
pcDNArc-KLIETYFAK	5.1 kb	amp^R, bls^R	Expression of KLIETYFAK peptide in COS-7 cells
pcDNArc-LIGEVFIL	5.1 kb	amp^R, bls^R	Expression of LIGEVFIL peptide in COS-7 cells
pcDNArc-LIGEVYVL	5.1 kb	amp^R, bls^R	Expression of LIGEVYVL peptide in COS-7 cells
pcDNArc-LIGEVFVI	5.1 kb	amp^R, bls^R	Expression of LIGEVFVI peptide in COS-7 cells
pcDNArc-LIGEIFEL	5.1 kb	amp^R, bls^R	Expression of LIGEIFEL peptide in COS-7 cells
pcDNArc-LIGEMFEL	5.1 kb	amp^R, bls^R	Expression of LIGEMFEL peptide in COS-7 cells
pcDNArc-LAGEVFAL	5.1 kb	amp^R, bls^R	Expression of LAGEVFAL peptide in COS-7 cells
pcDNArc-IVGEVYVL	5.1 kb	amp^R, bls^R	Expression of IVGEVYVL peptide in COS-7 cells
pcDNArc-LIGEVWVL	5.1 kb	amp^R, bls^R	Expression of LIGEVWVL peptide in COS-7 cells
pcDNArc-LLGNVFVL	5.1 kb	amp^R, bls^R	Expression of LLGNVFVL peptide in COS-7 cells
pcDNArc-LVGDLWNL	5.1 kb	amp^R, bls^R	Expression of LVGDLWNL peptide in COS-7 cells
pcDNArc-LIGEVFAL	5.1 kb	amp^R, bls^R	Expression of LIGEVFAL peptide in COS-7 cells
pcDNArc-LVGEIFVL	5.1 kb	amp^R, bls^R	Expression of LVGEIFVL peptide in COS-7 cells
pcDNArc-LIGEGFVL	5.1 kb	amp^R, bls^R	Expression of LIGEGFVL peptide in COS-7 cells
pcDNArc-LIGEAFIL	5.1 kb	amp^R, bls^R	Expression of LIGEAFIL peptide in COS-7 cells
pcDNArc-LLGEVFIL	5.1 kb	amp^R, bls^R	Expression of LLGEVFIL peptide in COS-7 cells
pcDNArc-LIGDLFVL	5.1 kb	amp^R, bls^R	Expression of LIGDLFVL peptide in COS-7 cells
pcDNArc-IIGEVWGL	5.1 kb	amp^R, bls^R	Expression of IIGEVWGL peptide in COS-7 cells
pcDNArc-LVGDVWGV	5.1 kb	amp^R, bls^R	Expression of LVGDVWGV peptide in COS-7 cells
pcDNArc-MVGEVWSL	5.1 kb	amp^R, bls^R	Expression of MVGEVWSL peptide in COS-7 cells
pcDNArc-LLGEVWHL	5.1 kb	amp^R, bls^R	Expression of LLGEVWHL peptide in COS-7 cells
pcDNArc-LIGEVFNI	5.1 kb	amp^R, bls^R	Expression of LIGEVFNI peptide in COS-7 cells
pcDNArc-LGGEVYRL	5.1 kb	amp^R, bls^R	Expression of LGGEVYRL peptide in COS-7 cells
pcDNArc-LPGEVWEL	5.1 kb	amp^R, bls^R	Expression of LPGEVWEL peptide in COS-7 cells
pcDNArc-LVGEVFGT	5.1 kb	amp^R, bls^R	Expression of LVGEVFGT peptide in COS-7 cells
pcDNArc-LGGEVWLL	5.1 kb	amp^R, bls^R	Expression of LGGEVWLL peptide in COS-7 cells
pcDNArc-LAGEVFNL	5.1 kb	amp^R, bls^R	Expression of LAGEVFNL peptide in COS-7 cells
pcDNArc-LPGEVHVL	5.1 kb	amp^R, bls^R	Expression of LPGEVHVL peptide in COS-7 cells
pcDNArc-LTGEVAKL	5.1 kb	amp^R, bls^R	Expression of LTGEVAKL peptide in COS-7 cells
pcDNArc-LVGEVGEL	5.1 kb	amp^R, bls^R	Expression of LVGEVGEL peptide in COS-7 cells
pcDNArc-LVGEVDFL	5.1 kb	amp^R, bls^R	Expression of LVGEVDFL peptide in COS-7 cells
pcDNArc-LTGEVVAL	5.1 kb	amp^R, bls^R	Expression of LTGEVVAL peptide in COS-7 cells
pcDNArc-LTGEVFPL	5.1 kb	amp^R, bls^R	Expression of LTGEVFPL peptide in COS-7 cells
pcDNArc-LYGEVFPL	5.1 kb	amp^R, bls^R	Expression of LYGEVFPL peptide in COS-7 cells

Plasmid	Size	Resistance Genes	Application
pcDNArc-LVGQVFAL	5.1 kb	amp^R, bls^R	Expression of LVGQVFAL peptide in COS-7 cells
pcDNArc-LLGQVFEL	5.1 kb	amp^R, bls^R	Expression of LLGQVFEL peptide in COS-7 cells
pcDNArc-LGGDVFVL	5.1 kb	amp^R, bls^R	Expression of LGGDVFVL peptide in COS-7 cells
pcDNArc-LHGEVYNL	5.1 kb	amp^R, bls^R	Expression of LHGEVYNL peptide in COS-7 cells
pcDNArc-LPGEVFAI	5.1 kb	amp^R, bls^R	Expression of LPGEVFAI peptide in COS-7 cells
pcDNArc-LLGELWCL	5.1 kb	amp^R, bls^R	Expression of LLGELWCL peptide in COS-7 cells
pcDNArc-LGGEVFYV	5.1 kb	amp^R, bls^R	Expression of LGGEVFYV peptide in COS-7 cells
pcDNArc-LLGEVQAL	5.1 kb	amp^R, bls^R	Expression of LLGEVQAL peptide in COS-7 cells
pcDNArc-LEGEGFIL	5.1 kb	amp^R, bls^R	Expression of LEGEGFIL peptide in COS-7 cells
pcDNArc-MEGEVWGL	5.1 kb	amp^R, bls^R	Expression of MEGEVWGL peptide in COS-7 cells
pcDNArc-LRGEVWQL	5.1 kb	amp^R, bls^R	Expression of LRGEVWQL peptide in COS-7 cells
pcDNArc-LRGEVWAL	5.1 kb	amp^R, bls^R	Expression of LRGEVWAL peptide in COS-7 cells
pcDNArc-LIGEVWLA	5.1 kb	amp^R, bls^R	Expression of LIGEVWLA peptide in COS-7 cells
pcDNArc-LLGEVVAL	5.1 kb	amp^R, bls^R	Expression of LLGEVVAL peptide in COS-7 cells
pcDNArc-LIGEAFCL	5.1 kb	amp^R, bls^R	Expression of LIGEAFCL peptide in COS-7 cells
pcDNArc-LLGEVWNA	5.1 kb	amp^R, bls^R	Expression of LLGEVWNA peptide in COS-7 cells
pcDNArc-LLGAVWLL	5.1 kb	amp^R, bls^R	Expression of LLGAVWLL peptide in COS-7 cells
pcDNArc-LEGEAFPL	5.1 kb	amp^R, bls^R	Expression of LEGEAFPL peptide in COS-7 cells
pcDNArc-LSGEVFGM	5.1 kb	amp^R, bls^R	Expression of LSGEVFGM peptide in COS-7 cells
pcDNArc-LPGEVWMV	5.1 kb	amp^R, bls^R	Expression of LPGEVWMV peptide in COS-7 cells
pcDNArc-LSGEVHLL	5.1 kb	amp^R, bls^R	Expression of LSGEVHLL peptide in COS-7 cells
pcDNArc-LEGEVFIV	5.1 kb	amp^R, bls^R	Expression of LEGEVFIV peptide in COS-7 cells
pcDNArc-LQGEVFGA	5.1 kb	amp^R, bls^R	Expression of LQGEVFGA peptide in COS-7 cells

5.6 Primer Position for Quantitative PCR of Potential Parent Mouse Proteins

Sequence information for mRNA and genomic DNA was obtained from www.ncbi.nlm.nih.gov/gene. Yellow highlight: qPCR primers, gray highlight: qPCR probes, red letters: mimotope peptide-coding sequence, blue letters: comments.

Alox12b arachidonate 12-lipoxygenase, 12R type [Mus musculus]

Gene ID: 11686

exon 8 - **AGGGGGAATATTTACCTGGCAGACTACCGCATCCTGGATGGCATCCCCACCGTGGAGCTCAA TGGTCAGCAGCAGCATCACTGTGCCCCGATGTGCTTGCTGCACTTTGGTCCTGATGGCAACATGATGC CCATCGCCATTCAG** - intron - (1375 bp) - exon 9 - **CTCAGTCAGACTCCTGGGCCTGATTGTCCTATCT TCCTGCCGAATGATTCTGAGTGGGACTGGCTGTTGGCTAAAACGTGGGTGCGCTACGCGGAGTTCTAC AGCCACGAGGCCGTGGCACACTTGCTGGAGAGCCACCTCATCGGGGAAGCTTTCTGCTTGGCCCTCCT GAGGAACCTGCCCATGTGCCACCCCCTGTATAAG**

Ap5s1 adaptor-related protein 5 complex, sigma 1 subunit [Mus musculus]

Gene ID: 69596

exon 2 - **ACAGGTGGAGTCACTGTGTAGGCTGCAGCAGCAAGCGGCTGGATGTTCCTCCACAGACCTTC AGCCTCAGTTCTCAGCTGAACCTGTGTCCCTGCATGAGGCCCCTCATGGAGCCTTCCACCTGGCAGCC GGGGACCCTTTCCAGGAGCCTCGGACAGTGCTATGGCTGGGTATACTCTCCTTAGGTTTCGCCCTGGT GTTGGACACCCATGAGAACCTGCTGCTGGCTGAGCGCACGCTCCGGCTCTTGGCTCGCCTCCTCCTTG ACCACCTCCGGCTGCTGACACCA** - intron (89 bp) - exon 3 - **GTTTGTCCAGGATCTGGAGAAGGAATT CAGTGCTGCTTGGCCCCGCTGACCCCTCACCAGACAAAGAGCGAGGGTAAAGGTTGCATACTGCTAGG GGAAGTGTGGCATCTGCCTCTTGCCCAGCCTGCTCCCTGCTCTGATGTGTGGCCACGCTCAGGACATA CGGATTGGGCAAGCCCGAAGGAAGGGACCTGGGTAGAAGGCTGTCTGTGCCTGTCCTCAGGCCACTGG AATTGTAAAGTATTCATTGTAGAGCATCCTGAAGCTGGAACCGCCCCGTGA**

Dmxl2 Dmx-like 2 [Mus musculus]

Gene ID: 235380

exon 13 - **GGCACATACTGCAATTCTGCAAGTGCTTGCTTTGTTGCATCTGATGGCAAAAATCTAAGACT CTATCAAGCTGTGGTCGATGCAAGAAAATTATTAGATGAACTGTCAGACCCAGAAGCCTCA** - intron (1 7259 bp) - exon 14 - **AAACTGATCGGAGAAGTGTTTAACATTGTGAGCCAACAGTCCACTGCTCGTCCA GGCTGCATTATTGAGCTTGATGCCATAACTGACCAA** - intron (1528 bp) - exon 15 - **TGTGGATCAAA TACACAGCTACTGCACGTGTTTCAAGAAGACTTCATTATTGGATATAAGCCACACAAAGAAGATATGG AGAAAAAGGAAAAGGAGTCAGAAATATTTTTCCAGCCATCACAAGG**

Eml5 echinoderm microtubule associated protein like 5 [Mus musculus]

Gene ID: 319670

exon 20 - **CTGCTCTTGGAAGATAACCCATCTATACGTGCCATATCATTAGGGCATGGTCATATTTTGGT TGGCACAAAGAATGGTGAGATATTAGAAGTGGATAAGAGTGGCCCAATCACTCTTCTGGTCCAGG** - intr on (4166 bp) - exon 21 - **GACACATGGAAGGAGAGGTGTGGGGTTTGGCCACACATCCTTACCTGCCCAT CTGTGCTACTGTAAGTGATGATAAGACCTTAAGAATATGGGATCTCTCTCCTAGTCATTGTATGTTGG CAGTCCGGAAACTGAAAAAGGG**

Eml6 echinoderm microtubule associated protein like 6 [Mus musculus]

Gene ID: 237711

exon 20 - **ACTGCTTTTGGAGGATAACCCTTCAATTCGTGCAATTACCCTAGGGCATGGACACATTCTCG TGGGGACAAAAAATGGAGAGATTCTAGAAATTGATAAGAGTGGCCCGATGACCCTGCTTGTTCAGG** - in tron (7067 bp) - exon 21 - **GACACATGGAAGGGGAAGTGTGGGGGCTGGCAGCACACCCGCTCCTGCCC ATCTGCGCGACAGTAAGTGATGACAAAACACTTCGGATCTGGGAATTATCCTCCCAGCACCGCATGCT GGCTGTACGGAAACTTAAAAAAGG**

Gpcpd1 glycerophosphocholine phosphodiesterase GDE1 homolog (Saccharomyces cerevisiae) [Mus musculus]

Gene ID: 74182

untranslated 3' sequence - **CAGA** - exon 1 - **ATGACACCTTCTCAGG**TCACTTTTGAAATAAGAGGAACT
CTTT**TACCAGG** intron (3468 bp) - exon 2 - **AGAGGTCTTTGCAATA**TGTGGAAGCTGTGATGCCCTGGG
AAACTGGAAT**CCTCAAAATGCTGTGGCTCT**TATTAATGAAAACGAGACAGGAGACAG

Klhl28 kelch-like 28 [Mus musculus]

Gene ID: 66689

exon 2 - TGTGGAGATGTACTTTCCCCAGAATGACTCTTGGATTGGTCTGGCGCCCTTAAATATTCCTC
GCTATGAATTCGGAATATGTGTTTTAGACCAAAAAGTCTTTGTTATAGGTGGTATTGAAACTAGCGTG
CGTCCTGGTATGACTGTCAGAAAACATGAAAATTCAGTGGAATGTTGGAATCCTGATACAAACACCTG
GACTTCTCTCGAGAGAATGAACGAGAGCCGGAGTA**CTCTCGGAGTGGCAGTG**CTCGCGGGAGAAGTTT
TTGCCTTA**GGTGGATATGACGGGCAGTCTTACTTGCAATCTGTAGAAAAATACATCCCCAAAATAAGG
CAGTGGCAACCTGTGGCCCCAATGACAACCACAAGAAGTTGTTTTGCTGCAGCTGTCCTGGATGGAAT
GCTATACGCCATTGGAGGCTA**TGGCCCCGCTCACATGAACAG - intron (1153 bp) - exon 3 - TGT**GGA**
GCGTTACGATCCGAGTAAGGACTCCTGGGAGATGGTTGCGCCCATGGCTGATAAGAGGATTCACTTTG
GCGTCGGAGTCATGCTAGGTTTTATTTTCGTGGTAGGTGGGCATAACGGTGTCTCACATTTGTCAAGC
ATTGAAAGATATGATCCTCATCAAAATCAGTGGACTGTGTGTAGACCAATGAAAGAGCCCAGGACAGG

Mdh1b malate dehydrogenase 1B, NAD (soluble) [Mus musculus]

Gene ID: 76668

exon 4 - CTTTACTATGGTGTCACTTCCAACATGACGACGGAGTTGATGATGGTCATCGCTAAAGAGAA
CATGCAGACGCATACAGAACAACAGTTGGATAAAGAA**ACCATGAAAGATCTCATCAGC**CCTTTGCAGG
TCTGGATTGCCAG - intron (1469 bp) - exon 5 - TGCAGGTACTTACGTGTGCTGCCACTTAATTCCCC
TCTTG**CTAAGCGGGGAAGTGTTT**GGGATGCACACAGAGATCAGCCTGACCCTGTTTGACCAGGAGCAA
AGGGAGGACTGCCTCAGAAGCATAGTGATGGAAACCCAGGACTTGGCCTCACCAGTGCTCCGCACTGT
GTCCTTCTGCACCACGGTAAAGGAGGCCTTCCTTCAGGCCCAGGTCATCATCATCCTGGATGACAGTA
CAGAGGAAGAGGTGTACAGCCTGGAGAGCTGCCTCCGGAGCAGGGTGCCGCTGTGCCGCCTCTACGGC
TACCTGATAGAGAAAAACGCTCACAAGTCTGTCAAGGTCATCGTGGGAGGGAAAAACTTTGTAAATCT
GAAAACAACTTTGCTCATGCAATATGCCCCTAACATCGCGAGCAACATTATCGCAGTGGCTCTGGGGG
TAGAAGGCCAAGCAAAAGCAGTACTGGCCCGAAAGATGAAAACCACTTCAGCCA

Ncan neurocan [Mus musculus]

Gene ID: 13004

exon 5 - ACCCGATCACTCAGTCGCGTCCTGGTTGCTATGGTGACCGCAGCAGTCTCCCGGGTGTTCGG
AGCTACGGGAGACGCGACCCGCAGGAACTCT**ACGATGTCTACTGCTTTGCC**CGCGAG**CTAGGGGG** - intr
on (313 bp) - exon 6 - **TGAAGTCTTTTACGTG**GGCCCGGCCCGCCGACTGACCCTGGCGGGCGCGCGGG
CACAATGTCAGCGGCAGGGT**GCAGCGCTGGCCTCGGT**GGGGCAGTTGCACCTGGCCTGGCACGAGGGC
CTGGACCAGTGCGACCCGGGCTGGCTGGCAGACGGCAGCGTGCGCTACCCCATCCAGACTCCGCGCCG
GCGTTGCGGGGGCCCCGCCCCAGGTGTGCGCACTGTGTACCGCTTCGCCAACCGCACCGGCTTTCC

Gapdh glyceraldehyde-3-phosphate dehydrogenase [Mus musculus]

Gene ID: 14433

exon 2 - **ATTTGGCCGTATTGGGCGCCTGGTCACCAGGGCTGCCATTTGCAGTGGCAAAGTGGAGATTG TTGCCATCAACGACCCCTTCATTGACCTCAACTACATGGTCTACATGTTCCAGTATGACTCCACTCAC GGCAAATTCAACGGCACAGTCAAGGCCGAGAATGGGAAGCTTGTCATCAACGGGAAGCCCATCACCAT CTTCCAGGAGCGAGACCCCACTAACATCAAATGGGGTGAGGCCGGTGCTGAGTATGTCGTGGAGTCTA CTGGTGTCTTCACCACCATGGAGAAGGCCGGGG** - intron (98 bp) - exon 3 - **CCCACTTGAAGGGTGGA GCCAAAAGGGTCATCATCTCCGCCCCTTCTGCCGATGCCCCCATGTTTGTGATGGGTGTGAACCACGA GAAATATGACAACTCACTCAAGATTGTCAGCAATGCATCCTGCACCACCAACTGCTTAGCCCCCCTGG CCAAGGTCATCCATGACAACTTTGGCATTGTGGAAGGGCTCATG**

5.7 Plasmid Information

5.7.1 pcDNA6/V5-HisA

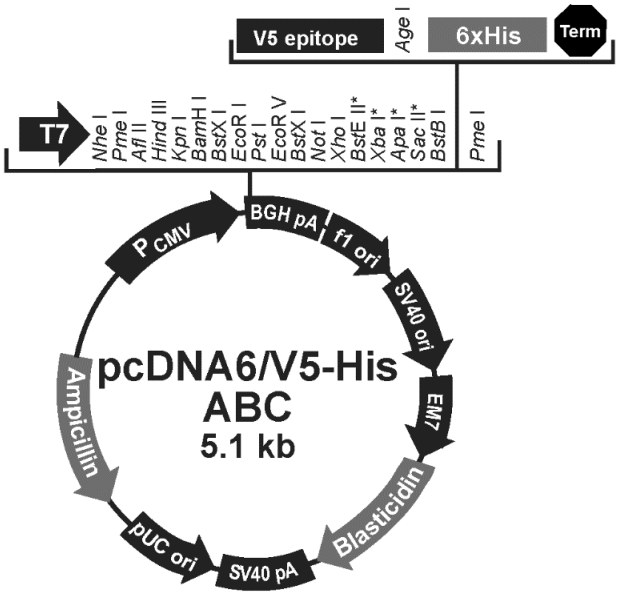

Comments for pcDNA6/V5-His A
5144 nucleotides

CMV promoter: bases 209-863
T7 promoter priming site: bases 863-882
Multiple cloning site: bases 895-1008
V5 epitope: bases 1009-1050
Polyhistidine tag: bases 1060-1077
BGH reverse priming site: bases 1100-1117
BGH polyadenylation sequence: bases 1103-1330
f1 origin: bases 1376-1804
SV40 promoter and origin: bases 1832-2139
EM7 promoter: bases 2187-2242
Blasticidin resistance gene (ORF): bases 2261-2659
SV40 early polyadenylation sequence: bases 2817-2947
pUC origin: bases 3330-4003
Ampicillin resistance gene (ORF): bases 4148-5008

* Frame-dependent variations.
Sac II is only found in version B.
*Bst*E II is only found in version C. In addition, there are no *Xba* I or *Apa* I sites in version C.

Invitrogen™
life technologies

Black letters: plasmid backbone, red letters: truncated protein-coding region, gray highlight: pcDNA-for-1 / pcDNA-rev-1 primer, solid line: EcoRI / NotI restriction site, dotted line: mimotope-coding region, dashed line: V5 tag.

pcDNA6/V5-HisA-DMXL2$_{748-926}$-V5 (Mimotope: DMXL2$_{813-820}$)

CACTGCTTACTGGCTTATCGAAATTAATACGACTCACTATAGGGAGACCCAAGCTGGCTAGCGTTTAAACTTAAG
CTTGGTACCGAGCTCGGATCCACTAGTCCAGTGTGGTGGAATTCCACCATGAACTCTTTACATACCTCAGCCTTC
TCTAATGTGGCATGGCTTCCAACTCTTATTCCTAGTTACTGTCTTGGCACATACTGCAATTCTGCAAGTGCTTGC
TTTGTTGCATCTGATGGCAAAAATCTAAGACTCTATCAAGCTGTGGTCGATGCAAGAAAATTATTAGATGAACTG
TCAGACCCAGAAGCCTCAAAACTGATCGGAGAAGTGTTTAACATTGTGAGCCAACAGTCCACTGCTCGTCCAGGC
TGCATTATTGAGCTTGATGCCATAACTGACCAATGTGGATCAAATACACAGCTACTGCACGTGTTTCAAGAAGAC
TTCATTATTGGATATAAGCCACACAAAGAAGATATGGAGAAAAAGGAAAAGGAGTCAGAAATATTTTTCCAGCCA
TCACAAGGATATCGACCACCACCATTTTCAGAAAAATTCTTTTTAGTAGTCATTGAGAAGGATGGAAATAATAAC
TCTATTCTCCATATGTGGCACCTTCATCTTAAGTCTGTACAAGCGTGCTTAGCCAAAGCTGCAGGTAAGCCTATC
CCTAACCCTCTCCTCGGTCTCGATTCTACGTAGGCGGCCGCTCGAGTCTAGAGGGCCCTTCGAAGGTAAGCCTAT
CCCTAACCCTCTCCTCGGTCTCGATTCTACGCGTACCGGTCATCATCACCATCACCATTGAGTTTAAACCCGCTG
ATCAGCCTCGACTGTGCCTTCTAGT

pcDNA6-EML5$_{897-1038}$-V5 (Mimotope: EML5/6$_{997-1004}$)

CACTGCTTACTGGCTTATCGAAATTAATACGACTCACTATAGGGAGACCCAAGCTGGCTAGCGTTTAAACTTAAG
CTTGGTACCGAGCTCGGATCCACTAGTCCAGTGTGGTGGAATTCCACCATGAAAACAGTTAAAGCCCATGATGGG
CCCGTGTTCAGTATGCATGCATTGGAGAAAGGATTTGTAACTGGAGGAAAAGATGGTATGGTAGCCCTTTGGGAT
GATTCCTTTGAAAGATGCCTCAAGACCTATGCTATAAAAAGAGCTGATTTAGCCCCAGGATCTAAAGGTCTGCTC
TTGGAAGATAACCCATCTATACGTGCCATATCATTAGGGCATGGTCATATTTTGGTTGGCACAAAGAATGGTGAG
ATATTAGAAGTGGATAAGAGTGGCCCAATCACTCTTCTGGTCCAGGGACACATGGAAGGAGAGGTGTGGGGTTTG
GCCACACATCCTTACCTGCCCATCTGTGCTACTGTAAGTGATGATAAGACCTTAAGAATATGGGATCTCTCTCCT
AGTCATTGTATGTTGGCAGTCCGGAAAGGTAAGCCTATCCCTAACCCTCTCCTCGGTCTCGATTCTACGTAGGCG
GCCGCTCGAGTCTAGAGGGCCCTTCGAAGGTAAGCCTATCCCTAACCCTCTCCTCGGTCTCGATTCTACGCGTAC
CGGTCATCATCACCATCACCATTGAGTTTAAACCCGCTGATCAGCCTCGACTGTGCCTTCTAGT

pcDNA6-GPCPD1$_{1-118}$-V5 (Mimotope: GPCPD1$_{15-22}$)

CACTGCTTACTGGCTTATCGAAATTAATACGACTCACTATAGGGAGACCCAAGCTGGCTAGCGTTTAAACTTAAG
CTTGGTACCGAGCTCGGATCCACTAGTCCAGTGTGGTGGAATTCCACCATGACACCTTCTCAGGTCACTTTTGAA
ATAAGAGGAACTCTTTTACCAGGAGAGGTCTTTGCAATATGTGGAAGCTGTGATGCCCTGGGAAACTGGAATCCT
CAAAATGCTGTGGCTCTTATTAATGAAAACGAGACAGGAGACAGTGTGTTGTGGAAAGCAGTGATTGCTCTCAAT
AGAGGAGTGTCAGTGAAGTACCGCTACTTCAGAGGCTGCTTTTTAGAACCAAAGACTATCGGTGGTCCATGTCAA
GTCATAGTTCACAAGTGGGAGACTCATCTACAACCACGATCAATAACCCCTTTAGAAAGTGAAATCATTATTGAC
GATGGACAGTTTGGCATCCACAATGGTGGTAAGCCTATCCCTAACCCTCTCCTCGGTCTCGATTCTACGTAGGCG
GCCGCTCGAGTCTAGAGGGCCCTTCGAAGGTAAGCCTATCCCTAACCCTCTCCTCGGTCTCGATTCTACGCGTAC
CGGTCATCATCACCATCACCATTGAGTTTAAACCCGCTGATCAGCCTCGACTGTGCCTTCTAGT

pcDNA6-NCAN$_{156-359}$-V5 (Mimotope: NCAN$_{257-264}$)

CACTGCTTACTGGCTTATCGAAATTAATACGACTCACTATAGGGAGACCCAAGCTGGCTAGCGTTTAAACTTAAG
CTTGGTACCGAGCTCGGATCCACTAGTCCAGTGTGGTGGAATTCCACCATGGTGACAGGCGTCGTGTTCCATTAT
CGGGCGGCCCGGGACCGCTATGCGCTGACCTTCGCTGAGGCCCAGGAGGCTTGTCGCCTAAGCTCTGCTACCATC
GCTGCCCCACGGCACCTGCAGGCTGCCTTTGAAGATGGCTTTGACAACTGCGACGCGGGCTGGCTCTCAGACCGC
ACGGTTCGGTACCCGATCACTCAGTCGCGTCCTGGTTGCTATGGTGACCGCAGCAGTCTCCCGGGTGTTCGGAGC
TACGGGAGACGCGACCCGCAGGAACTCTACGATGTCTACTGCTTTGCCCGCGAGCTAGGGGGTGAAGTCTTTTAC
GTGGGCCCGGCCCGCCGACTGACCCTGGCGGGCGCGCGGGCACAATGTCAGCGGCAGGGTGCAGCGCTGGCCTCG
GTGGGGCAGTTGCACCTGGCCTGGCACGAGGGCCTGGACCAGTGCGACCCGGGCTGGCTGGCAGACGGCAGCGTG
CGCTACCCCATCCAGACTCCGCGCCGGCGTTGCGGGGGCCCCGCCCCAGGTGTGCGCACTGTGTACCGCTTCGCC
AACCGCACCGGCTTTCCTGCGCCAGGAGCACGCTTCGACGCCTACTGCTTCCGAGCTCATCACGGTAAGCCTATC
CCTAACCCTCTCCTCGGTCTCGATTCTACGTAGGCGGCCGCTCGAGTCTAGAGGGCCCTTCGAAGGTAAGCCTAT
CCCTAACCCTCTCCTCGGTCTCGATTCTACGCGTACCGGTCATCATCACCATCACCATTGAGTTTAAACCCGCTG
ATCAGCCTCGACTGTGCCTTCTAGT

5.7.2 pQE-30

pQE-30

Positions of elements in bases	pQE-30
Vector size (bp)	3461
Start of numbering at *Xho*I (CTCGAG)	1–6
T5 promoter/lac operator element	7–87
T5 transcription start	61
6xHis-tag coding sequence	127–144
Multiple cloning site	145–192
Lambda t_0 transcriptional termination region	208–302
rrnB T1 transcriptional termination region	1064–1162
ColE1 origin of replication	1638
β-lactamase coding sequence	3256–2396

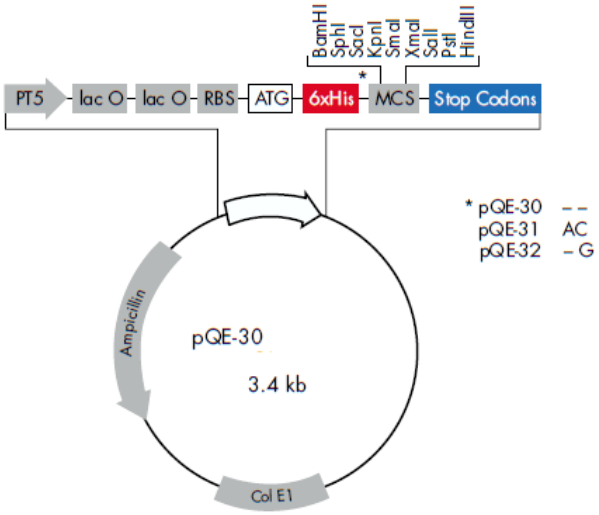

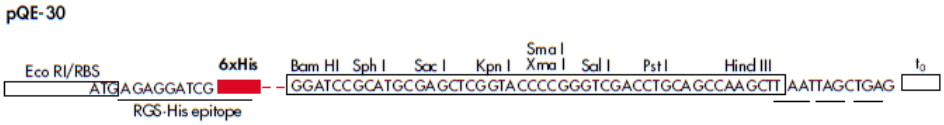

Black letters: plasmid backbone, red letters: truncated protein-coding region, gray highlight: pQE-for / pQE-rev primer, solid line: BamHI / SalI restriction site, waved line: His_6 tag, dotted line: mimotope-coding region, dashed line: V5 tag.

pQE-30-His_6-$DMXL2_{748-926}$-V5 (Mimotope: $DMXL2_{813-820}$)

CCCGAAAAGTGCCACCTGACGTCTAAGAAACCATTATTATCATGACATTAACCTATAAAAATAGGCGTATCACGA
GGCCCTTTCGTCTTCACCTCGAGAAATCATAAAAAATTTATTTGCTTTGTGAGCGGATAACAATTATAATAGATT
CAATTGTGAGCGGATAACAATTTCACACAGAATTCATTAAAGAGGAGAAATTAACTATGAGAGGATCGCATCACC
ATCACCATCACGGATCCAACTCTTTACATACCTCAGCCTTCTCTAATGTGGCATGGCTTCCAACTCTTATTCCTA
GTTACTGTCTTGGCACATACTGCAATTCTGCAAGTGCTTGCTTTGTTGCATCTGATGGCAAAAATCTAAGACTCT
ATCAAGCTGTGGTCGATGCAAGAAAATTATTAGATGAACTGTCAGACCCAGAAGCCTCAAAACTGATCGGAGAAG
TGTTTAACATTGTGAGCCAACAGTCCACTGCTCGTCCAGGCTGCATTATTGAGCTTGATGCCATAACTGACCAAT
GTGGATCAAATACACAGCTACTGCACGTGTTTCAAGAAGACTTCATTATTGGATATAAGCCACACAAAGAAGATA
TGGAGAAAAAGGAAAAGGAGTCAGAAATATTTTTCCAGCCATCACAAGGATATCGACCACCACCATTTTCAGAAA
AATTCTTTTTAGTAGTCATTGAGAAGGATGGAAATAATAACTCTATTCTCCATATGTGGCACCTTCATCTTAAGT
CTGTACAAGCGTGCTTAGCCAAAGCTGCAGGTAAGCCTATCCCTAACCCTCTCCTCGGTCTCGATTCTACGTAGG
TCGACCTGCAGCCAAGCTTAATTAGCTGAGCTTGGACTCCTGTTGATAGATCCAGTAATGACCTCAGAAC

pQE-30-His$_6$-EML5$_{897\text{-}1038}$-V5 (Mimotope: EML5/6$_{997\text{-}1004}$)

CCCGAAAAGTGCCACCTGACGTCTAAGAAACCATTATTATCATGACATTAACCTATAAAAATAGGCGTATCACGA
GGCCCTTTCGTCTTCACCTCGAGAAATCATAAAAAATTTATTTGCTTTGTGAGCGGATAACAATTATAATAGATT
CAATTGTGAGCGGATAACAATTTCACACAGAATTCATTAAAGAGGAGAAATTAACTATGAGAGGATCGCATCACC
ATCACCATCACGGATCCAAAACAGTTAAAGCCCATGATGGGCCCGTGTTCAGTATGCATGCATTGGAGAAAGGAT
TTGTAACTGGAGGAAAAGATGGTATGGTAGCCCTTTGGGATGATTCCTTTGAAAGATGCCTCAAGACCTATGCTA
TAAAAAGAGCTGATTTAGCCCCAGGATCTAAAGGTCTGCTCTTGGAAGATAACCCATCTATACGTGCCATATCAT
TAGGGCATGGTCATATTTTGGTTGGCACAAAGAATGGTGAGATATTAGAAGTGGATAAGAGTGGCCCAATCACTC
TTCTGGTCCAGGGACACATGGAAGGAGAGGTGTGGGGTTTGGCCACACATCCTTACCTGCCCATCTGTGCTACTG
TAAGTGATGATAAGACCTTAAGAATATGGGATCTCTCTCCTAGTCATTGTATGTTGGCAGTCCGGAAAGGTAAGC
CTATCCCTAACCCTCTCCTCGGTCTCGATTCTACGTAGGTCGACCTGCAGCCAAGCTTAATTAGCTGAGCTTGGA
CTCCTGTTGATAGATCCAGTAATGACCTCAGAAC

pQE-30-His$_6$-GPCPD1$_{1\text{-}118}$-V5 (Mimotope: GPCPD1$_{15\text{-}22}$)

CCCGAAAAGTGCCACCTGACGTCTAAGAAACCATTATTATCATGACATTAACCTATAAAAATAGGCGTATCACGA
GGCCCTTTCGTCTTCACCTCGAGAAATCATAAAAAATTTATTTGCTTTGTGAGCGGATAACAATTATAATAGATT
CAATTGTGAGCGGATAACAATTTCACACAGAATTCATTAAAGAGGAGAAATTAACTATGAGAGGATCGCATCACC
ATCACCATCACGGATCCATGACACCTTCTCAGGTCACTTTTGAAATAAGAGGAACTCTTTTACCAGGAGAGGTCT
TTGCAATATGTGGAAGCTGTGATGCCCTGGGAAACTGGAATCCTCAAAATGCTGTGGCTCTTATTAATGAAAACG
AGACAGGAGACAGTGTGTTGTGGAAAGCAGTGATTGCTCTCAATAGAGGAGTGTCAGTGAAGTACCGCTACTTCA
GAGGCTGCTTTTTAGAACCAAAGACTATCGGTGGTCCATGTCAAGTCATAGTTCACAAGTGGGAGACTCATCTAC
AACCACGATCAATAACCCCTTTAGAAAGTGAAATCATTATTGACGATGGACAGTTTGGCATCCACAATGGTGGTA
AGCCTATCCCTAACCCTCTCCTCGGTCTCGATTCTACGTAGGTCGACCTGCAGCCAAGCTTAATTAGCTGAGCTT
GGACTCCTGTTGATAGATCCAGTAATGACCTCAGAAC

pQE-30-His$_6$-NCAN$_{156\text{-}359}$-V5 (Mimotope: NCAN$_{257\text{-}264}$)

CCCGAAAAGTGCCACCTGACGTCTAAGAAACCATTATTATCATGACATTAACCTATAAAAATAGGCGTATCACGA
GGCCCTTTCGTCTTCACCTCGAGAAATCATAAAAAATTTATTTGCTTTGTGAGCGGATAACAATTATAATAGATT
CAATTGTGAGCGGATAACAATTTCACACAGAATTCATTAAAGAGGAGAAATTAACTATGAGAGGATCGCATCACC
ATCACCATCACGGATCCGTGACAGGCGTCGTGTTCCATTATCGGGCGGCCCGGGACCGCTATGCGCTGACCTTCG
CTGAGGCCCAGGAGGCTTGTCGCCTAAGCTCTGCTACCATCGCTGCCCCACGGCACCTGCAGGCTGCCTTTGAAG
ATGGCTTTGACAACTGCGACGCGGGCTGGCTCTCAGACCGCACGGTTCGGTACCCGATCACTCAGTCGCGTCCTG
GTTGCTATGGTGACCGCAGCAGTCTCCCGGGTGTTCGGAGCTACGGGAGACGCGACCCGCAGGAACTCTACGATG
TCTACTGCTTTGCCCGCGAGCTAGGGGGGTGAAGTCTTTTACGTGGGCCCGGCCCGCCGACTGACCCTGGCGGGCG
CGCGGGCACAATGTCAGCGGCAGGGTGCAGCGCTGGCCTCGGTGGGGCAGTTGCACCTGGCCTGGCACGAGGGCC
TGGACCAGTGCGACCCGGGCTGGCTGGCAGACGGCAGCGTGCGCTACCCCATCCAGACTCCGCGCCGGCGTTGCG
GGGGCCCCGCCCCAGGTGTGCGCACTGTGTACCGCTTCGCCAACCGCACCGGCTTTCCTGCGCCAGGAGCACGCT
TCGACGCCTACTGCTTCCGAGCTCATCACGGTAAGCCTATCCCTAACCCTCTCCTCGGTCTCGATTCTACGTAGG
TCGACCTGCAGCCAAGCTTAATTAGCTGAGCTTGGACTCCTGTTGATAGATCCAGTAATGACCTCAGAAC

5.7.3 pcDNA™3.1D/V5-His-TOPO®

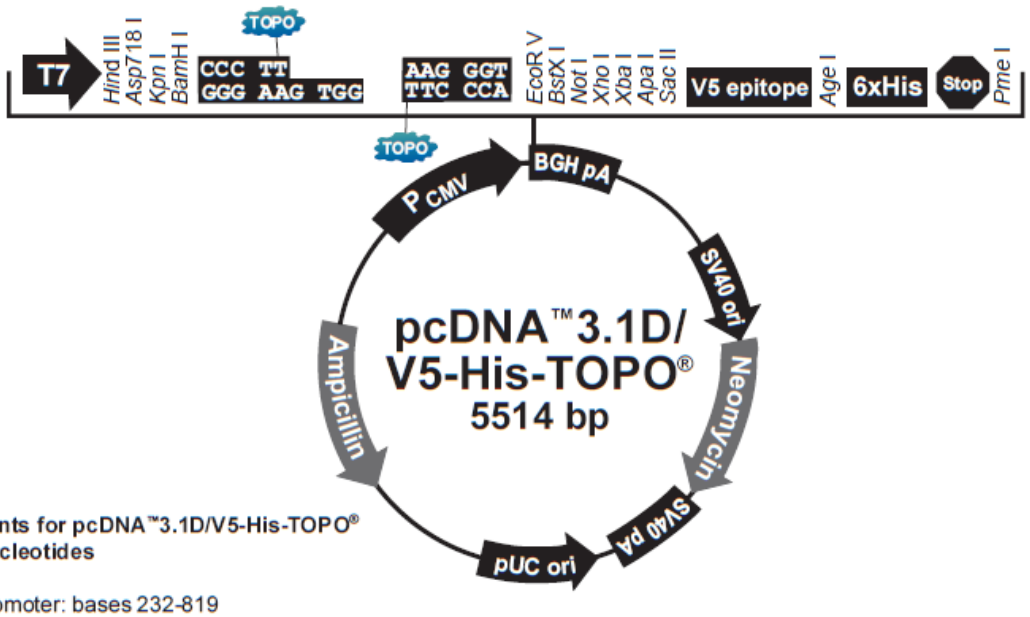

Comments for pcDNA™3.1D/V5-His-TOPO®
5514 nucleotides

CMV promoter: bases 232-819
T7 promoter/priming site: bases 863-882
TOPO® recognition site 1: bases 930-934
Overhang sequence (complementary strand): bases 935-938
TOPO® recognition site 2: bases 939-943
V5 epitope: bases 1011-1052
Polyhistidine (6xHis) tag: bases 1062-1079
BGH reverse priming site: bases 1102-1119
BGH polyadenylation signal: bases 1108-1332
SV40 early promoter and origin: bases 1833-2142
Neomycin resistance gene: bases 2217-3011
SV40 early polyadenylation signal: bases 3189-3319
pUC origin: bases 3700-4373 (complementary strand)
Ampicillin (*bla*) resistance gene: bases 4518-5378 (complementary strand)
bla promoter: bases 5379-5477 (complementary strand)

Invitrogen™
life technologies

5.7.4 13AAG64P_Ncan-V5_pMA-RQ

Plasmid DNA Description:

The synthetic gene Ncan-V5 was assembled from synthetic oligonucleotides and/or PCR products. The fragment was cloned into pMA-RQ (ampR) using SfiI and SfiI cloning sites. The plasmid DNA was purified from transformed bacteria and concentration determined by UV spectroscopy. The final construct was verified by sequencing. The sequence congruence within the used restriction sites was 100%. See the accompanying data sheets for sequences and find the original ABI trace files as well as the assembled sequences electronically on disk.
5 µg of the plasmid preparation were lyophilized for shipping.

Plasmid Map:

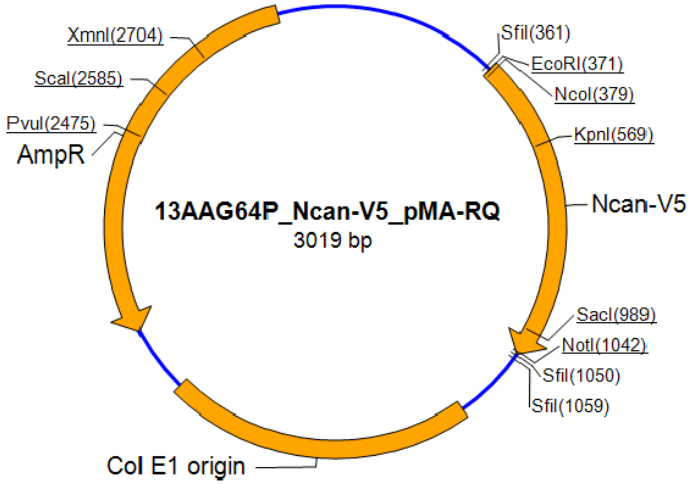

life technologie

Quality Assurance Documentation: 13AAG64P

Ref. No.: 1323637

Designation:	E.coli K12 (dam+ dcm+ tonA rec-)
Gene name:	**Ncan-V5**
Gene size:	678 bp
Vector backbone:	pMA-RQ (ampR)
Cloning sites:	SfiI / SfiI
Quantity:	~5 µg Plasmid DNA
Note:	Please dissolve lyophilized DNA in 50 µl distilled water or 10 mM Tris-HCl (pH 8.0). We recommend sequence verification after each transformation step.
Date:	18 March 2013

Meike Brodt
Quality control

GeneArt AG **www.lifetechnologies.com** **GeneArtSupport@lifetech.com**

5.8 Protein Truncation

Protein sequences were truncated according to predicted/known domains obtained from www.uniprot.org. Given are protein sequences with highlighted domains and mRNA sequences. Green highlight: domains, yellow highlight: mimotope sequence, red letters: truncated protein sequence.

DMXL2 Dmx-like [Mus musculus]
GenBank: AAH23075.1

http://www.uniprot.org/uniprot/Q8BPN8

```
         10          20          30          40          50          60
MHLHQVLTGA VNPGDNCYSV GSVGDVPFTA YGSGCDIVIL ASDFECVQII PGAKHGNIQV
         70          80          90         100         110         120
SCVECSNQHG RVAASYGNAV CIFEPLGVNS HKRNSQLKCQ WLKTGQFFLS SVTYNLAWDP
WD1    130         140         150         160         170         180
QDNRLLTATD SIQLWAPPGG DILEEEEDVD NRAPPVLNDW KCIWQCKTSV SVHLMEWSPD
WD2    190         200         210         220         230         240
GEYFATAGKD DCLLKVWYPM TGWKSSIIPQ DPHEVKRRRA STQFSFVYLA HPRAVTGFSW
WD3    250         260         270         280         290         300
RKTSKYMPRG SVCNVLLTSC HDGVCRLWAE TLLPEDCLLG EQICETTTSS VASNLSSAGK
       310         320         330         340         350         360
HKDRIQHALE TIHHLKNLRK GQRRSSVLVT HAELMPDKTA THEVHRHISH HANALCHFHI
       370         380         390         400         410         420
AASINPTTDI PNVLVGTAFN IDDINGGFVV HWLNNKEFHF TSSTEIFMHQ LRKLSEKQLD
       430         440         450         460         470         480
HESDDADRED EERSQDERER GLRMKLDHEL SLDRESEAGT GSSEHEDGER EGSPRTHPRP
       490    WD4  500         510         520         530         540
SISMPLPTVL LDRKIETLLT EWNKNPDMLF TIHPVDGTFL VWHVKYLDEY NPGIFRQVQV
       550         560         570         580         590         600
SFSSRIPVAF PSGDANSLSK NIMMYACVNA TKDSYNPSQQ EMMSVDSPHG SQLHSPSHST
WD5    610         620         630         640         650         660
DMNILAPTVM MVSKHIDGSL NQWAVTFADK SAFTTVLTVS HKFRYCGHRF HLNDLACHSV
       670         680         690         700         710         720
LPLLLTSSHH NALLTPESDC QWDSDSKVNR LIDPVKHTKA SSKQPLRNAA TRTFHDPNAI
       730         740         750         760         770         780
YSELILWRVD PIGPLSYTGG VSELARINSL HTSAFSNVAW LPTLIPSYCL GTYCNSASAC
WD6    790         800         810         820         830         840
FVASDGKNLR LYQAVVDARK LLDELSDPEA SKLIGEVFNI VSQQSTARPG CIIELDAITD
       850         860         870         880         890         900
QCGSNTQLLH VFQEDFIIGY KPHKEDMEKK EKESEIFFQP SQGYRPPPFS EKFFLVVIEK
WD7    910         920         930         940         950         960
DGNNNSILHM WHLHLKSVQA CLAKAAEGIS SDSLLSVPGQ KNLDSSPETS SSMSSVPHSS
       970         980         990        1000   WD8  1010        1020
SIANLQTASK LILSSRLVYS QPLDLPEAVE VIRATPSAGH LSSSSIYPVC LAPYLVVTTC
      1030        1040        1050        1060        1070        1080
SDNKVRFWKC CMETNSLGNT SDESETYHWR RWPLMNDEGE DNSSTVSIVG RPVAVSCSYT
      1090        1100        1110        1120        1130        1140
GRLAVAYKQP IHHNGFISKE FSMHVCIFEC ESTGGSEWVL EQTIHLDDLV KVGSVLDSRV
      1150        1160        1170   WD9  1180        1190        1200
SVDSNLFVYS KSDAFLSKDR YLIPNIKHLV HLDWVSKEDG SHILTVGVGA NIFMYGRLSG
      1210        1220        1230        1240        1250 WD10  1260
IVSDQTNSKD GVAVITLPLG GSIKQGVKSR WVLLRSIDLV SSVDGTPSLP VSLSWVRDGI
      1270        1280        1290        1300        1310        1320
LVVGMDCEMH VYAQWKHSVK FGNVDADSPV EETIQDHSAL KSSMLARKSI VEGAAIPDDV
```

```
      1330        1340        1350        1360        1370        1380
FCSPTVVQDG GLFEAAHALS PTLPQYHPTQ LLELMDLGKV RRAKAILSHL VKCIAGEVAI
      1390        1400        1410        1420        1430        1440
VRDPDAGEGT KRHLSRTISV SGSTAKDTVT IGKDGTRDYT EIDSIPPLPL HALLAADQDT
      1450        1460        1470        1480        1490        1500
SYRISEDSTK KPQSYEDHIE SQSEDQYSEL FQVQEITTDD IDLEPEKREN KSKVINLSQY
      1510        1520        1530        1540        1550        1560
GPACFGQEHA RVLSSHLMHS SLPGLTRLEQ MFLVALADTV ATTSTELDEN RDKNYSGRDT
      1570        1580        1590        1600        1610        1620
LDECGLRYLL AMRLHTCLLT SLPPLYRVQL LHQGVSTCHF AWAFHSEAEE ELINMIPAIQ
      1630        1640        1650        1660        1670        1680
RGDPQWSELR AMGIGWWVRN VNTLRRCIEK VAKAAFQRNN EALDAALFYL SMKKKAVVWG
      1690        1700        1710        1720        1730        1740
LFRSQHDEKM TTFFSHNFNE DRWRKAALKN AFSLLGKQRF EQSAAFFLLA GSLKDAIEVC
      1750        1760        1770        1780        1790        1800
LEKMEDIQLA MVIARLFESE FETSSTYISI LNQKILGCQK DGTGFDCKRL HPDPFLRSLA
      1810        1820        1830        1840        1850        1860
YWVVKDYTRA LDTLLEQTPK EDDEQQVIIK SCNPVVFSFY NYLRTHPLLI RRNLASPEGT
      1870        1880        1890        1900        1910        1920
LATLGLKTEK NIADKINLIE RKLFFTTANA HFKVGCPVLA LEVLSKIPKV TKISSLTAKK
      1930        1940        1950        1960        1970        1980
DQLDSVSGRM ENGPSESKPV SRSDGGSGAD WSAVTSSQFD WSQPMVTVDE EPLRLDWGDD
      1990        2000        2010        2020        2030        2040
HDGALEEDDG GGLVMKTTDA KKAGQEQSAS DPRALLTPQD EECADGDTEV DVIAEQLKFR
      2050        2060        2070        2080        2090        2100
ACLKILMTEL RTLATGYEVD GGKLRFQLYN WLEKEIAALH EICNHESVIK EYSSKAHSTV
      2110        2120        2130        2140        2150        2160
ETERLDQEEM VDKPDIGSYE RHQIERRRLQ AKREHAERRK LWLQKNQDLL RVFLSYCSLH
      2170        2180        2190        2200        2210        2220
GAQGGGLASV RMELKFLLQE SQQETTVKQL QSPLPLPTTL PLLSASIAST KTVIANPVLY
      2230        2240        2250        2260        2270        2280
LNNHIHDILY TIVQMKTPPH PSVEDVKVHT LHSLAASLSA SIYQALCDSH SYSQSEGNQF
      2290        2300        2310        2320        2330        2340
TGMAYQGLLL SDRRRLRTES IEEHATPNSA PAQWPGVSSL INLLSSAQDE DQPKLNVLLC
      2350        2360        2370        2380        2390        2400
EAVVAVYLSL LIHALATNSS NELFRLAAHP LNNRMWAAVF GGGVKLVVKP RRQSESIAAP
      2410        2420        2430        2440        2450        2460
PVASEDMDKH RRRFNMRMLV PGRPVKDATP PPVPAERPSY KEKFIPPELS MWDYFVAKPF
      2470        2480        2490        2500        2510        2520
LPLSDSGVIY DSDESVHSDD EEDDAFFSDT QIQEHQDPNS YSWALLHLTM VKLALHNIKN
      2530        2540        2550        2560        2570        2580
FFPIAGLEFS ELPVTSPLGI AVIKNLENWE QILQEKMDHF EGPPPNYVNT YPTDLSVGAG
      2590        2600        2610        2620        2630        2640
PAILRNKAML EPENTPFKSR DSSALPVKRL WHFLVKQEVL QETFIRYIFT KKRKQSEVEA
      2650        2660        2670        2680        2690        2700
DLGYPGGKAK VIHKESDMIM AFSINKANCN EIVLASTHDV QELDVTSLLA CQSYIWIGEE
      2710        2720        2730        2740        2750        2760
YDRESKSSDD IDYRGSTTTL YQPGAASHSS SQPHPPPSLP WLGSGQTSTG ATVLMKRNLH
 WD11 2770        2780        2790        2800        2810        2820
NVKRMTSHPV HQYYLTGAQD GSVRMFEWTR PQQLVCFRQA GNARVTRLYF NSQGNKCGVA
 WD12 2830        2840        2850  WD13 2860        2870        2880
DGEGFLSIWQ VNQTASNPKP YMSWQCHSKA TSDFAFITSS SLVATSGHSN DNRNVCLWDT
      2890        2900  WD14 2910        2920        2930        2940
LISPGNSLIH GFTCHDHGAT VLQYAPKQQL LISGGRKGYI CIFDIRQRQL IHTFQAHDSA
 WD15 2950        2960        2970        2980        2990  WD16 3000
IKALALDSCE EYFTTGSAEG NIKVWRLTGH GLIHSFKSEH AKQSIFRNIG AGVMQIAISQ
      3010        3020        3030
DNRLFSCGAD GTLKTRVLPS AFNIPNRILD IL
```

```
 M   H   L   H   Q   V   L   T   G   A   V   N   P   G   D   N   C   Y   S   V
ATG CAT CTG CAT CAG GTC CTC ACC GGG GCT GTC AAC CCT GGG GAC AAC TGC TAT TCG GTG
 G   S   V   G   D   V   P   F   T   A   Y   G   S   G   C   D   I   V   I   L
GGC AGC GTC GGG GAC GTC CCC TTC ACG GCA TAT GGA TCA GGC TGT GAT ATT GTT ATT CTG
 A   S   D   F   E   C   V   Q   I   I   P   G   A   K   H   G   N   I   Q   V
GCG AGT GAC TTT GAA TGT GTG CAG ATC ATC CCT GGT GCT AAG CAT GGG AAC ATC CAA GTC
 S   C   V   E   C   S   N   Q   H   G   R   V   A   A   S   Y   G   N   A   V
AGT TGT GTG GAA TGC TCC AAC CAG CAT GGG AGA GTT GCA GCT TCA TAT GGG AAT GCT GTG
 C   I   F   E   P   L   G   V   N   S   H   K   R   N   S   Q   L   K   C   Q
TGT ATT TTT GAA CCC CTG GGT GTA AAT TCT CAT AAG AGA AAC AGT CAA CTC AAG TGT CAG
 W   L   K   T   G   Q   F   F   L   S   S   V   T   Y   N   L   A   W   D   P
TGG CTT AAA ACT GGA CAG TTT TTT TTG AGT TCC GTG ACA TAC AAC TTA GCA TGG GAC CCT
 Q   D   N   R   L   L   T   A   T   D   S   I   Q   L   W   A   P   P   G   G
CAA GAT AAC AGA TTG CTG ACA GCA ACG GAT TCG ATT CAG CTG TGG GCT CCT CCA GGC GGT
 D   I   L   E   E   E   E   D   V   D   N   R   A   P   P   V   L   N   D   W
GAT ATT CTA GAA GAG GAG GAA GAT GTT GAT AAT AGA GCC CCT CCT GTT TTA AAT GAT TGG
 K   C   I   W   Q   C   K   T   S   V   S   V   H   L   M   E   W   S   P   D
AAG TGC ATC TGG CAG TGC AAA ACC TCA GTG TCT GTA CAT CTG ATG GAA TGG TCT CCT GAT
 G   E   Y   F   A   T   A   G   K   D   D   C   L   L   K   V   W   Y   P   M
GGT GAA TAC TTT GCC ACT GCT GGA AAG GAT GAC TGT CTT CTG AAA GTC TGG TAC CCT ATG
 T   G   W   K   S   S   I   I   P   Q   D   P   H   E   V   K   R   R   R   A
ACT GGC TGG AAG TCT TCA ATC ATA CCT CAA GAT CCC CAT GAA GTG AAG AGG AGA CGG GCT
 S   T   Q   F   S   F   V   Y   L   A   H   P   R   A   V   T   G   F   S   W
TCC ACT CAG TTC TCC TTT GTT TAC TTG GCA CAC CCT CGA GCC GTG ACA GGT TTC TCA TGG
 R   K   T   S   K   Y   M   P   R   G   S   V   C   N   V   L   L   T   S   C
CGG AAA ACT AGC AAG TAT ATG CCC AGG GGC TCT GTC TGT AAT GTC TTA CTG ACT TCA TGT
 H   D   G   V   C   R   L   W   A   E   T   L   L   P   E   D   C   L   L   G
CAT GAT GGT GTG TGT CGG CTC TGG GCA GAA ACA TTG TTA CCT GAA GAC TGC CTT TTG GGT
 E   Q   I   C   E   T   T   T   S   S   V   A   S   N   L   S   S   A   G   K
GAG CAG ATT TGT GAG ACC ACT ACC TCC AGC GTT GCC AGC AAC CTC TCT TCT GCT GGG AAA
 H   K   D   R   I   Q   H   A   L   E   T   I   H   H   L   K   N   L   R   K
CAC AAA GAC AGG ATC CAG CAT GCT CTT GAG ACA ATA CAC CAT TTG AAG AAT TTA AGG AAA
 G   Q   R   R   S   S   V   L   V   T   H   A   E   L   M   P   D   K   T   A
GGA CAA AGG AGG TCT TCT GTT CTT GTA ACT CAC GCT GAA CTG ATG CCT GAC AAG ACT GCA
 T   H   E   V   H   R   H   I   S   H   H   A   N   A   L   C   H   F   H   I
ACC CAC GAG GTT CAC AGA CAC ATT TCT CAC CAT GCC AAC GCA CTG TGC CAC TTT CAC ATC
 A   A   S   I   N   P   T   T   D   I   P   N   V   L   V   G   T   A   F   N
GCG GCG AGC ATC AAT CCT ACT ACA GAT ATT CCA AAT GTC CTG GTT GGC ACT GCA TTT AAT
 I   D   D   I   N   G   G   F   V   V   H   W   L   N   N   K   E   F   H   F
ATT GAT GAT ATC AAT GGA GGA TTT GTA GTT CAT TGG TTA AAT AAC AAG GAA TTT CAT TTT
 T   S   S   T   E   I   F   M   H   Q   L   R   K   L   S   E   K   Q   L   D
ACA TCA TCA ACT GAA ATA TTT ATG CAC CAA TTA CGA AAA CTT TCT GAA AAA CAA TTA GAT
 H   E   S   D   D   A   D   R   E   D   E   E   R   S   Q   D   E   R   E   R
CAT GAA AGT GAT GAT GCA GAT AGA GAA GAT GAG GAG CGC TCA CAG GAC GAG AGA GAG AGG
 G   L   R   M   K   L   D   H   E   L   S   L   D   R   E   S   E   A   G   T
GGC TTA CGC ATG AAA CTG GAC CAT GAA TTA TCT CTG GAT AGA GAA TCT GAG GCA GGT ACA
 G   S   S   E   H   E   D   G   E   R   E   G   S   P   R   T   H   P   R   P
GGA TCA TCA GAA CAT GAA GAT GGA GAA CGA GAG GGA AGT CCT AGA ACC CAT CCA CGA CCT
 S   I   S   M   P   L   P   T   V   L   L   D   R   K   I   E   T   L   L   T
AGC ATC TCA ATG CCA CTG CCT ACA GTA CTG CTG GAC CGG AAG ATT GAA ACG CTG CTG ACA
 E   W   N   K   N   P   D   M   L   F   T   I   H   P   V   D   G   T   F   L
GAG TGG AAC AAG AAC CCT GAC ATG TTA TTC ACG ATA CAC CCT GTA GAT GGA ACT TTT CTA
 V   W   H   V   K   Y   L   D   E   Y   N   P   G   I   F   R   Q   V   Q   V
GTG TGG CAT GTA AAG TAT TTG GAT GAA TAT AAC CCT GGA ATA TTT AGA CAA GTT CAG GTT
 S   F   S   S   R   I   P   V   A   F   P   S   G   D   A   N   S   L   S   K
TCT TTT TCC TCT CGG ATT CCT GTT GCA TTT CCC TCT GGG GAC GCC AAC TCT CTT AGT AAA
 N   I   M   M   Y   A   C   V   N   A   T   K   D   S   Y   N   P   S   Q   Q
AAC ATC ATG ATG TAT GCT TGT GTG AAT GCT ACA AAA GAT TCA TAC AAC CCA TCC CAG CAA
 E   M   M   S   V   D   S   P   H   G   S   Q   L   H   S   P   S   H   S   T
GAG ATG ATG TCT GTA GAT AGT CCC CAT GGA TCA CAG CTA CAC TCT CCA TCA CAC AGC ACC
 D   M   N   I   L   A   P   T   V   M   M   V   S   K   H   I   D   G   S   L
GAT ATG AAT ATT TTA GCA CCT ACG GTA ATG ATG GTC TCT AAA CAC ATA GAT GGG TCT TTG
 N   Q   W   A   V   T   F   A   D   K   S   A   F   T   T   V   L   T   V   S
AAT CAG TGG GCA GTC ACG TTT GCT GAC AAG TCA GCC TTT ACC ACT GTT CTG ACT GTG TCC
 H   K   F   R   Y   C   G   H   R   F   H   L   N   D   L   A   C   H   S   V
CAC AAA TTC AGA TAC TGT GGT CAC CGA TTC CAC CTC AAT GAC CTG GCA TGC CAT TCT GTT
 L   P   L   L   L   T   S   S   H   H   N   A   L   L   T   P   E   S   D   C
TTA CCC CTC TTG CTG ACA TCT TCC CAT CAT AAT GCT CTG TTG ACT CCT GAA TCA GAC TGT
 Q   W   D   S   D   S   K   V   N   R   L   I   D   P   V   K   H   T   K   A
CAG TGG GAC TCC GAC AGT AAA GTA AAT AGA TTA ATA GAT CCT GTA AAA CAC ACA AAA GCT
```

```
 S   S   K   Q   P   L   R   N   A   A   T   R   T   F   H   D   P   N   A   I
TCA TCA AAA CAG CCT CTG AGA AAT GCA GCA ACC CGT ACA TTT CAT GAC CCA AAT GCA ATC
 Y   S   E   L   I   L   W   R   V   D   P   I   G   P   L   S   Y   T   G   G
TAC AGT GAA CTT ATT TTG TGG CGT GTA GAC CCC ATT GGA CCT TTG TCA TAT ACT GGA GGA
 V   S   E   L   A   R   I   N   S   L   H   T   S   A   F   S   N   V   A   W
GTG TCA GAA TTG GCT CGA ATT AAC TCT TTA CAT ACC TCA GCC TTC TCT AAT GTG GCA TGG
 L   P   T   L   I   P   S   Y   C   L   G   T   Y   C   N   S   A   S   A   C
CTT CCA ACT CTT ATT CCT AGT TAC TGT CTT GGC ACA TAC TGC AAT TCT GCA AGT GCT TGC
 F   V   A   S   D   G   K   N   L   R   L   Y   Q   A   V   V   D   A   R   K
TTT GTT GCA TCT GAT GGC AAA AAT CTA AGA CTC TAT CAA GCT GTG GTC GAT GCA AGA AAA
 L   L   D   E   L   S   D   P   E   A   S   K   L   I   G   E   V   F   N   I
TTA TTA GAT GAA CTG TCA GAC CCA GAA GCC TCA AAA CTG ATC GGA GAA GTG TTT AAC ATT
 V   S   Q   Q   S   T   A   R   P   G   C   I   I   E   L   D   A   I   T   D
GTG AGC CAA CAG TCC ACT GCT CGT CCA GGC TGC ATT ATT GAG CTT GAT GCC ATA ACT GAC
 Q   C   G   S   N   T   Q   L   L   H   V   F   Q   E   D   F   I   I   G   Y
CAA TGT GGA TCA AAT ACA CAG CTA CTG CAC GTG TTT CAA GAA GAC TTC ATT ATT GGA TAT
 K   P   H   K   E   D   M   E   K   K   E   K   E   S   E   I   F   F   Q   P
AAG CCA CAC AAA GAA GAT ATG GAG AAA AAG GAA AAG GAG TCA GAA ATA TTT TTC CAG CCA
 S   Q   G   Y   R   P   P   P   F   S   E   K   F   F   L   V   V   I   E   K
TCA CAA GGA TAT CGA CCA CCA CCA TTT TCA GAA AAA TTC TTT TTA GTA GTC ATT GAG AAG
 D   G   N   N   N   S   I   L   H   M   W   H   L   H   L   K   S   V   Q   A
GAT GGA AAT AAT AAC TCT ATT CTC CAT ATG TGG CAC CTT CAT CTT AAG TCT GTA CAA GCG
 C   L   A   K   A   A   E   G   I   S   S   D   S   L   L   S   V   P   G   Q
TGC TTA GCC AAA GCT GCA GAG GGC ATC TCA TCT GAC AGT CTG CTC TCA GTC CCG GGG CAG
 K   N   L   D   S   S   P   E   T   S   S   S   M   S   S   V   P   H   S   S
AAG AAC CTG GAC TCT TCT CCA GAA ACC TCC TCT AGT ATG AGC TCC GTG CCA CAT TCC TCG
 S   I   A   N   L   Q   T   A   S   K   L   I   L   S   S   R   L   V   Y   S
TCA ATT GCC AAT CTT CAA ACT GCT AGT AAG CTT ATT CTG AGC TCC AGA CTT GTA TAT AGC
 Q   P   L   D   L   P   E   A   V   E   V   I   R   A   T   P   S   A   G   H
CAG CCC CTG GAT CTG CCG GAA GCT GTT GAA GTA ATA AGA GCA ACG CCT TCA GCA GGT CAT
 L   S   S   S   S   I   Y   P   V   C   L   A   P   Y   L   V   V   T   T   C
CTG AGT TCC TCT TCA ATT TAC CCA GTG TGC CTT GCA CCT TAT TTA GTG GTT ACA ACT TGC
 S   D   N   K   V   R   F   W   K   C   C   M   E   T   N   S   L   G   N   T
TCC GAC AAT AAA GTA CGC TTC TGG AAA TGT TGT ATG GAA ACT AAC TCA CTG GGC AAT ACA
 S   D   E   S   E   T   Y   H   W   R   R   W   P   L   M   N   D   E   G   E
AGT GAT GAG AGT GAG ACC TAT CAT TGG AGG AGA TGG CCC TTG ATG AAT GAT GAA GGA GAA
 D   N   S   S   T   V   S   I   V   G   R   P   V   A   V   S   C   S   Y   T
GAT AAC AGC AGT ACT GTG AGC ATC GTG GGA AGA CCT GTT GCT GTT AGC TGC TCA TAC ACA
 G   R   L   A   V   A   Y   K   Q   P   I   H   H   N   G   F   I   S   K   E
GGC CGC CTT GCA GTG GCT TAC AAG CAA CCC ATC CAC CAC AAT GGT TTT ATT TCT AAA GAA
 F   S   M   H   V   C   I   F   E   C   E   S   T   G   G   S   E   W   V   L
TTC TCT ATG CAT GTC TGT ATA TTT GAA TGC GAA TCT ACA GGA GGG TCA GAA TGG GTT TTA
 E   Q   T   I   H   L   D   D   L   V   K   V   G   S   V   L   D   S   R   V
GAA CAG ACG ATC CAT CTT GAT GAT TTA GTT AAG GTT GGA AGT GTA CTT GAT TCA AGG GTC
 S   V   D   S   N   L   F   V   Y   S   K   S   D   A   F   L   S   K   D   R
AGT GTT GAC AGT AAT CTG TTT GTA TAT AGC AAA TCA GAT GCA TTT TTA AGT AAG GAT AGA
 Y   L   I   P   N   I   K   H   L   V   H   L   D   W   V   S   K   E   D   G
TAC CTT ATT CCA AAT ATC AAG CAT TTA GTA CAT TTG GAC TGG GTG TCA AAA GAA GAT GGC
 S   H   I   L   T   V   G   V   G   A   N   I   F   M   Y   G   R   L   S   G
TCT CAC ATC CTC ACA GTG GGG GTT GGT GCT AAT ATC TTC ATG TAT GGG AGA CTT TCA GGA
 I   V   S   D   Q   T   N   S   K   D   G   V   A   V   I   T   L   P   L   G
ATT GTA AGT GAC CAA ACC AAC AGT AAG GAT GGA GTA GCT GTC ATC ACT TTA CCA CTA GGT
 G   S   I   K   Q   G   V   K   S   R   W   V   L   L   R   S   I   D   L   V
GGT AGT ATC AAG CAA GGA GTT AAG TCA AGA TGG GTT CTT CTG AGA TCT ATA GAC TTA GTA
 S   S   V   D   G   T   P   S   L   P   V   S   L   S   W   V   R   D   G   I
TCC TCT GTG GAT GGC ACA CCT TCA CTG CCT GTT TCT CTC TCT TGG GTA AGA GAT GGA ATA
 L   V   V   G   M   D   C   E   M   H   V   Y   A   Q   W   K   H   S   V   K
TTG GTG GTG GGA ATG GAT TGT GAA ATG CAT GTA TAT GCC CAA TGG AAG CAT TCT GTC AAA
 F   G   N   V   D   A   D   S   P   V   E   E   T   I   Q   D   H   S   A   L
TTT GGA AAC GTT GAC GCT GAT AGT CCA GTT GAA GAG ACA ATA CAA GAT CAC TCT GCC CTT
 K   S   S   M   L   A   R   K   S   I   V   E   G   A   A   I   P   D   D   V
AAA TCC TCT ATG CTG GCA AGA AAA AGT ATT GTT GAA GGA GCA GCT ATC CCT GAT GAT GTT
 F   C   S   P   T   V   V   Q   D   G   G   L   F   E   A   A   H   A   L   S
TTC TGT TCA CCT ACT GTG GTT CAA GAT GGT GGC TTA TTT GAG GCT GCA CAT GCA CTC TCT
 P   T   L   P   Q   Y   H   P   T   Q   L   L   E   L   M   D   L   G   K   V
CCT ACT CTG CCA CAG TAT CAT CCA ACT CAG CTG TTA GAA TTA ATG GAC TTA GGG AAA GTT
 R   R   A   K   A   I   L   S   H   L   V   K   C   I   A   G   E   V   A   I
AGA AGA GCT AAG GCC ATT CTT TCC CAT TTG GTA AAG TGC ATC GCA GGT GAA GTT GCA ATA
 V   R   D   P   D   A   G   E   G   T   K   R   H   L   S   R   T   I   S   V
GTT CGG GAT CCT GAT GCT GGA GAA GGA ACT AAG CGG CAT CTC TCT CGG ACC ATT AGT GTG
```

```
 S   G   S   T   A   K   D   T   V   T   I   G   K   D   G   T   R   D   Y   T
AGC GGC AGT ACA GCA AAG GAT ACA GTT ACC ATT GGG AAG GAT GGT ACT CGG GAT TAT ACC
 E   I   D   S   I   P   P   L   P   L   H   A   L   L   A   A   D   Q   D   T
GAG ATA GAC TCT ATT CCT CCA CTA CCA CTA CAC GCA TTG CTT GCT GCA GAC CAG GAC ACA
 S   Y   R   I   S   E   D   S   T   K   K   P   Q   S   Y   E   D   H   I   E
TCC TAC AGA ATT TCA GAG GAC AGT ACA AAA AAG CCA CAG AGC TAT GAG GAC CAT ATT GAA
 S   Q   S   E   D   Q   Y   S   E   L   F   Q   V   Q   E   I   T   T   D   D
AGC CAA TCA GAG GAT CAA TAT TCA GAG CTG TTT CAA GTC CAG GAG ATA ACA ACA GAT GAT
 I   D   L   E   P   E   K   R   E   N   K   S   K   V   I   N   L   S   Q   Y
ATT GAT TTA GAG CCA GAA AAG AGA GAG AAC AAA TCA AAA GTA ATA AAC CTG TCA CAG TAT
 G   P   A   C   F   G   Q   E   H   A   R   V   L   S   S   H   L   M   H   S
GGA CCA GCC TGT TTT GGC CAG GAA CAT GCT AGA GTA CTT TCA AGT CAT CTA ATG CAC TCA
 S   L   P   G   L   T   R   L   E   Q   M   F   L   V   A   L   A   D   T   V
AGT CTG CCA GGC CTT ACC CGC TTG GAG CAG ATG TTC CTT GTA GCA CTG GCG GAT ACT GTG
 A   T   T   S   T   E   L   D   E   N   R   D   K   N   Y   S   G   R   D   T
GCA ACC ACC AGT ACG GAG CTT GAT GAA AAC AGG GAT AAG AAC TAC TCA GGA AGA GAC ACC
 L   D   E   C   G   L   R   Y   L   L   A   M   R   L   H   T   C   L   L   T
TTA GAT GAG TGT GGT TTG AGA TAC CTG TTA GCT ATG CGC TTG CAC ACA TGC CTG TTA ACA
 S   L   P   P   L   Y   R   V   Q   L   L   H   Q   G   V   S   T   C   H   F
TCA CTG CCT CCT TTA TAC CGA GTC CAG CTC CTT CAC CAA GGA GTG TCT ACC TGC CAC TTT
 A   W   A   F   H   S   E   A   E   E   E   L   I   N   M   I   P   A   I   Q
GCC TGG GCT TTT CAT TCT GAA GCT GAG GAA GAA CTG ATC AAT ATG ATT CCA GCA ATC CAA
 R   G   D   P   Q   W   S   E   L   R   A   M   G   I   G   W   W   V   R   N
AGA GGG GAC CCT CAG TGG TCT GAA TTA AGA GCT ATG GGA ATA GGC TGG TGG GTG AGG AAT
 V   N   T   L   R   R   C   I   E   K   V   A   K   A   A   F   Q   R   N   N
GTT AAC ACA CTC CGA AGA TGC ATT GAA AAG GTT GCC AAA GCT GCT TTT CAG AGG AAC AAC
 E   A   L   D   A   A   L   F   Y   L   S   M   K   K   K   A   V   V   W   G
GAG GCC TTA GAT GCC GCT TTG TTC TAC CTT TCC ATG AAG AAG AAA GCG GTA GTG TGG GGT
 L   F   R   S   Q   H   D   E   K   M   T   T   F   F   S   H   N   F   N   E
CTG TTC AGG TCA CAA CAT GAT GAA AAA ATG ACA ACA TTC TTC AGC CAC AAC TTT AAT GAA
 D   R   W   R   K   A   A   L   K   N   A   F   S   L   L   G   K   Q   R   F
GAT AGA TGG CGG AAA GCT GCT TTG AAA AAC GCC TTT TCT TTA CTT GGA AAG CAG CGC TTT
 E   Q   S   A   A   F   F   L   L   A   G   S   L   K   D   A   I   E   V   C
GAG CAG TCT GCT GCT TTT TTC TTG TTA GCT GGT TCA TTG AAA GAT GCA ATT GAG GTA TGT
 L   E   K   M   E   D   I   Q   L   A   M   V   I   A   R   L   F   E   S   E
CTT GAA AAA ATG GAA GAT ATT CAA CTA GCC ATG GTT ATT GCC CGT TTA TTT GAA TCT GAA
 F   E   T   S   S   T   Y   I   S   I   L   N   Q   K   I   L   G   C   Q   K
TTT GAG ACT TCA TCT ACT TAC ATC TCT ATC TTG AAT CAG AAA ATT TTG GGT TGT CAG AAA
 D   G   T   G   F   D   C   K   R   L   H   P   D   P   F   L   R   S   L   A
GAC GGC ACA GGA TTC GAT TGT AAA AGA TTA CAT CCT GAC CCT TTT CTG CGT AGT CTT GCC
 Y   W   V   V   K   D   Y   T   R   A   L   D   T   L   L   E   Q   T   P   K
TAT TGG GTA GTG AAA GAT TAT ACC CGA GCC TTG GAT ACC TTA CTG GAA CAG ACA CCA AAG
 E   D   D   E   Q   Q   V   I   I   K   S   C   N   P   V   V   F   S   F   Y
GAA GAT GAC GAG CAA CAA GTC ATC ATC AAA TCT TGT AAC CCA GTG GTG TTC AGT TTT TAC
 N   Y   L   R   T   H   P   L   L   I   R   R   N   L   A   S   P   E   G   T
AAC TAC CTT CGA ACA CAT CCT TTA CTT ATT CGA AGA AAT CTT GCT TCC CCT GAA GGA ACT
 L   A   T   L   G   L   K   T   E   K   N   I   A   D   K   I   N   L   I   E
TTG GCA ACT TTA GGT CTC AAA ACT GAG AAA AAC ATT GCT GAT AAA ATT AAC CTC ATA GAA
 R   K   L   F   F   T   T   A   N   A   H   F   K   V   G   C   P   V   L   A
AGA AAA TTA TTT TTT ACC ACC GCT AAT GCT CAT TTT AAA GTT GGA TGT CCT GTT TTA GCC
 L   E   V   L   S   K   I   P   K   V   T   K   I   S   S   L   T   A   K   K
CTT GAA GTA CTT TCT AAA ATT CCT AAA GTA ACC AAA ATA TCC TCC TTA ACT GCA AAA AAA
 D   Q   L   D   S   V   S   G   R   M   E   N   G   P   S   E   S   K   P   V
GAT CAG CTT GAC TCT GTT TCT GGA AGG ATG GAG AAC GGG CCA TCA GAA TCA AAA CCA GTG
 S   R   S   D   G   G   S   G   A   D   W   S   A   V   T   S   S   Q   F   D
AGC AGG AGT GAT GGT GGT TCT GGG GCT GAC TGG TCG GCT GTG ACT TCC TCC CAG TTT GAC
 W   S   Q   P   M   V   T   V   D   E   E   P   L   R   L   D   W   G   D   D
TGG AGT CAG CCA ATG GTT ACA GTT GAC GAG GAG CCT CTT AGG CTC GAT TGG GGT GAC GAT
 H   D   G   A   L   E   E   D   D   G   G   G   L   V   M   K   T   T   D   A
CAT GAC GGT GCC TTA GAA GAG GAT GAT GGC GGT GGC TTA GTA ATG AAA ACT ACA GAT GCC
 K   K   A   G   Q   E   Q   S   A   S   D   P   R   A   L   L   T   P   Q   D
AAG AAG GCT GGC CAG GAG CAG AGT GCC TCA GAC CCT CGT GCT TTG CTG ACT CCT CAG GAC
 E   E   C   A   D   G   D   T   E   V   D   V   I   A   E   Q   L   K   F   R
GAG GAG TGT GCT GAC GGC GAT ACT GAG GTC GAT GTG ATT GCT GAA CAA CTC AAG TTC CGA
 A   C   L   K   I   L   M   T   E   L   R   T   L   A   T   G   Y   E   V   D
GCT TGC TTG AAG ATC CTT ATG ACT GAG TTA AGA ACT TTG GCT ACA GGT TAT GAA GTA GAT
 G   G   K   L   R   F   Q   L   Y   N   W   L   E   K   E   I   A   A   L   H
GGA GGG AAG CTG AGA TTT CAG CTC TAT AAC TGG CTT GAA AAG GAA ATT GCT GCC TTG CAT
 E   I   C   N   H   E   S   V   I   K   E   Y   S   S   K   A   H   S   T   V
GAG ATA TGC AAC CAT GAA TCA GTT ATT AAA GAA TAT TCG AGC AAA GCG CAT TCT ACA GTA
```

```
 E   T   E   R   L   D   Q   E   E   M   V   D   K   P   D   I   G   S   Y   E
GAG ACT GAG CGT CTG GAT CAG GAG GAA ATG GTG GAC AAG CCG GAT ATC GGT TCC TAT GAG
 R   H   Q   I   E   R   R   R   L   Q   A   K   R   E   H   A   E   R   R   K
CGC CAC CAA ATA GAA CGA CGA CGG CTG CAG GCT AAA AGG GAG CAT GCA GAA AGA CGA AAG
 L   W   L   Q   K   N   Q   D   L   L   R   V   F   L   S   Y   C   S   L   H
CTG TGG TTG CAG AAA AAC CAA GAT CTC CTG AGA GTA TTT CTC AGT TAC TGT AGC CTT CAT
 G   A   Q   G   G   G   L   A   S   V   R   M   E   L   K   F   L   L   Q   E
GGA GCC CAG GGC GGT GGT CTG GCT TCA GTA AGA ATG GAA CTC AAA TTT TTG CTG CAA GAG
 S   Q   Q   E   T   T   V   K   Q   L   Q   S   P   L   P   L   P   T   T   L
TCA CAG CAG GAA ACT ACA GTG AAG CAG CTC CAG TCC CCA CTG CCA CTA CCT ACC ACG TTG
 P   L   L   S   A   S   I   A   S   T   K   T   V   I   A   N   P   V   L   Y
CCT CTG CTT TCA GCA AGT ATC GCA TCA ACA AAA ACA GTC ATA GCT AAC CCT GTA TTG TAT
 L   N   N   H   I   H   D   I   L   Y   T   I   V   Q   M   K   T   P   P   H
TTA AAT AAC CAC ATC CAT GAT ATA CTT TAT ACT ATT GTG CAG ATG AAA ACA CCA CCT CAT
 P   S   V   E   D   V   K   V   H   T   L   H   S   L   A   A   S   L   S   A
CCC AGT GTT GAA GAT GTG AAG GTG CAC ACA CTT CAT TCA CTA GCA GCA TCA CTT TCT GCA
 S   I   Y   Q   A   L   C   D   S   H   S   Y   S   S   Q   S   E   G   N   Q
TCA ATT TAC CAG GCA TTA TGT GAC AGT CAT AGC TAC AGC AGT CAG TCG GAA GGA AAT CAG
 F   T   G   M   A   Y   Q   G   L   L   L   S   D   R   R   R   L   R   T   E
TTC ACA GGA ATG GCC TAT CAA GGG CTT CTT CTA AGT GAT CGA CGA CGC CTC AGG ACA GAA
 S   I   E   E   H   A   T   P   N   S   A   P   A   Q   W   P   G   V   S   S
AGC ATC GAA GAG CAT GCA ACA CCA AAC TCA GCT CCT GCT CAG TGG CCT GGT GTG AGC TCA
 L   I   N   L   L   S   S   A   Q   D   E   D   Q   P   K   L   N   V   L   L
CTC ATT AAT CTC TTG AGT TCT GCC CAA GAT GAA GAC CAG CCA AAA TTG AAT GTT CTG TTG
 C   E   A   V   V   A   V   Y   L   S   L   L   I   H   A   L   A   T   N   S
TGT GAA GCT GTT GTT GCT GTT TAC TTA AGT TTA CTG ATA CAT GCT CTT GCC ACA AAT TCT
 S   N   E   L   F   R   L   A   A   H   P   L   N   N   R   M   W   A   A   V
TCC AAT GAA TTG TTT CGG CTT GCA GCC CAC CCG TTA AAT AAT CGA ATG TGG GCT GCT GTT
 F   G   G   G   V   K   L   V   V   K   P   R   R   Q   S   E   S   I   A   A
TTC GGA GGG GGT GTA AAA CTT GTT GTG AAG CCT CGG AGG CAA TCA GAA AGT ATC GCA GCA
 P   P   V   A   S   E   D   M   D   K   H   R   R   R   F   N   M   R   M   L
CCT CCT GTG GCC TCT GAG GAC ATG GAC AAG CAC CGC AGG AGA TTC AAC ATG AGG ATG CTG
 V   P   G   R   P   V   K   D   A   T   P   P   P   V   P   A   E   R   P   S
GTC CCT GGG AGG CCT GTA AAA GAT GCC ACC CCA CCC CCA GTG CCT GCA GAA AGA CCA TCT
 Y   K   E   K   F   I   P   P   E   L   S   M   W   D   Y   F   V   A   K   P
TAC AAG GAA AAA TTT ATT CCC CCA GAA CTT AGT ATG TGG GAC TAC TTT GTT GCA AAG CCG
 F   L   P   L   S   D   S   G   V   I   Y   D   S   D   E   S   V   H   S   D
TTC CTC CCT TTG TCT GAT AGT GGT GTC ATA TAT GAT TCT GAT GAA AGT GTA CAC AGT GAT
 D   E   E   D   D   A   F   F   S   D   T   Q   I   Q   E   H   Q   D   P   N
GAT GAA GAG GAT GAT GCC TTT TTT TCA GAC ACA CAA ATA CAG GAG CAT CAA GAT CCT AAT
 S   Y   S   W   A   L   L   H   L   T   M   V   K   L   A   L   H   N   I   K
TCT TAT AGC TGG GCT CTT CTG CAT TTG ACA ATG GTT AAG CTG GCG CTT CAC AAT ATC AAG
 N   F   F   P   I   A   G   L   E   F   S   E   L   P   V   T   S   P   L   G
AAT TTT TTT CCT ATT GCT GGG CTG GAA TTC TCT GAG CTC CCT GTG ACA TCA CCG CTA GGA
 I   A   V   I   K   N   L   E   N   W   E   Q   I   L   Q   E   K   M   D   H
ATC GCT GTC ATT AAA AAC TTG GAG AAC TGG GAA CAG ATT CTG CAG GAG AAA ATG GAT CAC
 F   E   G   P   P   P   N   Y   V   N   T   Y   P   T   D   L   S   V   G   A
TTT GAA GGC CCA CCC CCT AAC TAT GTC AAC ACA TAC CCA ACT GAC CTC TCA GTG GGA GCG
 G   P   A   I   L   R   N   K   A   M   L   E   P   E   N   T   P   F   K   S
GGG CCA GCT ATT CTC CGA AAT AAA GCA ATG TTA GAG CCG GAA AAC ACT CCA TTC AAA TCC
 R   D   S   S   A   L   P   V   K   R   L   W   H   F   L   V   K   Q   E   V
CGG GAT TCG TCT GCA CTT CCT GTC AAG CGA CTC TGG CAT TTC CTT GTC AAA CAG GAA GTT
 L   Q   E   T   F   I   R   Y   I   F   T   K   K   R   K   Q   S   E   S   V
CTT CAG GAG ACA TTT ATT AGA TAC ATT TTC ACT AAG AAA AGA AAG CAG AGT GAG TCT GTA
 E   E   H   V   E   Q   V   K   H   N   S   V   A   E   D   C   H   I   K   V
GAA GAA CAT GTG GAG CAG GTC AAA CAC AAC TCC GTA GCA GAA GAT TGC CAC ATC AAG GTC
 E   A   D   L   G   Y   P   G   G   K   A   K   V   I   H   K   E   S   D   M
GAA GCT GAT CTG GGC TAC CCA GGA GGG AAG GCG AAG GTC ATT CAT AAG GAA TCT GAC ATG
 I   M   A   F   S   I   N   K   A   N   C   N   E   I   V   L   A   S   T   H
ATC ATG GCA TTC TCT ATT AAT AAG GCA AAC TGT AAT GAA ATT GTT TTG GCT TCA ACA CAT
 D   V   Q   E   L   D   V   T   S   L   L   A   C   Q   S   Y   I   W   I   G
GAT GTT CAA GAA CTC GAT GTC ACT TCT CTA CTG GCT TGT CAA TCA TAT ATA TGG ATC GGA
 E   E   Y   D   R   E   S   K   S   S   D   D   I   D   Y   R   G   S   T   T
GAA GAA TAT GAC AGA GAG TCG AAA AGT TCA GAT GAT ATT GAT TAC CGT GGT TCC ACT ACA
 T   L   Y   Q   P   G   A   A   S   H   S   S   S   Q   P   H   P   P   P   S
ACC CTG TAC CAG CCT GGT GCA GCC TCC CAT TCC TCA AGC CAG CCA CAC CCA CCT CCA TCT
 L   P   W   L   G   S   G   Q   T   S   T   G   A   T   V   L   M   K   R   N
CTG CCA TGG CTA GGC AGT GGA CAG ACC AGC ACT GGG GCT ACT GTG CTC ATG AAA AGG AAT
 L   H   N   V   K   R   M   T   S   H   P   V   H   Q   Y   Y   L   T   G   A
CTA CAT AAT GTT AAG AGA ATG ACA TCA CAC CCC GTC CAT CAG TAC TAT CTC ACA GGT GCC
```

```
 Q   D   G   S   V   R   M   F   E   W   T   R   P   Q   Q   L   V   C   F   R
CAG GAC GGC AGT GTC CGC ATG TTT GAG TGG ACA CGA CCT CAG CAA CTT GTC TGT TTC CGT
 Q   A   G   N   A   R   V   T   R   L   Y   F   N   S   Q   G   N   K   C   G
CAA GCT GGC AAT GCA AGA GTT ACT AGA TTA TAT TTT AAT TCA CAA GGC AAC AAG TGT GGT
 V   A   D   G   E   G   F   L   S   I   W   Q   V   N   Q   T   A   S   N   P
GTT GCA GAC GGA GAG GGT TTT CTG AGT ATC TGG CAA GTT AAC CAA ACT GCA TCG AAT CCT
 K   P   Y   M   S   W   Q   C   H   S   K   A   T   S   D   F   A   F   I   T
AAA CCG TAC ATG AGT TGG CAG TGC CAC AGT AAG GCC ACA AGT GAC TTT GCA TTT ATC ACC
 S   S   S   L   V   A   T   S   G   H   S   N   D   N   R   N   V   C   L   W
TCT TCA AGC CTA GTT GCA ACC TCT GGA CAT TCC AAT GAC AAT AGA AAC GTA TGC CTC TGG
 D   T   L   I   S   P   G   N   S   L   I   H   G   F   T   C   H   D   H   G
GAC ACA TTG ATA TCA CCT GGA AAC AGC CTC ATT CAC GGT TTT ACT TGT CAT GAC CAT GGT
 A   T   V   L   Q   Y   A   P   K   Q   Q   L   L   I   S   G   G   R   K   G
GCC ACA GTA CTC CAA TAT GCC CCC AAG CAA CAA CTC CTA ATC TCT GGG GGT AGG AAA GGC
 Y   I   C   I   F   D   I   R   Q   R   Q   L   I   H   T   F   Q   A   H   D
TAC ATC TGC ATT TTT GAC ATC AGA CAG AGA CAG CTA ATA CAC ACC TTC CAG GCA CAC GAC
 S   A   I   K   A   L   A   L   D   S   C   E   E   Y   F   T   T   G   S   A
TCG GCT ATT AAG GCT TTG GCT CTG GAT TCG TGT GAG GAG TAC TTC ACT ACA GGC TCA GCA
 E   G   N   I   K   V   W   R   L   T   G   H   G   L   I   H   S   F   K   S
GAG GGC AAT ATA AAA GTA TGG AGA TTG ACA GGC CAT GGC CTG ATT CAT TCA TTT AAG AGC
 E   H   A   K   Q   S   I   F   R   N   I   G   A   G   V   M   Q   I   A   I
GAG CAT GCT AAG CAG TCC ATA TTT CGG AAC ATT GGC GCT GGA GTC ATG CAG ATT GCT ATC
 S   Q   D   N   R   L   F   S   C   G   A   D   G   T   L   K   T   R   V   L
AGC CAG GAC AAT CGG CTC TTC TCC TGT GGC GCA GAC GGC ACG CTG AAA ACC AGG GTT CTG
 P   S   A   F   N   I   P   N   R   I   L   D   I   L   *
CCC AGT GCT TTT AAC ATC CCT AAT AGA ATT CTT GAC ATT CTG TAG
```

EML5 echinoderm microtubule associated protein like 5 [Mus musculus]

GenBank: AAI58138.1

http://www.uniprot.org/uniprot/Q8BQM8

```
        10          20          30          40          50          60
MAARSAPSCH LRLEWVYGYR GHQCRNNLYY TAAKEIVYFV AGVGVVYSPR EHRQKFFRGH
  WD1     70          80          90         100         110   WD2   120
SDDIISLALH PERVLVATGQ VGKEPYICVW DSYTVQTVSV LKDVHTHGIA CLAFDLDGQR
       130         140         150   WD3   160         170         180
LVSVGLDSKN AVCVWDWKRG RMLSMAPGHT DRIFDISWDL YQPNKLVSCG VKHIKFWSLC
       190         200   WD4   210         220         230         240
GNALTPKRGV FGKTGDLQTI LCLACARDEL TYSGALNGDI YVWKGINLIR TIQGAHTAGI
  WD5   250         260         270         280   WD6   290         300
FSMNSCEEGF ATGGRDGCIR LWDLTFKPIT VIDLRETEQG YKGLSVRSVC WRGDHILVGT
       310         320     WD7 330         340         350         360
QDSEIFEIVV HERNKPFLIM QGHCEGELWA LAVHPTKPLA VTGSDDRSVR IWSLVDHALI
       370         380         390         400         410   WD8   420
ARCNMEEPIR CAAVNVDGIH LALGMKDGSF TVLRVRDMTE VVHIKDRKEA IHELKYSPDG
       430         440         450   WD9   460         470         480
AYLAVGCNDS SVDIYGVAQR YKKVGECVGS LSFITHLDWS SDSRYLQTND GSGKRLLYKM
       490         500         510         520         530         540
PGGKEVTSKE EIKGMHWASW TCVAGLEVNG IWPKYSDIND INSVDGNYVG QVLVTADDYG
       550         560   WD10  570         580         590         600
VVKLFRYPCL RKGAKFRKYI GHSAHVTNVR WSHDYQWVIS IGGADHSVFQ WKFIPERKLK
       610         620         630         640         650         660
DALHIAPQES LAESNSDESD SDLSDVPELD SEIEQETQLT YHRQVYKEDL PQLKEQCKEK
       670         680         690         700         710         720
QKSATSKRRE RTPGTSIRLH FIHGYRGYDC RSNLFYTQIG EIVYHVAAVG VIYNRQQNTQ
       730   WD11  740         750         760         770   WD12  780
RFYLGHDDDI LCLAIHPLKD YVATGQVGRD PSIHVWDTET IKPLSILKGY HQYGICAVDF
       790         800         810         820   WD13  830         840
SADGKRLASV GIDDSHTIVL WDWKKGEKLS VTRGSKDKIF VVKMNPYVPD KLITAGIKHM
```

```
       850         860  WD14  870         880         890         900
KFWRRAGGGL IGKKGYVGTL GKNDTMMCAV YGWTEEMAFS GTSTGDVCIW RDVFLVKTVK
 WD15  910         920         930         940         950         960
AHDGPVFSMH ALEKGFVTGG KDGMVALWDD SFERCLKTYA IKRADLAPGS KGLLLEDNPS
       970         980         990        1000        1010  WD16 1020
IRAISLGHGH ILVGTKNGEI LEVDKSGPIT LLVQGHMEGE VWGLATHPYL PICATVSDDK
      1030        1040  WD17 1050        1060        1070        1080
TLRIWDLSPS HCMLAVRKLK KGGRCCCFSP DGKALAVGLN DGSFLMANAD TLEDLVSFHH
 WD18 1090        1100        1110        1120        1130        1140
RKDIISDIRF SPGSGKYLAV ASHDSFVDIY NVTSSKRVGV CKGATSYITH IDWDSRGKLL
      1150        1160        1170        1180        1190        1200
QVNTGAKEQL FFEAPRGKRQ TIPSVEVEKI SWATWTSVLG LCCEGIWPVI GEVTEVTASC
      1210        1220        1230        1240  WD19 1250        1260
LTSDKMVLAT GDDLGFVKLF RYPAKGKFGK FKKYVAHSTH VTNVRWTYDD SMLVTLGGAD
      1270        1280        1290        1300        1310        1320
MSLMVWTNEV ESHREKKYCD SEESDIDSEE DGGYDSDVTR ENEISYTIRA LSTNIRPMFG
      1330        1340        1350        1360        1370        1380
VKPHLQQKEP SVDERQGVVR GSRPPVSRAP PQPEKLQSNN VGKKKRPIED LVLELAFGYR
      1390        1400        1410        1420  WD20 1430        1440
GRDCRNNVHY LNDGDDIIYH TASIGILHNV ATGTQSFYQE HNDDILCLTV NQHPKFINIV
      1450        1460        1470        1480  WD21 1490        1500
ATGQVGDSAD MSATAPSVHI WDAVNKQTLS ILRCSHSKGV CSVSFSATGK LLLSVGLDPE
      1510        1520  WD22 1530        1540        1550        1560
HTVTIWRWQE GAKIASRGGH NQRIFVAEFR PDSDTQFVSV GIKHVKFWTL AGRALLSKKG
      1570  WD23 1580        1590        1600        1610  WD24 1620
LLSSLEDARM QTMLAVAFGA NNLTFTGTIS GDVCVWKDHI LCRVVARAHN GPVFAMYTTL
      1630        1640        1650        1660        1670        1680
RDGLIVTGGK ERPSKEGGAV KLWDQELRRC RAFRLETGQV TDCVRSVCRG KGKILVGTRN
      1690        1700  WD25 1710        1720        1730        1740
SEIIEVGEKN AACNILVNGH VDGPIWGLAT HPSRDFFLSA AEDGTVRLWD IADKKMLNKV
 WD26 1750        1760        1770        1780   |    1790  WD27 1800
NLGHAARTVC YSPEGDMVAI GMKNGEFIIL LVSSLKIWGK KRDRRCAIHD IRFSPDSRYL
      1810        1820        1830        1840        1850        1860
AVGSSENSVD FYDLTLGPTL NRISYCKDIP SFVIQMDFSA DSRHLQVSSG CYKRHVYEVP
      1870        1880        1890        1900  WD28 1910        1920
SGKHLVDHAA IDRITWATWT SILGDEVMGI WSRHAEKADV TCACVSHSGI SLVTGDDFGM
      1930        1940  WD29 1950        1960        1970
VKLYDFPCPE KFAKHKRFLG HSPHVTNIRF TSGDRHVVSA GGDDCSLFVW KCVHMPH
```

```
 M   A   A   R   S   A   P   S   C   H   L   R   L   E   W   V   Y   G   Y   R
ATG GCG GCT CGG AGC GCC CCG AGC TGC CAC CTG CGG CTC GAG TGG GTG TAC GGC TAC CGG
 G   H   Q   C   R   N   N   L   Y   Y   T   A   A   K   E   I   V   Y   F   V
GGC CAC CAG TGC CGC AAC AAC CTC TAC TAC ACG GCG GCC AAG GAG ATC GTG TAC TTC GTG
 A   G   V   G   V   V   Y   S   P   R   E   H   R   Q   K   F   F   R   G   H
GCG GGG GTC GGC GTG GTG TAT AGT CCG CGG GAG CAT CGG CAG AAG TTC TTC CGC GGC CAC
 S   D   D   I   I   S   L   A   L   H   P   E   R   V   L   V   A   T   G   Q
AGC GAC GAC ATC ATC AGT CTT GCA CTG CAT CCT GAG CGA GTG TTG GTA GCA ACA GGA CAA
 V   G   K   E   P   Y   I   C   V   W   D   S   Y   T   V   Q   T   V   S   V
GTT GGG AAA GAG CCT TAC ATC TGT GTT TGG GAT TCT TAC ACT GTC CAG ACC GTG TCG GTT
 L   K   D   V   H   T   H   G   I   A   C   L   A   F   D   L   D   G   Q   R
CTG AAG GAT GTT CAT ACA CAT GGT ATA GCT TGT TTG GCA TTT GAC TTG GAT GGA CAG CGC
 L   V   S   V   G   L   D   S   K   N   A   V   C   V   W   D   W   K   R   G
TTG GTT TCA GTT GGA CTC GAT TCA AAG AAT GCA GTT TGT GTT TGG GAC TGG AAA AGG GGG
 R   M   L   S   M   A   P   G   H   T   D   R   I   F   D   I   S   W   D   L
AGA ATG CTG TCT ATG GCT CCA GGT CAC ACC GAC AGA ATA TTT GAT ATT TCT TGG GAT TTG
 Y   Q   P   N   K   L   V   S   C   G   V   K   H   I   K   F   W   S   L   C
TAC CAG CCA AAT AAA CTC GTC AGC TGT GGT GTA AAA CAC ATC AAG TTC TGG AGT TTG TGT
 G   N   A   L   T   P   K   R   G   V   F   G   K   T   G   D   L   Q   T   I
GGA AAT GCT CTG ACC CCA AAA CGC GGA GTT TTT GGT AAA ACA GGT GAC CTT CAG ACA ATA
 L   C   L   A   C   A   R   D   E   L   T   Y   S   G   A   L   N   G   D   I
TTG TGC CTC GCC TGT GCT CGG GAT GAG CTA ACA TAT TCT GGT GCA CTC AAT GGG GAT ATA
 Y   V   W   K   G   I   N   L   I   R   T   I   Q   G   A   H   T   A   G   I
TAT GTA TGG AAA GGA ATC AAT CTT ATA CGA ACA ATA CAA GGA GCC CAT ACT GCA GGG ATT
```

```
 F   S   M   N   S   C   E   E   G   F   A   T   G   G   R   D   G   C   I   R
TTT AGT ATG AAC TCT TGT GAA GAA GGC TTT GCT ACT GGT GGC AGA GAT GGC TGT ATT CGT
 L   W   D   L   T   F   K   P   I   T   V   I   D   L   R   E   T   E   Q   G
CTT TGG GAT TTA ACT TTT AAA CCA ATT ACT GTG ATT GAT CTC AGG GAA ACA GAA CAA GGA
 Y   K   G   L   S   V   R   S   V   C   W   R   G   D   H   I   L   V   G   T
TAC AAA GGT TTA TCT GTG AGG AGT GTT TGT TGG CGA GGT GAC CAC ATT TTA GTG GGA ACG
 Q   D   S   E   I   F   E   I   V   V   H   E   R   N   K   P   F   L   I   M
CAG GAC AGT GAA ATT TTT GAA ATT GTT GTG CAT GAA AGA AAT AAA CCT TTC CTA ATT ATG
 Q   G   H   C   E   G   E   L   W   A   L   A   V   H   P   T   K   P   L   A
CAA GGG CAT TGC GAA GGT GAA CTT TGG GCG CTT GCT GTT CAC CCT ACT AAG CCT TTG GCT
 V   T   G   S   D   D   R   S   V   R   I   W   S   L   V   D   H   A   L   I
GTG ACC GGA AGT GAT GAT CGT TCA GTC AGG ATT TGG AGC CTT GTA GAT CAT GCT TTA ATA
 A   R   C   N   M   E   E   P   I   R   C   A   A   V   N   V   D   G   I   H
GCA AGA TGT AAT ATG GAA GAG CCA ATT CGG TGT GCT GCT GTA AAT GTA GAT GGA ATT CAT
 L   A   L   G   M   K   D   G   S   F   T   V   L   R   V   R   D   M   T   E
CTT GCC CTT GGA ATG AAG GAT GGG TCG TTC ACT GTC CTT AGA GTG AGA GAC ATG ACT GAA
 V   V   H   I   K   D   R   K   E   A   I   H   E   L   K   Y   S   P   D   G
GTT GTA CAT ATT AAA GAC AGG AAA GAA GCA ATC CAT GAG CTA AAA TAT TCA CCA GAT GGC
 A   Y   L   A   V   G   C   N   D   S   S   V   D   I   Y   G   V   A   Q   R
GCT TAC CTT GCT GTT GGC TGC AAT GAC AGC TCA GTT GAC ATC TAT GGA GTT GCT CAG CGT
 Y   K   K   V   G   E   C   V   G   S   L   S   F   I   T   H   L   D   W   S
TAT AAA AAG GTC GGT GAA TGT GTC GGC TCC CTT AGC TTC ATC ACT CAC TTG GAC TGG TCT
 S   D   S   R   Y   L   Q   T   N   D   G   S   G   K   R   L   L   Y   K   M
TCA GAT AGT AGA TAC TTA CAG ACA AAT GAT GGC AGT GGA AAG CGA CTT CTC TAC AAG ATG
 P   G   G   K   E   V   T   S   K   E   E   I   K   G   M   H   W   A   S   W
CCA GGA GGA AAG GAG GTG ACA AGC AAA GAA GAA ATA AAA GGC ATG CAC TGG GCT TCC TGG
 T   C   V   A   G   L   E   V   N   G   I   W   P   K   Y   S   D   I   N   D
ACA TGC GTT GCA GGC CTT GAA GTC AAT GGA ATT TGG CCC AAG TAT TCT GAT ATC AAT GAT
 I   N   S   V   D   G   N   Y   V   G   Q   V   L   V   T   A   D   D   Y   G
ATA AAC TCA GTC GAT GGC AAT TAT GTT GGC CAG GTT TTA GTT ACA GCT GAT GAC TAC GGA
 V   V   K   L   F   R   Y   P   C   L   R   K   G   A   K   F   R   K   Y   I
GTT GTA AAA TTA TTC CGA TAC CCA TGT TTG AGA AAA GGG GCC AAG TTT AGA AAG TAC ATT
 G   H   S   A   H   V   T   N   V   R   W   S   H   D   Y   Q   W   V   I   S
GGC CAT TCA GCT CAT GTA ACT AAT GTC AGA TGG TCA CAT GAT TAT CAG TGG GTT ATC TCT
 I   G   G   A   D   H   S   V   F   Q   W   K   F   I   P   E   R   K   L   K
ATT GGT GGA GCA GAT CAT TCT GTC TTT CAG TGG AAA TTT ATT CCT GAG AGA AAA CTA AAA
 D   A   L   H   I   A   P   Q   E   S   L   A   E   S   N   S   D   E   S   D
GAT GCT CTT CAC ATA GCA CCG CAA GAA AGT CTG GCT GAG TCC AAC AGT GAT GAA TCA GAT
 S   D   L   S   D   V   P   E   L   D   S   E   I   E   Q   E   T   Q   L   T
TCA GAT CTG TCT GAT GTT CCA GAA CTG GAT TCT GAG ATT GAG CAA GAG ACA CAG CTT ACT
 Y   H   R   Q   V   Y   K   E   D   L   P   Q   L   K   E   Q   C   K   E   K
TAC CAC CGG CAG GTT TAC AAA GAA GAT CTA CCT CAA CTT AAA GAA CAA TGC AAA GAG AAG
 Q   K   S   A   T   S   K   R   R   E   R   T   P   G   T   S   I   R   L   H
CAG AAA AGT GCT ACT TCT AAA CGA AGA GAA CGC ACT CCA GGA ACT AGT ATT CGA TTG CAC
 F   I   H   G   Y   R   G   Y   D   C   R   S   N   L   F   Y   T   Q   I   G
TTT ATT CAT GGT TAC AGA GGT TAT GAC TGT CGA AGT AAT CTT TTC TAC ACT CAA ATT GGT
 E   I   V   Y   H   V   A   A   V   G   V   I   Y   N   R   Q   Q   N   T   Q
GAA ATT GTG TAC CAC GTG GCA GCA GTG GGT GTC ATA TAT AAT AGA CAA CAG AAC ACA CAG
 R   F   Y   L   G   H   D   D   D   I   L   C   L   A   I   H   P   L   K   D
CGT TTT TAC TTG GGT CAT GAT GAT GAT ATT CTG TGT TTG GCT ATT CAT CCT TTG AAA GAC
 Y   V   A   T   G   Q   V   G   R   D   P   S   I   H   V   W   D   T   E   T
TAT GTG GCA ACA GGC CAG GTA GGT AGA GAT CCC TCA ATT CAT GTA TGG GAC ACA GAA ACC
 I   K   P   L   S   I   L   K   G   Y   H   Q   Y   G   I   C   A   V   D   F
ATT AAA CCA TTG TCT ATA TTA AAG GGC TAC CAC CAA TAT GGC ATC TGT GCT GTT GAT TTC
 S   A   D   G   K   R   L   A   S   V   G   I   D   D   S   H   T   I   V   L
TCA GCT GAT GGG AAA CGC CTG GCT TCA GTT GGA ATA GAT GAC AGC CAC ACC ATT GTA TTG
 W   D   W   K   K   G   E   K   L   S   V   T   R   G   S   K   D   K   I   F
TGG GAC TGG AAG AAA GGG GAG AAA CTT TCA GTG ACA AGA GGC AGT AAA GAT AAG ATT TTT
 V   V   K   M   N   P   Y   V   P   D   K   L   I   T   A   G   I   K   H   M
GTT GTG AAA ATG AAC CCC TAT GTG CCT GAT AAA CTA ATT ACA GCT GGG ATT AAA CAC ATG
 K   F   W   R   R   A   G   G   G   L   I   G   K   K   G   Y   V   G   T   L
AAA TTT TGG CGT AGA GCA GGG GGA GGA TTA ATT GGA AAA AAA GGC TAC GTA GGC ACT CTG
 G   K   N   D   T   M   M   C   A   V   Y   G   W   T   E   E   M   A   F   S
GGG AAA AAC GAC ACA ATG ATG TGT GCA GTG TAC GGA TGG ACT GAA GAG ATG GCT TTT TCT
 G   T   S   T   G   D   V   C   I   W   R   D   V   F   L   V   K   T   V   K
GGA ACA TCC ACA GGA GAT GTG TGC ATC TGG AGA GAT GTT TTT CTT GTA AAA ACA GTT AAA
 A   H   D   G   P   V   F   S   M   H   A   L   E   K   G   F   V   T   G   G
GCC CAT GAT GGG CCC GTG TTC AGT ATG CAT GCA TTG GAG AAA GGA TTT GTA ACT GGA GGA
 K   D   G   M   V   A   L   W   D   D   S   F   E   R   C   L   K   T   Y   A
AAA GAT GGT ATG GTA GCC CTT TGG GAT GAT TCC TTT GAA AGA TGC CTC AAG ACC TAT GCT
```

```
 I   K   R   A   D   L   A   P   G   S   K   G   L   L   L   E   D   N   P   S
ATA AAA AGA GCT GAT TTA GCC CCA GGA TCT AAA GGT CTG CTC TTG GAA GAT AAC CCA TCT
 I   R   A   I   S   L   G   H   G   H   I   L   V   G   T   K   N   G   E   I
ATA CGT GCC ATA TCA TTA GGG CAT GGT CAT ATT TTG GTT GGC ACA AAG AAT GGT GAG ATA
 L   E   V   D   K   S   G   P   I   T   L   L   V   Q   G   H   M   E   G   E
TTA GAA GTG GAT AAG AGT GGC CCA ATC ACT CTT CTG GTC CAG GGA CAC ATG GAA GGA GAG
 V   W   G   L   A   T   H   P   Y   L   P   I   C   A   T   V   S   D   D   K
GTG TGG GGT TTG GCC ACA CAT CCT TAC CTG CCC ATC TGT GCT ACT GTA AGT GAT GAT AAG
 T   L   R   I   W   D   L   S   P   S   H   C   M   L   A   V   R   K   L   K
ACC TTA AGA ATA TGG GAT CTC TCT CCT AGT CAT TGT ATG TTG GCA GTC CGG AAA CTG AAA
 K   G   G   R   C   C   C   F   S   P   D   G   K   A   L   A   V   G   L   N
AAG GGG GGC CGC TGC TGC TGC TTT TCC CCT GAT GGA AAA GCT TTG GCT GTG GGT CTC AAC
 D   G   S   F   L   M   A   N   A   D   T   L   E   D   L   V   S   F   H   H
GAC GGA AGC TTC TTA ATG GCC AAT GCT GAC ACT CTG GAG GAT CTT GTG TCC TTT CAC CAC
 R   K   D   I   I   S   D   I   R   F   S   P   G   S   G   K   Y   L   A   V
AGA AAA GAT ATT ATT TCA GAC ATC CGG TTT TCA CCT GGT TCT GGG AAA TAC CTA GCT GTG
 A   S   H   D   S   F   V   D   I   Y   N   V   T   S   S   K   R   V   G   V
GCA TCC CAT GAC AGC TTC GTT GAT ATA TAC AAC GTG ACG AGT AGT AAA CGA GTG GGG GTT
 C   K   G   A   T   S   Y   I   T   H   I   D   W   D   S   R   G   K   L   L
TGC AAA GGA GCA ACC AGC TAC ATC ACC CAT ATC GAC TGG GAC AGC AGA GGA AAG CTT TTA
 Q   V   N   T   G   A   K   E   Q   L   F   F   E   A   P   R   G   K   R   Q
CAA GTC AAC ACT GGT GCT AAA GAA CAG CTA TTC TTT GAA GCT CCC AGA GGA AAA AGA CAA
 T   I   P   S   V   E   V   E   K   I   S   W   A   T   W   T   S   V   L   G
ACC ATC CCC AGT GTG GAG GTG GAA AAA ATT AGT TGG GCA ACA TGG ACA AGT GTT CTT GGT
 L   C   C   E   G   I   W   P   V   I   G   E   V   T   E   V   T   A   S   C
TTA TGC TGT GAG GGA ATT TGG CCG GTG ATT GGA GAA GTC ACA GAA GTA ACC GCC TCT TGC
 L   T   S   D   K   M   V   L   A   T   G   D   D   L   G   F   V   K   L   F
CTC ACC AGT GAC AAA ATG GTC CTA GCC ACA GGG GAT GAC TTG GGA TTC GTG AAG CTG TTC
 R   Y   P   A   K   G   K   F   G   K   F   K   K   Y   V   A   H   S   T   H
AGA TAC CCA GCT AAA GGA AAA TTT GGA AAG TTT AAG AAG TAT GTG GCT CAC AGC ACA CAT
 V   T   N   V   R   W   T   Y   D   D   S   M   L   V   T   L   G   G   A   D
GTC ACA AAT GTT CGC TGG ACT TAT GAT GAC AGC ATG CTG GTT ACC CTG GGA GGA GCA GAT
 M   S   L   M   V   W   T   N   E   V   E   S   H   R   E   K   K   Y   C   D
ATG TCC TTA ATG GTA TGG ACA AAT GAA GTG GAG AGC CAT CGA GAA AAG AAG TAC TGT GAC
 S   E   E   S   D   I   D   S   E   E   D   G   G   Y   D   S   D   V   T   R
AGT GAA GAG TCT GAT ATA GAT TCT GAA GAA GAT GGA GGC TAT GAC AGC GAT GTT ACA AGA
 E   N   E   I   S   Y   T   I   R   A   L   S   T   N   I   R   P   M   F   G
GAG AAT GAA ATT AGC TAT ACC ATC AGA GCC TTA TCA ACA AAT ATT CGC CCA ATG TTT GGA
 V   K   P   H   L   Q   Q   K   E   P   S   V   D   E   R   Q   G   V   V   R
GTC AAG CCT CAT TTG CAA CAG AAA GAG CCA TCA GTT GAT GAA AGA CAG GGG GTA GTA AGA
 G   S   R   P   P   V   S   R   A   P   P   Q   P   E   K   L   Q   S   N   N
GGA TCT AGG CCT CCA GTG AGT AGG GCC CCA CCA CAG CCA GAG AAA CTT CAG TCA AAC AAT
 V   G   K   K   K   R   P   I   E   D   L   V   L   E   L   A   F   G   Y   R
GTT GGC AAG AAG AAG AGA CCT ATA GAG GAC CTT GTG TTG GAG CTT GCT TTT GGC TAT CGG
 G   R   D   C   R   N   N   V   H   Y   L   N   D   G   D   D   I   I   Y   H
GGC AGA GAC TGC AGG AAC AAT GTG CAC TAT TTA AAT GAT GGT GAT GAT ATA ATT TAT CAC
 T   A   S   I   G   I   L   H   N   V   A   T   G   T   Q   S   F   Y   Q   E
ACT GCC TCT ATT GGA ATT CTA CAC AAT GTT GCC ACA GGG ACT CAG AGT TTT TAT CAA GAG
 H   N   D   D   I   L   C   L   T   V   N   Q   H   P   K   F   I   N   I   V
CAT AAT GAT GAT ATT TTG TGC CTC ACT GTA AAT CAG CAC CCC AAA TTT ATC AAC ATA GTG
 A   T   G   Q   V   G   D   S   A   D   M   S   A   T   A   P   S   V   H   I
GCA ACT GGC CAA GTA GGT GAT TCT GCA GAC ATG TCA GCT ACA GCC CCA TCT GTC CAC ATC
 W   D   A   V   N   K   Q   T   L   S   I   L   R   C   S   H   S   K   G   V
TGG GAT GCA GTG AAC AAG CAG ACG TTG TCT ATA CTA AGA TGC TCC CAC TCA AAG GGT GTG
 C   S   V   S   F   S   A   T   G   K   L   L   L   S   V   G   L   D   P   E
TGT TCT GTC AGC TTC AGT GCT ACT GGG AAG CTG CTG CTG TCT GTA GGG CTA GAC CCC GAG
 H   T   V   T   I   W   R   W   Q   E   G   A   K   I   A   S   R   G   G   H
CAC ACT GTA ACC ATT TGG AGA TGG CAG GAA GGG GCC AAA ATT GCC AGC AGA GGT GGG CAC
 N   Q   R   I   F   V   A   E   F   R   P   D   S   D   T   Q   F   V   S   V
AAC CAA CGT ATT TTT GTA GCA GAA TTT CGA CCA GAT TCA GAT ACC CAG TTT GTC TCT GTG
 G   I   K   H   V   K   F   W   T   L   A   G   R   A   L   L   S   K   K   G
GGT ATA AAG CAC GTG AAG TTC TGG ACC CTG GCA GGA AGG GCT CTT CTC AGC AAA AAG GGA
 L   L   S   S   L   E   D   A   R   M   Q   T   M   L   A   V   A   F   G   A
CTT CTG AGC AGC CTG GAG GAT GCC CGG ATG CAG ACG ATG CTT GCT GTT GCA TTT GGT GCA
 N   N   L   T   F   T   G   T   I   S   G   D   V   C   V   W   K   D   H   I
AAT AAC TTG ACG TTT ACA GGT ACC ATC AGT GGT GAT GTC TGT GTG TGG AAA GAT CAC ATA
 L   C   R   V   V   A   R   A   H   N   G   P   V   F   A   M   Y   T   T   L
TTG TGC AGA GTG GTG GCT AGA GCG CAC AAT GGG CCT GTG TTT GCC ATG TAC ACC ACC CTG
 R   D   G   L   I   V   T   G   G   K   E   R   P   S   K   E   G   G   A   V
CGA GAC GGA CTG ATT GTG ACC GGT GGC AAG GAA AGG CCG TCA AAG GAA GGA GGC GCA GTT
```

```
 K   L   W   D   Q   E   L   R   R   C   R   A   F   R   L   E   T   G   Q   V
AAA CTG TGG GAT CAG GAA CTG AGG CGA TGC CGG GCC TTC AGG CTT GAG ACA GGA CAA GTC
 T   D   C   V   R   S   V   C   R   G   K   G   K   I   L   V   G   T   R   N
ACA GAT TGT GTT CGG TCT GTG TGC AGA GGC AAA GGC AAG ATA CTA GTT GGG ACA AGG AAT
 S   E   I   I   E   V   G   E   K   N   A   A   C   N   I   L   V   N   G   H
TCG GAA ATA ATT GAA GTT GGA GAG AAA AAT GCA GCA TGT AAC ATT TTA GTT AAT GGC CAT
 V   D   G   P   I   W   G   L   A   T   H   P   S   R   D   F   F   L   S   A
GTG GAT GGG CCA ATC TGG GGA CTC GCA ACA CAT CCC TCC AGG GAC TTC TTC CTT TCT GCT
 A   E   D   G   T   V   R   L   W   D   I   A   D   K   K   M   L   N   K   V
GCT GAA GAT GGG ACA GTG AGA CTC TGG GAC ATT GCT GAT AAA AAG ATG CTA AAC AAA GTG
 N   L   G   H   A   A   R   T   V   C   Y   S   P   E   G   D   M   V   A   I
AAT TTG GGA CAC GCT GCT CGG ACA GTG TGT TAT AGC CCC GAA GGG GAC ATG GTG GCT ATT
 G   M   K   N   G   E   F   I   I   L   L   V   S   S   L   K   I   W   G   K
GGA ATG AAA AAT GGA GAA TTT ATT ATA TTA CTT GTG AGT TCT CTA AAA ATA TGG GGA AAG
 K   R   D   R   R   C   A   I   H   D   I   R   F   S   P   D   S   R   Y   L
AAG AGA GAC AGG CGA TGT GCA ATC CAT GAT ATC AGA TTT AGC CCA GAT TCC CGG TAT TTG
 A   V   G   S   S   E   N   S   V   D   F   Y   D   L   T   L   G   P   T   L
GCG GTG GGT TCC AGT GAG AAC TCA GTG GAC TTT TAT GAC CTG ACA CTG GGT CCC ACA CTT
 N   R   I   S   Y   C   K   D   I   P   S   F   V   I   Q   M   D   F   S   A
AAC AGA ATC AGC TAC TGC AAA GAC ATT CCA AGC TTT GTC ATT CAG ATG GAC TTC TCT GCA
 D   S   R   H   L   Q   V   S   S   G   C   Y   K   R   H   V   Y   E   V   P
GAT AGC AGA CAT CTC CAG GTT TCT AGT GGC TGC TAT AAA CGG CAT GTC TAT GAA GTG CCT
 S   G   K   H   L   V   D   H   A   A   I   D   R   I   T   W   A   T   W   T
TCA GGA AAA CAC CTT GTG GAT CAT GCT GCC ATT GAC AGG ATC ACG TGG GCT ACC TGG ACT
 S   I   L   G   D   E   V   M   G   I   W   S   R   H   A   E   K   A   D   V
AGT ATT CTA GGA GAT GAA GTT ATG GGA ATC TGG TCC AGA CAT GCT GAG AAG GCG GAT GTC
 T   C   A   C   V   S   H   S   G   I   S   L   V   T   G   D   D   F   G   M
ACC TGT GCC TGT GTG TCT CAC TCA GGA ATC AGC CTT GTG ACA GGA GAT GAC TTT GGC ATG
 V   K   L   Y   D   F   P   C   P   E   K   F   A   K   H   K   R   F   L   G
GTT AAA TTA TAT GAC TTT CCA TGC CCA GAA AAA TTT GCA AAG CAC AAG AGG TTC TTG GGT
 H   S   P   H   V   T   N   I   R   F   T   S   G   D   R   H   V   V   S   A
CAT TCC CCT CAT GTG ACA AAT ATT CGA TTT ACC AGT GGT GAT CGG CAT GTT GTC AGT GCT
 G   G   D   D   C   S   L   F   V   W   K   C   V   H   M   P   H   *
GGA GGC GAT GAC TGC AGT TTG TTT GTC TGG AAA TGT GTA CAC ATG CCT CAC TGA
```

GPCPD1 glycerophosphocholine phosphodiesterase GDE1 homolog (Saccharomyces cerevisiae) [Mus musculus]

GenBank: NP_001036136.1

http://www.uniprot.org/uniprot/Q8C0L9

```
CBM20   10          20          30          40          50          60
MTPSQVTFEI RGTLLPGEVF AICGSCDALG NWNPQNAVAL INENETGDSV LWKAVIALNR
        70          80          90          100         110         120
GVSVKYRYFR GCFLEPKTIG GPCQVIVHKW ETHLQPRSIT PLESEIIIDD GQFGIHNGVE
       130         140         150         160         170         180
TLDSGWLTCQ TEIRLRLHFS EKPPVSISKK KFKKSRFRVK LTLEGLEEDE DDDDDKVSPT
       190         200         210         220         230         240
VLHKMSNSLE ISLISDNEFK CRHSQPECGY GLQPDRWTEY SIQTMEPDNL ELIFDFFEED
       250         260         270         280         290         300
LSEHVVQGDV LPGHVGTACL LSSTIAESGR SAGILTLPIM SRNSRKTIGK VRVDFIIIKP
       310         320         330  GDPD   340         350         360
LPGYSCSMQS SFSKYWKPRI PLDVGHRGAG NSTTTAKLAK VQENTIASLR NAASHGAAFV
       370         380         390         400         410         420
EFDVHLSKDF VPVVYHDLTC CLTMKRKYEA DPVELFEIPV KELTFDQLQL LKLSHVTALK
       430         440         450         460         470         480
TKDRKQSLYE EENFFSENQP FPSLKMVLES LPENVGFNIE IKWICQHRDG VWDGNLSTYF
       490         500         510         520         530         540
DMNVFLDIIL KTVLENSGKR RIVFSSFDAD ICTMVRQKQN KYPILFLTQG KSDIYPELMD
       550         560         570         580         590         600
LRSRTTPIAM SFAQFENILG INAHTEDLLR NPSYVQEAKA KGLVIFCWGD DTNDPENRRK
```

```
        610         620         630         640         650         660
LKEFGVNGLI YDRIYDWMPE QPNIFQVEQL ERLKQELPEL KNCLCPTVSH FIPSSFCVEP
        670
DIHVDANGID SVENA
```

```
 M   T   P   S   Q   V   T   F   E   I   R   G   T   L   L   P   G   E   V   F
ATG ACA CCT TCT CAG GTC ACT TTT GAA ATA AGA GGA ACT CTT TTA CCA GGA GAG GTC TTT
 A   I   C   G   S   C   D   A   L   G   N   W   N   P   Q   N   A   V   A   L
GCA ATA TGT GGA AGC TGT GAT GCC CTG GGA AAC TGG AAT CCT CAA AAT GCT GTG GCT CTT
 I   N   E   N   E   T   G   D   S   V   L   W   K   A   V   I   A   L   N   R
ATT AAT GAA AAC GAG ACA GGA GAC AGT GTG TTG TGG AAA GCA GTG ATT GCT CTC AAT AGA
 G   V   S   V   K   Y   R   Y   F   R   G   C   F   L   E   P   K   T   I   G
GGA GTG TCA GTG AAG TAC CGC TAC TTC AGA GGC TGC TTT TTA GAA CCA AAG ACT ATC GGT
 G   P   C   Q   V   I   V   H   K   W   E   T   H   L   Q   P   R   S   I   T
GGT CCA TGT CAA GTC ATA GTT CAC AAG TGG GAG ACT CAT CTA CAA CCA CGA TCA ATA ACC
 P   L   E   S   E   I   I   I   D   D   G   Q   F   G   I   H   N   G   V   E
CCT TTA GAA AGT GAA ATC ATT ATT GAC GAT GGA CAG TTT GGC ATC CAC AAT GGT GTT GAA
 T   L   D   S   G   W   L   T   C   Q   T   E   I   R   L   R   L   H   F   S
ACA CTG GAT TCT GGA TGG CTT ACA TGT CAG ACT GAA ATA AGA TTG CGT CTG CAT TTT TCT
 E   K   P   P   V   S   I   S   K   K   K   F   K   K   S   R   F   R   V   K
GAG AAA CCT CCT GTT TCA ATT AGC AAG AAA AAG TTC AAA AAA TCG AGA TTT AGG GTA AAG
 L   T   L   E   G   L   E   E   D   E   D   D   D   D   D   K   V   S   P   T
CTC ACA CTC GAG GGT CTG GAG GAA GAT GAA GAT GAT GAT GAC GAT AAG GTC TCT CCC ACT
 V   L   H   K   M   S   N   S   L   E   I   S   L   I   S   D   N   E   F   K
GTT CTT CAC AAA ATG TCC AAC AGC CTG GAG ATA TCC TTA ATA AGT GAC AAT GAG TTC AAG
 C   R   H   S   Q   P   E   C   G   Y   G   L   Q   P   D   R   W   T   E   Y
TGC AGG CAC TCA CAG CCA GAA TGT GGG TAT GGC TTA CAG CCC GAT CGT TGG ACA GAG TAC
 S   I   Q   T   M   E   P   D   N   L   E   L   I   F   D   F   F   E   E   D
AGC ATA CAG ACA ATG GAA CCA GAT AAT CTG GAG CTC ATC TTT GAC TTT TTT GAG GAA GAT
 L   S   E   H   V   V   Q   G   D   V   L   P   G   H   V   G   T   A   C   L
CTC AGT GAG CAT GTA GTT CAG GGT GAT GTT CTT CCT GGA CAC GTG GGC ACA GCA TGC CTC
 L   S   S   T   I   A   E   S   G   R   S   A   G   I   L   T   L   P   I   M
CTG TCT TCT ACC ATT GCT GAG AGT GGA AGA AGC GCT GGA ATC CTT ACT CTT CCC ATC ATG
 S   R   N   S   R   K   T   I   G   K   V   R   V   D   F   I   I   I   K   P
AGC AGA AAT TCC AGA AAA ACT ATA GGC AAA GTC AGA GTT GAT TTT ATC ATC ATC AAG CCA
 L   P   G   Y   S   C   S   M   Q   S   S   F   S   K   Y   W   K   P   R   I
TTA CCT GGA TAT AGT TGT TCT ATG CAG TCT TCA TTT TCC AAG TAT TGG AAA CCA AGA ATA
 P   L   D   V   G   H   R   G   A   G   N   S   T   T   T   A   K   L   A   K
CCA TTG GAC GTT GGA CAT CGT GGT GCA GGG AAC TCA ACA ACG ACT GCC AAG CTA GCT AAA
 V   Q   E   N   T   I   A   S   L   R   N   A   A   S   H   G   A   A   F   V
GTA CAG GAA AAT ACT ATC GCT TCT TTA AGA AAT GCT GCC AGT CAT GGC GCA GCA TTT GTA
 E   F   D   V   H   L   S   K   D   F   V   P   V   V   Y   H   D   L   T   C
GAA TTT GAT GTC CAC CTT TCA AAG GAC TTT GTG CCC GTG GTG TAT CAT GAC CTC ACC TGC
 C   L   T   M   K   R   K   Y   E   A   D   P   V   E   L   F   E   I   P   V
TGT CTG ACC ATG AAG AGG AAA TAT GAA GCT GAT CCA GTT GAA TTG TTT GAA ATC CCA GTA
 K   E   L   T   F   D   Q   L   Q   L   L   K   L   S   H   V   T   A   L   K
AAA GAA TTA ACA TTT GAC CAA CTC CAG TTA TTG AAG CTT TCT CAT GTG ACT GCA TTA AAA
 T   K   D   R   K   Q   S   L   Y   E   E   E   N   F   F   S   E   N   Q   P
ACC AAA GAC CGG AAA CAA TCT TTG TAT GAG GAG GAA AAT TTC TTT TCT GAA AAT CAG CCA
 F   P   S   L   K   M   V   L   E   S   L   P   E   N   V   G   F   N   I   E
TTT CCT TCT CTT AAG ATG GTT TTA GAA TCA TTG CCA GAA AAT GTA GGA TTT AAT ATA GAA
 I   K   W   I   C   Q   H   R   D   G   V   W   D   G   N   L   S   T   Y   F
ATA AAA TGG ATT TGC CAA CAC AGG GAT GGA GTA TGG GAT GGC AAC TTA TCA ACA TAT TTT
 D   M   N   V   F   L   D   I   I   L   K   T   V   L   E   N   S   G   K   R
GAT ATG AAT GTG TTT TTG GAT ATA ATT TTA AAA ACT GTT TTA GAA AAT TCT GGG AAG AGG
 R   I   V   F   S   S   F   D   A   D   I   C   T   M   V   R   Q   K   Q   N
AGA ATA GTG TTT TCT TCT TTT GAT GCA GAT ATT TGT ACA ATG GTT CGG CAG AAG CAG AAC
 K   Y   P   I   L   F   L   T   Q   G   K   S   D   I   Y   P   E   L   M   D
AAA TAT CCC ATA TTA TTT TTG ACC CAA GGA AAG TCT GAT ATT TAC CCC GAA CTC ATG GAC
 L   R   S   R   T   T   P   I   A   M   S   F   A   Q   F   E   N   I   L   G
CTC AGA TCT CGG ACA ACA CCC ATT GCA ATG AGT TTT GCA CAG TTT GAA AAT ATT TTG GGG
 I   N   A   H   T   E   D   L   L   R   N   P   S   Y   V   Q   E   A   K   A
ATA AAT GCC CAT ACT GAA GAC CTC CTT AGA AAC CCA TCC TAT GTC CAA GAG GCA AAA GCT
 K   G   L   V   I   F   C   W   G   D   D   T   N   D   P   E   N   R   R   K
AAG GGA TTG GTC ATA TTC TGC TGG GGT GAT GAT ACC AAC GAT CCT GAA AAC AGA AGG AAA
 L   K   E   F   G   V   N   G   L   I   Y   D   R   I   Y   D   W   M   P   E
CTG AAG GAA TTT GGA GTA AAT GGT CTA ATA TAT GAT AGG ATA TAT GAT TGG ATG CCT GAA
```

```
 Q   P   N   I   F   Q   V   E   Q   L   E   R   L   K   Q   E   L   P   E   L
CAG CCA AAT ATA TTC CAA GTG GAG CAG TTG GAG CGC CTG AAG CAA GAA TTG CCA GAG CTT
 K   N   C   L   C   P   T   V   S   H   F   I   P   S   S   F   C   V   E   P
AAG AAC TGT TTG TGT CCC ACT GTT AGC CAC TTC ATC CCT TCT TCT TTC TGT GTG GAG CCT
 D   I   H   V   D   A   N   G   I   D   S   V   E   N   A   *
GAT ATC CAC GTG GAT GCC AAC GGC ATT GAT AGT GTG GAG AAC GCT TAG
```

NCAN neurocan [Mus musculus]

GenBank: AAH65118.1

http://www.uniprot.org/uniprot/P55066

```
        10          20          30          40 Ig-like 50          60
MGAGSVWASG LLLLWLLLLV AGDQDTQDTT ATEKGLRMLK SGSGPVRAAL AELVALPCFF
        70          80          90         100         110         120
TLQPRLSSLR DIPRIKWTKV QTASGQRQDL PILVAKDNVV RVAKGWQGRV SLPAYPRHRA
       130         140         150         160 Link1  170         180
NATLLLGPLR ASDSGLYRCQ VVKGIEDEQD LVTLEVTGVV FHYRAARDRY ALTFAEAQEA
       190         200         210         220         230         240
CRLSSATIAA PRHLQAAFED GFDNCDAGWL SDRTVRYPIT QSRPGCYGDR SSLPGVRSYG
       250         260 Link2  270         280         290         300
RRDPQELYDV YCFARELGGE VFYVGPARRL TLAGARAQCQ RQGAALASVG QLHLAWHEGL
       310         320         330         340         350         360
DQCDPGWLAD GSVRYPIQTP RRRCGGPAPG VRTVYRFANR TGFPAPGARF DAYCFRAHHH
       370         380         390         400         410         420
TAQHGDSEIP SSGDEGEIVS AEGPPGRELK PSLGEQEVIA PDFQEPLMSS GEGEPPDLTW
       430         440         450         460         470         480
TQAPEETLGS TPGGPTLASW PSSEKWLFTG APSSMGVSSP SDMGVDMEAT TPLGTQVAPT
       490         500         510         520         530         540
PTMRRGRFKG LNGRHFQQQG PEDQLPEVAE PSAQPPTLGA TANHMRPSAA TEASESDQSH
       550         560         570         580         590         600
SPWAILTNEV DEPGAGSLGS RSLPESLMWS PSLISPSVPS TESTPSPKPG AAEAPSVKSA
       610         620         630         640         650         660
IPHLPRLPSE PPAPSPGPSE ALSAVSLQAS SADGSPDFPI VAMLRAPKLW LLPRSTLVPN
       670         680         690         700         710         720
MTPVPLSPAS PLPSWVPEEQ AVRPVSLGAE DLETPFQTTI AAPVEASHRS PDADSIEIEG
       730         740         750         760         770         780
TSSMRATKHP ISGPWASLDS SNVTMNPVPS DAGILGTESG VLDLPGSPTS GGQATVEKVL
       790         800         810         820         830         840
ATWLPLPGQG LDPGSQSTPM EAHGVAVSME PTVALEGGAT EGPMEATREV VPSTADATWE
       850         860         870         880         890         900
SESRSAISST HIAVTMARAQ GMPTLTSTSS EGHPEPKGQM VAQESLEPLN TLPSHPWSSL
       910         920         930         940         950         960
VVPMDEVASV SSGEPTGLWD IPSTLIPVSL GLDESVLNVV AESPSVEGFW EEVASGQEDP
EGF11  970         980         990        1000 EGF12 1010        1020
TDPCENNPCL HGGTCHTNGT VYGCSCDQGY AGENCEIDID DCLCSPCENG GTCIDEVNGF
      1030        1040 CtypL 1050        1060        1070        1080
ICLCLPSYGG SLCEKDTEGC DRGWHKFQGH CYRYFAHRRA WEDAERDCRR RAGHLTSVHS
      1090        1100        1110        1120        1130        1140
PEEHKFINSF GHENSWIGLN DRTVERDFQW TDNTGLQYEN WREKQPDNFF AGGEDCVVMV
      1150        1160        1170 Sushi 1180        1190        1200
AHESGRWNDV PCNYNLPYVC KKGTVLCGPP PAVENASLVG VRKIKYNVHA TVRYQCDEGF
      1210        1220        1230        1240        1250        1260
SQHRVATIRC RNNGKWDRPQ IMCIKPRRSH RMRRHHHHPH RHHKPRKEHR KHKRHPAEDW

EKDEGDFC
```

```
 M   G   A   G   S   V   W   A   S   G   L   L   L   L   W   L   L   L   L   V
ATG GGG GCC GGA TCT GTG TGG GCC TCA GGC CTC CTG CTG CTG TGG CTG CTT CTC CTA GTG
 A   G   D   Q   D   T   Q   D   T   T   A   T   E   K   G   L   R   M   L   K
GCT GGG GAT CAG GAC ACA CAG GAC ACC ACC GCC ACG GAA AAG GGG CTT CGC ATG CTG AAG
 S   G   S   G   P   V   R   A   A   L   A   E   L   V   A   L   P   C   F   F
TCA GGG TCA GGA CCC GTC CGT GCT GCC CTG GCA GAG CTA GTG GCC CTG CCC TGC TTC TTT
 T   L   Q   P   R   L   S   S   L   R   D   I   P   R   I   K   W   T   K   V
ACC CTG CAA CCA CGG CTA AGC TCC CTG CGA GAC ATT CCT CGG ATC AAG TGG ACT AAG GTT
 Q   T   A   S   G   Q   R   Q   D   L   P   I   L   V   A   K   D   N   V   V
CAG ACT GCA TCA GGC CAG CGA CAG GAT TTG CCA ATC TTG GTG GCC AAA GAC AAC GTG GTG
 R   V   A   K   G   W   Q   G   R   V   S   L   P   A   Y   P   R   H   R   A
CGT GTG GCC AAG GGC TGG CAG GGA CGG GTG TCA TTG CCT GCT TAT CCC CGG CAC AGA GCC
 N   A   T   L   L   L   G   P   L   R   A   S   D   S   G   L   Y   R   C   Q
AAT GCT ACC CTT CTG CTG GGG CCA CTT CGA GCA AGC GAC TCT GGG CTG TAT CGC TGC CAA
 V   V   K   G   I   E   D   E   Q   D   L   V   T   L   E   V   T   G   V   V
GTG GTA AAG GGT ATC GAA GAT GAG CAG GAC CTG GTA ACC CTG GAA GTG ACA GGC GTC GTG
 F   H   Y   R   A   A   R   D   R   Y   A   L   T   F   A   E   A   Q   E   A
TTC CAT TAT CGG GCG GCC CGG GAC CGC TAT GCG CTG ACC TTC GCT GAG GCC CAG GAG GCT
 C   R   L   S   S   A   T   I   A   A   P   R   H   L   Q   A   A   F   E   D
TGT CGC CTA AGC TCT GCT ACC ATC GCT GCC CCA CGG CAC CTG CAG GCT GCC TTT GAA GAT
 G   F   D   N   C   D   A   G   W   L   S   D   R   T   V   R   Y   P   I   T
GGC TTT GAC AAC TGC GAC GCG GGC TGG CTC TCA GAC CGC ACG GTT CGG TAC CCG ATC ACT
 Q   S   R   P   G   C   Y   G   D   R   S   S   L   P   G   V   R   S   Y   G
CAG TCG CGT CCT GGT TGC TAT GGT GAC CGC AGC AGT CTC CCG GGT GTT CGG AGC TAC GGG
 R   R   D   P   Q   E   L   Y   D   V   Y   C   F   A   R   E   L   G   G   E
AGA CGC GAC CCG CAG GAA CTC TAC GAT GTC TAC TGC TTT GCC CGC GAG CTA GGG GGT GAA
 V   F   Y   V   G   P   A   R   R   L   T   L   A   G   A   R   A   Q   C   Q
GTC TTT TAC GTG GGC CCG GCC CGC CGA CTG ACC CTG GCG GGC GCG CGG GCA CAA TGT CAG
 R   Q   G   A   A   L   A   S   V   G   Q   L   H   L   A   W   H   E   G   L
CGG CAG GGT GCA GCG CTG GCC TCG GTG GGG CAG TTG CAC CTG GCC TGG CAC GAG GGC CTG
 D   Q   C   D   P   G   W   L   A   D   G   S   V   R   Y   P   I   Q   T   P
GAC CAG TGC GAC CCG GGC TGG CTG GCA GAC GGC AGC GTG CGC TAC CCC ATC CAG ACT CCG
 R   R   R   C   G   G   P   A   P   G   V   R   T   V   Y   R   F   A   N   R
CGC CGG CGT TGC GGG GGC CCC GCC CCA GGT GTG CGC ACT GTG TAC CGC TTC GCC AAC CGC
 T   G   F   P   A   P   G   A   R   F   D   A   Y   C   F   R   A   H   H   H
ACC GGC TTT CCT GCG CCA GGA GCA CGC TTC GAC GCC TAC TGC TTC CGA GCT CAT CAC CAT
 T   A   Q   H   G   D   S   E   I   P   S   S   G   D   E   G   E   I   V   S
ACA GCA CAA CAT GGA GAT TCT GAG ATC CCC TCA TCT GGA GAT GAG GGG GAG ATT GTG TCA
 A   E   G   P   P   G   R   E   L   K   P   S   L   G   E   Q   E   V   I   A
GCA GAG GGG CCT CCA GGC CGA GAA CTA AAG CCC AGC TTG GGG GAA CAG GAG GTG ATA GCA
 P   D   F   Q   E   P   L   M   S   S   G   E   G   E   P   P   D   L   T   W
CCT GAC TTC CAG GAA CCT CTC ATG TCC AGT GGA GAA GGC GAA CCC CCA GAC TTG ACT TGG
 T   Q   A   P   E   E   T   L   G   S   T   P   G   G   P   T   L   A   S   W
ACA CAA GCA CCT GAG GAG ACC CTT GGT TCT ACT CCA GGG GGT CCC ACG CTG GCC TCA TGG
 P   S   S   E   K   W   L   F   T   G   A   P   S   S   M   G   V   S   S   P
CCC TCT TCA GAA AAG TGG CTC TTT ACG GGT GCC CCA AGC TCC ATG GGT GTC TCC AGT CCC
 S   D   M   G   V   D   M   E   A   T   T   P   L   G   T   Q   V   A   P   T
AGC GAC ATG GGA GTA GAT ATG GAA GCG ACA ACA CCC TTG GGC ACA CAG GTA GCA CCC ACC
 P   T   M   R   R   G   R   F   K   G   L   N   G   R   H   F   Q   Q   Q   G
CCC ACG ATG AGG AGG GGC CGC TTT AAA GGG TTG AAT GGT CGA CAC TTC CAG CAG CAG GGC
 P   E   D   Q   L   P   E   V   A   E   P   S   A   Q   P   P   T   L   G   A
CCA GAA GAC CAG CTG CCT GAG GTA GCA GAG CCC AGT GCC CAG CCT CCC ACC CTG GGA GCT
 T   A   N   H   M   R   P   S   A   A   T   E   A   S   E   S   D   Q   S   H
ACT GCC AAC CAC ATG AGG CCT TCT GCA GCC ACA GAG GCT TCA GAG AGT GAC CAG AGC CAC
 S   P   W   A   I   L   T   N   E   V   D   E   P   G   A   G   S   L   G   S
AGT CCT TGG GCC ATT CTG ACC AAC GAA GTG GAT GAG CCA GGA GCA GGC TCT CTT GGC AGC
 R   S   L   P   E   S   L   M   W   S   P   S   L   I   S   P   S   V   P   S
AGG AGT CTC CCA GAG TCC CTG ATG TGG TCC CCG TCG TTG ATC TCA CCC AGT GTC CCA AGC
 T   D   S   T   P   S   A   K   P   G   A   A   E   A   P   S   V   K   S   A
ACC GAC AGT ACT CCT AGC GCG AAG CCA GGG GCA GCC GAG GCA CCC AGT GTG AAG TCA GCC
 I   P   H   L   P   R   L   P   S   E   P   P   A   P   S   P   G   P   S   E
ATC CCC CAC CTG CCC CGG CTG CCC TCA GAG CCC CCT GCT CCC TCT CCC GGG CCC TCA GAG
 A   L   S   A   V   S   L   Q   A   S   S   A   D   G   S   P   D   F   P   I
GCC CTA AGT GCT GTC TCC CTC CAG GCA TCC TCT GCT GAT GGC TCC CCT GAC TTC CCC ATT
 V   A   M   L   R   A   P   K   L   W   L   L   P   R   S   T   L   V   P   N
GTA GCC ATG CTT CGA GCC CCC AAA CTG TGG CTT CTG CCA CGC TCT ACA CTT GTC CCC AAT
 M   T   P   V   P   L   S   P   A   S   P   L   P   S   W   V   P   E   E   Q
ATG ACC CCA GTC CCA CTG TCC CCA GCT TCT CCA CTT CCC TCC TGG GTC CCA GAA GAA CAG
 A   V   R   P   V   S   L   G   A   E   D   L   E   T   P   F   Q   T   T   I
GCT GTC AGG CCT GTC AGC CTT GGA GCG GAA GAC CTC GAA ACC CCA TTT CAG ACC ACC ATA
```

```
 A   A   P   V   E   A   S   H   R   S   P   D   A   D   S   I   E   I   E   G
GCT GCC CCA GTT GAA GCC AGC CAC AGA TCC CCT GAT GCA GAT TCT ATA GAA ATC GAG GGG
 T   S   S   M   R   A   T   K   H   P   I   S   G   P   W   A   S   L   D   S
ACC AGC TCC ATG CGG GCT ACA AAG CAC CCC ATC TCT GGC CCA TGG GCT TCT TTG GAC TCT
 S   N   V   T   M   N   P   V   P   S   D   A   G   I   L   G   T   E   S   G
AGT AAT GTG ACG ATG AAT CCT GTC CCT TCT GAT GCT GGC ATC CTA GGG ACT GAG TCT GGG
 V   L   D   L   P   G   S   P   T   S   G   G   Q   A   T   V   E   K   V   L
GTC TTG GAC TTA CCA GGG AGT CCC ACA TCA GGC GGA CAG GCC ACT GTG GAG AAG GTG CTG
 A   T   W   L   P   L   P   G   Q   G   L   D   P   G   S   Q   S   T   P   M
GCC ACC TGG CTA CCA CTG CCT GGC CAA GGA CTA GAC CCT GGC TCC CAG TCC ACA CCC ATG
 E   A   H   G   V   A   V   S   M   E   P   T   V   A   L   E   G   G   A   T
GAA GCC CAT GGG GTT GCC GTG AGC ATG GAA CCT ACA GTG GCT TTG GAG GGA GGT GCC ACC
 E   G   P   M   E   A   T   R   E   V   V   P   S   T   A   D   A   T   W   E
GAG GGC CCT ATG GAG GCC ACC AGG GAG GTG GTC CCC AGC ACT GCT GAT GCC ACT TGG GAG
 S   E   S   R   S   A   I   S   S   T   H   I   A   V   T   M   A   R   A   Q
TCT GAA TCC AGA AGT GCC ATT TCT AGC ACC CAC ATA GCT GTG ACC ATG GCT AGG GCT CAG
 G   M   P   T   L   T   S   T   S   S   E   G   H   P   E   P   K   G   Q   M
GGC ATG CCC ACA CTG ACC TCT ACA AGC TCC GAA GGC CAC CCA GAG CCT AAG GGC CAG ATG
 V   A   Q   E   S   L   E   P   L   N   T   L   P   S   H   P   W   S   S   L
GTG GCC CAG GAG TCA CTG GAG CCT CTC AAC ACT CTG CCT TCG CAC CCC TGG TCA TCC CTG
 V   V   P   M   D   E   V   A   S   V   S   S   G   E   P   T   G   L   W   D
GTG GTC CCC ATG GAT GAA GTG GCC TCA GTT TCC TCA GGG GAA CCC ACA GGA CTG TGG GAC
 I   P   S   T   L   I   P   V   S   L   G   L   D   E   S   D   L   N   V   V
ATA CCC AGC ACT CTG ATA CCT GTA TCC TTG GGC TTG GAT GAA TCA GAC CTG AAT GTT GTG
 A   E   S   P   S   V   K   G   F   W   E   E   V   A   S   G   Q   E   D   P
GCT GAG AGT CCA AGC GTG AAG GGC TTC TGG GAA GAG GTG GCC AGC GGG CAG GAA GAT CCC
 T   D   P   C   E   N   N   P   C   L   H   G   G   T   C   H   T   N   G   T
ACA GAT CCC TGC GAG AAC AAC CCC TGC CTG CAT GGG GGC ACC TGC CAC ACC AAC GGC ACC
 V   Y   G   C   S   C   D   Q   G   Y   A   G   E   N   C   E   I   D   I   D
GTG TAT GGC TGT AGT TGT GAC CAG GGC TAT GCT GGG GAG AAT TGT GAA ATT GAC ATT GAT
 D   C   L   C   S   P   C   E   N   G   G   T   C   I   D   E   V   N   G   F
GAC TGC TTA TGC AGC CCT TGC GAG AAT GGG GGC ACC TGC ATC GAC GAG GTG AAT GGT TTC
 I   C   L   C   L   P   S   Y   G   G   S   L   C   E   K   D   T   E   G   C
ATC TGC CTC TGC CTC CCC AGC TAT GGG GGC AGC CTG TGT GAG AAG GAC ACA GAA GGC TGC
 D   R   G   W   H   K   F   Q   G   H   C   Y   R   Y   F   A   H   R   R   A
GAC CGT GGC TGG CAC AAA TTC CAG GGA CAC TGC TAC CGG TAC TTT GCC CAT CGC CGG GCC
 W   E   D   A   E   R   D   C   R   R   R   A   G   H   L   T   S   V   H   S
TGG GAG GAT GCA GAG AGA GAT TGC AGG CGC CGA GCT GGT CAC CTG ACA AGC GTC CAT TCG
 P   E   E   H   K   F   I   N   S   F   G   H   E   N   S   W   I   G   L   N
CCA GAA GAG CAC AAG TTC ATT AAC AGT TTT GGA CAT GAG AAT TCG TGG ATC GGC CTG AAT
 D   R   T   V   E   R   D   F   Q   W   T   D   N   T   G   L   Q   Y   E   N
GAC CGG ACA GTA GAG AGG GAC TTC CAG TGG ACA GAC AAC ACA GGA CTG CAA TAT GAG AAC
 W   R   E   K   Q   P   D   N   F   F   A   G   G   E   D   C   V   V   M   V
TGG AGG GAG AAG CAG CCG GAT AAT TTC TTC GCA GGT GGG GAG GAT TGT GTG GTG ATG GTG
 A   H   E   S   G   R   W   N   D   V   P   C   N   Y   N   L   P   Y   V   C
GCA CAT GAG AGT GGG CGC TGG AAT GAT GTC CCC TGC AAC TAC AAC CTA CCC TAT GTC TGC
 K   K   G   T   V   L   C   G   P   P   P   A   V   E   N   A   S   L   V   G
AAG AAG GGT ACA GTG CTG TGT GGT CCC CCT CCA GCA GTG GAG AAT GCC TCT CTT GTT GGT
 V   R   K   I   K   Y   N   V   H   A   T   V   R   Y   Q   C   D   E   G   F
GTG CGC AAG ATC AAG TAC AAT GTC CAT GCC ACT GTG CGA TAC CAG TGT GAT GAA GGA TTC
 S   Q   H   R   V   A   T   I   R   C   R   N   N   G   K   W   D   R   P   Q
TCC CAG CAC CGA GTG GCC ACT ATC CGC TGC CGT AAC AAT GGG AAG TGG GAC CGG CCT CAG
 I   M   C   I   K   P   R   R   S   H   R   M   R   R   H   H   H   H   P   H
ATC ATG TGC ATC AAA CCC AGG CGG TCA CAT CGG ATG CGT AGA CAC CAC CAC CAT CCA CAC
 R   H   H   K   P   R   K   E   H   R   K   H   K   R   H   P   A   E   D   W
CGA CAT CAC AAG CCT CGC AAG GAG CAC AGA AAA CAC AAG AGA CAC CCA GCG GAA GAC TGG
 E   K   D   E   G   D   F   C   *
GAG AAA GAC GAA GGG GAT TTC TGC TAA
```

5.9 Mass Spectrometry of the Protein Sequences His_6-$DMXL2_{748-926}$-V5, His_6-$EML5_{897-1038}$-V5, His_6-$GPCPD1_{1-118}$-V5 and His_6-$NCAN_{156-359}$-V5

Protein sequences were entered at http://web.expasy.org/peptide_mass. All samples were digested using trypsin setting the maximum number of missed cleavages to 1. Cysteins have been treated with iodoacetamide to form carbamidomethyl-cysteine. Methionines have not been oxidized. Only peptides

with a mass bigger than 0.5 kDa were displayed using monoisotopic masses of the occurring amino acid residues and giving peptide masses as $[M+H]^+$. Data output was compared to mass spectrum provided by Reinhard Mentele (Section 2.6.3, p. 44). Yellow: Sequence yielding peak in mass spectrum.

His_6-$DMXL2_{748-926}$-V5

```
        10         20         30         40         50         60         70
MRGSHHHHHH GSNSLHTSAF SNVAWLPTLI PSYCLGTYCN SASACFVASD GKNLRLYQAV VDARKLLDEL
        80         90        100        110        120        130        140
SDPEASKLIG EVFNIVSQQS TARPGCIIEL DAITDQCGSN TQLLHVFQED FIIGYKPHKE DMEKKEKESE
       150        160        170        180        190        200
IFFQPSQGYR PPPFSEKFFL VVIEKDGNNN SILHMWHLHL KSVQACLAKA AGKPIPNPLL GLDST
```

mass	position	#MC	artif.modification(s)		peptide sequence
7083.5757	66-129	1	Cys_CAM: 96, 107	7197.6186	LLDELSDPEASKLIGEVFNIVSQQSTARPGCIIELDAITDQCGSNTQLLHVFQEDFIIGYKPHK
6418.1831	78-134	1	Cys_CAM: 96, 107	6532.2261	LIGEVFNIVSQQSTARPGCIIELDAITDQCGSNTQLLHVFQEDFIIGYKPHKEDMEK
5785.9356	78-129	0	Cys_CAM: 96, 107	5899.9785	LIGEVFNIVSQQSTARPGCIIELDAITDQCGSNTQLLHVFQEDFIIGYKPHK
5689.6447	3-55	1	Cys_CAM: 34, 39, 45	5860.7091	GSHHHHHHGSNSLHTSAFSNVAWLPTLIPSYCLGTYCNSASACFVASDGKNLR
5593.5582	1-52	1	Cys_CAM: 34, 39, 45	5764.6226	MRGSHHHHHHGSNSLHTSAFSNVAWLPTLIPSYCLGTYCNSASACFVASDGK
5306.4166	3-52	0	Cys_CAM: 34, 39, 45	5477.4810	GSHHHHHHGSNSLHTSAFSNVAWLPTLIPSYCLGTYCNSASACFVASDGK
3345.7193	138-165	1			ESEIFFQPSQGYRPPPFSEKFFLVVIEK
2904.5341	158-181	1			FFLVVIEKDGNNNSILHMWHLHLK
2729.3762	166-189	1	Cys_CAM: 186	2786.3977	DGNNNSILHMWHLHLKSVQACLAK
2627.2776	136-157	1			EKESEIFFQPSQGYRPPPFSEK
2370.1400	138-157	0			ESEIFFQPSQGYRPPPFSEK
2364.2955	182-205	1	Cys_CAM: 186	2421.3169	SVQACLAKAAGKPIPNPLLGLDST
1928.9548	166-181	0			DGNNNSILHMWHLHLK
1563.8740	190-205	0			AAGKPIPNPLLGLDST
1444.7529	65-77	1			KLLDELSDPEASK
1417.7910	53-64	1			NLRLYQAVVDAR
1316.6580	66-77	0			LLDELSDPEASK
1162.6578	56-65	1			LYQAVVDARK
1034.5629	56-64	0			LYQAVVDAR
994.5971	158-165	0			FFLVVIEK
819.4393	182-189	0	Cys_CAM: 186	876.4607	SVQACLAK
779.3604	130-135	1			EDMEKK
651.2654	130-134	0			EDMEK

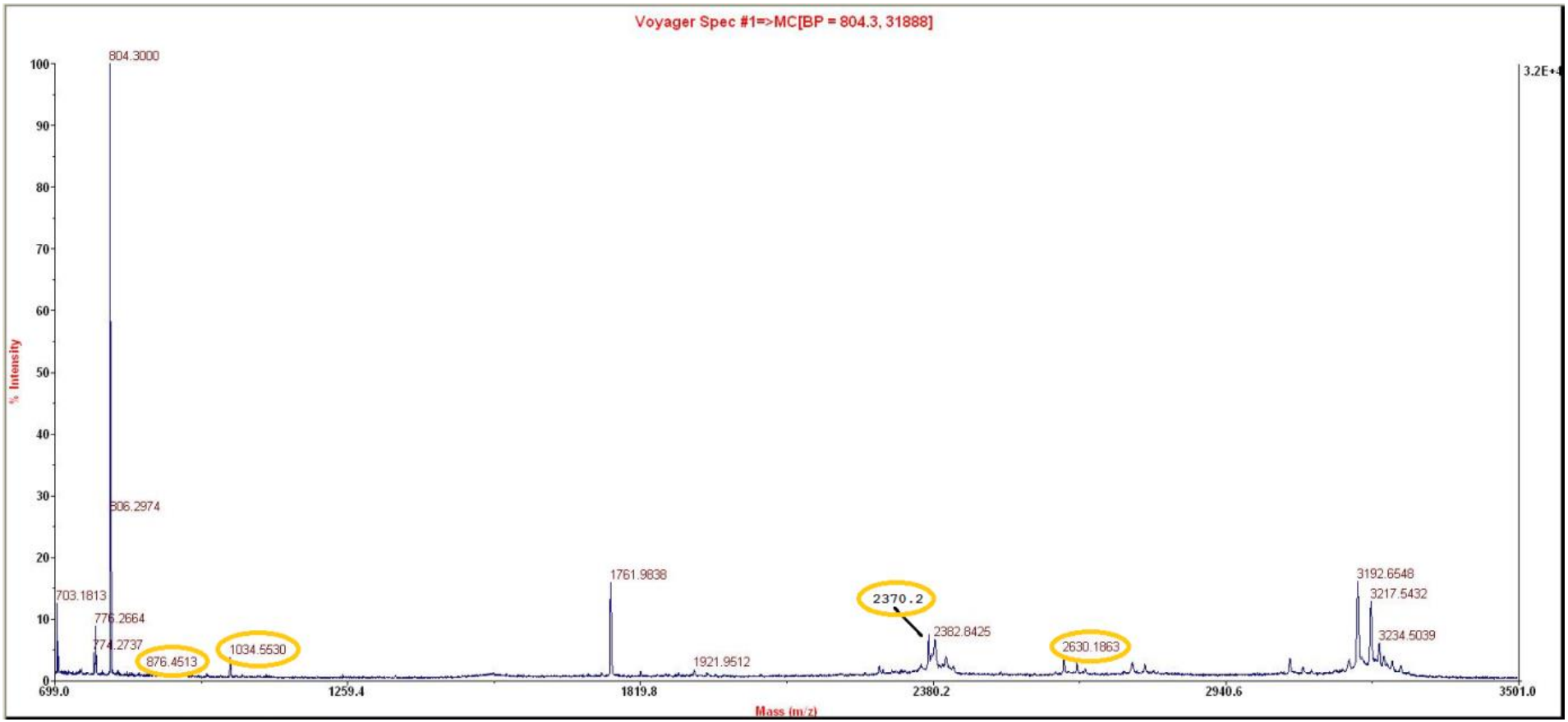
Voyager Spec #1=>MC[BP = 804.3, 31888]
804.3000
806.2974
703.1813
776.2664
774.2737
876.4513
1034.5530
1761.9838
1921.9512
2370.2
2382.8425
2630.1863
3192.6548
3217.5432
3234.5039
% Intensity
Mass (m/z)
699.0
1259.4
1819.8
2380.2
2940.6
3501.0

His_6-$EML5_{897-1038}$-V5

```
         10         20         30         40         50         60         70
MRGSHHHHHH GSKTVKAHDG PVFSMHALEK GFVTGGKDGM VALWDDSFER CLKTYAIKRA DLAPGSKGLL
         80         90        100        110        120        130        140
LEDNPSIRAI SLGHGHILVG TKNGEILEVD KSGPITLLVQ GHMEGEVWGL ATHPYLPICA TVSDDKTLRI
        150        160
WDLSPSHCML AVRKGKPIPN PLLGLDST
```

mass	position	#MC	artif.modification(s)		peptide sequence
4732.3636	93-136	1	Cys_CAM: 129	4789.3851	NGEILEVDKSGPITLLVQGH MEGEVWGLATHPYLPICATV SDDK
4105.0884	102-139	1	Cys_CAM: 129	4162.1099	SGPITLLVQGHMEGEVWGLA THPYLPICATVSDDKTLR
3734.8556	102-136	0	Cys_CAM: 129	3791.8771	SGPITLLVQGHMEGEVWGLA THPYLPICATVSDDK
2610.4725	68-92	1			GLLLEDNPSIRAISLGHGHI LVGTK
2400.3245	79-101	1			AISLGHGHILVGTKNGEILE VDK
2187.0175	31-50	1			GFVTGGKDGMVALWDDSFER
2185.0858	17-37	1			AHDGPVFSMHALEKGFVTGG K
1998.0411	137-153	1	Cys_CAM: 148	2055.0626	TLRIWDLSPSHCMLAVR
1966.0603	60-78	1			ADLAPGSKGLLLEDNPSIR
1884.8618	38-53	1	Cys_CAM: 51	1941.8833	DGMVALWDDSFERCLK
1866.9530	14-30	1			TVKAHDGPVFSMHALEK
1755.9033	140-154	1	Cys_CAM: 148	1812.9247	IWDLSPSHCMLAVRK
1627.8083	140-153	0	Cys_CAM: 148	1684.8298	IWDLSPSHCMLAVR
1585.7843	3-16	1			GSHHHHHHGSKTVK
1549.8948	154-168	1			KGKPIPNPLLGLDST
1544.7148	1-13	1			MRGSHHHHHHGSK
1540.6736	38-50	0			DGMVALWDDSFER
1538.7420	17-30	0			AHDGPVFSMHALEK
1421.7998	155-168	0			GKPIPNPLLGLDST
1402.8165	79-92	0			AISLGHGHILVGTK
1257.5732	3-13	0			GSHHHHHHGSK
1226.6739	68-78	0			GLLLEDNPSIR
1016.5258	93-101	0			NGEILEVDK
939.5332	51-58	1	Cys_CAM: 51	996.5546	CLKTYAIK
914.5054	59-67	1			RADLAPGSK
758.4043	60-67	0			ADLAPGSK
751.4461	54-59	1			TYAIKR
665.3617	31-37	0			GFVTGGK
595.3450	54-58	0			TYAIK

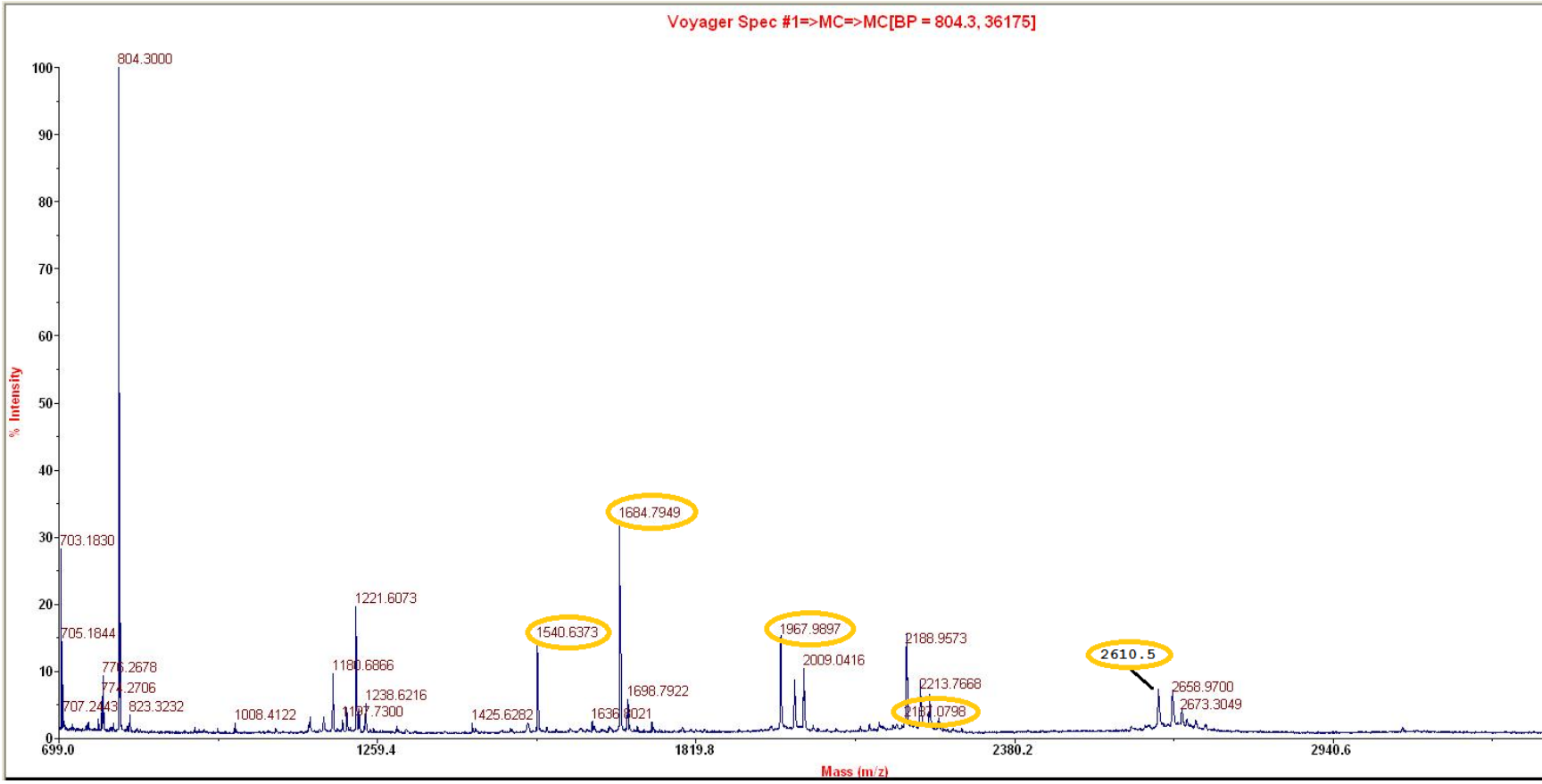
Voyager Spec #1=>MC=>MC[BP = 804.3, 36175]
% Intensity
Mass (m/z)
804.3000
703.1830
705.1844
776.2678
774.2706
707.2443
823.3232
1008.4122
1180.6866
1221.6073
1197.7300
1238.6216
1425.6282
1540.6373
1636.6021
1684.7949
1698.7922
1967.9897
2009.0416
2188.9573
2213.7668
2167.0798
2610.5
2658.9700
2673.3049
100
90
80
70
60
50
40
30
20
10
0
699.0
1259.4
1819.8
2380.2
2940.6

His_6-$GPCPD1_{1-118}$-V5

```
         10         20         30         40         50         60         70
MRGSHHHHHH GSMTPSQVTF EIRGTLLPGE VFAICGSCDA LGNWNPQNAV ALINENETGD SVLWKAVIAL
         80         90        100        110        120        130        140
NRGVSVKYRY FRGCFLEPKT IGGPCQVIVH KWETHLQPRS ITPLESEIII DDGQFGIHNG GKPIPNPLLG

LDST
```

mass	position	#MC	artif.modification(s)		peptide sequence
6816.2316	3-65	1	Cys_CAM: 35, 38	6930.2746	GSHHHHHHGSMTPSQVTFEI RGTLLPGEVFAICGSCDALG NWNPQNAVALINENETGDSV LWK
5153.5822	24-72	1	Cys_CAM: 35, 38	5267.6251	GTLLPGEVFAICGSCDALGN WNPQNAVALINENETGDSVL WKAVIALNR
4705.4259	102-144	1			WETHLQPRSITPLESEIIID DGQFGIHNGGKPIPNPLLGL DST
4416.1274	24-65	0	Cys_CAM: 35, 38	4530.1703	GTLLPGEVFAICGSCDALGN WNPQNAVALINENETGDSVL WK
3657.9009	110-144	0			SITPLESEIIIDDGQFGIHN GGKPIPNPLLGLDST
2706.2637	1-23	1			MRGSHHHHHHGSMTPSQVTF EIR
2419.1221	3-23	0			GSHHHHHHGSMTPSQVTFEI R
2299.2128	90-109	1	Cys_CAM: 95	2356.2342	TIGGPCQVIVHKWETHLQPR
2026.0612	83-101	1	Cys_CAM: 84, 95	2140.1041	GCFLEPKTIGGPCQVIVHK
1259.6241	80-89	1	Cys_CAM: 84	1316.6456	YFRGCFLEPK
1251.6878	90-101	0	Cys_CAM: 95	1308.7092	TIGGPCQVIVHK
1226.7579	66-77	1			AVIALNRGVSVK
1066.5428	102-109	0			WETHLQPR
808.4675	73-79	1			GVSVKYR
804.4151	78-82	1			YRYFR
793.3913	83-89	0	Cys_CAM: 84	850.4127	GCFLEPK
756.4726	66-72	0			AVIALNR

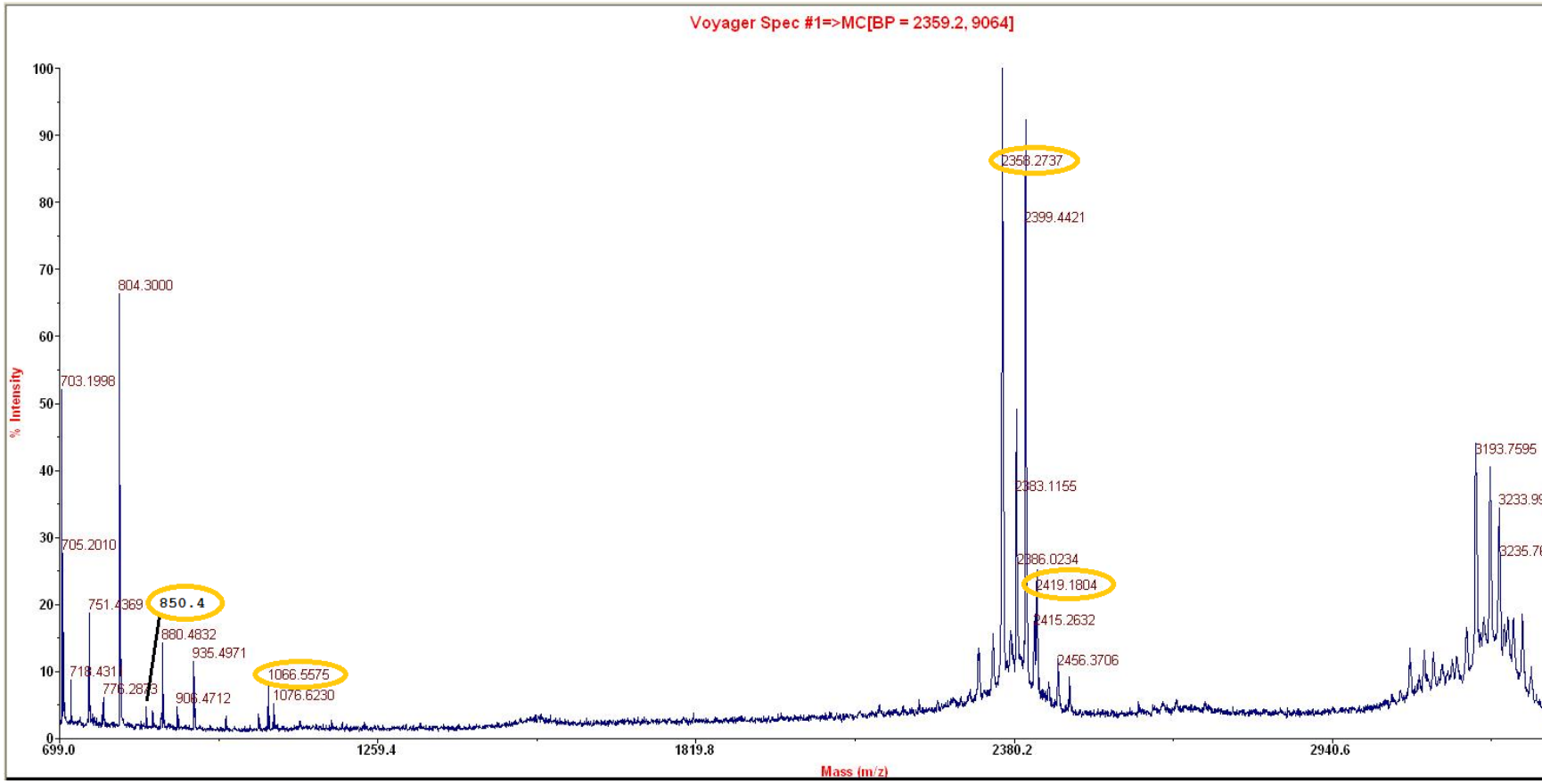
Voyager Spec #1=>MC[BP = 2359.2, 9064]
% Intensity
Mass (m/z)
2358.2737
2399.4421
804.3000
703.1998
705.2010
751.4369
850.4
880.4832
935.4971
718.431
776.2873
906.4712
1066.5575
1076.6230
2383.1155
2386.0234
2419.1804
2415.2632
2456.3706
3193.7595
3233.99
3235.76

His_6-$NCAN_{156-359}$-V5

```
        10         20         30         40         50         60         70
MRGSHHHHHH GSVTGVVFHY RAARDRYALT FAEAQEACRL SSATIAAPRH LQAAFEDGFD NCDAGWLSDR
        80         90        100        110        120        130        140
TVRYPITQSR PGCYGDRSSL PGVRSYGRRD PQELYDVYCF ARELGGEVFY VGPARRLTLA GARAQCQRQG
       150        160        170        180        190        200        210
AALASVGQLH LAWHEGLDQC DPGWLADGSV RYPIQTPRRR CGGPAPGVRT VYRFANRTGF PAPGARFDAY
       220        230
CFRAHHGKPI PNPLLGLDST
```

mass	position	#MC	artif.modification(s)		peptide sequence
4313.1308	139-178	1	Cys_CAM: 160	4370.1522	QGAALASVGQLHLAWHEGLD QCDPGWLADGSVRYPIQTPR
4043.9351	134-171	1	Cys_CAM: 136, 160	4157.9780	AQCQRQGAALASVGQLHLAW HEGLDQCDPGWLADGSVR
3457.6705	139-171	0	Cys_CAM: 160	3514.6920	QGAALASVGQLHLAWHEGLD QCDPGWLADGSVR
3334.5545	40-70	1	Cys_CAM: 62	3391.5759	LSSATIAAPRHLQAAFEDGF DNCDAGWLSDR
2993.4137	100-125	1	Cys_CAM: 109	3050.4352	DPQELYDVYCFARELGGEVF YVGPAR
2723.2266	50-73	1	Cys_CAM: 62	2780.2481	HLQAAFEDGFDNCDAGWLSD RTVR
2669.3292	207-230	1	Cys_CAM: 211	2726.3507	FDAYCFRAHHGKPIPNPLLG LDST
2486.2197	3-24	1			GSHHHHHHGSVTGVVFHYRA AR
2475.1860	1-21	1			MRGSHHHHHHGSVTGVVFHY R
2440.2289	27-49	1	Cys_CAM: 38	2497.2503	YALTFAEAQEACRLSSATIA APR
2367.0094	50-70	0	Cys_CAM: 62	2424.0309	HLQAAFEDGFDNCDAGWLSD R
2309.1455	74-94	1	Cys_CAM: 83	2366.1669	YPITQSRPGCYGDRSSLPGV R
2188.0444	3-21	0			GSHHHHHHGSVTGVVFHYR
1968.9708	71-87	1	Cys_CAM: 83	2025.9923	TVRYPITQSRPGCYGDR
1775.8322	198-213	1	Cys_CAM: 211	1832.8536	TGFPAPGARFDAYCFR
1774.8217	99-112	1	Cys_CAM: 109	1831.8432	RDPQELYDVYCFAR
1766.9547	214-230	0			AHHGKPIPNPLLGLDST
1743.8119	25-39	1	Cys_CAM: 38	1800.8333	DRYALTFAEAQEACR
1618.7206	100-112	0	Cys_CAM: 109	1675.7420	DPQELYDVYCFAR
1612.7536	74-87	0	Cys_CAM: 83	1669.7751	YPITQSRPGCYGDR
1549.8121	113-126	1			ELGGEVFYVGPARR
1472.6838	27-39	0	Cys_CAM: 38	1529.7053	YALTFAEAQEACR
1393.7110	113-125	0			ELGGEVFYVGPAR
1361.7072	194-206	1			FANRTGFPAPGAR
1332.6841	181-193	1	Cys_CAM: 181	1389.7055	CGGPAPGVRTVYR
1287.6950	127-138	1	Cys_CAM: 136	1344.7164	LTLAGARAQCQR
1178.6276	88-98	1			SSLPGVRSYGR
1030.5792	172-179	1			YPIQTPRR
1026.5479	190-197	1			TVYRFANR
986.5629	40-49	0			LSSATIAAPR
969.5047	180-189	1	Cys_CAM: 181	1026.5261	RCGGPAPGVR

921.3923	207-213	0	Cys_CAM: 211	978.4138	FDAYCFR
874.4781	172-178	0			YPIQTPR
873.4577	198-206	0			TGFPAPGAR
857.5315	126-133	1			RLTLAGAR
813.4035	181-189	0	Cys_CAM: 181	870.4250	CGGPAPGVR
715.4097	88-94	0			SSLPGVR
701.4304	127-133	0			LTLAGAR
638.3369	95-99	1			SYGRR
605.2824	134-138	0	Cys_CAM: 136	662.3039	AQCQR
588.3212	22-26	1			AARDR
538.2984	190-193	0			TVYR
507.2674	194-197	0			FANR

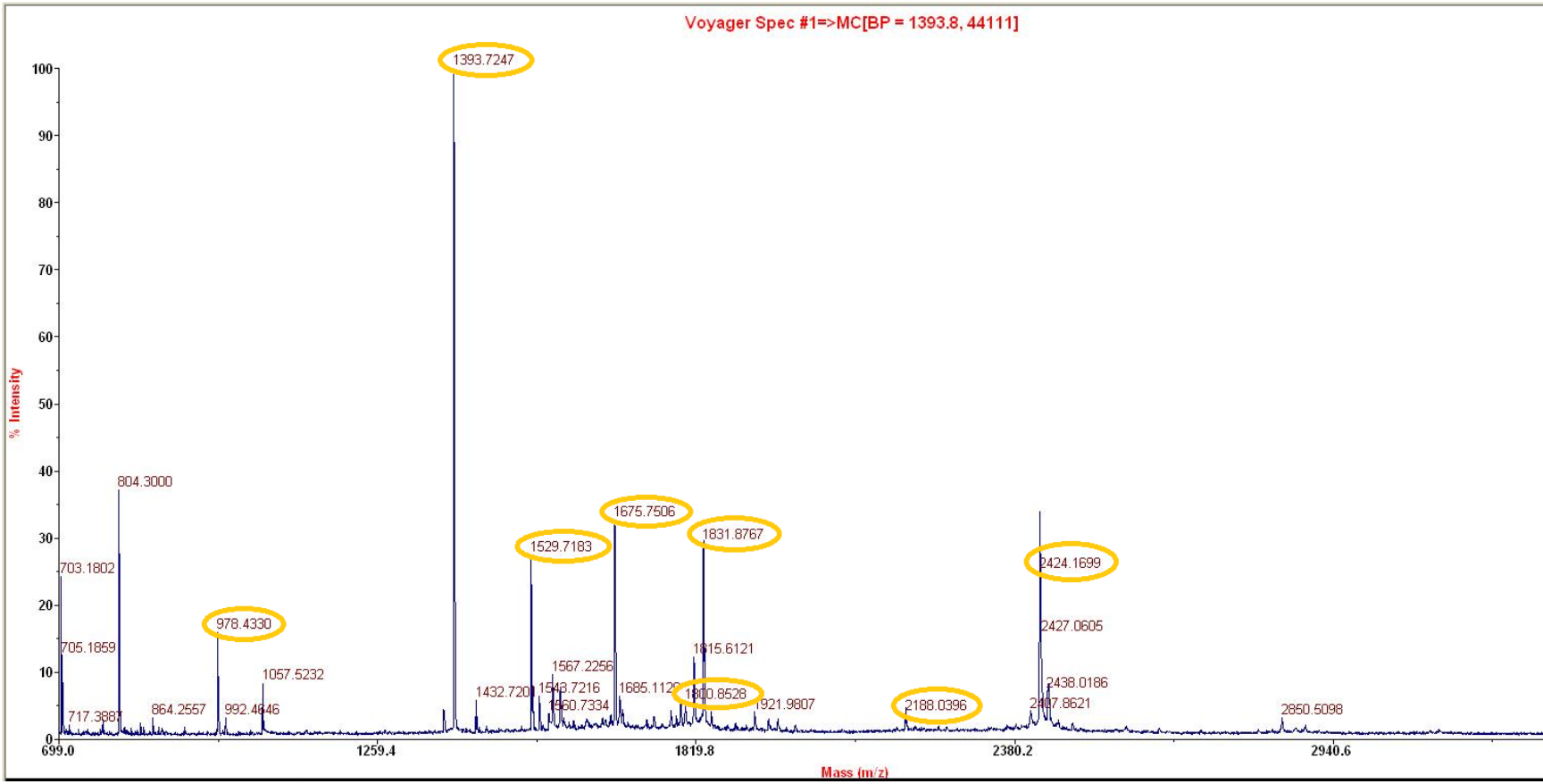
Voyager Spec #1=>MC[BP = 1393.8, 44111]
% Intensity
Mass (m/z)
1393.7247
804.3000
1675.7506
1529.7183
1831.8767
2424.1699
703.1802
978.4330
2427.0605
705.1859
1815.6121
1567.2256
1057.5232
2438.0186
1432.7201
1548.7216
1685.1120
1800.8528
1921.9807
2188.0396
1560.7334
717.3887
864.2557
992.4646
2850.5098
699.0
1259.4
1819.8
2380.2
2940.6

List of Abbreviations

AA	Amino Acid
AC	TCR Alpha chain Constant gene segment
aFITC-Alexa488	Goat anti FITC IgG labeled with Alexa Fluor 488
AJ	TCR Alpha chain Joining gene segment
ALOX12B	Arachidonate 12-Lipoxygenase, 12R-type
AP5S1	Adaptor-related Protein 5 Complex, Sigma 1 Subunit
APC	Antigen Presenting Cell
AV	TCR Alpha chain Variable gene segment
BC	TCR Beta chain Constant gene segment
BD	TCR Beta chain Diversity gene segment
BJ	TCR Beta chain Joining gene segment
BS^3	Bis(Sulfsuccinimidyl)Suberate
BSA	Bovine Serum Albumin
BV	TCR Beta chain Variable gene segment
CDR	Complementarity Determining Region
CNS	Central Nervous System
DEPC	Diethylpyrocarbonate
DMSO	Dimethyl Sulfoxide
ECL	Enhanced Chemiluminescence
EML5	Echinoderm Microtubule-associated Protein-Like 5
EML6	Echinoderm Microtubule-associated Protein-Like 6
ESI-MS	Electrospray Ionization Mass Spectrometry
FCS	Fetal Calf Serum
FITC	Fluorescein-Isothiocyanat
FPLC	Fast Protein Liquid Chromatography
FU	Fluorescence Unit
GAPDH	Glyceraldehyde-3-Phosphate Dehydrogenase
GFP	Green Fluorescent Protein
GPCPD1	Glycerophosphocholine Phosphodiesterase 1
HLA	Human Leukocyte Antigen
HRP	Horseradish Peroxydase
IB	Inclusion Body
IL-2	Interleukin 2
IPTG	Isopropyl β-D-1-thiogalactopyranoside
KLHL28	Kelch-Like protein 28
MALDI-TOF-MS	Matrix Assisted Laser Desorption Ionization - Time Of Flight Mass Spectrometry
MDH1B	Malate Dehydrogenase 1B
MOG	Myelin Oligodendrocyte Protein
MS	Multiple Sclerosis
NCAN	Neurocan
NFAT	Nuclear Factor of Activated T Cells
OD	Optical Density
ori	Origin of Replication
PBMC	Peripheral Blood Mononuclear Cell
PCR	Polymerase Chain Reaction
PECP library	Plasmid-Encoded Combinatorial Peptide Library
PLP	Proteolipid Protein 1
PMSF	Phenylmethanesulfonyl Fluoride
qPCR	Quantitative PCR
RIN	RNA Integrity Number
RT-PCR	Reverse Transcription PCR
SDS	Sodium Dodecyl Sulfate
SDS-PAGE	SDS Polyacrylamide Gel Electrophoresis
SPDL1	Spindle Apparatus Coiled-Coil Protein 1
TAP1	Transporter 1
TCR	T Cell Receptor
T_m	Melting Temperature
WDR25	WD Repeat Domain 25

List of References

Ackerman AL, Cresswell P. (2004) Cellular mechanisms governing cross-presentation of exogenous antigens. *Nat Immunol*. 5(7):678-84.

Adams JM, Imagawa DT. (1962) Measles antibodies in multiple sclerosis. *Proc Soc Exp Biol Med*. 111:562-6.

Agostini HT, Ryschkewitsch CF, Baumhefner RW, Tourtellotte WW, Singer EJ, Komoly S, Stoner GL. (2000) Influence of JC virus coding region genotype on risk of multiple sclerosis and progressive multifocal leukoencephalopathy. *J Neurovirol*. 6 Suppl 2:S101-8.

Altman JD, Davis MM. (2003) MHC-peptide tetramers to visualize antigen-specific T cells. *Curr Protoc Immunol.* Chapter 17: Unit 17.3.

Anderson G, Takahama Y. (2012) Thymic epithelial cells: working class heroes for T cell development and repertoire selection. *Trends Immunol.* 33(6):256-63.

Arden B, Clark SP, Kabelitz D, Mak TW. (1995) Human T-cell receptor variable gene segment families. *Immunogenetics.* 42(6):455-500.

Arens R, Schoenberger SP. (2010) Plasticity in programming of effector and memory CD8 T-cell formation. *Immunol Rev.* 235(1):190-205.

Arstila TP, Casrouge A, Baron V, Even J, Kanellopoulos J, Kourilsky P. (1999) A direct estimate of the human alphabeta T cell receptor diversity. *Science.* 286(5441):958-61.

Babbe H, Roers A, Waisman A, Lassmann H, Goebels N, Hohlfeld R, Friese M, Schröder R, Deckert M, Schmidt S. (2000) Clonal Expansions of CD8+ T Cells Dominate the T Cell Infiltrate in Active Multiple Sclerosis Lesions as Shown by Micromanipulation and Single Cell Polymerase Chain Reaction. *J Exp Med.* 192(3):393-404.

Backes A. (2010) Untersuchungen zur Charakterisierung autoaggressiver $CD8^+$ T-Zellen aus Patienten mit Multipler Sklerose.

Baranzini SE, Mudge J, van Velkinburgh JC, Khankhanian P, Khrebtukova I, Miller NA, Zhang L, Farmer AD, Bell CJ, Kim RW, May GD, Woodward JE, Caillier SJ, McElroy JP, Gomez R, Pando MJ, Clendenen LE, Ganusova EE, Schilkey FD, Ramaraj T, Khan OA, Huntley JJ, Luo S, Kwok PY, Wu TD, Schroth GP, Oksenberg JR, Hauser SL, Kingsmore SF. (2010) Genome, epigenome and RNA sequences of monozygotic twins discordant for multiple sclerosis. *Nature*. 464(7293):1351-6.

Bennett SR, Carbone FR, Toy T, Miller JF, Heath WR. (1998) B cells directly tolerize CD8 (+) T cells. *J Exp Med*. 188(11):1977-83.

Berer K, Mues M, Koutrolos M, Rasbi ZA, Boziki M, Johner C, Wekerle H, Krishnamoorthy G. (2011) Commensal microbiota and myelin autoantigen cooperate to trigger autoimmune demyelination. *Nature*. 479(7374):538-41.

Bhonsle L. (2011) Characterization of potentially autoaggressive brain infiltrating CD8+ T cells in multiple sclerosis patients.

Biddison WE, Beall SS, Concannon P, Charmley P, Gatti RA, Hood LE, McFarland HF, McFarlin DE. (1989) the germline repertoire of T-cell receptor beta-chain genes in patients with multiple sclerosis. *Res Immunol*. 140(2):212-5.

Booss J, Esiri MM, Tourtellotte WW, Mason DY. (1983) Immunohistological analysis of T lymphocyte subsets in the central nervous system in chronic progressive multiple sclerosis. *J Neurol Sci*. 62(1-3):219-32.

Brück W, Stadelmann C. (2003) Inflammation and degeneration in multiple sclerosis. *Neurological Sciences.* 24, p. 265 - 267.

Brynedal B, Duvefelt K, Jonasdottir G, Roos IM, Akesson E, Palmgren J, Hillert J. (2007) HLA-A confers an HLA-DRB1 independent influence on the risk of multiple sclerosis. *PLoS One*. 2(7):e664.

Burfoot RK, Jensen CJ, Field J, Stankovich J, Varney MD, Johnson LJ, Butzkueven H, Booth D, Bahlo M, Tait BD, Taylor BV, Speed TP, Heard R, Stewart GJ, Foote SJ, Kilpatrick TJ, Rubio JP. (2008) SNP mapping and candidate gene sequencing in the class I region of the HLA complex: searching for multiple sclerosis susceptibility genes in Tasmanians. *Tissue Antigens*. 71(1):42-50.

van der Bruggen P, Traversari C, Chomez P, Lurquin C, De Plaen E, Van den Eynde BJ, Knuth A, Boon T. (2007) A gene encoding an antigen recognized by cytolytic T lymphocytes on a human melanoma. *Cancer Res*. 62(19):5510-6.

Chaplin DD. (2010) Overview of the immune response. *J Allergy Clin Immunol*. 125(2 Suppl 2):S3-23.

Clevers H, Alarcon B, Wileman T, Terhorst C. (1988) The T cell receptor/CD3 complex: a dynamic protein ensemble. *Annu Rev Immunol*. 6:629-62.

Colf LA, Bankovich AJ, Hanick NA, Bowerman NA, Jones LL, Kranz DM, Garcia KC. (2007) How a single T cell receptor recognizes both self and foreign MHC. *Cell*. 129(1):135–46.

Collins SM, Surette M, Bercik P. (2012) The interplay between the intestinal microbiota and the brain. *Nat Rev Microbiol*. 10(11):735-42.

Compston A, Coles A. (2008) Multiple Sclerosis. *Lancet.* 372(9648):1502-17.

Cusick MF, Libbey JE, Fujinami RS. (2012) Molecular mimicry as a mechanism of autoimmune disease. *Clin Rev Allergy Immunol.* 42(1):102-11.

Davis MM, Bjorkman PJ. (1988) T-cell antigen receptor genes and T-cell recognition. *Nature* 334(6181):395-402.

Davis MM, Boniface JJ, Reich Z, Lyons D, Hampl J, Arden B, Chien Y. (1998) Ligand recognition by alpha beta T cell receptors. *Annu Rev Immunol*. 16:523-44.

Derbinski J, Schulte A, Kyewski B, Klein L. (2001) Promiscuous gene expression in medullary thymic epithelial cells mirrors the peripheral self. *Nat Immunol*. 2(11):1032-9.

Ding YH, Smith KJ, Garboczi DN, Utz U, Biddison WE, Wiley DC. (1998) Two human T cell receptors bind in a similar diagonal mode to the HLA-A2/Tax peptide complex using different TCR amino acids. *Immunity*. 8(4):403-11.

D'Orsogna LJ, Nguyen TH, Claas FH, Witt C, Mifsud NA. (2013) Endogenous-peptide-dependent alloreactivity: new scientific insights and clinical implications. *Tissue Antigens*. 81(6):399-407.

Dyment DA, Ebers GC, Sadovnick AD. (2004) Genetics of multiple sclerosis. *Lancet Neurology*. 3:104-110.

Ebers GC. (2008) Environmental factors and multiple sclerosis. *Lancet Neurol*. 7(3):268-77.

Ehling R, Berger T, Reindl M. (2010) Multiple sclerosis - established and novel therapeutic approaches. *Cent Nerv Syst Agents Med Chem*. 10(1):3-15.

Falk K, Rötzschke O, Stevanović S, Jung G, Rammensee HG. (1991) Allele-specific motifs revealed by sequencing of self-peptides eluted from MHC molecules. *Nature.* 351(6324):290-6.

Felix NJ, Allen PM. (2007) Specificity of T-cell alloreactivity. *Nat Rev Immunol.* 7(12):942-53.

Friese MA, Fugger L. (2009) Pathogenic CD8(+) T cells in multiple sclerosis. *Ann Neurol*. 66(2):132-41.

Friese MA, Jakobsen KB, Friis L, Etzensperger R, Craner MJ, McMahon RM, Jensen LT, Huygelen V, Jones EY, Bell JI, Fugger L. (2008) Opposing effects of HLA class I molecules in tuning autoreactive CD8+ T cells in multiple sclerosis. *Nat Med*. 14(11):1227-35.

Frohman EM, Racke MK, Raine CS. (2006) Multiple sclerosis - the plaque and its pathogenesis. *N Engl J Med.* 354(9):942-55.

Fung I, Garrett JP, Shahane A, Kwan M. (2012) Do bugs control our fate? The influence of the microbiome on autoimmunity. *Curr Allergy Asthma* Rep. 12(6):511-9.

Gangadharan D, Cheroutre H. (2004) The CD8 isoform CD8alphaalpha is not a functional homologue of the TCR co-receptor CD8alphabeta. *Curr Opin Immunol*. 16(3):264-70.

Garcia KC, Adams EJ. (2005) How the T cell receptor sees antigen--a structural view. *Cell.* 122(3):333-6.

Gáspár R Jr, Bagossi P, Bene L, Matkó J, Szöllosi J, Tozsér J, Fésüs L, Waldmann TA, Damjanovich S. (2001) Clustering of class I HLA oligomers with CD8 and TZR: three-dimensional models based on fluorescence resonance energy transfer and crystallographic data. *J Immunol*. 166(8):5078-86.

Gluzman Y. (1981) SV40-transformed simian cells support the replication of early SV40 mutants. *Cell.* 23(1):175-82.

Gnjatic S, Atanackovic D, Matsuo M, Jäger E, Lee SY, Valmori D, Chen YT, Ritter G, Knuth A, Old LJ. (2003) Cross-presentation of HLA class I epitopes from exogenous NY-ESO-1 polypeptides by nonprofessional APCs. *J Immunol*. 170(3):1191-6.

Godelaine D, Carrasco J, Brasseur F, Neyns B, Thielemans K, Boon **T**, Van Pel A. (2007) A new tumor-specific antigen encoded by MAGE-C2 and presented to cytolytic T lymphocytes by HLA-B44. *Cancer Immunol Immunother*. 56(6):753-9.

Goverman J, Perchellet A, Huseby ES. (2005) The role of CD8(+) T cells in multiple sclerosis and its animal models. *Curr Drug Targets Inflamm Allergy*. 4(2):239-45.

Greer JM, McCombe PA. (2011) Role of gender in multiple sclerosis: clinical effects and potential molecular mechanisms. *J Neuroimmunol*. 234(1-2):7-18.

Griesemer AD, Sorenson EC, Hardy MA. (2010) The role of the thymus in tolerance. *Transplantation*, 90: 465–74

Groothuis TA, Neefjes J. 2005 The many roads to cross-presentation. *J Exp Med*. 202(10):1313-8.

Hahn M, Nicholson MJ, Pyrdol J, Wucherpfennig KW. 2005. Unconventional topology of self peptide-major histocompatibility complex binding by a human autoimmune T cell receptor. *Nat. Immunol.* 6:490–496.

Harty JT, Tvinnereim AR, White DW. (2000) CD8+ T cell effector mechanisms in resistance to infection. *Annu Rev Immunol.* 18:275-308.

Hauser SL, Bhan AK, Gilles F, Kemp M, Kerr C, Weiner HL. (1986) Immunohistochemical analysis of the cellular infiltrate in multiple sclerosis lesions. *Ann Neurol*. 19(6):578-87.

Hausmann S, Biddison WE, Smith KJ, Ding YH, Garboczi DN, Utz U, Wiley DC, Wucherpfennig KW. (1999) Peptide recognition by two HLA-A2/Tax11-19-specific T cell clones in relationship to their MHC/peptide/TCR crystal structures. *J Immunol.* 162(9):5389-97.

Hohlfeld R, Wekerle H. (2001) Immunological update on multiple sclerosis. *Curr. Opin. Neurol*. 14(3):299-304.

Honma K, Parker KC, Becker KG, McFarland HF, Coligan JE, Biddison WE. (1997) Identification of an epitope derived from human proteolipid protein that can induce autoreactive CD8+ cytotoxic T lymphocytes restricted by HLA-A3: evidence for cross-reactivity with an environmental microorganism. *J Neuroimmunol*. 73(1-2):7-14.

Hu W, Lucchinetti CF. (2009) The pathological spectrum of CNS inflammatory demyelinating diseases. *Semin Immunopathol.* 31(4):439-53.

Huesmann M, Scott B, Kisielow P, von Boehmer H. (1991) Kinetics and efficacy of positive selection in the thymus of normal and T cell receptor transgenic mice. *Cell.* 66(3):533-40.

Ibrahim S, Dawson DV, Sanfilippo F. (1995) Predominant infiltration of rejecting human renal allografts with T cells expressing CD8 and CD45RO. *Transplantation*. 59(5):724–8.

International Multiple Sclerosis Genetics Consortium; Wellcome Trust Case Control Consortium 2 (2011) Genetic risk and a primary role for cell-mediated immune mechanisms in multiple sclerosis. *Nature*. 476(7359):214-9.

Irvine DJ, Purbhoo MA, Krogsgaard M, Davis MM. (2002) Direct observation of ligand recognition by T cells. *Nature.* 419(6909):845-9.

Jersild C, Svejgaard A, Fog T. (1972) HL-A antigens and multiple sclerosis. *Lancet*. 1(7762):1240-1.

Junker A, Ivanidze J, Malotka J, Eiglmeier I, Lassmann H, Wekerle H, Meinl E, Hohlfeld R, Dornmair K. (2007) Multiple sclerosis: T-cell receptor expression in distinct brain regions. *Brain.* 130(Pt 11):2789-99.

Kim SM, Bhonsle L, Besgen P, Nickel J, Backes A, Held K, Vollmer S, Dornmair K, Prinz JC. (2012) Analysis of the paired TCR α- and β-chains of single human T cells. *PLoS One*. 7(5):e37338.

Krangel MS. (2009) Mechanics of T cell receptor gene rearrangement. *Curr Opin Immunol*. 21(2):133-9.

Kronenberg M, Siu G, Hood LE, Shastri N. (1986) The molecular genetics of the T-cell antigen receptor and T-cell antigen recognition. *Annu Rev Immunol.* 4:529-91.

Lassmann H, Brück W, Lucchinetti C. (2001) Heterogeneity of multiple sclerosis pathogenesis: implications for diagnosis and therapy. *Trends Mol Med.* 7(3):115-21.

Lefranc MP, Lefranc G. (2001) The T Cell Receptor Facts Book. (London, UK: Academic Press).

Lennon VA, Wilks AV, Carnegie PR. (1970) Immunologic properties of the main encephalitogenic peptide from the basic protein of human myelin. *J Immunol*. 105(5),1223-30.

Long EO, Rosen-Bronson S, Karp DR, Malnati M, Sekaly RP, Jaraquemada D. (1991) Efficient cDNA expression vectors for stable and transient expression of HLA-DR in transfected fibroblast and lymphoid cells. *Hum Immunol.* 31(4):229-35.

Love PE, Hayes SM. (2010) ITAM-mediated signaling by the T-cell antigen receptor. *Cold Spring Harb Perspect Biol.* 2(6):a002485.

Lucas RM, Hughes AM, Lay ML, Ponsonby AL, Dwyer DE, Taylor BV, Pender MP. (2011) Epstein-Barr virus and multiple sclerosis. *J Neurol Neurosurg Psychiatry*. 82(10),1142-8.

Lucchinetti C, Brück W, Parisi J, Scheithauer B, Rodriguez M, Lassmann H. (2000) Heterogeneity of multiple sclerosis lesions: implications for the pathogenesis of demyelination. *Ann Neurol*. 47(6):707-17.

MacDonald KP, Shlomchik WD, Reddy P. (2013) Biology of graft-versus-host responses: recent insights. *Biol Blood Marrow Transplant*. 19(1 Suppl):S10-4.

Madden DR, Garboczi DN, Wiley DC. (1993) The antigenic identity of peptide-MHC complexes: a comparison of the conformations of five viral peptides presented by HLA-A2. *Cell*. 19;75(4):693-708.

Mars LT, Saikali P, Liblau RS, Arbour N. (2010) Contribution of CD8 T lymphocytes to the immuno-pathogenesis of multiple sclerosis and its animal models. *Biochim Biophys Acta*. 1812(2):151-61.

Mason D. (1998) A very high level of crossreactivity is an essential feature of the T-cell receptor. *Immunol Today*. 19:395–404.

Matsumoto Y, Yoon WK, Jee Y, Fujihara K, Misu T, Sato S, Nakashima I, Itoyama Y. (2003). Complementarity-determining region 3 spectratyping analysis of the TCR repertoire in multiple sclerosis. *J Immunol*. 170, 4846-53.

McMahon RM, Friis L, Siebold C, Friese MA, Fugger L, Jones EY. (2011) Structure of HLA-A*0301 in complex with a peptide of proteolipid protein: insights into the role of HLA-A alleles in susceptibility to multiple sclerosis. *Acta Crystallogr D Biol Crystallogr.* 67(Pt 5):447-54.

Miller E. (2012) Multiple Sclerosis. *Adv Exp Med Biol*. 724:222-38.

Mohme M, Hotz C, Stevanovic S, Binder T, Lee JH, Okoniewski M, Eiermann T, Sospedra M, Rammensee HG, Martin R. (2013) HLA-DR15-derived self-peptides are involved in increased autologous T cell proliferation in multiple sclerosis. *Brain*. 136(Pt 6):1783-98.

Morris GP, Allen PM. (2012) How the TCR balances sensitivity and specificity for the recognition of self and pathogens. *Nat Immunol.* 13(2):121-8.

Murphy K, Travers P, Walport M. (2008) Janeway's Immunobiology. 7. edition, Garland Science, New York and London.

Nagai K, Thøgersen HC. (1987) Synthesis and sequence-specific proteolysis of hybrid proteins produced in Escherichia coli. *Methods Enzymol*. 153:461-81.

Naito S, Namerow N, Mickey MR, Terasaki PI. (1972) Multiple sclerosis: association with HL-A3. *Tissue Antigens*. 2(1):1-4.

Nakayamada S, Takahashi H, Kanno Y, O'Shea JJ. (2012) Helper T cell diversity and plasticity. *Curr Opin Immunol*, 24(3):297-302.

Nikolic-Zugic J, Bevan MJ. (1990) Role of self-peptides in positively selecting the T-cell repertoire. *Nature*. 344:65–7.

Nino-Vasquez JJ, Allicotti G, Borras E, Wilson DB, Valmori D, Simon R, Martin R, Pinilla C. (2004) A powerful combination: the use of positional scanning libraries and biometrical analysis to identify cross-reactive T cell epitopes. *Mol Immunol*. 40(14-15):1063-74.

Noseworthy JH, Lucchinetti C, Rodriguez M, Weinshenker BG. (2000) Multiple sclerosis. *N Engl J Med*. 343(13):938-52.

Olival GS, Lima BM, Sumita LM, Serafim V, Fink MC, Nali LH, Romano CM, Thomaz RB, Cavenaghi VB, Tilbery CP, Penalva-de-Oliveira AC. (2013) Multiple sclerosis and herpesvirus interaction. *Arq Neuropsiquiatr*. 71(9B):727-30.

van Oosten BW, Lai M, Hodgkinson S, Barkhof F, Miller DH, Moseley IF, Thompson AJ, Rudge P, McDougall A, McLeod JG, Adèr HJ, Polman CH. (1997) Treatment of multiple sclerosis with the monoclonal anti-CD4 antibody cM-T412: results of a randomized, double-blind, placebo-controlled, MR-monitored phase II trial. *Neurology*. 49(2):351-7.

Owens GP, Bennett JL. (2012) Trigger, pathogen, or bystander: the complex nexus linking Epstein- Barr virus and multiple sclerosis. *Mult Scler*. 18(9):1204-8.

Owens GP, Gilden D, Burgoon MP, Yu X, Bennett JL. (2011) Viruses and multiple sclerosis. *Neuroscientist*. 17(6):659-76.

Pakpoor J, Giovannoni G, Ramagopalan SV. (2013) Epstein-Barr virus and multiple sclerosis: association or causation? *Expert Rev Neurother*. 13(3):287-97.

Pannetier C, Even J, Kourilsky P. (1995) T-cell repertoire diversity and clonal expansions in normal and clinical samples. *Immunol Today* 16:176-181.

Paterson DJ, Jefferies WA, Green JR, Brandon MR, Corthesy P, Puklavec M, Williams AF. (1987) Antigens of activated rat T lymphocytes including a molecule of 50,000 Mr detected only on CD4 positive T blasts. *Mol Immunol*. 24(12):1281-90.

Pircher H, Mak TW, Lang R, Ballhausen W, Rüedi E, Hengartner H, Zinkernagel RM, Bürki K. (1989) T cell tolerance to Mlsa encoded antigens in T cell receptor V beta 8.1 chain transgenic mice. *EMBO J.* 8(3):719-27.

Poser CM, Roman GC, Vernant JC. (1990) Multiple sclerosis or HTLV-I myelitis? *Neurology*. 40(7):1020-2.

Prineas JW, Wright RG. (1978) Macrophages, lymphocytes, and plasma cells in the perivascular compartment in chronic multiple sclerosis. *Lab Invest*. 38(4):409-21.

Rainey-Barger EK, Blakely PK, Huber AK, Segal BM, Irani DN. (2013) Virus-induced CD8+ T cells accelerate the onset of experimental autoimmune encephalomyelitis: implications for how viral infections might trigger multiple sclerosis exacerbations. *J Neuroimmunol*. 259(1-2):47-54.

Rock KL, York IA, Saric T, Goldberg AL. (2002) Protein degradation and the generation of MHC class I-presented peptides. Adv Immunol. 2002;80:1-70.

Roers A, Montesinos-Rongen M, Hansmann ML, Rajewsky K, Küppers R. (1998) Amplification of TCRbeta gene rearrangements from micromanipulated single cells: T cells rosetting around Hodgkin and Reed-Sternberg cells in Hodgkin's disease are polyclonal. *Eur J Immunol*. 28(8):2424-31.

Rose AM, Bell LC. (2012) Epistasis and immunity: the role of genetic interactions in autoimmune diseases. *Immunology*. 137(2):131-8.

Rostasy K, Reiber H, Pohl D, Lange P, Ohlenbusch A, Eiffert H, Maass M, Hanefeld F. (2003) Chlamydia pneumoniae in children with MS: frequency and quantity of intrathecal antibodies. *Neurology*. 61(1):125-8.

Rowen L, Koop BF, Hood L. (1996) The complete 685-kilobase DNA sequence of the human b T cell receptor locus. *Science*, 272(5269):1755-62.

Rudolph MG, Stanfield RL, Wilson IA. (2006) How TCRs bind MHCs, peptides, and coreceptors. *Annu Rev Immunol*. 24:419-66.

Schluesener HJ, Sobel RA, Linington C, Weiner HL. (1987) A monoclonal antibody against a myelin oligodendrocyte glycoprotein induces relapses and demyelination in central nervous system autoimmune disease. *J Immunol*. 139(12):4016-21.

Seitz S, Schneider CK, Malotka J, Nong X, Engel AG, Wekerle H, Hohlfeld R, Dornmair K. (2006) Reconstitution of paired T cell receptor α- and β-chains from microdissected single cells of human inflammatory tissues. *PNAS*. 103(32):12057-62.

Serafini B, Rosicarelli B, Franciotta D, Magliozzi R, Reynolds R, Cinque P, Andreoni L, Trivedi P, Salvetti M, Faggioni A, Aloisi F. (2007) Dysregulated Epstein-Barr virus infection in the multiple sclerosis brain. *J Exp Med*. 204(12):2899-912.

Serafini B, Severa M, Columba-Cabezas S, Rosicarelli B, Veroni C, Chiappetta G, Magliozzi R, Reynolds R, Coccia EM, Aloisi F. (2010). Epstein-Barr virus latent infection and BAFF expression in B cells in the multiple sclerosis brain: implications for viral persistence and intrathecal B-cell activation. *J Neuropathol Exp Neurol*. 69(7):677-93.

Sethi DK, Schubert DA, Anders AK, Heroux A, Bonsor DA, Thomas CP, Sundberg EJ, Pyrdol J, Wucherpfennig KW. (2011) A highly tilted binding mode by a self-reactive T cell receptor results in altered engagement of peptide and MHC. *J Exp Med.* 208(1):91-102.

Sewell AK. (2012) Why must T cells be cross-reactive? *Nat Rev Immunol*. 12(9):669-77.

Shevchenko A, Wilm M, Vorm O, Mann M. (1996) Mass spectrometric sequencing of proteins silver-stained polyacrylamide gels. *Analytical chemistry.* 68, 850–858.

Siewert K. (2011) Autoaggressive Human T Cell Receptors and their Antigen Specificities.

Siewert K, Malotka J, Kawakami N, Wekerle H, Hohlfeld R, Dornmair K. (2012) Unbiased identification of target antigens of CD8+ T cells with combinatorial libraries coding for short peptides. *Nat Med.* 18(5):824-8.

Silva AM, Bettencourt A, Pereira C, Santos E, Carvalho C, Mendonça D, Costa PP, Monteiro L, Martins B. (2009) Protective role of the HLA-A*02 allele in Portuguese patients with multiple sclerosis. *Mult Scler*. 15(6):771-4.

Skulina C, Schmidt S, Dornmair K, Babbe H, Roers A, Rajewsky K, Wekerle H, Hohlfeld R, Goebels N. (2004) Multiple sclerosis: Brain-infiltrating CD8+ T cells persist as clonal expansions in the cerebrospinal fluid and blood. *PNAS*. 101(8):2428-33.

Smith-Garvin JE, Koretzky GA, Jordan MS. (2009) T cell activation. *Annu Rev Immunol*. 27:591-619.

Sospedra M, Pinilla C, Martin R. (2003) Use of combinatorial peptide libraries for T-cell epitope mapping. *Methods*. 29(3):236-47.

Speir JA, Stevens J, Joly E, Butcher GW, Wilson IA. (2001) Two different, highly exposed, bulged structures for an unusually long peptide bound to rat MHC class I RT1-Aa. *Immunity.* 14(1):81-92.

Sumaya CV, Myers LW, Ellison GW. (1980) Epstein-Barr virus antibodies in multiple sclerosis. *Arch Neurol*. 37(2), 94-6.

Sun X, Saito M, Sato Y, Chikata T, Naruto T, Ozawa T, Kobayashi E, Kishi H, Muraguchi A, Takiguchi M. (2012) Unbiased analysis of TCRα/β chains at the single-cell level in human CD8+ T-cell subsets. *PLoS One*. 7(7):e40386.

Sundqvist E, Bergström T, Daialhosein H, Nyström M, Sundström P, Hillert J, Alfredsson L, Kockum I, Olsson T. (2013) Cytomegalovirus seropositivity is negatively associated with multiple sclerosis. *Mult Scler*. [Epub ahead of print]

Trapp BD, Nave KA. (2008) Multiple sclerosis: an immune or neurodegenerative disorder? *Annu Rev Neurosci.* 31:247-69.

Virtanen JO, Jacobson S. (2012) Viruses and multiple sclerosis. *CNS Neurol Disord Drug Targets*. 11(5):528-44.

Wang JH, Reinherz EL. (2012) The structural basis of αβ T-lineage immune recognition: TCR docking topologies, mechanotransduction, and co-receptor function. *Immunol Rev.* 250(1):102-19.

Weinberg AD, Bourdette DN, Sullivan TJ, Lemon M, Wallin JJ, Maziarz R, Davey M, Palida F, Godfrey W, Engleman E, Fulton RJ, Offner H, Vandenbark AA. (1996) Selective depletion of myelin-reactive T cells with the anti-OX-40 antibody ameliorates autoimmune encephalomyelitis. *Nat Med*. 2(2):183-9.

Wekerle H. (1992) Myelin specific, autoaggressive T cell clones in the normal immune repertoire: their nature and their regulation. *Int Rev Immunol*. 9(3),231-41.

Wooldridge L, Ekeruche-Makinde J, van den Berg HA, Skowera A, Miles JJ, Tan MP, Dolton G, Clement M, Llewellyn-Lacey S, Price DA, Peakman M, Sewell AK. (2012) A single autoimmune T cell receptor recognizes more than a million different peptides. *J Biol Chem*. 287(2):1168-77.

Wucherpfennig KW, Newcombe J, Li H, Keddy C, Cuzner ML, Hafler DA. (1992) T cell receptor V alpha-V beta repertoire and cytokine gene expression in active multiple sclerosis lesions. *J Exp Med.* 175(4), 993-1002.

Yewdell JW, Reits E, Neefjes J. (2003) Making sense of mass destruction: quantitating MHC class I antigen presentation. *Nat Rev Immunol*. 3(12):952-61.

Eidesstattliche Versicherung

Gemäß §7 Abs. 2 der Promotionsordnung der Ludwig-Maximilians-Universität München für die medizinische Fakultät zur Erlangung des akademischen Doktorgrades der Naturwissenschaften (Dr. rer. nat.):

Hiermit erkläre ich an Eides statt, dass ich die vorliegende Dissertation mit dem Thema „Characterization of Disease-Related $CD8^+$ T Cells and their Antigens from Patients with Multiple Sclerosis“ selbstständig verfasst, mich außer der angegebenen keiner weiteren Hilfsmittel bedient und alle Erkenntnisse, die aus dem Schrifttum ganz oder annähernd übernommen sind, als solche kenntlich gemacht und nach ihrer Herkunft unter Bezeichnung der Fundstelle einzeln nachgewiesen habe.

Ich erkläre des Weiteren, dass die hier vorgelegte Dissertation nicht in gleicher oder in ähnlicher Form bei einer anderen Stelle zur Erlangung eines akademischen Grades eingereicht wurde.

Wolfratshausen, den 07.11.2013

_____

Anna Gabriele Niedl